Functional analysis of *Penicillium paxilli* genes required for biosynthesis of paxilline

This thesis is presented in partial fulfilment of the requirements

for the degree of

Doctor of Philosophy (PhD)

in

Biochemistry

at

Massey University, Palmerston North,

New Zealand

Sanjay Saikia

2006

ABSTRACT

Paxilline belongs to a large, structurally and functionally diverse group of indole-diterpenes and is synthesised by the filamentous fungus *Penicillium paxilli*. A gene cluster for paxilline biosynthesis in *P. paxilli* has been identified and characterised. However, none of the steps proposed in the biosynthesis of paxilline or paxilline-like indole-diterpenes have been validated. In some diterpene-producing filamentous fungi, including *P. paxilli*, two distinct copies of geranylgeranyl diphosphate (GGPP) synthase, that catalyses the committed step in diterpene biosynthesis, have been identified. However, the biological significance of the presence of two distinct GGPP synthases is not known. In this study, biochemical analysis of the paxilline gene products in *P. paxilli* and subcellular localisation of the two *P. paxilli* GGPP synthases, Ggs1 and PaxG, were carried out.

Transfer of constructs containing different combinations of *pax* genes into a *pax* cluster negative deletion derivative of *P. paxilli* identified four Pax proteins that are required for the biosynthesis of a paxilline intermediate, paspaline. These proteins are PaxG, a GGPP synthase, PaxM, a FAD-dependent monooxygenase, PaxB, a putative membrane protein, and PaxC, a prenyltransferase. Using precursor feeding experiments, it was confirmed that the indole-diterpenes paspaline and β-PC-M6 are substrates for the cytochrome P450 monooxygenase, PaxP, and are converted to 13-desoxypaxilline. Further, it was confirmed that the indole-diterpene 13-desoxypaxilline is a substrate for PaxQ, a cytochrome P450 monooxygenase, and is converted to paxilline. Unlike PaxQ, PaxP is specific for indole-diterpene substrates that have a β-stereochemistry. The detection of the indole-diterpene products was related to the expression of the transgene in the *pax* cluster negative background.

Reporter fusion studies of the two *P. paxilli* GGPP synthases, Ggs1 and PaxG, showed that the Ggs1-EGFP fusion protein was localised to punctuate structures whose identity could not be established, and the EGFP-GRV fusion

protein, containing the C-terminal tripeptide GRV of PaxG, was localised to peroxisomes.

ACKNOWLEDGEMENTS

I would like to express my extreme sense of thankfulness and appreciation to my supervisor, Barry Scott, for his invaluable and judicious guidance, constructive criticism and incessant encouragement throughout the period of my research and preparation of this thesis. Thank you Barry for giving me this opportunity to work on this project and for being an excellent supervisor! I would also like to thank my co-supervisor, Emily Parker, who with her knowledge, guidance and unremitting encouragement helped for a practical approach towards my research. I am thankful to the Royal Society of New Zealand for funding this project. I am also thankful to IMBS and NZSBMB for financial support for conference attendance.

I would like to express my sincere thanks to all my lab members, past and present, for their help, support and invaluable suggestions throughout my research. Andrea thanks a lot for your ever willingness to help and providing all the technical support in the lab. I really appreciate it. Jonathan thank you for helping me work on the HPLC and also for introducing me to the indoor cricket team. Carolyn thank you for supplying me with some of your lambda clones. Aiko and Daigo thank you for your friendship and unflinching help and support both inside and outside the lab. Matthew, Michelle and Ruth thank you for reading parts of my thesis and giving me critical and valuable suggestions. Ruth thank you for providing technical support in the lab. Thanks are also due to Shuguang, Rohan, Xiuwen, Brendon, Kim, Simon, Carla, Damien and Andrew for their helpful suggestions.

I would like to thank Albert for all the LC-MSMS analysis and for making me understand what the spectra meant. I would also like to thank Brian for discussions on indole-diterpene biosynthesis. I would like to thank Sarah for providing me with authentic samples of some indole-diterpenes.

I would like to thank Gill, Trev and Santanu for their help with HPLC. I would also like to thank Chad and Jeremy for their help and discussions on cellular

staining and supplying me with a stain. Thanks also to Liz for helping me with the use of microscope. I would like to thank Cynthia for her help in the printing of my thesis.

I am extremely grateful to my friends Afreen, Asela, Nadika, Nilu, Tehzeeb, Nihad, Fahd, Karthik, Corey, Wayne, Olivia, Arne, Abhimanyu, Vivek and Sanj for sharing all my myriad moments of joy and despair. Words are inadequate to express my gratitude for Khura and Khuri who provided me with the much needed homely milieu during all these years in Palmy. Thanks also to my indoor and outdoor cricket team mates for a very good time both in winning and losing.

Finally, I could not have reached this stage without the support of my dear family. Ma and Baba words at my discretion are simply inadequate to express my veneration for you two. Your sacrifices have made me reach this echelon of education. I am heartfelt when I think of the love and care rendered by my sister Junu and brother Montu, who selflessly prayed for my success.

TABLE OF CONTENTS

CHAPTER ONE
INTRODUCTION

1.1 Fungal secondary metabolism

Fungi produce many secondary metabolites that are not directly involved in normal growth but may serve diverse survival functions. Production of such metabolites is genus or species specific and is only activated during particular stages of growth and development, or during periods of stress caused by nutrient limitation or interaction with other organisms. Although such pathways are dispensable, there has been considerable interest in secondary metabolites due to their medical, industrial and agricultural importance. Secondary metabolites are used as competitive weapons against other organisms, metal transporting agents, symbiosis agents, sexual hormones and differentiation effectors. The main types of biosynthetic pathways involved form peptides, polyketides, isoprenes, oligosaccharides, aromatic compounds and β-lactam rings (Demain, 1992).

1.2 Secondary metabolite gene clusters

Although the clustering of functionally related genes is less common in eukaryotes than in prokaryotes (Keller and Hohn, 1997), this concept is rapidly changing with the identification of many fungal gene clusters involved in secondary metabolism (Table 1.1). Generally, fungal gene clusters can be defined as two or more genes that are closely linked, co-regulated, and participate in a common metabolic or developmental pathway. Gene clusters are often associated with dispensable metabolic pathways such as nutrient utilisation pathways (e.g. proline, quinate) and secondary metabolite biosynthesis pathways (e.g. antibiotics, mycotoxins). Dispensable metabolic pathways are either not vital for growth or are only important for growth under particular physiological conditions. Such pathways are characteristically expressed under suboptimal growth conditions or during interactions with other organisms, and thereby enhance survival of the producing organism. Besides having genes for biosynthetic enzymes, the dispensable metabolic pathway gene clusters also contain genes encoding for transcription factors, transporters, and also for products that provide self-protection.

Table 1.1 Fungal secondary metabolite gene clusters

Secondary metabolite	Organism*	Type	Biological function
Aflatoxins	*Aspergillus parasiticus, Aspergillus nidulans*	polyketide	carcinogen
Aflatrem	*Aspergillus flavus*	indole-diterpene	tremorgen
AF-toxin	*Alternaria alternata*	polyketide	pathogenicity factor
AK-toxin	*A. alternata*	polyketide	pathogenicity factor
AM-toxin	*A. alternata*	peptide	pathogenicity factor
Aphidicolin	*Phoma betae*	isoprenoid	antiviral
Aurofusarin	*Fusarium graminearum*	polyketide	electron transport inhibitor
Cephalosporin	*Acremonium chrysogenum*	peptide	antibiotic
Compactin	*Penicillium citrinum*	polyketide	HMG CoA reductase inhibitor
Dothistromin	*Dothistroma pini*	polyketide	pathogenicity factor
Ergot alkaloids/ Ergopeptines	*Claviceps purpurea*	peptide	plant protection/ anti-mammalian
Fumonisins	*Fusarium verticillioides*	polyketide	sphingolipid metabolism inhibitor
Gibberellins	*Fusarium fujikuroi*	isoprenoid	plant hormone
Gliotoxin	*Aspergillus fumigatus*	peptide	immunosuppressant
HC-toxin	*Cochliobolus carbonum*	peptide	virulence factor
Lolitrem B	*Neotyphodium lolii*	indole-diterpene	tremorgen
Lovastatin	*Aspergillus terrus*	polyketide	HMG CoA reductase inhibitor
Melanin	*A. alternata*	polyketide	fungal survival
Paxilline	*Penicillium paxilli*	indole-diterpene	tremorgen
Penicillin	*A. nidulans, P. chrysogenum*	peptide	antibiotic
Peramine	*Epichloë festucae*	peptide	anti-insect
Sirodesmin	*Leptosphaeria maculans*	peptide	phytotoxin
Sterigmatocystin	*A. nidulans, P. chrysogenum*	polyketide	carcinogen
Trichothecenes	*Fusarium sporotrichioides, F. graminearum*	isoprenoid	protein synthesis inhibitor
T-toxin	*Cochliobolus heterostrophus*	polyketide	virulence factor
Zearalenone	*F. graminearum*	polyketide	estrogen

* Well characterised organism in relation to the secondary metabolite. References cited elsewhere in the thesis.

1.3 Chemical diversity of fungal secondary metabolites

Secondary metabolites can be classified into three main classes: polyketides, non-ribosomal peptides and isoprenoids/ terpenoids.

1.3.1 Polyketides

Polyketides (Figure 1.1) are one of the most structurally diverse classes of natural products produced by filamentous bacteria, fungi, and plants through the successive condensation of simple carboxylic acid units. This group includes fungal aflatoxins, many clinically important antibiotics and plant flavonoids. The biosynthesis of these secondary metabolites is carried out by polyketide synthases (PKSs), and is related to fatty acid metabolism. The PKSs contain various catalytic domains, namely acyl transferase (AT), β-ketoacyl synthase (KS), acyl carrier protein (ACP), β-keto reductase (KR), dehydratase (DH), enoyl reductase (ER) and thiol esterase (TE) domains (Figure 1.1). These domains determine the order of substrate selection for chain elongation and the degree of reduction of each extension unit. The minimal PKS is composed of the AT, KS and ACP domains (the core domain), responsible for chain elongation. The ketoester produced by the core domain is then processed by the reductive domains consisting of ER, KR and DH domains. The TE domain is responsible for the release of the growing polyketide. Polyketide synthesis differs from fatty acid synthesis in using different primer and extender units, the extent that the nascent chain is processed during each elongation cycle, the introduction of chiral centres, and release of the processed chain after cyclisation, lactonisation, or amide bond formation. Thus, variations in primer units, processing sequences, chiral centres and cyclisation reactions makes the polyketides structurally diverse.

Based on enzyme architecture, PKSs are categorised into three families. Type I PKSs are multifunctional enzymes containing one or more modules, each with catalytic domains for the different biosynthetic steps. Macrocyclic polyketides like rifamycin, erythromycin, rapamycin, monensin and avermectin are synthesised by type I enzymes. Several bacterial type I PKS genes have been sequenced, in whole or part, for secondary metabolites including erythromycin

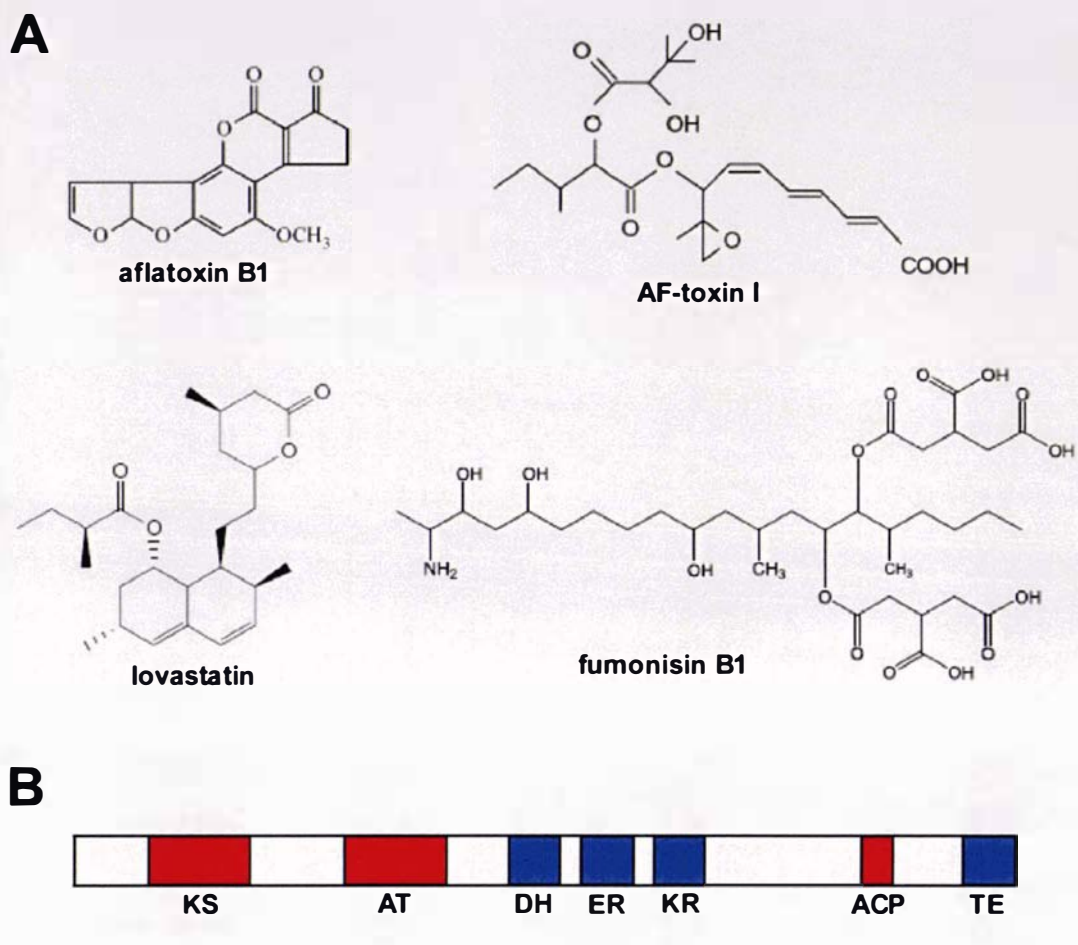

Figure 1.1 Polyketides

(A) Chemical structures of polyketides. **(B)** Domain structure of fungal polyketide synthase. The domains that form the minimal structure are coloured red and the domains that are optional are coloured blue. KS=β-ketoacyl synthase; AT=acyl transferase; DH=dehydratase; ER=enoyl reductase; KR=β-keto reductase; ACP=acyl carrier protein; TE=thiol esterase.

(Cortes *et al.*, 1990), FK506 (Motamedi and Shafiee, 1998), rapamycin (Ruan *et al.*, 1997) and avermectin (Yoon *et al.*, 2004). Various fungal type I PKS genes have been discovered including those for aflatoxin (Yu *et al.*, 2004), AF-toxin (Hatta *et al.*, 2002; Ito *et al.*, 2004), AK-toxin (Tanaka *et al.*, 1999), aurofusarin (Malz *et al.*, 2005), compactin (Abe *et al.*, 2002), dothistromin (Bradshaw *et al.*, 2006), fumonisins (Proctor *et al.*, 2003), lovastatin (Kennedy *et al.*, 1999), sterigmatocystin (Brown *et al.*, 1996), T-toxin (Yang *et al.*, 1996) and zearalenone (Gaffoor *et al.*, 2005; Kim *et al.*, 2005; Lysoe *et al.*, 2006).

Type II PKSs are found in bacteria and plants and consist of many separate, largely single-function proteins in which each catalytic site is on a separate protein subunit. These enzyme complexes catalyse the formation of cyclic, aromatic compounds that do not require extensive reduction or reduction-dehydration cycles. Polyketides synthesised by type II PKSs include actinorhodin, tetracenomycin, anthracyclins and tetracyclins.

Type III PKS enzymes are homodimers that are structurally and mechanistically different from type I and type II PKSs. These enzymes act directly on the acyl-CoA substrates without the involvement of acyl carrier proteins. These belong to the plant chalcone synthase superfamily of condensing enzymes, and are involved in chalcone and stilbene biosynthesis in plants and polyhydroxyphenol biosynthesis in bacteria.

1.3.2 Non-ribosomal peptides

Non-ribosomal peptides (Figure 1.2) are mainly produced by soil bacteria and filamentous fungi. These are secondary metabolites that are synthesised non-ribosomally via a thiotemplate mechanism on large multi-enzyme complexes called peptide synthetases (Figure 1.2). Peptide synthetases incorporate a wide range of amino acids, including non-proteinogenic or modified amino acids, such as *N*-methylated amino acids, hydroxylated amino acids and D-amino acids, into both cyclic and linear peptides to form structurally diverse peptidic secondary metabolites (Moffitt and Neilan, 2000). Non-ribosomal peptide synthetases are composed of modules that may be subdivided into domains (Doekel and Marahiel, 2001). The minimal elongation module

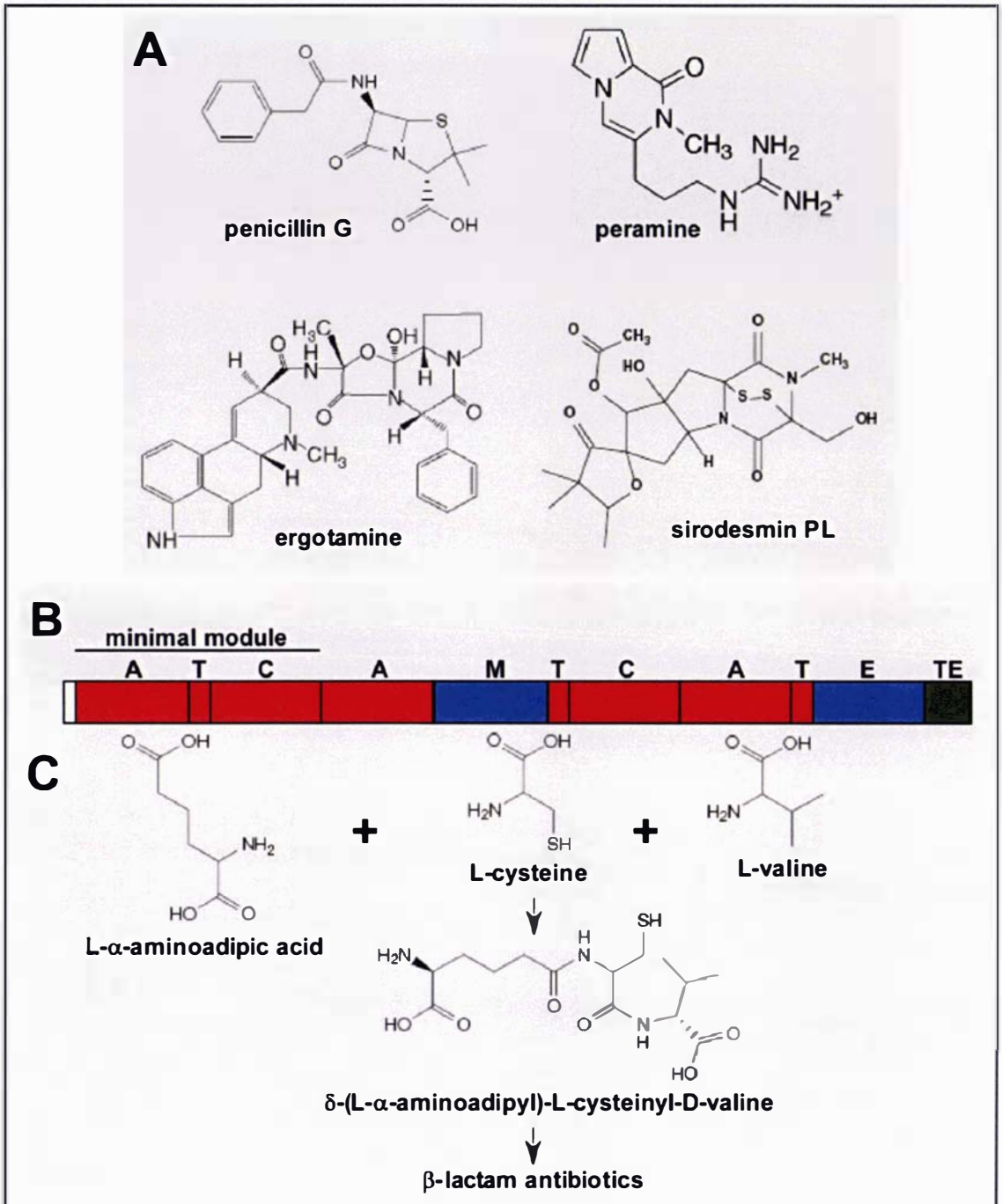

Figure 1.2 Non-ribosomal peptides

(A) Chemical structures of non-ribosomal peptides. **(B)** Modular structure of peptide synthetase. The minimal module contains the adenylation (A), the thiolation (T) and the condensation domains (C), and are coloured red. The optional domains are coloured blue. **(C)** Committed step in the biosynthesis of β-lactam antibiotics such as penicillin G, cephalosporin C. M=N-methylation domain; E=epimerisation domain; TE=thioesterase domain.

comprises at least three domains: an adenylation domain for substrate recognition and activation, a thiolation domain for covalent incorporation as thioesters on an enzyme-bound 4'-phosphopantetheinyl (4'PP) moiety and a condensation domain for condensation of precursor, which act together to form a peptide concatenated to the 4'PP moiety of the next module. Thioesterase-like domains implement the release of the processed peptide from the terminal 4'PP moiety. The substrate can be further modified by other catalytic domains such as epimerisation domains (for epimerisation of α-carbon atoms) or *N*-methylation domains (for *N*-methylation of α-amino groups). In fungi, a single multifunctional protein catalyses the multi-step assembly process, but in bacteria more than one multifunctional protein may be required.

Many bacterial and fungal genes encoding peptide synthetases have been cloned including those for AM-toxin (Johnson *et al.*, 2000), ergot alkaloids/ ergopeptines (Correia *et al.*, 2003; Coyle and Panaccione, 2005; Haarmann *et al.*, 2005; Haarmann *et al.*, 2006; Panaccione *et al.*, 2001; Riederer *et al.*, 1996; Tsai *et al.*, 1995; Tudzynski *et al.*, 1999b; Tudzynski *et al.*, 2001b; Wang *et al.*, 2004), gliotoxin (Cramer *et al.*, 2006; Gardiner and Howlett, 2005), HC-toxin (Ahn *et al.*, 2002; Panaccione *et al.*, 1992; Scott-Craig *et al.*, 1992), penicillin (Barredo *et al.*, 1989; Diez *et al.*, 1990; Smith *et al.*, 1990b), peramine (Tanaka *et al.*, 2005) and sirodesmin (Gardiner *et al.*, 2004; Gardiner and Howlett, 2005).

Non-ribosomal peptides may also act as a backbone for the biosynthesis of more complex structures, or may be incorporated with fatty acids or polyketides. Such structures may be synthesised by mixed or hybrid peptide synthetase and polyketide synthase systems. The number of identified structurally novel secondary metabolites produced via this thiotemplate mechanism is rapidly expanding.

1.3.3 Isoprenoids/ Terpenoids

Isoprenoids (Figure 1.3) are the largest group of natural products, comprising more than 30,000 known compounds. These metabolites are synthesised by

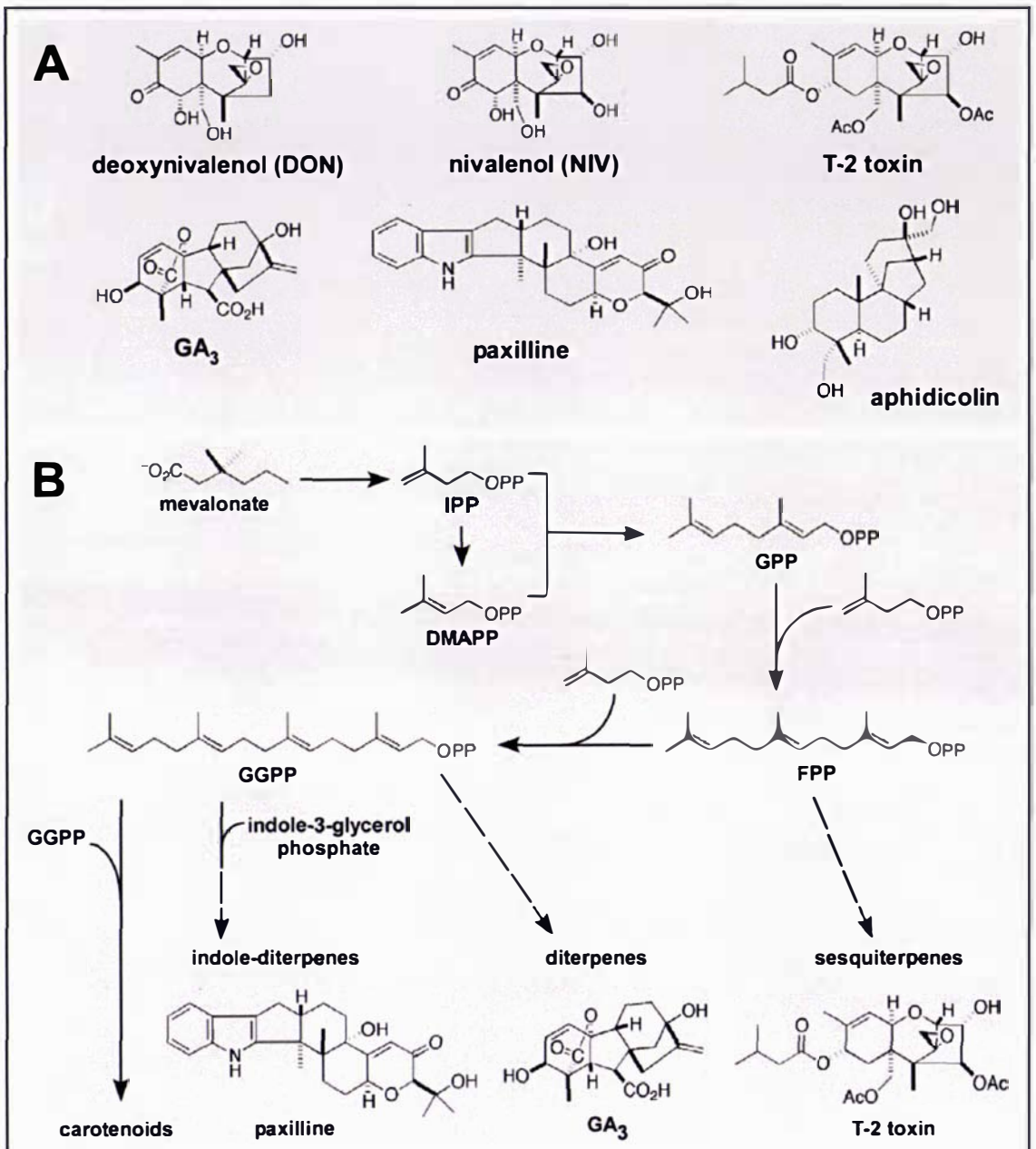

Figure 1.3 Isoprenoids

(A) Chemical structures of isoprenoids. **(B)** Isoprenoid biosynthesis in fungi (adapted from Scott *et al.*, 2004). IPP=isopentenyl diphosphate; DMAPP=dimethylallyl diphosphate; GPP=geranyl diphosphate; FPP=farnesyl diphosphate; GGPP=geranylgeranyl diphosphate

consecutive condensations of five-carbon compound isopentenyl diphosphate (IPP) to the isomer dimethylallyl diphosphate (DMAPP) by a family of prenyltransferases (Figure 1.3). The isoprenoid substrates can be derived from either a mevalonate pathway that occurs in eukaryotes, archaebacteria, and cytosols of higher plants, or from a mevalonate-independent pathway (via 1-deoxyxylulose-5-phosphate) that operates in many eubacteria, green algae and chloroplasts of higher plants. Linear C10, C15 and C20 isoprenyl pyrophosphates are synthesised by geranyl diphosphate (GPP) synthase, farnesyl diphosphate (FPP) synthase and geranylgeranyl diphosphate (GGPP) synthase, respectively. FPP and GGPP are key branching points and serve as substrates for various prenyltransferases involved in the biosynthesis of sesquiterpenes, sterols, dolichols, diterpenes, indole-diterpenes and carotenoids.

1.3.3.1 Trichothecenes

Trichothecenes are toxic sesquiterpenoid secondary metabolites produced by fungi including *Fusarium*, *Stachybotrys*, *Myrothecium*, *Trichothecium*, *Trichoderma*, and *Cephalosporium*, as well as two plant species (Brown *et al.*, 2001; Sharma and Kim, 1991). Trichothecenes are strong inhibitors of protein synthesis and act as virulence factors in plant pathogenesis (Harris *et al.*, 1999; Proctor *et al.*, 1995a). These secondary metabolites have a common trichothecene skeleton that consists of cyclopentane, cyclohexane, and a six-member oxyrane ring with four methyl groups.

Trichothecene biosynthesis has been extensively studied in *Fusarium graminearum* (mainly producing the trichothecenes deoxynivalenol and nivalenol) and *Fusarium sporotrichioides* (mainly producing the trichothecene T-2 toxin). In these organisms, trichothecenes are synthesised by the cyclisation of the primary metabolite FPP by the *Tri5* gene product, trichodiene synthase, followed by multiple oxygenation, cyclisation and esterification steps. Based on genetic and metabolite feeding studies, trichothecene biosynthesis genes in *Fusarium* have been identified at four different genomic locations. The main 12-gene cluster includes the *Tri5* sesquiterpene cyclase gene (Desjardins *et al.*, 1993; Hohn and Beremand, 1989), the *Tri4*, *Tri11* and *Tri13* cytochrome

P450 monooxygenase genes (Alexander *et al.*, 1998; Brown *et al.*, 2002; Hohn *et al.*, 1995; Lee *et al.*, 2002b), the *Tri3* and *Tri7* acetyltransferase genes (Brown *et al.*, 2001; Kimura *et al.*, 2003; Lee *et al.*, 2002b; McCormick *et al.*, 1996), the *Tri8* esterase gene (McCormick and Alexander, 2002), the *Tri6* and *Tri10* regulatory genes (Kimura *et al.*, 2003; Peplow *et al.*, 2003b; Proctor *et al.*, 1995b; Tag *et al.*, 2001), and the *Tri12* transport pump gene (Alexander *et al.*, 1999). A two-gene mini cluster includes the *Tri1* cytochrome P450 monooxygenase gene (Meek *et al.*, 2003) and the *Tri16* acyltransferase gene (Peplow *et al.*, 2003a). Another two single-gene locus contains the *Tri101* trichothecene 3-*O*-acetyltransferase gene (Kimura *et al.*, 1998; McCormick *et al.*, 1999) and the *Tri15* regulatory gene (Alexander *et al.*, 2004).

The trichothecene diversity in *Fusarium* spp. occurs due to the differences in their *Tri* gene structure, although the arrangement of the core cluster genes is almost identical. Unlike *F. sporotrichioides*, *F. graminearum* contains a non-functional *Tri7* that gives it a trichothecene phenotype different from that of *F. sporotrichioides* (Brown *et al.*, 2001). Another *F. graminearum* strain, F15, does not contain *Tri7* and produces 3-acetyldeoxynivalenol by the action of only *Tri4*, *Tri5*, and *Tri11* gene products (Kimura *et al.*, 2003). However, the organisation and orientation of the homologues of *Tri4*, *Tri5* and *Tri6* in *Myrothecium roridum* differ significantly giving rise to more complex trichothecenes (Trapp *et al.*, 1998).

1.3.3.2 Gibberellins

Gibberellins (GAs) are a large family of structurally related diterpenoid acids produced by green plants, fungi and bacteria, some of which act as plant hormones. *Fusarium fujikuroi* (sexual stage *Gibberella fujikuroi* MP-C) is the largest commercial source of GAs, although other fungi such as *Sphaceloma manihoticola*, *Neurospora crassa* and *Phaeosphaeria* spp. also produce GAs.

The gibberellin biosynthesis genes have been cloned and characterised in *F. fujikuroi*. Seven genes required for GA biosynthesis are organised in a cluster and include a GA-specific GGPP synthase (*ggs2*) (Mende *et al.*, 1997; Tudzynski and Holter, 1998), a bi-functional *ent*-copalyl-*ent*-kaurene synthase

(*cps/ks*) (Tudzynski *et al.*, 1998), four cytochrome P450 monooxygenases (*P450-1* to *P450-4*) (Rojas *et al.*, 2001; Tudzynski *et al.*, 2001a; Tudzynski *et al.*, 2002; Tudzynski *et al.*, 2003) and a desaturase gene (*des*) (Tudzynski and Holter, 1998; Tudzynski *et al.*, 2003). *P450-3* is the only gene in the GA biosynthesis cluster that is not under the control of the major nitrogen regulator, AREA. This is consistent with the absence of the double GATA sequence elements, which bind the AREA transcriptional regulator, in its promoter. These elements are present in the promoters of the other six genes in the GA gene cluster. A *cpr* gene encoding a NADPH-cytochrome P450 reductase (functions as an electron donor to P450 monooxygenases) was identified outside the gibberellin gene cluster and was found to be essential for gibberellin biosynthesis (Malonek *et al.*, 2004). Gene function has been determined by gene disruption and by expression of individual genes in mutants lacking the GA biosynthesis gene cluster, where the function of the gene products could be determined in isolation. The GGPP synthase encoded by *ggs2* was specific for supplying GGPP for GA production and its deletion was not complemented by the presence of *ggs1* gene that was specific for the central isoprenoid pathway (Mende *et al.*, 1997; Tudzynski and Holter, 1998). A series of oxidation reactions, within the gibberellin pathway, are catalysed by the two cytochrome P450 monooxygenases, P450-1 and P450-4, showing the versatility of the P450 monooxygenases (Rojas *et al.*, 2001; Tudzynski *et al.*, 2001a).

1.3.3.3 Aphidicolin

Aphidicolin is a fungal diterpene that specifically inhibits DNA polymerase α. A gene cluster for aphidicolin biosynthesis was identified from the fungus *Phoma betae* (Oikawa *et al.*, 2001; Toyomasu *et al.*, 2004). This cluster contains the *PbGGS* GGPP synthase gene, the *ACS* aphidicolin-16β-ol synthase gene, the *Pb450-1* and *Pb450-2* cytochrome P450 monooxygenase genes, the *PbTP* ABC transporter gene and the *PbTF* transcription factor gene.

1.3.3.4 Indole-diterpenes

Indole-diterpenes are a large, structurally diverse group of secondary metabolites produced mainly by the *Penicillium*, *Aspergillus*, *Claviceps* and

Neotyphodium species of filamentous fungi (Parker and Scott, 2004; Scott *et al.*, 2004). Most of these metabolites are potent tremorgenic mammalian toxins (Steyn and Vleggaar, 1985) and some have anti-insect properties (Gloer, 1995). These metabolites share a common cyclic diterpene skeleton obtained from GGPP and an indole moiety derived from tryptophan or a tryptophan precursor (Byrne *et al.*, 2002; de Jesus *et al.*, 1983; Laws and Mantle, 1989). Biosynthetic schemes have been proposed on the basis of chemical identification of likely intermediates and precursor feeding studies from the organism of interest and related filamentous fungi (Gatenby *et al.*, 1999; Mantle and Weedon, 1994; Munday-Finch *et al.*, 1996). Until recently, none of the proposed steps had been validated by biochemical or genetic studies.

Indole-diterpenes can be broadly categorised into paxilline-like and other indole-diterpenes (Parker and Scott, 2004). Paxilline-like indole-diterpenes possess the basic ring structure of paxilline and includes the penitrems, janthitrems, lolitrems, aflatrem, paxilline, paspaline/ paspalinine/ paspalitrems, terpendoles, shearinines and sulphinines. Other indole-diterpenes do not possess the paxilline-like carbon skeleton and includes emindoles, nodulisporic acid, petromindole, nominine, aflavinines, radarins and thiersinines (Figure 1.4).

Much work has been done to demonstrate the origin of indole and diterpene parts of these metabolites from tryptophan and mevalonate, respectively (Acklin *et al.*, 1977; de Jesus *et al.*, 1983; Laws and Mantle, 1989). Recently, it was found that radiolabelled anthranilic acid and not tryptophan was incorporated into nodulisporic acid suggesting that the indole precursor for nodulisporic acid is indole-3-glycerol phosphate (Byrne *et al.*, 2002). Very little is known about the biosynthetic pathways of indole-diterpenes. However, the cloning and characterization of a cluster of genes from *Penicillium paxilli* necessary for biosynthesis of the indole-diterpene, paxilline, has helped to understand the genetics and biochemistry of this important class of secondary metabolites (Young *et al.*, 2001). Based on gene disruption and chemical complementation studies, a cluster of five genes including *paxG* (encoding a GGPP synthase), *paxM* (encoding a FAD-dependent monooxygenase), *paxC*

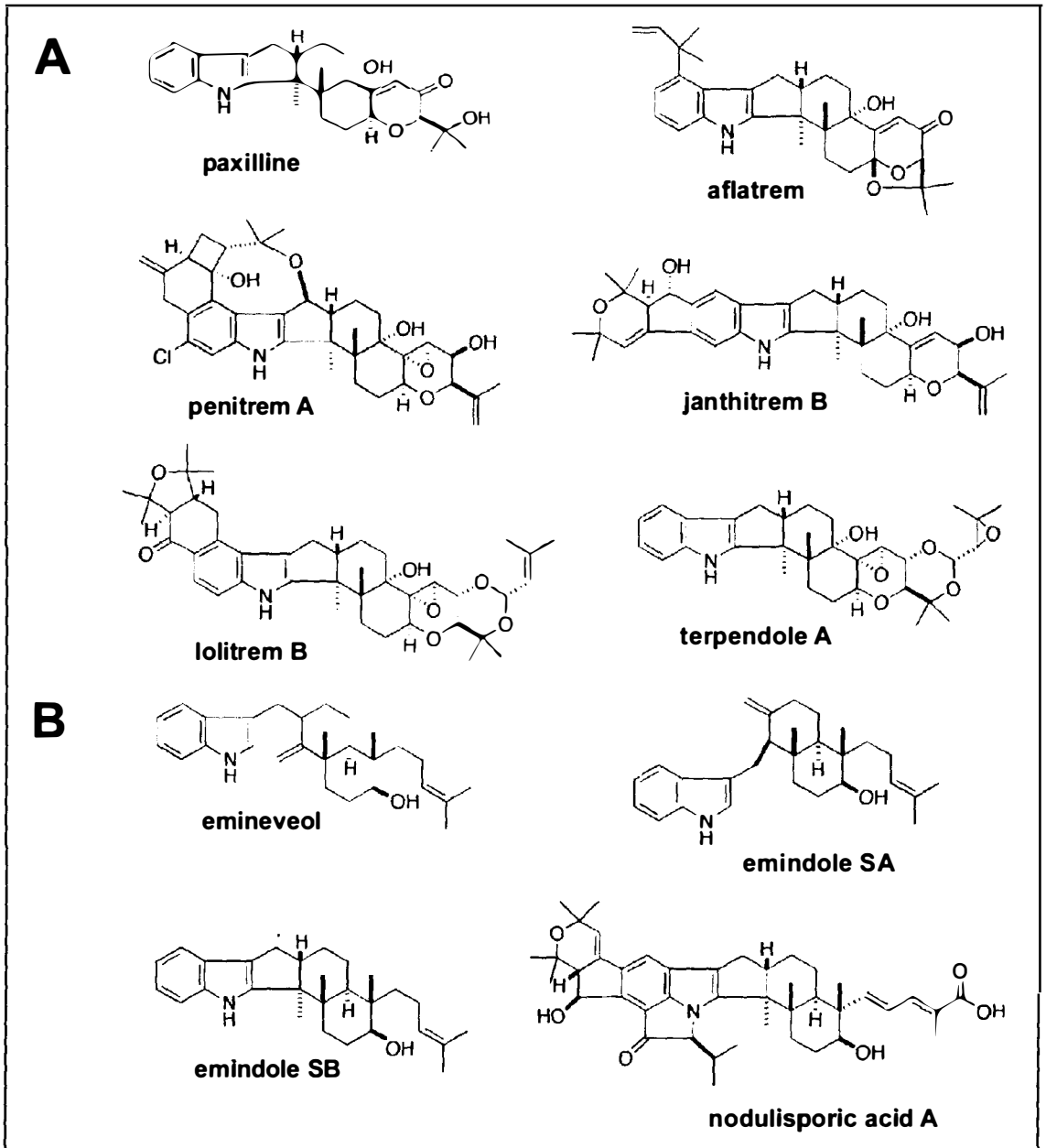

Figure 1.4 Indole-diterpenes

(A) Chemical structures of paxilline-like indole-diterpenes. **(B)** Chemical structures of other indole-diterpenes.

(encoding a prenyltransferase), *paxP* and *paxQ* (encoding two cytochrome P450 monooxygenases) has been shown to be essential for paxilline biosynthesis (McMillan *et al.*, 2003; Young *et al.*, 2001). Recently, two additional genes, *paxA* and *paxB* (encoding two putative membrane proteins), have been identified within the core cluster and were found to be essential for paxilline biosynthesis (Monahan and Scott, unpublished results). No stable indole-diterpenes have been identified in deletion mutants of *paxG* (Young *et al.*, 2001), *paxM* (McMillan and Scott, unpublished results) or *paxC* (Young *et al.*, unpublished results). However, *paxP* and *paxQ* deletion mutants accumulate paspaline and 13-desoxypaxilline, respectively (McMillan *et al.*, 2003). Unlike the gene clusters for aflatoxin and trichothecene biosynthesis, no pathway-specific regulatory gene has been identified for the paxilline biosynthesis gene cluster. Although the *paxR* and *paxS* genes, which encode putative transcription factors, have been found to be associated with the paxilline cluster, their deletion had no effect on paxilline biosynthesis (McMillan *et al.*, unpublished results).

Orthologues of *paxG*, *paxM* and *paxC* have been identified in *Aspergillus flavus* (*atmG*, *atmM* and *atmC*, respectively) (Zhang *et al.*, 2004) and *Neotyphodium lolii* (*ltmG*, *ltmM* and *ltmC*, respectively) (Young *et al.*, 2005; Young *et al.*, 2006) that produce the indole-diterpenes aflatrem and lolitrem B, respectively. Like *P. paxilli* and *F. fujikuroi*, *N. lolii* also has a second copy of GGPP synthase (*ggs1*, earlier known as *ggsA*) specific for primary metabolism. The presence of two copies of GGPP synthases, one specific for primary metabolism and the other specific for secondary metabolism could mean compartmentalisation of the two pathways. Moreover, the presence of two GGPP synthase genes could be a molecular signature for diterpene biosynthesis.

1.4 Evolution of secondary metabolite gene clusters

Several hypotheses have been proposed to explain the clustering of fungal secondary metabolite genes. Horizontal gene transfer has been frequently proposed as an explanation for clustering of fungal genes (Walton, 2000). It is the process by which genetic information of one organism is incorporated into the genome of another organism of the same or a different species, a process

well known in the evolution of prokaryotes (Lawrence, 2000). In fungi some pathways, for instance those for penicillin and cephalosporin biosynthesis, are proposed to have arisen from prokaryotes by horizontal gene transfer (Brakhage *et al.*, 2005; Buades and Moya, 1996). In *Cochliobolus heterostrophus*, the *Tox1* locus responsible for T-toxin production was proposed to be derived from a horizontal transfer event. The origin of genes regulating HC-toxin, AK-toxin, and T-toxin was also attributed to horizontal gene transfer events (Ahn *et al.*, 2002; Tanaka *et al.*, 1999; Yang *et al.*, 1996). Co-regulation of genes in a cluster offers another possible explanation for gene clustering. However, the dispensable metabolic pathway genes may also be dispersed as has been found for melanin biosynthesis (Kimura and Tsuge, 1993). Another hypothesis proposed for distribution of gene clusters is vertical transmission. In many fungal gene clusters, including trichothecenes, fumonisins, gibberellins and paxilline, there is no evidence for horizontal transfer events (Brown *et al.*, 2001; Proctor *et al.*, 2003; Tudzynski and Holter, 1998; Young *et al.*, 2001). These gene clusters may be ancestral in origin. The discontinuous distributions of polyketide synthase genes among fungal species are attributed to gene duplication and gene loss in different lineages (Kroken *et al.*, 2003). In *N. crassa*, a lack of duplicated genes, probably due to repeat-induced point mutations, suggests the importance of gene duplication rather than horizontal gene transfer in gene diversity (Galagan *et al.*, 2003). In yet another observation, adaptive evolution as a consequence of simultaneous genomic rearrangements was suggested in the formation of the *Saccharomyces cerevisiae DAL* cluster involved in allantoin catabolism (Wong and Wolfe, 2005). The genomic reorganisation of the *DAL* genes coincided with a biochemical reorganisation of the purine degradation pathway which in turn was driven by selection for ability to grow in oxygen limiting environments.

1.5 Regulation of fungal secondary metabolism

Secondary metabolite production usually starts at the stationary or resting phase of the micro-organism. In fungi, factors governing induction of secondary metabolism are often complex and not well understood. Regulation of fungal secondary metabolism may be achieved either by global fungal regulators

activated by environmental conditions (like nutrient availability, pH of growth media) or by pathway-specific fungal regulators.

1.5.1 Nitrogen source regulation

Fungi are capable of using a wide array of nitrogen-containing compounds. In the absence of primary nitrogen sources such as ammonia, glutamine and glutamate, fungi can utilise nitrate, nitrite, purines, amides, most amino acids and proteins as alternate sources. The global nitrogen regulatory genes that facilitate the expression of structural genes for the metabolism of alternate nitrogen sources are *areA* in *Aspergillus*, *nit2* in *Neurospora*, *gln-3* in *Saccharomyces* and *nre* in *Penicillium* (Marzluf, 1997). These positive-acting regulatory genes encode transcription factors of the GATA family that carry a DNA-binding domain comprising a single Cys2/Cys2 zinc finger followed by an adjacent basic region that recognizes the consensus GATA motif in promoter sequences of target genes (Scazzocchio, 2000). Nitrogen metabolite repression affects both primary and secondary metabolism. In *Aspergillus parasiticus*, transcription of the *aflR* and *aflJ* genes, involved in aflatoxin biosynthesis, is regulated by AreA binding to GATA sites in the *aflR/aflJ* intergenic region (Chang *et al.*, 2000). Although nitrate negatively regulates AflR expression, resulting in decreased aflatoxin production (Liu and Chu, 1998), under certain conditions nitrate activates aflatoxin production by enhancing the expression of *aflJ* in a strain-specific manner (Ehrlich and Cotty, 2002). In *F. fujikuroi*, *areA-Gf* (a homologue of *areA/nit2*) regulates gibberellin and bikaverin (a polyketide) production though with different mechanisms (Linnemannstons *et al.*, 2002; Mihlan *et al.*, 2003; Tudzynski *et al.*, 1999a). Mutants without this gene could not utilise alternate nitrogen sources or produce gibberellin, but could produce bikaverin. The *pks4* gene involved in bikaverin biosynthesis is overexpressed in Δ*areA* mutants (Linnemannstons *et al.*, 2002). In addition to *areA-Gf*, *glnA-Gf* (encoding glutamine synthetase) is also involved in nitrogen regulation of secondary metabolite pathways, and its deletion blocks the production of both gibberellin and bikaverin (Teichert *et al.*, 2004). The homologue of *areA/nit2* in *Penicillium chrysogenum*, *nre*, mediates

the nitrogen metabolite regulation of penicillin biosynthesis genes (Haas and Marzluf, 1995; Litzka *et al.*, 1999).

1.5.2 Carbon source regulation

Carbon sources affect the metabolism of micro-organisms by the mechanism of carbon catabolite repression. In the presence of preferred carbon sources, such as glucose, the expression of genes encoding enzymes for utilising alternative carbon sources is repressed. The global regulator CreA, which functions as a negatively acting transcriptional repressor, is the main regulator of carbon catabolite repression. This gene has been isolated from many fungal species including *Aspergillus nidulans* and *Aspergillus niger* (*creA*) (Dowzer and Kelly, 1991; Drysdale *et al.*, 1993), *Trichoderma reesei* and *Trichoderma harzianum* (*cre1*) (Ilmen *et al.*, 1996; Takashima *et al.*, 1996), *Metarhizium anisopliae* (*crr1*) (Screen *et al.*, 1997), *Sclerotinia sclerotiorum* (*cre1*) (Vautard *et al.*, 1999), *F. fujikuroi* (*creA-Gf*) and *Botrytis cinerea* (*creA-Bc*) (Tudzynski *et al.*, 2000) and *Cochliobolus carbonum* (*CREA*) (Tonukari *et al.*, 2003). The *creA* gene encodes a protein with two Cys2/His2-type zinc fingers that binds to the consensus sequence 5'-SYGGRG-3' in the promoters of the target genes (Panozzo *et al.*, 1998). The zinc finger regions of CreA are significantly similar (84% at the amino-acid level) to those of *S. cerevisiae* glucose repressor Mig1 (Gancedo, 1998), suggesting glucose repression through a similar manner in related fungi. Transcription factors other than CreA may be involved in carbon catabolite repression/derepression. In *F. fujikuroi* and *B. cinerea*, high transcript levels of *creA* on all carbon sources indicate that catabolite repression occurs at a post-transcriptional level (Tudzynski *et al.*, 2000). In *A. nidulans*, penicillin biosynthesis is repressed by glucose by a *creA*-independent mechanism, suggesting the role of another carbon regulatory protein (Martin *et al.*, 1999). A role for additional transcriptional factors was also implied in *T. reesei* where catabolite repression was mediated through post-translational modification of Cre1 (Ilmen *et al.*, 1996). It was also shown that the phosphorylation of Cre1 was essential for binding to its target sequence (Cziferszky *et al.*, 2002).

1.5.3 pH regulation

Regulation of gene expression by ambient pH is found in both prokaryotes and eukaryotes. This regulatory system ensures micro-organisms can grow over a wide pH range. pH regulation is mediated by the global transcriptional regulator PacC (Tilburn *et al.*, 1995), which has three Cys2/His2 zinc fingers. PacC activates alkaline-expressed genes and represses acid-expressed genes and has been identified in many fungi including *A. nidulans*, *A. niger*, *P. chrysogenum*, *S. cerevisiae*, *Candida albicans*, *Yarrowia lipolytica* (Penalva and Arst, 2002). The aflatoxin and sterigmatocystin biosynthesis genes in *A. parasiticus* and *A. nidulans*, respectively, which contain PacC binding sites, are under negative regulation by PacC (Keller *et al.*, 1997). The *pks4* polyketide synthase gene in *F. fujikuroi* is also negatively regulated by PacC (Linnemannstons *et al.*, 2002). However, the penicillin biosynthesis gene clusters in *P. chrysogenum* and *A. nidulans* are under positive PacC regulation (Suarez and Penalva, 1996; Then Bergh and Brakhage, 1998). In *A. nidulans*, PacC also positively regulates the *sidA* gene involved in the biosynthesis of the siderophore, triacetylfusarinine C (Eisendle *et al.*, 2004). In *Fusarium verticillioides*, a PacC homologue (PAC1) represses fumonisin biosynthesis under alkaline conditions suggesting PAC1 is a negative regulator of fumonisin biosynthesis (Flaherty *et al.*, 2003).

1.5.4 LaeA regulation

LaeA is a nuclear-localised protein methyltransferase identified in *A. nidulans* that positively regulates expression of genes in the clusters including sterigmatocystin, penicillin and lovastatin gene clusters (Bok and Keller, 2004; Bok *et al.*, 2006). It was also shown to be a positive regulator of virulence factors in *Aspergillus fumigatus* by affecting the gliotoxin biosynthesis gene cluster (Bok *et al.*, 2005). This regulation of multiple gene clusters by LaeA was attributed to its possible involvement in chromatin remodelling. Although LaeA has been shown as a global regulator of secondary metabolism in *Aspergillus* species, whether the same occurs in other fungi remains to be shown.

1.5.5 Pathway-specific regulators

The secondary metabolite biosynthesis gene clusters often contain regulatory genes that encode transcriptional regulators of the other genes in the cluster (Keller and Hohn, 1997). In *Aspergillus* spp., aflatoxin and sterigmatocystin biosynthesis genes are co-regulated by the pathway-specific regulator gene *aflR*, which encodes a Cys6/Zn2-type DNA-binding protein (Ehrlich *et al.*, 1999). AflR regulates expression of aflatoxin-sterigmatocystin biosynthesis genes by binding to the consensus sequence 5'-TCGN_5CGA-3' found in the promoters of most of the biosynthetic genes (Bhatnagar *et al.*, 2003; Ehrlich *et al.*, 1999). The *aflJ* gene may also have a pathway-specific regulatory role in aflatoxin-sterigmatocystin gene cluster (Meyers *et al.*, 1998). In *Fusarium* spp., the *Tri6*, *Tri10* and *Tri15* genes regulate the expression of trichothecene pathway genes (Alexander *et al.*, 2004; Hohn *et al.*, 1999; Tag *et al.*, 2001). *Tri6* encodes a Cys2/His2 zinc finger DNA-binding protein that binds to the consensus sequence YNAGGCC found in the upstream region of all *Tri* biosynthetic genes except *Tri10*. *Tri10* acts upstream of *Tri6* and positively regulates *Tri6* expression, and together they regulate the expression of all *Tri* genes within and outside the core *Tri* cluster, and also regulate additional isoprenoid biosynthetic genes (Peplow *et al.*, 2003b). Unlike *Tri6* and *Tri10*, *Tri15*, which encodes a Cys2/His2 zinc finger protein, acts as a negative regulator of some of the trichothecene biosynthesis genes (Alexander *et al.*, 2004). In *F. verticillioides*, *ZFR1* (encoding a Cys6/Zn2-type DNA-binding protein) acts as a positive regulator of fumonisin biosynthesis genes (Flaherty and Woloshuk, 2004). Whether *ZFR1* only regulates the fumonisin pathway remains to be shown, as it is located outside the fumonisin gene cluster. In *C. carbonum*, expression of three HC-toxin biosynthesis genes is regulated by *TOXE*, which encodes TOXEp that contains the bZIP basic DNA-binding and the ankyrin domains (Ahn and Walton, 1998; Pedley and Walton, 2001). Recently, a Cys2/Zn6-type DNA-binding protein GIP2 was shown to positively regulate the biosynthesis of the pigment aurofusarin in *Gibberella zeae* (Kim *et al.*, 2006).

1.6 Localisation of proteins involved in fungal secondary metabolism

Although many gene clusters involved in fungal secondary metabolism have been isolated and the enzymes characterised, very few studies have been conducted on the subcellular localisation of these enzymes. Given the toxic nature of some of the fungal secondary metabolites, it is tempting to assume the enzymes of such pathways are compartmentalised to protect the host organism from the deleterious effects of the toxin accumulating in the fungal cell.

In *P. chrysogenum*, the penicillin biosynthesis enzymes, ACV-synthetase, IPN-synthetase and acyltransferase, are differentially localised in the fungal mycelium (Lendenfeld *et al.*, 1993; Muller *et al.*, 1991; Muller *et al.*, 1992). A combination of cell-fractionation, electron microscopy and labelling studies shows that ACV-synthetase is a vacuolar protein, IPN-synthetase is a cytosolic protein and acyltransferase is a peroxisomal protein. The C-terminal end of the acyltransferase contains a peroxisomal targeting signal type 1 (PTS1)-like tripeptide ARL. A truncated acyltransferase without the ARL sequence is not targeted to microbodies (peroxisomes), and transformants expressing the truncated protein do not produce penicillin (Muller *et al.*, 1992). An aryl-capping enzyme, PhI, which supplies an activated substrate to the acyltransferase, also contains a C-terminal consensus peroxisomal targeting sequence (SKI), indicating the presence of a functional complex for penicillin biosynthesis in peroxisomes (Lamas-Maceiras *et al.*, 2006). In *Acremonium chrysogenum*, *egfp* fusion studies show that the transcription factor CPCR1 that regulates cephalosporin C biosynthesis is a nuclear protein (Hoff *et al.*, 2005). A DNA-binding domain in CPCR1 is essential both for its localisation and function.

The occurrence of the final step of the penicillin biosynthesis pathway in peroxisomes suggests a role for this organelle in secondary metabolism. In *A. nidulans*, the first stable intermediate of aflatoxin and sterigmatocystin biosynthesis, norsolorinic acid, accumulates in peroxisomes (Maggio-Hall *et al.*, 2005). However, in *A. parasiticus*, Nor-1 and Ver-1, representing enzymes required for early and middle enzymatic steps in the aflatoxin biosynthesis pathway, are localised in the cytoplasm (Lee *et al.*, 2004). Another enzyme

required for catalysing a middle enzymatic step in the aflatoxin biosynthesis pathway, VBS, is also localised in the cytoplasm and in endoplasmic reticulum-like structures (Chiou *et al.*, 2004). The OmtA enzyme, representing an enzyme for a late step in this same pathway, is localised in the cytoplasm and in the vacuole, the locations depending on the age and/or physiological condition of the fungal cells.

Two distinct GGPP synthase genes have been found in *P. paxilli*, *F. fujikuroi* and *N. lolii*, one specific for secondary metabolism and the other for primary metabolism (Tudzynski and Holter, 1998; Young *et al.*, 2001; Young *et al.*, 2005). The authors have suggested differential localisation of the two metabolic pathways. Although knowledge of subcellular compartmentalisation of GGPP synthases in filamentous fungi is lacking, such studies have been done for plant GGPP synthases. GGPP synthases in two diterpene producing plants, *Scoparia dulcis* and *Croton sublyratus*, contain putative chloroplast targeting sequences. A fusion protein containing the putative transit peptide of the *S. dulcis* GGPP synthase fused to sGFP localises in the chloroplast after its introduction into *Arabidopsis* leaves (Sitthithaworn *et al.*, 2001). In *Arabidopsis*, five homologues of GGPP synthase (GGPS1, GGPS2, GGPS3, GGPS4, GGPS6) are localised into different subcellular compartments (Okada *et al.*, 2000). All of these GGPP synthases have putative localisation signals for subcellular targeting in their N-terminal regions. Reporter fusion studies using sGFP show that GGPS1 and GGPS3 are localised in the chloroplast, GGPS2 and GGPS4 are localised in the endoplasmic reticulum, and GGPS6 is localised in the mitochondrion (Okada *et al.*, 2000).

1.7 Significance of studying paxilline biosynthesis in *Penicillium paxilli*

Indole-diterpenes possess various bioactivities including insecticidal and tremorgenic activities. Although the biosynthesis of these metabolites by grass endophytes (filamentous fungi forming symbiotic associations with temperate grasses) has ecological benefits, it also has detrimental effects on grazing livestock (Fletcher and Harvey, 1981; Scott, 2001). Thus there is considerable interest in maximising the benefits of endophytes to pastoral agriculture by selecting fungal strains that retain the beneficial effects and not the detrimental

effects in a symbiotic association. In this context, it is important to understand the biosynthesis of these metabolites by the fungus. In contrast to grass endophytes like *Neotyphodium* that produces the animal neurotoxin, lolitrem B, grows slowly and not particularly amenable to genetic analysis, *P. paxilli* serves as a model organism to study the biosynthesis of the closely related indole-diterpene, paxilline.

1.8 Aims and objectives

The aim of this research was to carry out a biochemical analysis of the paxilline biosynthesis gene products in *P. paxilli* and also to understand the biological significance of the presence of two GGPP synthase genes, *ggs1* and *paxG* in *P. paxilli*. In order to achieve these aims the following objectives were proposed:

1. To define the minimum number of genes required for the biosynthesis of the first stable indole-diterpene, paspaline.
2. To identify the substrates and products for PaxP and PaxQ.
3. To test the involvement of proposed paxilline intermediates.
4. To test if the two GGPP synthases, Ggs1 and PaxG, are differentially compartmentalised in the cell.

In the first objective, different combinations of *paxG*, *paxA*, *paxM*, *paxB* and *paxC* genes were cloned into a paxilline-negative deletion derivative of *P. paxilli* and the resulting strains analysed for indole-diterpenes. In objectives two and three, precursor feeding experiments were carried out using *P. paxilli* strains containing *paxP* or *paxQ* only. To achieve the final objective, cellular targeting of Ggs1 and PaxG fusions with EGFP and DsRed in *P. paxilli* was analysed using fluorescence microscopy.

CHAPTER TWO

MATERIALS AND METHODS

2.1 Biological materials

The plasmids, lambda clones, fungal strains and bacterial strains reported in this study are listed in Table 2.1.

2.2 Media

All the media were prepared in Milli-Q® water and sterilised at 121°C and 15 psi for 15 min.

2.2.1 Bacterial media

2.2.1.1 Luria-Bertani (LB) medium

LB medium (Miller, 1972) contained 1% (w/v) tryptone (Merck, Darmstadt, Germany), 0.5% (w/v) NaCl and 0.5% (w/v) yeast extract (Merck, Darmstadt, Germany). The pH of the medium was adjusted to 7.0 before sterilising. LB agar was prepared by adding agar to a final concentration of 1.5% (w/v).

2.2.1.2 SOB medium

SOB medium contained 2% (w/v) tryptone (Merck, Darmstadt, Germany), 0.5% (w/v) yeast extract (Merck, Darmstadt, Germany), 10 mM NaCl, 2.5 mM KCl, 10 mM $MgCl_2$. The pH of the medium, without $MgCl_2$, was adjusted to 7.0 before sterilising and sterile $MgCl_2$ was added just before use.

2.2.1.3 SOC medium

SOC medium (Dower *et al.*, 1988) contained 2% (w/v) tryptone (Merck, Darmstadt, Germany), 0.5% (w/v) yeast extract (Merck, Darmstadt, Germany), 20 mM glucose, 10 mM NaCl, 2.5 mM KCl, 10 mM $MgCl_2$ and 10 mM $MgSO_4.7H_2O$.

2.2.2 Fungal media

2.2.2.1 *Aspergillus* Complete medium (ACM)

ACM contained 2% (w/v) malt extract (Oxoid, Basingstoke, England), 1% (w/v) mycological peptone (Oxoid, Basingstoke, England), 2% (w/v) glucose, 1.5% (w/v) agar.

Table 2.1 Biological materials

Biological Material	Strain/Identifier	Relevant Characteristics	Reference
Plasmids			
pBluescript II KS (+)		Amp^R	Stratagene
pGEM®-T Easy		Amp^R	Promega
	pII99	Amp^R/Gen^R (P*trpC-nptII*-T*trpC*)	Namiki *et al.*, 2001
pPN94		Amp^R/Hyg^R (P*trpC-hph*); P*TEF* T*trpC*	Tanaka, unpublished
pPN97		pPN94 containing *egfp* cDNA on a 0.7 kb *Xba*I/*Not*I fragment; Amp^R/Hyg^R	Tanaka, unpublished
	pSF16.17.cgi	Amp^R/Gen^R (P*trpC-nptII*-T*trpC*)	Foster, unpublished
	pSS1	pII99 containing *paxP* on a 2.7 kb *Eco*RI fragment; Amp^R/Gen^R	This study
	pSS2	pII99 containing *paxQ* on a 3.0 kb *Hin*dIII fragment; Amp^R/Gen^R	This study
	pSS7	pBlueScript II KS+ containing *paxP* on a 3.9 kb *Eco*RI/*Sma*I fragment; Amp^R	This study
	pSS8	pII99 containing *paxG-paxA-paxM-paxB-paxC* on a 11.0 kb *Hin*dIII fragment; Amp^R/Gen^R	This study
	pSS9	pSS8 Δ*paxA-paxM-paxB* on a 5.0 kb *Spe*I fragment; Amp^R/Gen^R	This study
	pSS16	pSS9 containing *paxM* on a 2.3 kb *Spe*I fragment; Amp^R/Gen^R	This study
	pSS17	pSS9 containing *paxM-paxB* on a 3.4 kb *Spe*I fragment; Amp^R/Gen^R	This study
	pSS20	pSS9 containing *paxA-paxM* on a 3.9 kb *Spe*I fragment; Amp^R/Gen^R	This study
	pSS27	pPN94 containing *paxG*::*egfp* cDNA; Amp^R/Hyg^R	This study
	pSS28	pPN94 containing *egfp*::*paxG* cDNA; Amp^R/Hyg^R	This study
	pSS29	pPN94 containing *ggs1*::*egfp* cDNA; Amp^R/Hyg^R	This study
	pSS30	pPN94 containing *egfp*::*ggs1* cDNA; Amp^R/Hyg^R	This study
	pSS37	pSF16.17.cgi containing P*TEF*-MCS-T*trpC* on a 1.4 kb *Sal*I/*Bgl*II fragment; Amp^R/Gen^R	This study
	pSS41	pSS37 containing *dsred*::*SKL* cDNA; Amp^R/Gen^R	This study
	pSS45	pSS37 containing *dsred* cDNA; Amp^R/Gen^R	This study
	pSS46	pPN94 containing *egfp*::*GRV* cDNA; Amp^R/Hyg^R	This study
Lambda clones			
	λCY55	λGEM-11 clone from *P. paxilli* containing *paxG-paxA-paxM-paxB-paxC*	Young, unpublished
	λCY56	λGEM-11 clone from *P. paxilli* containing *paxC-paxP-paxQ-paxD-paxO*	Young *et al.*, 2001

Biological Material	Strain/Identifier	Relevant Characteristics	Reference
***Penicillium paxilli* strains**			
PN2013		Wild-type; paxilline positive	Itoh *et al.*, 1994
PN2255	LMG23	PN2013/Δ*paxG-paxA*; Hyg^R; paxilline negative	Young *et al.*, 2001
PN2588	LMG23.V	PN2255/pII99; Hyg^R Gen^R; paxilline negative	This study
	LMG23.P8-1	PN2255/pSS8; Hyg^R Gen^R; paxilline positive	This study
PN2498	LMG23.P8-2	PN2255/pSS8; Hyg^R Gen^R; paxilline positive	This study
PN2499	LMG23.P8-3	PN2255/pSS8; Hyg^R GenR; paxilline positive	This study
	LMG23.P8-4	PN2255/pSS8; Hyg^R Gen^R; paxilline positive	This study
PN2290	ABC83	PN2013/Δ*paxC*; Hyg^R; paxilline negative	Bryant, unpublished
PN2500	ABC83.V	PN2290/pII99; Hyg^R Gen^R; paxilline negative	This study
PN2501	ABC83.P8-1	PN2290/pSS8; Hyg^R Gen^R; paxilline positive	This study
PN2502	ABC83.P8-2	PN2290/pSS8; Hyg^R Gen^R; paxilline positive	This study
	ABC83.P8-3	PN2290/pSS8; Hyg^R Gen^R; paxilline negative	This study
	ABC83.P8-4	PN2290/pSS8; Hyg^R Gen^R; paxilline negative	This study
PN2253	LM662	PN2013/Δ*paxT-paxD*; Hyg^R; paxilline negative	Young *et al.*, 2001
PN2503	LM662.V.1	PN2253/pII99; Hyg^R Gen^R; paxilline negative	This study
PN2504	LM662.P8-3	PN2253/pSS8; Hyg^R Gen^R; paxilline negative, paspaline positive	This study
	LM662.P8-4	PN2253/pSS8; Hyg^R Gen^R; paxilline negative, paspaline positive	This study
	LM662.P8-6	PN2253/pSS8; Hyg^R Gen^R; paxilline negative, paspaline positive	This study
PN2505	LM662.P8-9	PN2253/pSS8; Hyg^R Gen^R; paxilline negative, paspaline positive	This study
	LM662.P8-10	PN2253/pSS8; Hyg^R Gen^R; paxilline negative, paspaline positive	This study
	LM662.P8-11	PN2253/pSS8; Hyg^R Gen^R; paxilline negative, paspaline positive	This study
PN2506	LM662.P8-12	PN2253/pSS8; Hyg^R Gen^R; paxilline negative, paspaline positive	This study
PN2250	CY2	PN2013/Δ *pax* cluster and flanking sequences; Hyg^R; paxilline negative	Young *et al.*, 1998
PN2507	CY2.V.1	PN2250/pII99; Hyg^R Gen^R; paxilline negative	This study
	CY2.P8-1	PN2250/pSS8; Hyg^R Gen^R; paxilline negative, paspaline negative	This study
	CY2.P8-2	PN2250/pSS8; Hyg^R Gen^R; paxilline negative, paspaline positive	This study

Biological Material	Strain/Identifier	Relevant Characteristics	Reference
PN2508	CY2.P8-4	PN2250/pSS8; Hyg^R Gen^R; paxilline negative, paspaline positive	This study
	CY2.P8-5	PN2250/pSS8; Hyg^R Gen^R; paxilline negative, paspaline positive	This study
PN2509	CY2.P8-6	PN2250/pSS8; Hyg^R Gen^R; paxilline negative, paspaline positive	This study
PN2510	CY2.P8-8	PN2250/pSS8; Hyg^R Gen^R; paxilline negative, paspaline positive	This study
PN2511	CY2.P8-9	PN2250/pSS8; Hyg^R Gen^R; paxilline negative, paspaline positive	This study
PN2512	CY2.V.2	PN2250/pII99; Hyg^R Gen^R; paxilline negative	This study
PN2513	CY2.P16-1	PN2250/pSS16; Hyg^R Gen^R; paxilline negative, paspaline negative	This study
	CY2.P16-2	PN2250/pSS16; Hyg^R Gen^R; paxilline negative, paspaline negative	This study
	CY2.P16-3	PN2250/pSS16; Hyg^R Gen^R; paxilline negative, paspaline negative	This study
	CY2.P16-4	PN2250/pSS16; Hyg^R Gen^R; paxilline negative, paspaline negative	This study
	CY2.P16-5	PN2250/pSS16; Hyg^R Gen^R; paxilline negative, paspaline negative	This study
	CY2.P16-6	PN2250/pSS16; Hyg^R Gen^R; paxilline negative, paspaline negative	This study
	CY2.P16-7	PN2250/pSS16; Hyg^R Gen^R; paxilline negative, paspaline negative	This study
	CY2.P16-8	PN2250/pSS16; Hyg^R Gen^R; paxilline negative, paspaline negative	This study
	CY2.P16-9	PN2250/pSS16; Hyg^R Gen^R; paxilline negative, paspaline negative	This study
PN2514	CY2.V.3	PN2250/pII99; Hyg^R Gen^R; paxilline negative	This study
PN2515	CY2.P20-1	PN2250/pSS20; Hyg^R Gen^R; paxilline negative, paspaline negative	This study
	CY2.P20-2	PN2250/pSS20; Hyg^R Gen^R; paxilline negative, paspaline negative	This study
	CY2.P20-3	PN2250/pSS20; Hyg^R Gen^R; paxilline negative, paspaline negative	This study
	CY2.P20-4	PN2250/pSS20; Hyg^R Gen^R; paxilline negative, paspaline negative	This study
	CY2.P20-6	PN2250/pSS20; Hyg^R Gen^R; paxilline negative, paspaline negative	This study
	CY2.P20-8	PN2250/pSS20; Hyg^R Gen^R; paxilline negative, paspaline negative	This study
PN2516	CY2.V.4	PN2250/pII99; Hyg^R Gen^R; paxilline negative	This study
PN2517	CY2.P17-1	PN2250/pSS17; Hyg^R Gen^R; paxilline negative, paspaline positive	This study
	CY2.P17-2	PN2250/pSS17; Hyg^R Gen^R; paxilline negative, paspaline negative	This study
PN2518	CY2.P17-3	PN2250/pSS17; Hyg^R Gen^R; paxilline negative, paspaline positive	This study
PN2519	CY2.P17-4	PN2250/pSS17; Hyg^R Gen^R; paxilline negative, paspaline positive	This study
	CY2.P17-5	PN2250/pSS17; Hyg^R Gen^R; paxilline negative, paspaline negative	This study
	CY2.P17-6	PN2250/pSS17; Hyg^R Gen^R; paxilline negative, paspaline negative	This study
	CY2.P17-7	PN2250/pSS17; Hyg^R Gen^R; paxilline negative, paspaline negative	This study
	CY2.P17-8	PN2250/pSS17; Hyg^R Gen^R; paxilline negative, paspaline negative	This study

Biological Material	Strain/Identifier	Relevant Characteristics	Reference
	CY2.P17-9	PN2250/pSS17; Hyg^R Gen^R; paxilline negative, paspaline negative	This study
PN2520	CY2.P17-10	PN2250/pSS17; Hyg^R Gen^R; paxilline negative, paspaline positive	This study
PN2258	LMP1	PN2013/Δ*paxP*; Hyg^R; paxilline negative	McMillan *et al.*, 2003
PN2521	LMP1.V.1	PN2258/pII99; Hyg^R Gen^R; paxilline negative	This study
	LMP1.P1-1	PN2258/pSS1; Hyg^R Gen^R; paxilline negative	This study
PN2522	LMP1.P1-2	PN2258/pSS1; Hyg^R Gen^R; paxilline positive	This study
	LMP1.P1-3	PN2258/pSS1; Hyg^R Gen^R; paxilline negative	This study
PN2523	LMP1.P1-4	PN2258/pSS1; Hyg^R Gen^R; paxilline positive	This study
	LMP1.P1-5	PN2258/pSS1; Hyg^R Gen^R; paxilline positive	This study
	LMP1.P1-6	PN2258/pSS1; Hyg^R Gen^R; paxilline negative	This study
	LMP1.P1-7	PN2258/pSS1; Hyg^R Gen^R; paxilline positive	This study
PN2524	LMP1.P1-8	PN2258/pSS1; Hyg^R Gen^R; paxilline positive	This study
	LMP1.P1-9	PN2258/pSS1; Hyg^R Gen^R; paxilline positive	This study
PN2525	LMP1.P1-10	PN2258/pSS1; Hyg^R Gen^R; paxilline positive	This study
PN2259	LMQ226	PN2013/Δ*paxQ*; Hyg^R; paxilline negative	McMillan *et al.*, 2003
PN2526	LMQ226.V	PN2259/pII99; Hyg^R Gen^R; paxilline negative	This study
	LMQ226.P2-1	PN2259/pSS2; Hyg^R Gen^R; paxilline positive	This study
	LMQ226.P2-2	PN2259/pSS2; Hyg^R Gen^R; paxilline positive	This study
	LMQ226.P2-3	PN2259/pSS2; Hyg^R Gen^R; paxilline positive	This study
PN2527	LMQ226.P2-4	PN2259/pSS2; Hyg^R Gen^R; paxilline positive	This study
PN2528	LMQ226.P2-5	PN2259/pSS2; Hyg^R Gen^R; paxilline positive	This study
	LMQ226.P2-6	PN2259/pSS2; Hyg^R Gen^R; paxilline positive	This study
	LMQ226.P2-7	PN2259/pSS2; Hyg^R Gen^R; paxilline positive	This study
PN2529	LMQ226.P2-8	PN2259/pSS2; Hyg^R Gen^R; paxilline positive	This study
PN2530	LMQ226.P2-9	PN2259/pSS2; Hyg^R Gen^R; paxilline positive	This study
	LMQ226.P2-10	PN2259/pSS2; Hyg^R Gen^R; paxilline positive	This study
PN2531	LMP1.V.2	PN2258/pII99; Hyg^R Gen^R; paxilline negative	This study
	LMP1.V/P7-2	PN2258/pII99/pSS7; Hyg^R Gen^R; paxilline positive	This study
PN2532	LMP1.V/P7-7	PN2258/pII99/pSS7; Hyg^R Gen^R; paxilline positive	This study
	LMP1.V/P7-8	PN2258/pII99/pSS7; Hyg^R Gen^R; paxilline negative	This study
PN2533	LMP1.V/P7-13	PN2258/pII99/pSS7; Hyg^R Gen^R; paxilline positive	This study

Biological Material	Strain/Identifier	Relevant Characteristics	Reference
PN2534	LMP1.V/P7-23	PN2258/pII99/pSS7; Hyg^R Gen^R; paxilline positive	This study
PN2535	LMP1.V/P7-26	PN2258/pII99/pSS7; Hyg^R Gen^R; paxilline positive	This study
PN2536	LM662.V.2	PN2253/pII99; Hyg^R Gen^R; paxilline negative	This study
PN2537	LM662.P1-2	PN2253/pSS1; Hyg^R Gen^R; paxilline negative	This study
PN2538	LM662.P1-10	PN2253/pSS1; Hyg^R Gen^R; paxilline negative	This study
PN2539	CY2.V.5	PN2250/pII99; Hyg^R Gen^R; paxilline negative	This study
PN2540	CY2.P1-9	PN2250/pSS1; Hyg^R Gen^R; paxilline negative	This study
PN2541	CY2.P1-10	PN2250/pSS1; Hyg^R Gen^R; paxilline negative	This study
PN2542	LM662.V.3	PN2253/pII99; Hyg^R Gen^R; paxilline negative	This study
PN2543	LM662.P2-9	PN2253/pSS2; Hyg^R Gen^R; paxilline negative	This study
PN2544	LM662.P2-14	PN2253/pSS2; Hyg^R Gen^R; paxilline negative	This study
PN2545	CY2.V.6	PN2250/pII99; Hyg^R Gen^R; paxilline negative	This study
PN2546	CY2.P2-7	PN2250/pSS2; Hyg^R Gen^R; paxilline negative	This study
PN2547	CY2.P2-10	PN2250/pSS2; Hyg^R Gen^R; paxilline negative	This study
PN2548	WT.pPN97-10	PN2013/pPN97; P*TEF-egfp*; Hyg^R	This study
PN2549	WT.P30-5	PN2013/pSS30; P*TEF-egfp*::*ggs1*; Hyg^R	This study
PN2550	WT.P30-6	PN2013/pSS30; P*TEF-egfp*::*ggs1*; Hyg^R	This study
PN2551	WT.P30-7	PN2013/pSS30; P*TEF-egfp*::*ggs1*; Hyg^R	This study
PN2552	WT.P30-8	PN2013/pSS30; P*TEF-egfp*::*ggs1*; Hyg^R	This study
PN2553	WT.P29-7	PN2013/pSS29; P*TEF-ggs1*::*egfp*; Hyg^R	This study
PN2554	WT.P29-9	PN2013/pSS29; P*TEF-ggs1*::*egfp*; Hyg^R	This study
PN2555	WT.P29-12	PN2013/pSS29; P*TEF-ggs1*::*egfp*; Hyg^R	This study
PN2556	WT.P29-16	PN2013/pSS29; P*TEF-ggs1*::*egfp*; Hyg^R	This study
PN2557	WT.P27-2	PN2013/pSS27; P*TEF-paxG*::*egfp*; Hyg^R	This study
PN2558	WT.P27-4	PN2013/pSS27; P*TEF-paxG*::*egfp*; Hyg^R	This study
PN2559	WT.P27-13	PN2013/pSS27; P*TEF-paxG*::*egfp*; Hyg^R	This study
PN2560	WT.P27-14	PN2013/pSS27; P*TEF-paxG*::*egfp*; Hyg^R	This study
PN2561	WT.P46-1	PN2013/pSS46; P*TEF-egfp*::*GRV*; Hyg^R	This study
PN2562	WT.P46-5	PN2013/pSS46; P*TEF-egfp*::*GRV*; Hyg^R	This study
PN2563	WT.P46-8	PN2013/pSS46; P*TEF-egfp*::*GRV*; Hyg^R	This study
PN2564	WT.P46-10	PN2013/pSS46; P*TEF-egfp*::*GRV*; Hyg^R	This study
PN2565	WT.P45-1	PN2013/pSS45; P*TEF-dsred*; Gen^R	This study

Biological Material	Strain/Identifier	Relevant Characteristics	Reference
PN2566	WT.P41-1	PN2013/pSS41; P*TEF-dsred*::*SKL*; Gen^R	This study
PN2567	WT.P41-2	PN2013/pSS41; P*TEF-dsred*::*SKL*; Gen^R	This study
PN2568	WT.P41-9	PN2013/pSS41; P*TEF-dsred*::*SKL*; Gen^R	This study
PN2569	WT.P41-10	PN2013/pSS41; P*TEF-dsred*::*SKL*; Gen^R	This study
PN2570	WT.P41.1/P46-4	PN2566/pSS46; P*TEF-dsred*::*SKL* P*TEF-egfp*::*GRV*; Gen^R Hyg^R	This study
PN2571	WT.P41.1/P46-7	PN2566/pSS46; P*TEF-dsred*::*SKL* P*TEF-egfp*::*GRV*; Gen^R Hyg^R	This study
PN2572	WT.P41.1/P46-9	PN2566/pSS46; P*TEF-dsred*::*SKL* P*TEF-egfp*::*GRV*; Gen^R Hyg^R	This study
PN2573	WT.P41.1/P46-11	PN2566/pSS46; P*TEF-dsred*::*SKL* P*TEF-egfp*::*GRV*; Gen^R Hyg^R	This study
PN2574	WT.P29.12/P41-2	PN2555/pSS41; P*TEF-ggs1*::*egfp* P*TEF-dsred*::*SKL*; Hyg^R Gen^R	This study
PN2575	WT.P29.12/P41-1(2)	PN2555/pSS41; P*TEF-ggs1*::*egfp* P*TEF-dsred*::*SKL*; Hyg^R Gen^R	This study
Bacterial strains			
DH5α		*supE*44 Δ*lac*U169 (ϕ80 *lacZ* ΔM15) *hsdR*17 *recA*1 *endA*1 *gyrA*96 *thi*-1 *relA*1	Hanahan, 1983
XL 1-Blue		*supE*44 *hsdR*17 *recA*1 *endA*1 *gyrA*46 *thi relA*1 *lac*$^-$ F' [*proAB*$^+$ *lacI*^{q} *lacZ* ΔM15 Tn*10* (*Tet*^{R})]	Bullock *et al.*, 1987
PN1994		XL 1-Blue/pSS1	This study
PN1995		XL 1-Blue/pSS2	This study
PN1996		DH5α/pSS7	This study
PN1997		DH5α/pSS8	This study
PN1998		DH5α/pSS9	This study
PN1999		DH5α/pSS16	This study
PN4000		DH5α/pSS17	This study
PN4002		DH5α/pSS20	This study
PN4003		DH5α/pSS27	This study
PN4004		DH5α/pSS28	This study
PN4005		DH5α/pSS29	This study
PN4006		DH5α/pSS30	This study
PN4007		DH5α/pSS37	This study
PN4008		DH5α/pSS41	This study
PN4009		DH5α/pSS45	This study
PN4010		DH5α/pSS46	This study

PN numbers are assigned to the materials selected for laboratory culture stock.

2.2.2.2 Czapex-Dox Yeast Extract (CDYE) medium

CDYE medium contained 3.34% (w/v) Czapex-Dox (Oxoid, Basingstoke, England) and 0.5% (w/v) yeast extract (Merck, Darmstadt, Germany). CDYE medium was supplemented with 0.5% (v/v) trace elements mix (Section 2.2.2.5).

2.2.2.3 Potato Dextrose (PD) medium

PD medium contained 2.4% (w/v) PD broth (Difco™, Sparks, MD, USA). The pH of the medium was adjusted to 6.5 before sterilising. PD agar (PDA) was prepared by adding agar to a final concentration of 1.5% (w/v). Where necessary, PDA was supplemented with 5 mM oleic acid (Sigma) in methanol.

2.2.2.4 Regeneration (RG) medium

RG medium contained ACM medium (Section 2.2.2.1) supplemented with 0.8 M sucrose. RG medium, for an overlay, contained 0.8% (w/v) agar.

2.2.2.5 Trace elements mix

Trace elements mix contained 0.05% (w/v) $FeSO_4.7H_2O$, 0.05% (w/v) $ZnSO_4.7H_2O$, 0.01% (w/v) $MnSO_4.H_2O$, 0.005% (w/v) $CuSO_4.5H_2O$ and 0.004% (w/v) $CoCl_2.6H_2O$ in 0.6 N HCl. CDYE medium (Section 2.2.2.2) was supplemented with 0.5% (v/v) trace elements mix.

2.2.3 Media supplements

Where necessary the media were supplemented with ampicillin (100 μg/ml), hygromycin (100 μg/ml), geneticin (150 μg/ml), IPTG (40 μg/ml) and X-gal (40 μg/ml).

2.3 Growth conditions

2.3.1 Bacterial growth conditions

Escherichia coli cultures were grown at 37°C in LB broth or on LB agar plates (Section 2.2.1.1) supplemented with ampicillin (100 μg/ml), where necessary. When grown in liquid media, *E. coli* cultures were shaken at 150 – 200 rpm.

2.3.2 Fungal growth conditions

P. paxilli strains were routinely grown at 22°C on ACM plates (Section 2.2.2.1) and RG medium (Section 2.2.2.4) for 4 – 6 days. Cultures were then maintained at 4°C. Spore suspensions were made by resuspending a block of media, containing sporulating cultures, in 0.01% (v/v) Triton X-100. Spore concentration was then determined using a haemocytometer slide. Spore suspensions were stored at 4°C.

For protoplast preparation (Section 2.13.1), liquid cultures were started using an inoculum of 5×10^6 spores per 25 ml of CDYE medium supplemented with trace elements mix (Section 2.2.2.2), and incubated at 28°C with shaking at 200 rpm for 30 h.

For DNA isolation (Section 2.5.2), liquid cultures were started using an inoculum of 5×10^6 spores per 25 ml of PD broth (Section 2.2.2.3) and incubated at 22°C with shaking at 200 rpm for 2 – 3 days. For RNA isolation (Section 2.15) and indole-diterpene analysis (Section 2.20), liquid cultures were started using an inoculum of 5×10^6 spores per 25 ml of CDYE medium supplemented with trace elements mix (Section 2.2.2.2), and incubated at 28°C with shaking at 200 rpm for 6 – 7 days. After harvesting, mycelia were washed in Milli-Q® water and either freeze-dried (mycelia for DNA isolation and indole-diterpene analysis) or snap-frozen in liquid nitrogen (mycelia for RNA isolation).

2.4 Glycerol stocks

Bacterial and fungal cultures were stored at –80°C in 10% (v/v) glycerol.

2.5 DNA isolation and purification

2.5.1 Plasmid DNA isolation and purification

2.5.1.1 Quantum Prep® Plasmid Miniprep Kit (Bio-Rad)

E. coli cells were grown overnight at 37°C with shaking in 2 ml of LB broth (Section 2.2.1.1) containing the appropriate antibiotic (Section 2.2.3). Cells

were pelleted by centrifugation at 9,000 rpm for 30 sec and resuspended completely in 200 μl of cell resuspension solution. The resuspended cells were lysed by addition of 250 μl of cell lysis solution and then neutralised by addition of 250 μl of neutralisation solution. This suspension was centrifuged at 14,000 rpm for 5 min and the supernatant mixed with 200 μl of Quantum Prep matrix. The supernatant was then transferred to a spin filter and centrifuged at 14,000 rpm for 30 sec. The matrix in the spin filter was washed twice with 500 μl of wash buffer by centrifugation at 14,000 rpm for 30 sec and 2 min, respectively. DNA in the matrix was then eluted with sterile Milli-Q® water and its concentration determined by the method described in Section 2.6.2.

2.5.1.2 High Pure Plasmid Isolation Kit (Roche)

E. coli cells were grown overnight at 37°C with shaking in 2 ml of LB broth (Section 2.2.1.1) containing the appropriate antibiotic (Section 2.2.3). Cells were pelleted by centrifugation at 9,000 rpm for 30 sec and resuspended in 250 μl of suspension buffer containing RNase. The resuspended cells were lysed by addition of 250 μl of lysis buffer followed by incubation at room temperature for 5 min. The suspension was neutralised by addition of 350 μl of chilled binding buffer followed by incubation on ice for 5 min. It was then centrifuged at 14,000 rpm for 10 min. The supernatant was transferred to a High Pure filter tube and centrifuged at 14,000 rpm for 1 min. The filter was washed with 700 μl of wash buffer II by centrifugation at 14,000 rpm for 1 min. DNA in the filter was then eluted with 100 μl of elution buffer by centrifugation at 14,000 rpm for 30 sec and its concentration determined by the method described in Section 2.6.2.

2.5.1.3 Plasmid DNA purification by alkaline lysis

2.5.1.3.1 Solution I

Solution I contained 50 mM glucose, 25 mM Tris-HCl (pH 8.0) and 10 mM Na_2EDTA (pH 8.0).

2.5.1.3.2 Solution II

Solution II contained 0.2 N NaOH and 1% SDS.

2.5.1.3.3 Solution III

Solution III contained 3 M potassium acetate and 2 M glacial acetic acid.

2.5.1.3.4 Alkaline lysis method

E. coli cells were grown overnight at 37°C with shaking in 2 ml of LB broth (Section 2.2.1.1) containing the appropriate antibiotic (Section 2.2.3). Cells were pelleted by centrifugation at 9,000 rpm for 30 sec and resuspended in 100 µl of ice-cold Solution I (Section 2.5.1.3.1). Cells were then lysed by addition of 200 µl of Solution II (Section 2.5.1.3.2) followed by incubation on ice for 5 min. In order to neutralise the suspension, 150 µl of ice-cold Solution III (Section 2.5.1.3.3) was added, followed by incubation on ice for another 5 min. Cellular debris were then pelleted by centrifugation at 14,000 rpm for 10 min. The supernatant was extracted with an equal volume of phenol-chloroform and the DNA was precipitated with an equal volume of ice-cold isopropanol and pelleted by centrifugation at 14,000 rpm for 10 min. The DNA pellet was then washed in 70% ethanol and air dried at 37°C. DNA was then resuspended in sterile Milli-Q® water and its concentration determined by the method described in Section 2.6.2.

2.5.2 Genomic DNA isolation

2.5.2.1 Genomic DNA isolation from fungal spores for PCR screening

P. paxilli strains were grown for sporulation at 22°C on ACM plates (Section 2.2.2.1) for 4 – 6 days (Section 2.3.2). A 0.3 cm × 0.3 cm block of media containing spores was then suspended in 1 ml of TE (10 mM Tris-HCl, pH 7.5, 1 mM Na_2EDTA) with 0.01% (v/v) Triton X-100. One hundred µl of spore suspension was transferred into a 2 ml micro-tube PP (Sarstedt, Germany) containing sterile glass beads (425 – 600 µm). The spores were then disrupted in a FastPrep® Cell Disrupter FP120 (Thermo Savant, NY, USA) for 20 sec at 4 m/sec followed by centrifugation at 13,000 rpm for 10 min to pellet the cell debris and the glass beads. The supernatant was collected and a 5 µl sample was used as the template for PCR (Section 2.14.2).

2.5.2.2 Genomic DNA isolation from fungal mycelia using modified Yoder method

Genomic DNA was isolated from fungal mycelia using modifications of the method described by Yoder (Yoder, 1988). Freeze-dried mycelium (15 – 30 mg) was ground to a fine powder with liquid nitrogen in a 2 ml microcentrifuge tube. The powder was thoroughly suspended in 500 μl of extraction buffer (100 mM LiCl, 10 mM Na_2EDTA, 0.5% SDS, 10 mM Tris-HCl, pH 7.4). This suspension was extracted with 1 ml of phenol-chloroform-isoamyl alcohol (25:24:1) and centrifuged at 13,000 rpm for 10 min. The aqueous phase was then extracted with 500 μl of chloroform-isoamyl alcohol (24:1). DNA was precipitated with two volumes of 95% ethanol and pelleted by centrifugation at 13,000 rpm for 5 min. The DNA pellet was then washed in 70% ethanol and air dried at 37°C. The DNA was resuspended in sterile Milli-Q® water and its concentration determined by method described in Section 2.6.2.

2.5.3 Purification of PCR products using QIAquick PCR Purification Kit (Qiagen)

Five volumes of Buffer PB were added to 1 volume of the PCR product. The sample was applied to a QIAquick column and centrifuged at 13,000 rpm for 1 min. The DNA bound to the column was washed with 0.75 ml of Buffer PE and followed by centrifugation at 13,000 rpm for 1 min. The DNA was eluted with 30 – 50 μl of either Buffer EB or sterile Milli-Q® water by centrifugation at 13,000 rpm for 1 min.

2.5.4 Extraction and purification of DNA from agarose gels using QIAquick Gel Extraction Kit (Qiagen)

The gels were prepared and run as described in Section 2.9.2. The DNA fragment was excised from the agarose gel under long wavelength UV light. Three volumes of Buffer QG were added to 1 volume of gel (100 mg ~ 100 μl) and incubated at 50°C for 10 min. One gel volume of isopropanol was added to the sample and applied to a QIAquick column. The sample was centrifuged at 13,000 rpm for 1 min and the bound DNA was then washed with 0.75 ml of Buffer PE by centrifugation at 13,000 rpm for 1 min. DNA was eluted with 30 –

50 μl of either Buffer EB or sterile Milli-Q® water by centrifugation at 13,000 rpm for 1 min.

2.6 DNA quantitation using fluorometer

2.6.1 Solutions

2.6.1.1 10X TNE buffer stock solution

TNE buffer (10X) contained 100 mM Tris base, 10 mM Na_2EDTA and 1 M NaCl with the pH adjusted to 7.4.

2.6.1.2 Hoechst 33258 stock dye solution

Hoechst dye solution contained 1 mg/ml Hoechst 33258 dye (Sigma).

2.6.1.3 Calf thymus DNA

Calf thymus DNA was resuspended at 100 ng/μl in 1X TNE buffer (Section 2.6.1.1).

2.6.1.4 Assay solution

Assay solution contained 0.1 μg/ml Hoechst dye (Section 2.6.1.2) in 1X TNE buffer (Section 2.6.1.1).

2.6.2 Quantitation method

DNA concentration was measured using the Hoefer® DyNA Quant® 200 fluorometer (Amersham Pharmacia Biotech, San Francisco, CA, USA). The fluorometer was blanked against the assay solution (Section 2.6.1.4) and calibrated to 100 ng/ml using a 1000 fold dilution of calf thymus DNA (100 ng/μl) (Section 2.6.1.3) in the assay solution. The concentration of DNA was measured in a 1000 fold dilution of the sample in the assay solution.

2.7 Restriction endonuclease digestion of DNA

Restriction digests were carried out in the buffer that was supplied with the restriction endonuclease. The DNA was cut using an excess of enzyme at the

recommended temperature and then checked by agarose gel electrophoresis (Section 2.9.2).

2.8 DNA ligations

2.8.1 Dephosphorylation of plasmid DNA

Plasmid DNA (~ 5 μg) was cut using an excess of restriction enzyme. The restriction enzyme was inactivated by heating at 65°C for 10 min and an aliquot was removed as a pre-treatment control. The remaining linearised plasmid DNA was dephosphorylated by addition of 1/10 volume of 10X dephosphorylation buffer and 0.5 U of calf intestine alkaline phosphatase (Roche) followed by incubation at 37°C for 30 min. After the incubation period, the phosphatase enzyme was inactivated by addition of SDS and Na_2EDTA (pH 8.0) to final concentrations of 0.5% and 5 mM, respectively. To this mixture, Proteinase K (Roche) was added to a final concentration of 50 μg/ml and incubated at 56°C for 30 min. The mixture was extracted once with phenol and once with phenol-chloroform. The DNA was ethanol precipitated, resuspended in sterile Milli-Q® water and its concentration determined (Section 2.6.2). Both pre-treated and treated plasmid DNA was used for ligations.

2.8.2 Preparation of pBluescript II KS (+)-T vector

Five μg of pBluescript II KS (+) was cut in 1X SuRe/Cut Buffer B with 50 U of *Eco*RV (Roche) in a reaction volume of 100 μl by incubating overnight at 37°C. After incubation, the linearised vector was purified using the QIAquick Gel Extraction Kit (Qiagen) (Section 2.5.4) and finally eluted in 50 μl of sterile Milli-Q® water. A T residue was added to the terminal 3'-hydroxyl groups of the linearised vector by incubating 100 μl reaction volume containing 50 μl of linearised vector, 10 μl of 10X PCR reaction buffer, 2 μl of 100 mM dTTP (Roche), 1 μl of *Taq* DNA Polymerase (5 U/μl) (Roche) and 37 μl of sterile Milli-Q® water at 70°C for 2 h. The concentration of the pBluescript II KS (+)-T vector was determined (Section 2.6.2) and used in TA cloning (Section 2.8.3).

2.8.3 DNA ligations

PCR products were ligated either into the pGEM®-T Easy vector (Promega) or into the pBluescript II KS (+)-T vector (Section 2.8.2) using the pGEM®-T Easy Kit (Promega). The ligations were performed in a 10 µl reaction volume and contained 1X ligation buffer, either 25 ng of pGEM®-T Easy vector (Promega) or 22 ng of pBluescript II KS (+)-T vector, PCR products at a 1:3 vector:insert molar ratio and 3 Weiss units of T4 DNA ligase (Promega).

Ligations of restriction enzyme digested samples were performed after their purification on agarose gels (Section 2.5.4). Ligations were carried out in a 20 µl reaction volume and contained 1X ligation buffer, 15 – 20 ng of vector DNA, insert DNA at a 1:3 vector:insert molar ratio and 160 U of T4 DNA ligase (New England Biolabs).

Three-way ligations were performed in a 16 µl reaction volume and contained 1X ligation buffer, 15 ng of vector DNA, insert DNA at a 1:3 vector:insert molar ratio and 3 Weiss units of T4 DNA ligase (Promega).

All ligation reactions were incubated overnight at 4°C. After incubation, an aliquot of the ligation mixture was checked for completion of ligation by agarose gel electrophoresis (Section 2.9.2) before transforming *E. coli* cells (Section 2.12).

2.9 Agarose gel electrophoresis

2.9.1 Solutions

2.9.1.1 1X TBE buffer

TBE (1X) buffer contained 89 mM Tris (pH 8.2), 89 mM boric acid and 2.5 mM Na_2EDTA.

2.9.1.2 SDS gel-loading dye

SDS gel-loading dye contained 1% (w/v) SDS, 0.02% (w/v) bromophenol blue, 20% (w/v) sucrose and 5 mM Na_2EDTA (pH 8.0).

2.9.1.3 Ethidium bromide solution

Ethidium bromide solution contained 1 μg/ml ethidium bromide dissolved in Milli-Q® water.

2.9.2 Agarose gel electrophoresis

Horizontal agarose gel electrophoresis was performed either in a HORIZON® 58 (Gibco Brl) apparatus for 1 – 2 h or in a BIO-RAD SUB-CELL® GT apparatus for several hours to overnight. Agarose (Roche) gels at desired concentrations were made in 1X TBE buffer (Section 2.9.1.1). The gels were loaded with samples mixed with SDS dye (Section 2.9.1.2). Electrophoresis was performed at 100 V for shorter runs and at 20 – 30 V for longer overnight runs. After the SDS dye had travelled a desired distance, the gel was stained with ethidium bromide (Section 2.9.1.3) for 15 – 20 min and then destained in Milli-Q® water. The bands on the gel were visualised on a UV transilluminator and photographed using the Gel Doc system (Bio-Rad). DNA fragment sizes on the gel were then determined by comparing with molecular markers of known size such as 1 kb+ ladder, λ *Hin*dIII ladder.

2.10 Southern Blotting

2.10.1 Solutions

2.10.1.1 Depurination solution

Depurination solution contained 0.25 M HCl.

2.10.1.2 Denaturation solution

Denaturation solution contained 0.5 M NaOH and 0.5 M NaCl.

2.10.1.3 Neutralisation buffer

Neutralisation buffer contained 2.0 M NaCl and 0.5 M Tris-HCl (pH 7.4).

2.10.1.4 20X SSC

SSC (20X) contained 3.0 M NaCl and 0.3 M sodium citrate. This stock was also used to prepare appropriate dilutions as required.

2.10.1.5 Hybridisation solution

Hybridisation solution contained 50 mM HEPES (pH 7.0), 3X SSC (Section 2.10.1.4), 18 μg/ml phenol-extracted herring sperm DNA (Sigma), 20 μg/ml *E. coli* tRNA, 0.1% (w/v) SDS, 0.2% (w/v) Ficoll (Sigma), 0.2% (w/v) polyvinylpyrrolidone (Sigma), 0.2% (w/v) bovine serum albumin (Sigma).

2.10.1.6 STE buffer

STE buffer contained 100 mM NaCl, 10 mM Tris-HCl (pH 8.0) and 1 mM Na_2EDTA.

2.10.2 Southern blotting: capillary transfer

The fractionated DNA was transferred from the gel to a positively charged nylon membrane (Roche) using the method based on that of Southern (Southern, 1975). The DNA fragments to be transferred to the membrane were fractionated based on size by electrophoresis through agarose gel and then stained, visualised and photographed as described in Section 2.9.2. The gel containing the fractionated DNA was placed in a tray to prepare the gel for DNA transfer. The gel was gently agitated for 15 min in depurination solution (Section 2.10.1.1) to nick the DNA. After depurination, nicked DNA was denatured by gently agitating the gel for 30 – 45 min in alkaline denaturation solution (Section 2.10.1.2). This was followed by neutralisation by gentle agitation of the gel for 30 – 60 min in neutralisation buffer (Section 2.10.1.3). The gel was then soaked for 2 min in 2X SSC (Section 2.10.1.4) with constant gentle agitation.

The transfer apparatus for DNA transfer was assembled as described. Two sheets of 3 MM blotting paper (Whatman) were wetted with 20X SSC (Section 2.10.1.4) and placed on a plastic trough with wells at both ends. The ends of the paper draped over the edges of the trough into the wells and served as wicks. The wells were filled with 20X SSC and the whole set covered with plastic wrap. A rectangle with a slightly smaller size than the gel was cut from the wrap. The gel was then centred on the wet blotting paper so that it overlapped the cut edges of the plastic wrap. A positively charged nylon membrane (Roche) slightly larger in size than the gel was soaked in 2X SSC and placed on top of the gel. Two sheets of 3 MM blotting paper with a slightly smaller size than the gel were soaked in 2X SSC and placed on the wet membrane followed by another two dry sheets of 3 MM paper of the same size. A stack of paper towels was then placed on the blotting papers and weighed down with appropriate weight. The DNA was allowed to transfer overnight. Next day, the transfer apparatus was disassembled and the positions of the gel slots on the membrane were marked with a lead pencil. The membrane was then soaked in 2X SSC for 5 min with gentle agitation and irradiated to cross-link the DNA to the membrane using 120,000 $\mu J/cm^2$ of energy in a Cex-800 Ultra-Lum Electronic UV Crosslinker (Ultra-Lum Inc, Paramount, CA, USA).

2.10.3 Preparation of radiolabelled DNA probes

For radiolabelling, 30 ng of DNA in 12 µl volume was denatured by boiling for 3 min and then placed immediately on ice to cool. Four µl of High Prime solution (Roche) and 4 µl of [α^{32}P]-dCTP (3000 Ci/mmol, Amersham) was added to the denatured DNA, mixed and incubated at 37°C for 1 h. The reaction was stopped by addition of 35 µl of STE buffer (Section 2.10.1.6). The unincorporated labelled nucleotides were removed from the labelling reaction mixture using a ProbeQuant™ G-50 Micro Column (Amersham). The vortexed column was pre-spun at 2,050 rpm for 2 min to remove the void volume from the column in a 1.5 ml microcentrifuge tube. The labelled probe was applied to the column placed in a new 1.5 ml microcentrifuge tube and spun at 2,050 rpm for 2 min. The purified labelled probe collected in the microcentrifuge tube was boiled for 3 min to denature the probe and cooled on ice prior to use.

2.10.4 Hybridisation of labelled probes to DNA fixed on membranes

The membrane containing the fixed DNA (Section 2.10.2) was prehybridised for at least 2 h in hybridisation solution (Section 2.10.1.5) at 65°C. The denatured purified labelled probe (Section 2.10.3) was added and hybridised overnight at 65°C. Next day, the membrane was washed three times with gentle agitation in 2X SSC (Section 2.10.1.4) containing 0.1% SDS for 15 min at 50°C.

2.10.5 Autoradiography

The hybridised membrane (Section 2.10.4) was covered with plastic wrap and exposed to X-ray film (Fuji) for an appropriate time at –80°C with an intensifying screen. The film was developed using 100Plus™ Automatic X-ray Processor (All-Pro Imaging Corp, NY, USA).

2.10.6 Stripping of hybridised membranes

The hybridised membranes were stripped in a solution of boiling 0.1% SDS with gentle agitation until the solution had cooled to room temperature. This process was repeated several times and finally the stripped membrane was checked by autoradiography (Section 2.10.5) to ensure that no signal from the probe remained.

2.11 DNA sequencing

DNA fragments were sequenced by the dideoxynucleotide chain-termination method (Sanger *et al.*, 1977) using Big-Dye (Version 3) chemistry (Perkin-Elmer, Applied Biosystems, Foster City, CA, USA) with oligonucleotide primers (Sigma Genosys). For sequencing plasmids, 300 ng of plasmid DNA was mixed with 3.2 pmol of primer in a 20 µl reaction volume. For sequencing PCR products, 2ng/100 bp of PCR product was mixed with 3.2 pmol of primer in a 20 µl reaction volume. Products were separated on an ABI Prism 377 sequencer (Perkin-Elmer Applied Biosystems). DNA sequences were assembled into contigs using Sequencher™ 4.2.2 (Gene Codes Corporation). Sequences were then annotated and diagrammatically represented using either MacVector™ 7.2.3 (Accelrys) or Discovery Studio Gene v 1.5 (Accelrys).

2.12 *Escherichia coli* transformation

2.12.1 Preparation of electrocompetent *E. coli*

Electrocompetent *E. coli* cells of strain XL1-Blue were prepared by inoculating 1000 ml of LB broth (Section 2.2.1.1) with 10 ml of *E. coli* culture grown overnight in LB broth at 37°C with agitation. The culture was incubated at 37°C with agitation until the optical density (A_{600}) of the culture was between 0.5 and 1.0. The culture was then chilled on ice for 20 min and the cells harvested by centrifugation at 4,000 *g* for 10 min at 4°C. The cells were resuspended and harvested twice in ice-cold water, first in 1000 ml and then in 500 ml, and then in 20 ml of ice-cold 10% glycerol by centrifugation at 4,000 *g* for 10 min at 4°C. Finally, the cell pellet was resuspended in 4 ml of ice-cold 10% glycerol and stored in 40 μl aliquots at –80°C.

2.12.2 Transformation of *E. coli* by electroporation

Electrocompetent *E. coli* cells (40 μl) (Section 2.12.1) were thawed and mixed with 1 – 2 μl of ligation mixture (Section 2.8.3) and incubated on ice for 1 min. The electroporation apparatus Gene Pulser (Bio-Rad) was set to deliver an electrical pulse of 25 μF capacitance, 2.5 kV, and 200 ohm resistance. The DNA/cell mixture was pipetted into an ice-cold 0.2 cm electroporation cuvette (Bio-Rad) and pulsed at the settings indicated above. If a time constant of 4 – 5 millisecond was registered on the machine, 1 ml of SOC medium (Section 2.2.1.3) was immediately added to the electroporated mixture at room temperature. The electroporated cells were then incubated at 37°C for 30 min – 1 h with gentle agitation. After incubation, the cells were plated at suitable dilutions on LB agar plates (Section 2.2.1.1) containing ampicillin, IPTG and X-gal (Section 2.2.3), where necessary.

2.12.3 Preparation of competent *E. coli* using $CaCl_2$

E. coli cells of strain DH5α were incubated overnight in 2 ml of LB broth (Section 2.2.1.1) at 37°C with agitation. The overnight culture was transferred to 200 ml of SOB medium (Section 2.2.1.2) and incubated at 22°C with agitation until the optical density (A_{600}) of the culture was between 0.4 and 0.8.

The culture was then chilled on ice for 10 min and the cells harvested by centrifugation at 4,000 *g* for 10 min at 4°C. The cells were resuspended in 67 ml of ice-cold Inoue transformation buffer (55 mM $MnCl_2.4H_2O$, 15 mM $CaCl_2.2H_2O$, 250 mM KCl, 10 mM PIPES, pH 6.7) (Inoue e*t al.*, 1990) and incubated on ice for 10 min. The cells were harvested by centrifugation at 4,000 *g* for 10 min at 4°C and the cell pellet was gently resuspended in 16 ml of ice-cold Inoue transformation buffer followed by the addition of 1.2 ml of DMSO. The competent cells were then snap-frozen in liquid nitrogen in 50 µl aliquots and stored at –80°C.

2.12.4 Transformation of $CaCl_2$-treated *E. coli*

E. coli cells treated with $CaCl_2$ (Section 2.12.3) were thawed and mixed with 1 – 2 µl of ligation mixture (Section 2.8.3) and incubated on ice for 20 min. The DNA/cell mixture was incubated at 42°C in a water bath for exactly 1 min and then immediately cooled in ice for 1 – 2 min. After cooling, 450 µl of SOC medium (Section 2.2.1.3) was added to the sample and incubated at 37°C for 30 min – 1 h with agitation. After incubation, the cells were plated at suitable dilutions on LB agar plates (Section 2.2.1.1) containing ampicillin, IPTG and X-gal (Section 2.2.3), where necessary.

2.12.5 Screening of recombinant bacterial colonies

CloneChecker™ System (Gibco Brl) was used to screen recombinant bacterial colonies for the presence of target plasmid DNA. Bacterial colonies from overnight incubated LB agar plates (Section 2.2.1.1) were suspended in 6 µl of LB broth (Section 2.2.1.1) and mixed well. Three µl of suspended colonies were thoroughly mixed with 8 µl of Green Solution and incubated at 100°C for 30 sec and then cooled to room temperature. A digestion mix containing 1 µl of 10X reaction buffer and 1 µl (10 U) of restriction enzyme was added to each sample and incubated at the appropriate temperature for 10 min. Two µl of Blue Loading Buffer was added to each sample and analysed by agarose gel electrophoresis (Section 2.9.2). If a colony was found to contain the target plasmid DNA, its remaining 3 µl of suspended colony was used to inoculate an overnight culture for further analysis.

2.13 *Penicillium paxilli* transformation

2.13.1 Preparation of *P. paxilli* protoplasts

2.13.1.1 Solutions

2.13.1.1.1 OM buffer

OM buffer contained 1.2 M $MgSO_4$ and 10 mM Na_2HPO_4. The pH was adjusted to 5.8 with 100 mM $NaH_2PO_4.2H_2O$.

2.13.1.1.2 Glucanex solution

Glucanex was dissolved in OM buffer (Section 2.13.1.1.1) to a concentration of 10 mg/ml and filter sterilised before use.

2.13.1.1.3 ST buffer

ST buffer contained 0.6 M sorbitol and 100 mM Tris-HCl (pH 8.0).

2.13.1.1.4 STC buffer

STC buffer contained 1 M sorbitol, 50 mM $CaCl_2$ and 50 mM Tris-HCl (pH 8.0).

2.13.1.1.5 PEG buffer

PEG buffer contained 40% (w/v) PEG 4000, 50 mM $CaCl_2$, 1 M sorbitol and 50 mM Tris-HCl (pH 8.0).

2.13.1.2 Preparation of protoplasts

For protoplast preparation, five 25 ml liquid cultures of each fungal strain were grown for 30 h as described in Section 2.3.2. Liquid cultures for each strain were pooled and mycelia harvested by filtering through a sterile nappy liner, and washed three times with sterile Milli-Q® water. Mycelia were rinsed with OM buffer (Section 2.13.1.1.1), collected in a flask and resuspended in glucanex solution (Section 2.13.1.1.2) (20 ml glucanex solution/ g wet mycelia). Mycelia were then incubated at 30°C for 16 h with gentle shaking at 80 – 100 rpm. After incubation, a small sample was checked under the microscope for number of protoplasts. Protoplasts were collected by filtering the samples

through a sterile nappy liner into sterile centrifuge tubes with each tube containing approximately 5 ml of sample. The protoplast suspension from each tube was overlaid with 2 ml of ST buffer (Section 2.13.1.1.3) and the tubes were centrifuged at 2,210 *g* for 5 min at 4°C. Protoplasts, banded at the interface between glucanex and ST buffer solutions, were transferred to a fresh tube and washed three times in 5 ml of STC buffer (Section 2.13.1.1.4) by centrifugation at 2,210 *g* for 5 min at 4°C. Protoplasts were pooled after each wash and finally resuspended in STC buffer to a final concentration of 1.25×10^8 protoplasts per ml. At this stage, protoplasts (80 µl) were either used for fungal transformation or mixed with 20 µl of PEG buffer (Section 2.13.1.1.5) for storage at –80°C.

2.13.2 Transformation of *P. paxilli* protoplasts

Protoplasts of *P. paxilli* (Section 2.13.1.2) were transformed with 5 µg of circular plasmid DNA. For co-transformation, protoplasts were co-transformed with 5 µg each of geneticin-resistant vector pII99 and the recombinant plasmid. For each transformation, a "protoplast only" control, without any DNA, and a positive "vector only" control, with pII99, was also included.

Circular plasmid DNA was added to 80 µl of protoplasts with 20 µl of PEG buffer (Section 2.13.1.1.5), 5 µl of heparin (5 mg/ml in STC buffer, Section 2.13.1.1.4) and 2 µl of 50 mM spermidine, and incubated on ice for 30 min. Nine hundred µl of PEG buffer was added to the sample and incubated on ice for 15 – 20 min. A 100 µl aliquot of the sample was mixed by vortexing with 3 ml of 0.8% RG agar (Section 2.2.2.4) equilibrated to 50°C and overlaid on a RG medium agar plate (Section 2.2.2.4). This process was repeated for the remaining sample mix and all the plates incubated overnight at 22°C. Next day, another overlay with antibiotic selection (hygromycin to a final concentration of 100 µg/ml and geneticin to a final concentration of 150 µg/ml) (Section 2.2.3) was performed and the plates incubated at 22°C for 4 – 6 days.

2.13.3 Purification of transformants

Geneticin-resistant colonies of *P. paxilli* transformants were plated for single colonies on ACM (Section 2.2.2.1), with geneticin (Section 2.2.3), and incubated at 22°C for 4 days. Single colonies were picked into 50 µl of 0.01% Triton X-100 and plated on ACM, with geneticin, and incubated at 22°C for 4 – 6 days. After incubation, the transformants were either screened as described in Section 2.5.2.1 or used to prepare spore suspensions (Section 2.3.2) for further analysis.

2.14 PCR

2.14.1 Reagents

2.14.1.1 dNTPs

dNTPs (Roche) were prepared at concentrations of either 1.25 mM or 2 mM of each dNTP.

2.14.1.2 Oligonucleotide primers

Oligonucleotide primers were synthesised by Sigma Genosys and resuspended to a stock concentration of 100 pmol/µl. The primer stocks were diluted to 10 pmol/µl for PCR and to 3.2 pmol/µl for sequencing reactions. All primers were stored at –20°C. Primers cited in this thesis are listed in Table 2.2.

2.14.2 Standard PCR

Standard PCR was carried out in 25 or 50 µl reaction volume containing 1X PCR reaction buffer (1.5 mM $MgCl_2$), 100 µM of each dNTP, 200 nM of each primer, 1 or 2 U of *Taq* DNA polymerase (Roche) and either 10 ng of genomic DNA or 5 µl of genomic DNA prepared from spores (Section 2.5.2.1) as the template. The thermocycle conditions used were one cycle at 94°C for 2 min, 30 cycles at 94°C for 30 sec, 55°C for 30 sec and 72°C for 1 min (per kb) and one cycle at 72°C for 5 min.

Table 2.2 List of primers cited in this thesis

Primer name	Sequence (5' - 3')	Used for
ggpps16	TTGCTTCACTATTGCGAGTT	*paxGAMBC* PCR screening
ggpps31	GGGTAGTTGGGAACGGATTT	*paxGAMBC* PCR screening
pax214	CACCACAAGACTCCACAG	*paxGAMBC* PCR screening
CYP-6	GACAAGGGACATATCTTGAC	*paxGAMBC* PCR screening
pax122	GCAGATAGTAGGTACTAC	*paxGAMBC*, *paxGMC*, *paxGAMC* and *paxGMBC* PCR screening
pax127	GGATTTGACCATGATGCG	*paxGAMBC* PCR screening
pII99-3	GGCTGGCTTAACTATGCG	*paxGAMBC*, *paxGMC*, *paxGAMC* and *paxGMBC* PCR screening
pII99-4	CCCAGAATGCACAGGTAC	*paxGAMBC*, *paxGMC*, *paxGAMC* and *paxGMBC* PCR screening
Etub2	AGGCGTTGGCATTACGGC	*tub2* PCR
Etub3	CCGACGAGACCTTCTGTATC	*tub2* PCR
paxMSpeF2	GGACTAGTCCGCTTCTTAGGATCAAC	*paxM* PCR
paxMSpeR	GTACTAGTGTCAGAGTACCCCTCTGC	*paxM* and *paxMB* PCR
pax64	ACTGCATAGTTTGATATCTGC	*paxGMC*, *paxGAMC* and *paxGMBC* PCR screening
SS9	TGACTAGTCACAGGTCGTG	*paxAM* PCR
paxMSpeF1	TTACTAGTGATCGGCAGTTGAGGGTG	*paxAM* PCR
SS8	AGACTAGTTTAGATCTTGCAGGATCTCC	*paxMB* PCR
paxPEcoRIF2	TTGAATTCATGCATGGTAAGCAGCCG	*paxP* PCR
paxPEcoRIR	GGGAATTCCGGCCATTCAATCTCAAG	*paxP* PCR
paxQHindIIIF2	GAAAAGCTTTACTCTGACACACTCCGC	*paxQ* PCR
paxQHindIIIR	TTGAAGCTTCCTTATTGTGGCGCAGTC	*paxQ* PCR
SS1	TTCACGGACCACGTTGGTGG	*paxP* RT-PCR
SS2	TGCTCATGGCACTGGTGTGC	*paxP* RT-PCR
SS3	GGAAGTCTGCATCTGCAACG	*paxQ* RT-PCR
SS4	AGAACCTGGGTCGTGGTATG	*paxQ* RT-PCR
ggs1-Xb-F	CCTCTAGAATGAGTTCTTCCTTTC	Ggs1 PCR
ggs1-Xh-R	ACTCGAGTTGGGCACCTTCATC	Ggs1 PCR

Primer name	Sequence (5' - 3')	Used for
ggs1-Xh-F	CCTCGAGAGTTCTTCCTTTCAACC	Ggs1 PCR
ggs1-No-R	TGCGGCCGCCTATTGGGCAC	Ggs1 PCR
paxG-Sp-F	GCACTAGTATGTCCTACATCCTTGC	PaxG PCR
paxG-Xh-R	ACTCGAGAACTCTTCCTTTCTC	PaxG PCR
paxG-Xh-F2	GCTCGAGTCCTACATCCTTGCAGA	PaxG PCR
paxG-No-R2	GCGGCCGCTTAAACTCTTCCTTTCTC	PaxG PCR
EGFP-Xb-F	GTCTAGAATGGTGAGCAAGGG	EGFP and EGFP.GRV PCR
EGFP-Xh-R	TCTCGAGCTTGTACAGCTCGTC	EGFP PCR
EGFP-Xh-F	ATCTCGAGGTGAGCAAGG	EGFP PCR
EGFP-No-R	AGCGGCCGCTTACTTGTAC	EGFP PCR
PTEF-SalI-F	GTCGACGGTAGCAAACGGTGGTC	PTEF-TtrpC PCR
TtrpC-BglII-R	CCGGCAGATCTATTGTATACCC	PTEF-TtrpC PCR
DsRed-XbaI-F	TCTAGAATGGCCTCCTCCGAGGAC	DsRed and DsRed.SKL PCR
DsRed-No-R	GCGGCCGCCTACAGGAACAG	DsRed PCR
SKL-No-R	GCGGCCGCTTACAGCTTGCTCAGGAAC	DsRed.SKL PCR
GRV-No-R	GCGGCCGCTTAAACTCTTCCCTTGTACAG	EGFP.GRV PCR
TBg	CCGAGATCTATTGTATACCC	PCR Screening
TEFsl2	ATGTCGACGGTAGCAAACGG	PCR Screening

2.14.3 PCR using Expand High Fidelity PCR System (Roche)

High fidelity PCR was carried out in 25 or 50 μl reaction volume containing 1X Expand HF buffer (1.5 mM $MgCl_2$), 50 or 200 μM of each dNTP, 200 or 300 nM of each primer, 0.75 or 2.6 U of Expand High Fidelity Enzyme Mix (Roche) and either 10 ng of plasmid or 5 – 15 ng of genomic DNA as the template. The thermocycle conditions used were one cycle at 94°C for 2 min, 30 cycles at 94°C for 30 sec, 55°C for 30 sec and 72°C for 1 min (per kb) and one cycle at 72°C for 5 min.

2.14.4 PCR using TripleMaster® PCR System (Eppendorf)

TripleMaster® PCR was performed in 20 or 50 μl reaction volume containing 1X HighFidelity buffer (2.5 mM Mg^{2+}), 200 μM of each dNTP, 200 nM of each primer, 0.75 or 1.5 U of TripleMaster Polymerase Mix (Eppendorf) and either 1 ng of plasmid or 100 ng of genomic DNA as the template. Two different thermocycle conditions used were (a) one cycle at 94°C for 2 min, 30 cycles at 94°C for 20 sec, 55°C for 20 sec and 72°C for 1 min (per kb) and one cycle at 72°C for 3 min, and (b) one cycle at 94°C for 2 min, 25 cycles at 94°C for 20 sec, 50°C for 20 sec and 72°C for 1 min (per kb) and one cycle at 72°C for 3 min.

2.14.5 RT-PCR

2.14.5.1 RT-PCR using cDNA

RT-PCR was carried out using reactions and thermocycle conditions as described for Expand High Fidelity PCR System (Section 2.14.3) and TripleMaster® PCR System (Section 2.14.4) with 1 μl and 0.8 μl of cDNA (Section 2.18), respectively, as the template.

2.14.5.2 RT-PCR using SuperScript™ One-Step RT-PCR with Platinum® *Taq* (Invitrogen)

RT-PCR was performed in 25 μl reaction volume containing 1X Reaction Mix (200 μM of each dNTP, 1.2 mM $MgSO_4$), 200 nM of each primer, 0.5 μl of RT/ Platinum® *Taq* Mix (Invitrogen) and 100 ng of DNased RNA. The thermocycle

conditions used were one cycle at 50°C for 30 min and 94°C for 2 min, 35 cycles at 94°C for 30 sec, 55°C for 30 sec and 72°C for 1 min (per kb) and one cycle at 72°C for 10 min.

2.15 RNA isolation using TRIzol® Reagent (Invitrogen)

Total RNA was isolated from *P. paxilli* mycelia using TRIzol® reagent (Invitrogen). Snap-frozen mycelia (0.5 – 1 g) (Section 2.3.2) were ground to a powder with liquid nitrogen using a pestle and mortar. The powdered mycelia were mixed to a paste with 10 ml of TRIzol® reagent and left to thaw. The mixture was transferred to a 14 ml Falcon™ tube and centrifuged at 12,000 × *g* for 10 min at 4°C. The supernatant containing RNA was mixed thoroughly for 15 sec with 2 ml of chloroform and incubated at room temperature for 3 min. The mixture was then centrifuged at 12,000 × *g* for 15 min at 4°C. The upper aqueous phase was mixed with 5 ml of isopropanol to precipitate the RNA. The mixture was incubated at room temperature for 10 min and then centrifuged at 12,000 × *g* for 10 min at 4°C. The RNA pellet was washed with 10 ml of 75% ethanol and centrifuged at 7,500 × *g* for 5 min at 4°C. The RNA pellet was air-dried and resuspended in 200 µl of TE (10:1) buffer (10 mM Tris-HCl, pH 8.0, 1 mM Na_2EDTA).

2.16 RNA quantitation

The concentration and purity of isolated total RNA (Section 2.15) was determined by measuring the absorbance at 260 and 280 nm. To determine RNA concentration the absorbance of a 100 fold dilution of RNA in TE (10:1) buffer (Section 2.15) was measured. The absorbance at 260 nm was multiplied by the dilution factor and by 40 µg/ml, since an absorbance of 1 at 260 nm is equivalent to a concentration of 40 µg/ml. RNA purity was determined by calculating the A_{260}/ A_{280} ratio, with a ratio of 1.8 to 2.2 indicating pure RNA.

2.17 DNase I treatment of RNA

Before cDNA synthesis, RNA was treated with DNase I, Amplification Grade (Invitrogen). The treatment was performed in 50 µl reaction volume containing 5 µg of RNA, 1X DNase I Reaction Buffer and 5 U of DNase I, Amp Grade

(Invitrogen). The samples were incubated at room temperature for 15 min. After incubation, DNase I was inactivated by the addition of 5 μl of 25 mM EDTA followed by heating at 65°C for 10 min. The concentration of DNased RNA was then determined by measuring the absorbance of a 50 fold dilution of the DNased RNA in DEPC-treated water as described in Section 2.16.

2.18 cDNA synthesis using SuperScript™ First-Strand Synthesis System for RT-PCR (Invitrogen)

A 10 μl reaction volume containing approximately 5 μg of total RNA, 1 mM of dNTP mix and 0.5 μg of Oligo(dT)$_{12-18}$ (Invitrogen) was incubated at 65°C for 5 min and then placed on ice for at least 1 min. To this RNA/primer mixture, 9 μl of reaction mixture containing 2 μl of 10X RT buffer, 4 μl of 25 mM $MgCl_2$, 2 μl of 0.1 M DTT and 1 μl of RNaseOUT™ Recombinant RNase Inhibitor (Invitrogen) was added. This mixture was incubated at 42°C for 2 min and then 1 μl (50 U) of SuperScript™ II RT (Invitrogen) was added. The mixture was then incubated at 42°C for 50 min. After incubation, the reaction was terminated at 70°C for 15 min and chilled on ice. To this mixture, 1 μl of RNase H was added and incubated at 37°C for 20 min. Amplification of cDNA was then performed using either 0.8 or 1.0 μl of cDNA in a 20 μl or 25 μl reaction volume (Section 2.14.5.1), respectively.

2.19 Chemical synthesis of PC-M6 and paxitriol

Authentic PC-M6 and paxitriol were synthesised from 13-desoxypaxilline and paxilline, respectively, using the method described by Miles *et al.* (Miles *et al.*, 1992) since these indole-diterpenes were commercially not available.

2.19.1 Extraction and purification of 13-desoxypaxilline

In order to synthesise PC-M6, 13-desoxypaxilline was extracted and purified from the deletion mutant LMQ226 that accumulated 13-desoxypaxilline. Approximately 2 – 3 g of freeze-dried mycelium (Section 2.3.2) was extracted in 40 – 50 ml of chloroform-methanol (2:1) (Section 2.20). The extract was centrifuged at 10,000 rpm for 10 min and the supernatant dried *in vacuo*. The dried extract was redissolved in chloroform-acetone (9:1) and purified by flash

chromatography (chloroform-acetone 9:1). The purified substance was dried *in vacuo* and redissolved in methanol. On RP-HPLC analysis (Section 2.20), a major peak was observed at R_t = 7.5 min that corresponded to authentic 13-desoxypaxilline. The fractions corresponding to this peak were collected by RP-HPLC and pooled. The pooled fractions were snap-frozen in liquid nitrogen before freeze-drying. The purified 13-desoxypaxilline was checked by RP-HPLC to ensure that no other compound was present in it.

2.19.2 Synthesis of PC-M6

Conversion of 13-desoxypaxilline to PC-M6 required a reduction at the C-10 position, which was effected by the reducing agent sodium borohydride. Approximately 9 mg (0.021 mmol) of authentic 13-desoxypaxilline (Section 2.19.1) was dissolved in 9 ml of methanol. To this solution, approximately 12 mg (0.317 mmol) of sodium borohydride was added while stirring. The products of the reaction were checked by NP-TLC (chloroform-acetone 9.5:0.5) after 10 min, and no starting material could be detected. Ten ml of de-ionised water was added to the reaction mixture followed by the addition of 2 ml of 10% HCl. The products were extracted four times with 10 ml of dichloromethane and the pooled extract was analysed by NP-TLC (chloroform-acetone 9.5:0.5) for the products. The extracts were dried by the addition of anhydrous $MgSO_4$ and filtered through a sintered funnel. The filtrate was dried *in vacuo* and the residue redissolved in methanol. A sample of this was run on RP-HPLC (Section 2.20) which detected two peaks, one at R_t = 5.85 min and the other at 7.75 min (Appendix 5.1). A sample was also run on LC-MSMS (Section 2.20) and was confirmed to contain PC-M6. The fractions corresponding to the two peaks were separated by RP-HPLC and pooled. The pooled fractions were snap-frozen in liquid nitrogen and freeze-dried. The purified products were checked by RP-HPLC to ensure that no impurity was present. The reduction of 13-desoxypaxilline thus gave two diastereomers that were named as α-PC-M6 (R_t = 5.85 min) and β-PC-M6 (R_t = 7.75 min) based on their conversion products (Section 3.3.5).

2.19.3 Synthesis of paxitriol

Similar to the conversion of 13-desoxypaxilline to PC-M6, conversion of paxilline to paxitriol also required a C-10 reduction using sodium borohydride. Approximately 9 mg (0.021 mmol) of authentic paxilline (AgResearch, Ruakura, New Zealand) was dissolved in 9 ml of methanol. Approximately 9 mg (0.238 mmol) of sodium borohydride was added to the solution while stirring. The products of the reaction were checked by NP-TLC (chloroform-acetone 9.5:0.5) after 10 min, and no starting material could be detected. De-ionised water (10 ml) was added to the reaction mixture followed by the addition of 2 ml of 10% HCl. The products were extracted four times with 10 ml of dichloromethane and the pooled extract was analysed by NP-TLC (chloroform-acetone 9.5:0.5) for the products. The organic layer was dried by the addition of anhydrous $MgSO_4$ and filtered through a sintered funnel. The filtrate was dried *in vacuo* and the residue redissolved in methanol. A sample of this was run on RP-HPLC (Section 2.20) which detected two peaks, one at R_t = 3.55 min and the other at 4.30 min (Appendix 5.1). Since the two peaks observed did not resolve well with 85% methanol, 80% methanol was used for separating the two peaks. In 80% methanol, the two peaks had retention times of 4.75 min and 6.2 min. The fractions corresponding to these two peaks were separated by RP-HPLC using 80% methanol and pooled. The pooled fractions were snap-frozen in liquid nitrogen and freeze-dried. The purified products were checked by RP-HPLC to ensure that no impurity was present. The reduction of paxilline thus gave two diastereomers that were named as α-paxitriol (R_t = 4.30 min) and β-paxitriol (R_t = 3.55 min) based on comparison to authentic standards (AgResearch, Ruakura, New Zealand).

2.20 Feeding of precursor metabolites to *P. paxilli*

Mycelium from liquid cultures of *P. paxilli* was grown for 4 days in CDYE, supplemented with trace elements mix (Section 2.3.2). On day 4, mycelium was washed three times with 10 ml of 1 mM MOPS buffer (pH 6.5) and 0.5 g of washed mycelium resuspended in 12.5 ml of 20 mM MOPS buffer (pH 7.0) containing 4% (v/v) glycerol, in duplicates. To one set of cultures, precursor metabolite was added in two equal doses of 100 μg (in 100 μl of acetone) at 24

h interval during incubations at 28°C with shaking at 200 rpm. To the other set of cultures, 100 µl of acetone was added as an external control. On day 6, mycelium was harvested as described in Section 2.3.2 for indole-diterpene analysis (Section 2.21).

2.21 Indole-diterpene analysis

Approximately 0.2 – 0.5 g of freeze-dried mycelium (Section 2.3.2) was extracted with 10 ml of chloroform using a Virtis "45" Homogenizer. Five ml of methanol was added to the sample and mixed for 1 – 2 h by rotation on a spinning wheel. A 2 ml sample of each extract was centrifuged at 10,000 rpm for 10 min and the supernatant dried overnight in a fume hood.

For NP-TLC analysis, the dried extract was redissolved in 50 µl of chloroform-methanol (2:1). A 10 µl aliquot was spotted on a SIL G TLC plate (Macherey-Nagel, Germany) along with authentic indole-diterpenes. The samples were fractionated using chloroform-acetone (9:1) mixture. After fractionation, the indole-diterpenes were identified by spraying the TLC plate with Ehrlich's reagent [2% (w/v) *p*-dimethylaminobenzaldehyde in 12% (v/v) HCl and 50% ethanol] followed by heating at 120°C for 15 – 20 min.

For RP-HPLC analysis, the dried extract was redissolved in 1 ml of methanol and filtered through 0.2 µM nylon membrane (Phenomenex) before analysis. The analytical runs were performed with 10 – 50 µl of samples and 5 µg of authentic indole-diterpenes on a Dionex Summit (Dionex Corporation, CA, USA) HPLC system equipped with a Luna (Phenomenex, CA, USA) C18 column (5 µm particle size, 4.6 × 250 mm). Indole-diterpenes in the samples were eluted with 85% methanol at a flow rate of 1.5 ml/min and UV detection at either 230 or 280 nm. The characteristic feature of an indole moiety showing an absorption maximum at 230 nm and an absorption minimum at 280 nm was employed to confirm the presence of an indole-diterpene in a sample. However, in this thesis, all the RP-HPLC traces are shown for 230 nm wavelength.

For LC-MSMS analysis, an aliquot of the sample prepared for RP-HPLC analysis was provided to the LC-MSMS analytical facility at AgResearch Grasslands, Palmerston North, New Zealand. LC-MSMS analysis was performed on a Thermo Finnigan Surveyor (Thermo Finnigan, CA, USA) HPLC system equipped with a Luna (Phenomenex) C18 column (5 μm particle size, 2 × 150 mm) at a flow rate of 200 μl/min with a solvent gradient starting with acetonitrile-water (60:40) in 0.1% formic acid and increasing to 95% acetonitrile over 30 min followed by a column wash at 99% acetonitrile. Mass spectra were determined with linear ion trap mass spectrometer (Thermo LTQ, Thermo Finnigan, CA, USA) using electro spray ionization (ESI) in positive mode. The spray voltage was 5.0 kV and the capillary temperature was 275°C. The flow rates of sheath gas, auxiliary gas and sweep gas were set to 20, 5 and 10 (arbitrary units), respectively. Other parameters were optimized automatically by infusing authentic paspaline in water-acetonitrile-formic acid (75:25:0.1 v:v:v) at a flow rate of 200 μl/min. Indole-diterpenes were detected in single reaction monitoring (SRM) mode, selecting 422 *m/z* ± 2, 35% collision energy followed by data dependent fragmentation of the three most intense ions in the mass spectrum above a 1000 (arbitrary unit) threshold.

2.22 Staining of *P. paxilli* cultures

Samples were prepared by inoculating 10^6 spores in 1 ml of PD broth (Section 2.2.2.3) and incubating at 22°C with shaking at 150 rpm for approximately 2 days. For staining with MitoTracker® Red CMXRos (Molecular Probes) and FM 4-64 (Molecular Probes), 900 μl and 200 μl of mycelial suspension was used, respectively.

2.22.1 Staining with MitoTracker® Red CMXRos (Molecular Probes)

A working stock solution of 1 ng/μl was prepared in PD broth from a MitoTracker® stock solution of 1 μg/μl in DMSO. Hundred μl of working stock solution was added to 900 μl of mycelial suspension and mixed thoroughly. The sample was incubated for 30 min at 22°C with shaking at 150 rpm in dark. After incubation, the mycelia were pelleted by centrifugation at 13,000 rpm for 1 min and washed twice in 500 μl of PD broth at 13,000 rpm for 1 min. The pellet was

resuspended in 50 μl of 10% glycerol and a 10 μl aliquot was transferred to a microscope slide for microscopy (Section 2.23).

2.22.2 Staining with FM 4-64 (Molecular Probes)

A FM 4-64 stock solution of 1 μg/μl was prepared in DMSO. Two μl of stock solution was added to 200 μl of mycelial suspension and mixed thoroughly. The sample was incubated for 30 min at 22°C with shaking at 150 rpm in dark. After incubation, the mycelia were pelleted by centrifugation at 13,000 rpm for 1 min and washed twice in 500 μl of PD broth at 13,000 rpm for 1 min. The pellet was resuspended in 50 μl of 10% glycerol and a 10 μl aliquot was transferred to a microscopic slide for microscopy (Section 2.23).

2.23 Microscopy

For primary screening, the fungal strains were plated on ACM (Section 2.2.2.1) and incubated at 22°C for 3 – 4 days. After incubation, the samples were observed with an Olympus SZX12 microscope using a GFPA filter for EGFP fluorescence and a RFP1 filter for DsRed fluorescence.

For localisation studies, samples were prepared by inoculating 1 μl of 10^6 spores on PDA or PDA supplemented with oleic acid (Section 2.2.2.3) mounted on a sterile microscopic slide and incubating at 22°C for approximately 2 days. After incubation, 10% glycerol was added to the sample before microscopy. The stained samples for microscopy were prepared as described in Section 2.22. Fungal mycelia were observed with an Olympus BX51 fluorescence microscope using a FITC filter for EGFP fluorescence and a CY3 filter for MitoTracker® Red CMXRos and FM 4-64 fluorescence. All images were captured at 100X magnification with a MagnaFire™ digital camera and software (Optronics). The images were stored as TIF files and processed with Canvas 10 software (ACD Systems International).

CHAPTER THREE

RESULTS

3.1 Genes required for paspaline biosynthesis

Systematic gene disruption and chemical complementation studies have shown that at least five enzymes catalyse the formation of paxilline in *P. paxilli* (McMillan *et al.*, 2003; Young *et al.*, 2001). Deletion mutants of *paxG* (encodes a GGPP synthase), *paxM* (encodes a FAD-dependent monooxygenase) (McMillan and Scott, unpublished results) and *paxC* (encodes a prenyltransferase) (Young *et al.*, unpublished results) are unable to synthesise any detectable indole-diterpenes. However, deletion mutants of *paxP* and *paxQ* (both encode cytochrome P450 monooxygenases) accumulate the indole-diterpenes paspaline and 13-desoxypaxilline, respectively (McMillan *et al.*, 2003). These studies led Parker and Scott to propose that PaxG, PaxM and PaxC are required for biosynthesis of the first stable indole-diterpene product paspaline, and PaxP and PaxQ for the further transformations to paxilline (Parker and Scott, 2004). Recently, Monahan and Scott identified two additional *pax* genes within the cluster, *paxA* and *paxB* (putative membrane proteins), deletions of which are also unable to synthesise any detectable indole-diterpenes (Monahan and Scott, unpublished results). Taken together, these results suggest that at least five gene products (PaxG, PaxM, PaxC, PaxA and PaxB) are needed for paspaline biosynthesis. In order to determine how many of these genes are required for paspaline biosynthesis a series of constructs were prepared containing different combinations of these genes and transformed into paxilline-negative deletion derivatives.

3.1.1 Preparation and functional analysis of pSS8

A *Hin*dIII restriction fragment (~11 kb) from the lambda clone, λCY55, containing the five *pax* genes viz. *paxG*, *paxA*, *paxM*, *paxB* and *paxC* was cloned into the *Hin*dIII site of the geneticin-resistant vector pII99 to generate pSS8 (Figure 3.1). This fragment was missing the last six amino acids and the stop codon of PaxC. Hence, the functionality of the genes at either end of the restriction fragment, i.e. *paxG* and *paxC*, was checked by transforming pSS8 into the *P. paxilli* deletion mutants LMG23 (Δ*paxGA*) and ABC83 (Δ*paxC*) (Section 2.13.2). Subsequent to the generation of the LMG23 mutant Monahan

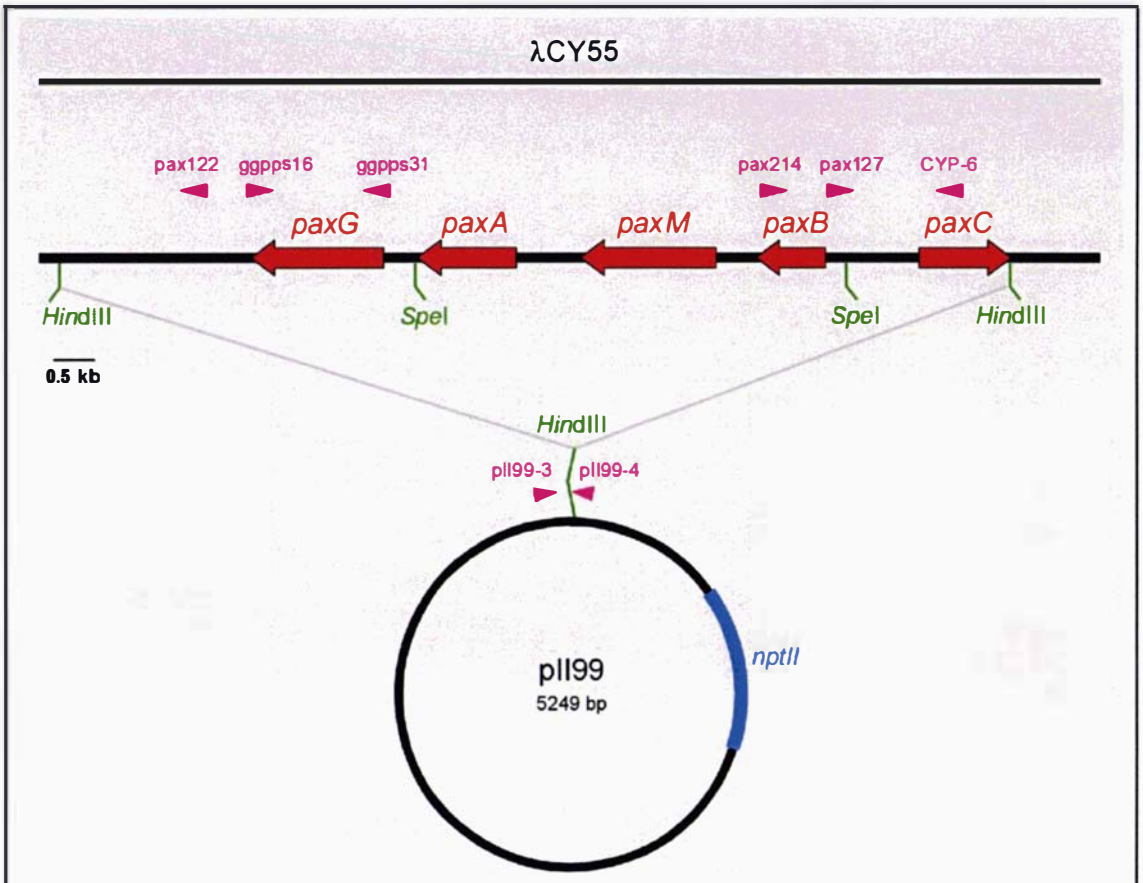

Figure 3.1 pSS8 (*paxGAMBC*) construct

The construct pSS8 was made by cloning the *Hin*dIII fragment containing *paxG*, *paxA*, *paxM*, *paxB* and *paxC* from the lambda clone, λCY55, into the *Hin*dIII site of pII99.
Restriction sites used for cloning and positions of primers used for screening transformants are shown in green and pink, respectively.

showed that the *paxG* deletion also included 370 bp of the 3' coding sequence of *paxA* (unpublished results).

Protoplasts of LMG23 and ABC83 were transformed with 5 μg of circular pII99 or pSS8. The transformants were selected on RG medium supplemented with 150 μg/ml of geneticin. Four to seven stable transformants were colony purified and screened by TLC analysis (Section 2.21) for their ability to synthesise paxilline or other indole-diterpenes, which stain green with Ehrlich's reagent (Figure 3.2). No indole-diterpenes were detected in extracts of the *paxGA* mutant or *paxGA* mutant with pII99 (Figure 3.2A). However, all the four LMG23 transformants containing pSS8, LMG23.P8-1 to 4, were able to complement the *paxGA* deletion. These transformants had intense green bands with R_f values similar to authentic paxilline. In addition to paxilline, other green bands, similar to those consistently observed in extracts of wild-type *P. paxilli*, were also observed. As will be shown later, these correspond to other indole-diterpenes including β-paxitriol, PC-M6, paspaline and 13-desoxypaxilline. These compounds have been proposed to be paxilline intermediates (Munday-Finch *et al.*, 1996).

Extracts of *paxC* mutant or *paxC* mutant with pII99 did not accumulate any detectable indole-diterpenes (Figure 3.2B). Two out of four ABC83 transformants containing pSS8, ABC83.P8-1 and ABC83.P8-2, were able to complement the *paxC* deletion. Since the transformants were not screened for the presence of intact copies of the integrating construct, and were arbitrarily selected as geneticin-resistant colonies, the indole-diterpene negative phenotype of the other two ABC83 transformants, ABC83.P8-3 and ABC83.P8-4, could be due to the absence of intact copies of pSS8. Unlike the *paxGA* complementation, *paxC* complementing transformants did not accumulate any indole-diterpene intermediates, but just the final product paxilline. These results confirmed that *paxG* and *paxC* present at either end of the *Hin*dIII restriction fragment were functional.

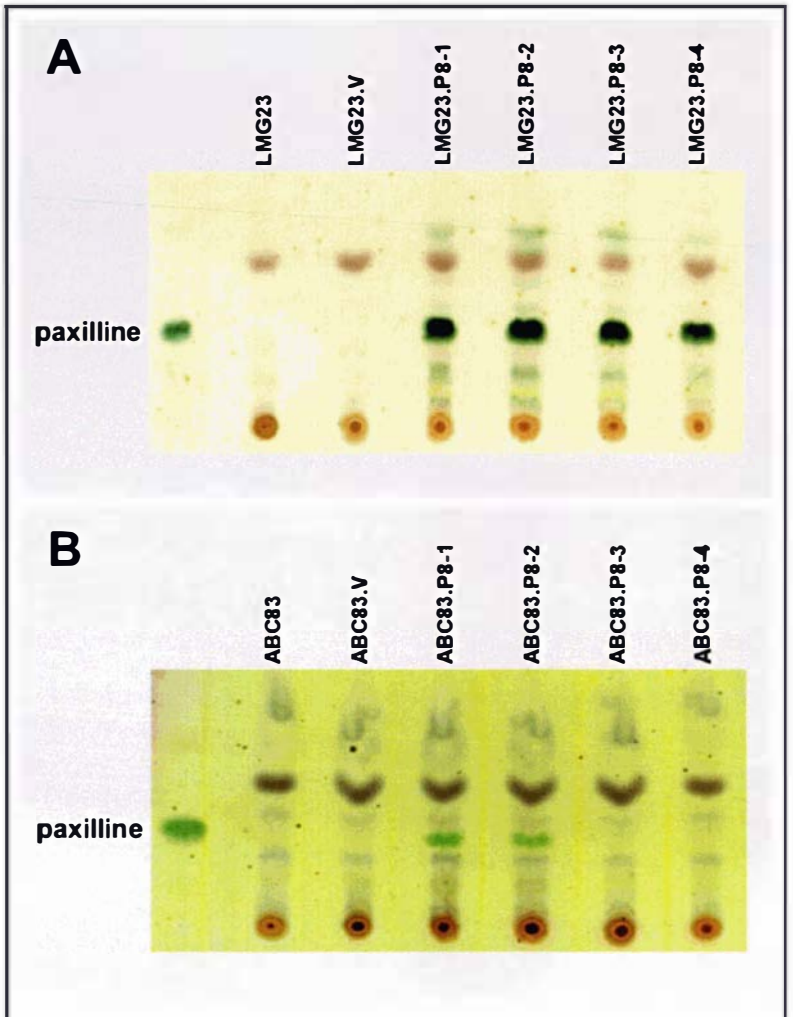

Figure 3.2 Normal Phase (NP)-TLC analysis of *paxG* and *paxC* complementations

NP-TLC analysis of **(A)** *paxGA* deletion mutant LMG23 and **(B)** *paxC* deletion mutant ABC83, containing the complementation construct pSS8 (*paxGAMBC*). Mycelium was grown for 7 days in CDYE, supplemented with trace element mix (Section 2.3.2), at 28ºC with shaking at 200 rpm, freeze-dried and extracted in 2:1 chloroform-methanol mixture (Section 2.21). V=pII99 vector; P8=pSS8.

3.1.2 pSS8 transformation of *pax* deletion mutants LM662 and CY2

In order to define the minimum number of genes required for paspaline biosynthesis pSS8 was introduced into two different genetic backgrounds. The first was LM662 (Young *et al.*, 2001) that lacks the entire *pax* cluster i.e. *paxG*, *paxA*, *paxM*, *paxB*, *paxC*, *paxP* and *paxQ*. The other background was CY2 (Young *et al.*, 1998) that lacks the entire *pax* cluster plus considerable flanking sequences. The reason for selecting two different *pax* negative backgrounds was to check if there were any other *pax* genes outside the region defined by the LM662 deletion. Protoplasts of LM662 and CY2 were transformed with 5 μg of circular pII99 or pSS8 (Section 2.13.2) and geneticin-resistant transformants selected on RG medium supplemented with 150 μg/ml of geneticin.

Twelve geneticin-resistant LM662/pSS8 transformants were arbitrarily selected and screened for integration of the pSS8 insert by PCR amplification (Section 2.14.2) with primer sets designed to amplify each end of the insert (Figure 3.3A). Seven out of twelve transformants were found to have both products. The absence of PCR products with *pax* primers was not due to DNA template quality as confirmed by the presence of products in all templates when amplified with primers to *tub2*. These positive transformants were analysed further by Southern blotting and hybridisation (Section 2.10) using a [^{32}P]-labelled *Hin*dIII fragment from pSS8 as the probe (Figure 3.3B). This analysis showed that all seven transformants contained at least one complete copy of the *Hin*dIII fragment. The copy number was calculated by comparing the signal obtained with wild-type. By this comparison, the additional weaker hybridising bands found in some transformants could be due to the integration of partial copies of the insert.

Extracts of the seven transformants that contained the pSS8 insert were then analysed by TLC (Section 2.21) for indole-diterpenes (Figure 3.4A). A green band with an R_f value similar to authentic paspaline was visible for three of the seven transformants viz. LM662.P8-3, LM662.P8-9 and LM662.P8-12. These transformants had at least three copies of the *Hin*dIII fragment containing *paxGAMBC* (Figure 3.3B). Extracts of all seven LM662/pSS8 transformants

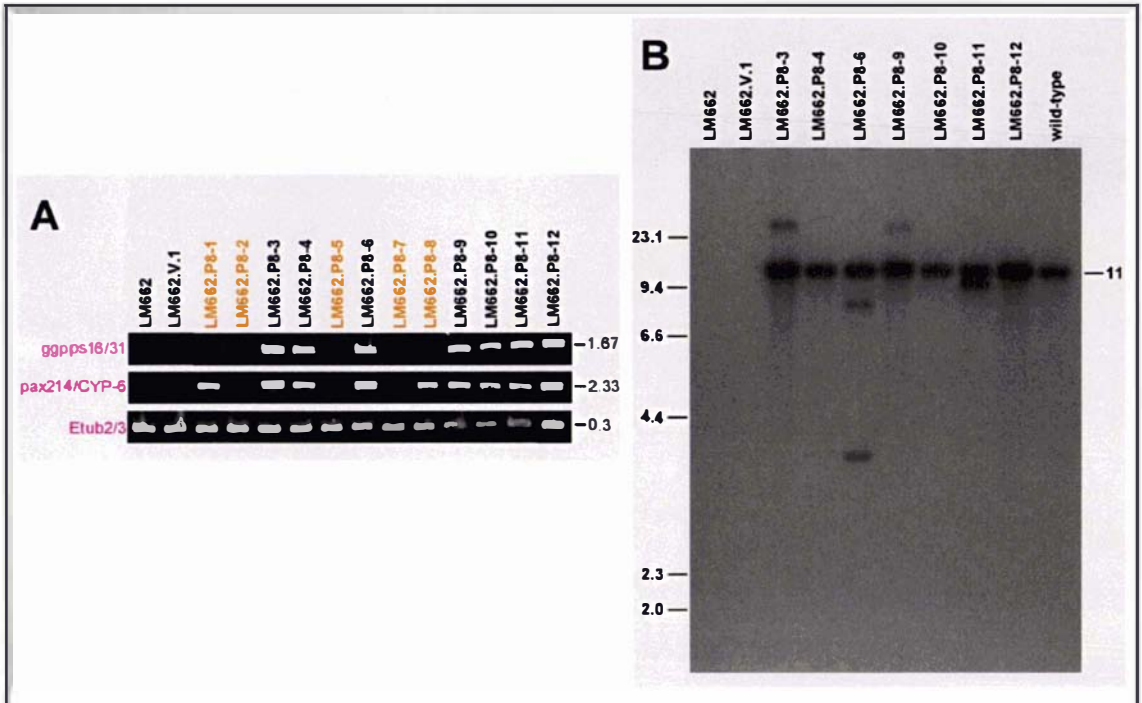

Figure 3.3 PCR screening and Southern analysis of LM662 transformants containing pSS8 (*paxGAMBC*)

(A) PCR screening for pSS8 (*paxGAMBC*) in LM662 background. Each transformant was screened with one primer set at either end of the construct (ggpps16/31 and pax214/CYP-6). The transformants (labelled black) that gave a PCR product for both sets of primers and also LM662 and LM662.V.1 (negative control and vector only control, respectively) were screened further by Southern analysis as shown in (B). See Figure 3.1 for primer positions. *tub2* was used as a control (amplified with primer set Etub2/3). **(B)** Southern analysis of LM662/*paxGAMBC* transformants. *Hin*dIII-digested genomic DNA from LM662/*paxGAMBC* transformants hybridised with the [^{32}P]-labelled *Hin*dIII fragment from the pSS8 construct. The numbers on the left correspond to the sizes of λDNA/*Hin*dIII fragments and that on the right correspond to the expected size of the restriction fragment that hybridised to the probe.
All fragment sizes are shown in kb. P8=pSS8; V=pII99 vector.

Standard PCR components (Section 2.14.2) were used with the following thermocycle conditions: 1 cycle of 94°C for 2 min; 30 cycles of 94°C for 30 sec, 55°C for 30 sec, 72°C for either 2 min (for ggpps16/31) or 3 min (for pax214/CYP-6) or 1 min (for Etub2/3); 1 cycle of 72°C for 5 min.

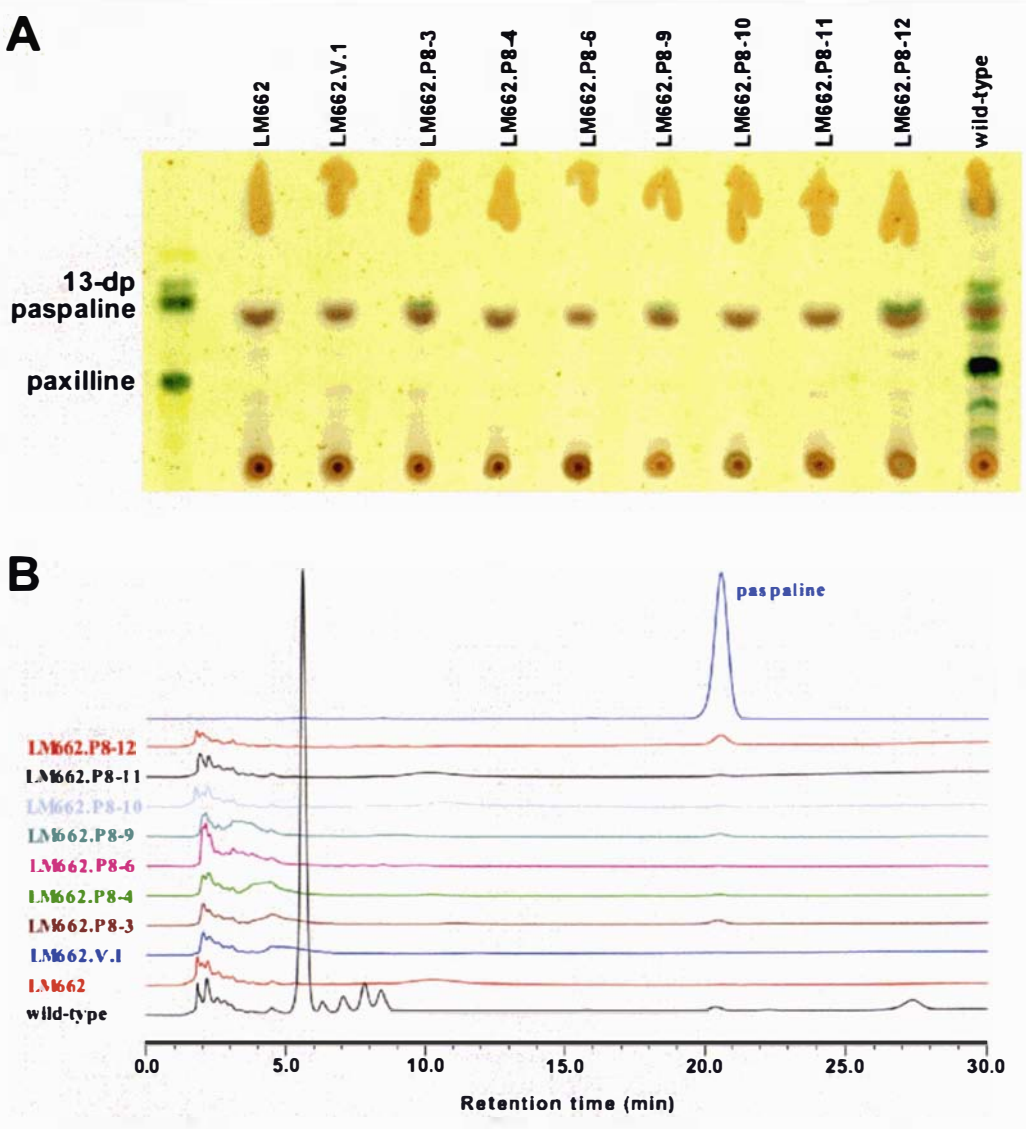

Figure 3.4 NP-TLC and Reverse Phase (RP)-HPLC analysis of LM662/pSS8 transformants

LM662 transformants containing the construct pSS8 (*paxGAMBC*) were analysed by **(A)** NP-TLC and **(B)** RP-HPLC for the presence of indole-diterpenes (Section 2.21). Mycelium was grown for 7 days in CDYE, supplemented with trace element mix (Section 2.3.2), at 28°C with shaking at 200 rpm, freeze-dried and extracted in 2:1 chloroform-methanol mixture. V=pII99 vector; P8=pSS8; 13-dp=13-desoxypaxilline.

were further analysed by HPLC (Section 2.21). This analysis showed that all transformants contained a metabolite that had the same retention time (R_t = 20.5 min) as authentic paspaline (Figure 3.4B) showing an absorption maximum at 230 nm and an absorption minimum at 280 nm characteristic of an indole moiety. The low levels of paspaline detected compared to wild-type probably reflects the ectopic integration of pSS8. The highest levels of paspaline coincided with transformants containing multiple copies of pSS8.

Ten arbitrarily selected geneticin-resistant CY2/pSS8 transformants were screened for integration of the pSS8 insert by PCR amplification (Section 2.14.2) with primer sets designed to amplify each end of the insert (Figure 3.5A). Seven out of ten transformants gave both products. All templates gave a product when amplified with primers to *tub2* confirming that the absence of products with the *pax* primers was not due to template quality. These positive transformants were further analysed by Southern blotting and hybridisation (Section 2.10) using a [^{32}P]-labelled *Hin*dIII fragment from pSS8 as the probe (Figure 3.5B). This analysis showed that at least one copy of the *Hin*dIII fragment was present in all transformants. The additional weaker hybridising bands observed in some transformants could be due to the integration of incomplete copies of the insert.

TLC analysis of extracts of the seven positive transformants (see above) showed a green band with an R_f value similar to authentic paspaline in all transformants except CY2.P8-1 (Figure 3.6A). This result was further confirmed by HPLC analysis (Figure 3.6B). The inability of the transformant CY2.P8-1 to synthesise paspaline, despite containing the five *pax* genes, could be due to the position of integration of the construct in the genome (Malonek *et al.*, 2005a).

It was confirmed that the introduction of pSS8 into LM662 and CY2 restored to these strains the ability to synthesise paspaline. The fact that both LM662/pSS8 and CY2/pSS8 transformants synthesised paspaline suggested that either genetic background was suitable for further complementation analysis and that there were no other *pax* genes outside the region defined by

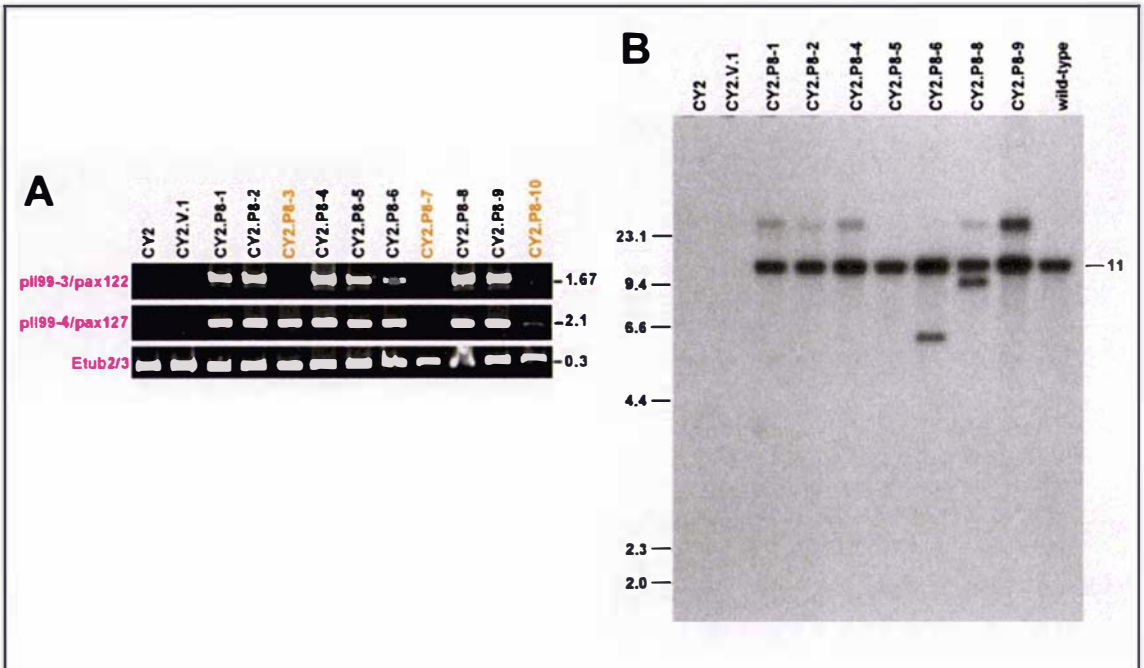

Figure 3.5 PCR screening and Southern analysis of CY2 transformants containing pSS8 (*paxGAMBC*)

(A) PCR screening for pSS8 (*paxGAMBC*) in CY2 background. Each transformant was screened with one primer set at either end of the construct (pII99-3/pax122 and pII99-4/pax127). The transformants (labelled black) that gave a PCR product for both sets of primers and also CY2 and CY2.V.1 (negative control and vector only control, respectively) were screened further by Southern analysis as shown in (B). See Figure 3.1 for primer positions. *tub2* was used as a control (amplified with primer set Etub2/3). **(B)** Southern analysis of CY2/*paxGAMBC* transformants. *Hin*dIII-digested genomic DNA from CY2/*paxGAMBC* transformants hybridised with the [^{32}P]-labelled *Hin*dIII fragment from the pSS8 construct. The numbers on the left correspond to the sizes of λDNA/*Hin*dIII fragments and that on the right correspond to the expected size of the restriction fragment that hybridised to the probe.
All fragment sizes are shown in kb. P8=pSS8; V=pII99 vector.

Standard PCR components (Section 2.14.2) were used with the following thermocycle conditions: 1 cycle of 94°C for 2 min; 30 cycles of 94°C for 30 sec, 55°C for 30 sec, 72°C for either 2 min (for pII99-3/pax122) or 3 min (for pII99-4/pax127) or 1 min (for Etub2/3); 1 cycle of 72°C for 5 min.

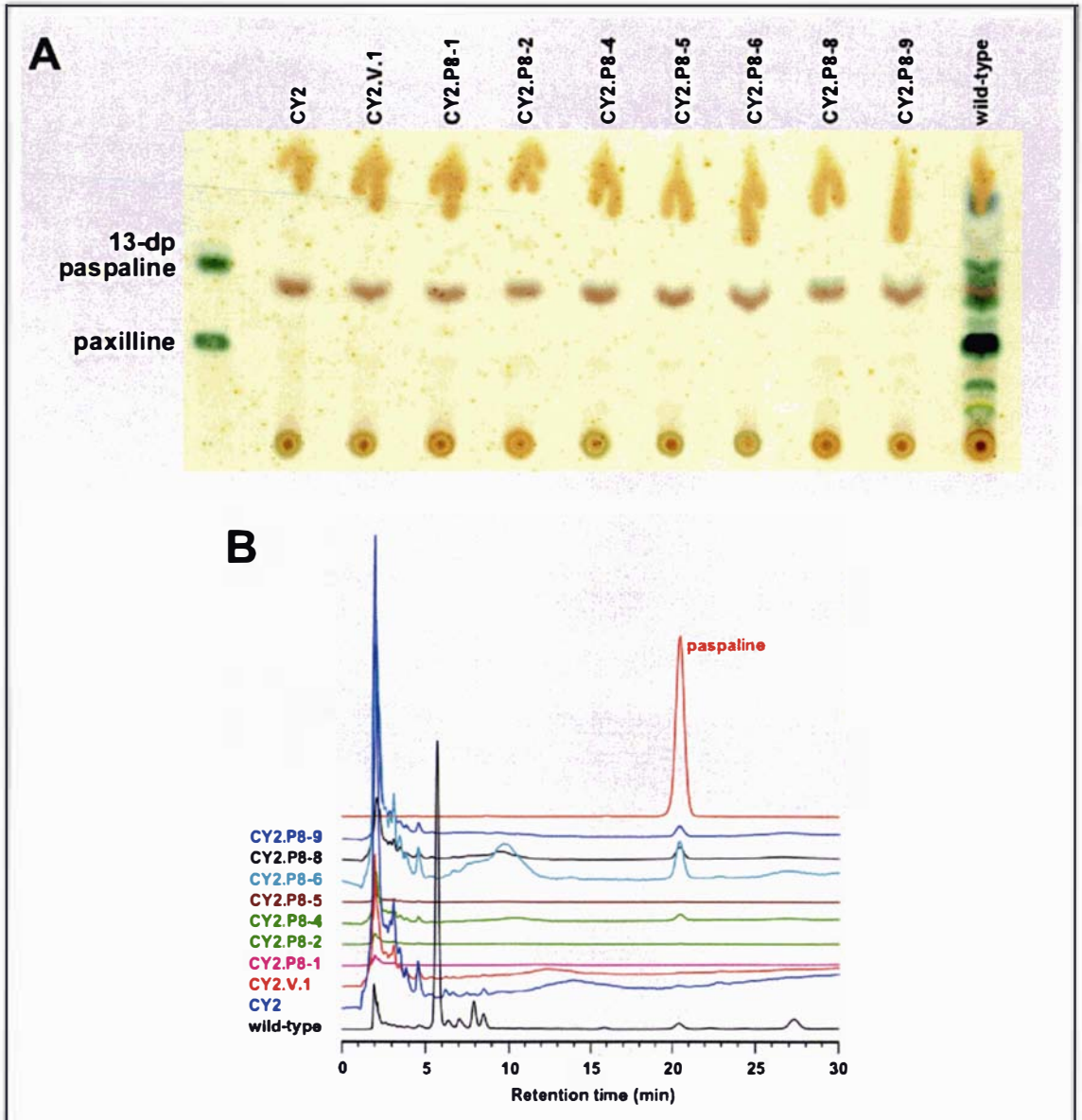

Figure 3.6 NP-TLC and RP-HPLC analysis of CY2/pSS8 transformants

CY2 transformants containing the construct pSS8 (*paxGAMBC*) were analysed by **(A)** NP-TLC and **(B)** RP-HPLC for the presence of indole-diterpenes (Section 2.21). Mycelium was grown for 7 days in CDYE, supplemented with trace element mix (Section 2.3.2), at 28ºC with shaking at 200 rpm, freeze-dried and extracted in 2:1 chloroform-methanol mixture. V=pII99 vector; P8=pSS8; 13-dp=13-desoxypaxilline.

the LM662 deletion. Hence, only one genetic background i.e. CY2 was used for further transformations.

3.1.3 Preparation of pSS16

To determine if the combination of *paxG*, *paxM* and *paxC* would be able to restore the paspaline biosynthesis ability to the *pax* deletion mutant CY2, the construct pSS16 was prepared. A *paxM* fragment containing 479 bp of the sequence 5' of the *paxM* ATG, all 1559 bp of the *paxM* gene sequence and 282 bp of the 3' sequence was amplified from pSS8 (Section 2.14.3) using the primers paxMSpeF2 and paxMSpeR, both with introduced *Spe*I sites (Figure 3.7). The product was subcloned into pGEM®-T Easy vector (Promega) to generate the plasmid pSS11 and subsequently sequenced. Sequence analysis showed no PCR-introduced errors. The *Spe*I fragment from this plasmid, containing *paxM*, was used to replace the *Spe*I fragment from pSS8, containing *paxA-paxM-paxB*, to generate pSS16 (*paxGMC*).

3.1.4 pSS16 transformation of *pax* deletion mutant CY2

Protoplasts of CY2 were transformed with 5 µg of circular pII99 or pSS16 and geneticin resistant transformants selected on RG medium supplemented with 150 µg/ml of geneticin (Section 2.13.2). Ten arbitrarily selected geneticin-resistant CY2/pSS16 transformants were screened for integration of the insert pSS16 by PCR (Section 2.14.2) using primer sets designed to amplify both ends of the insert (Figure 3.8A). Nine out of ten transformants gave both products. As a control for the quality of the DNA template *tub2* was amplified and this confirmed that the absence of products with *pax* primers was not due to template quality. These transformants were further analysed by Southern blotting and hybridisation (Section 2.10) using a [^{32}P]-labelled *Hin*dIII restriction fragment from pSS8 as the probe (Figure 3.8B). Since the *Spe*I fragment (5004 bp) in pSS8 was replaced by a *Spe*I-digested *paxM* PCR product of 2538 bp, the size of the *Hin*dIII-hybridising fragment in CY2/pSS16 transformants (~8.53 kb) was different from that in wild-type (~11 kb). Southern data showed that all CY2/pSS16 transformants had at least three copies of the *Hin*dIII fragment containing *paxGMC*, except CY2.P16-3, which did not contain any complete copies of the restriction fragment.

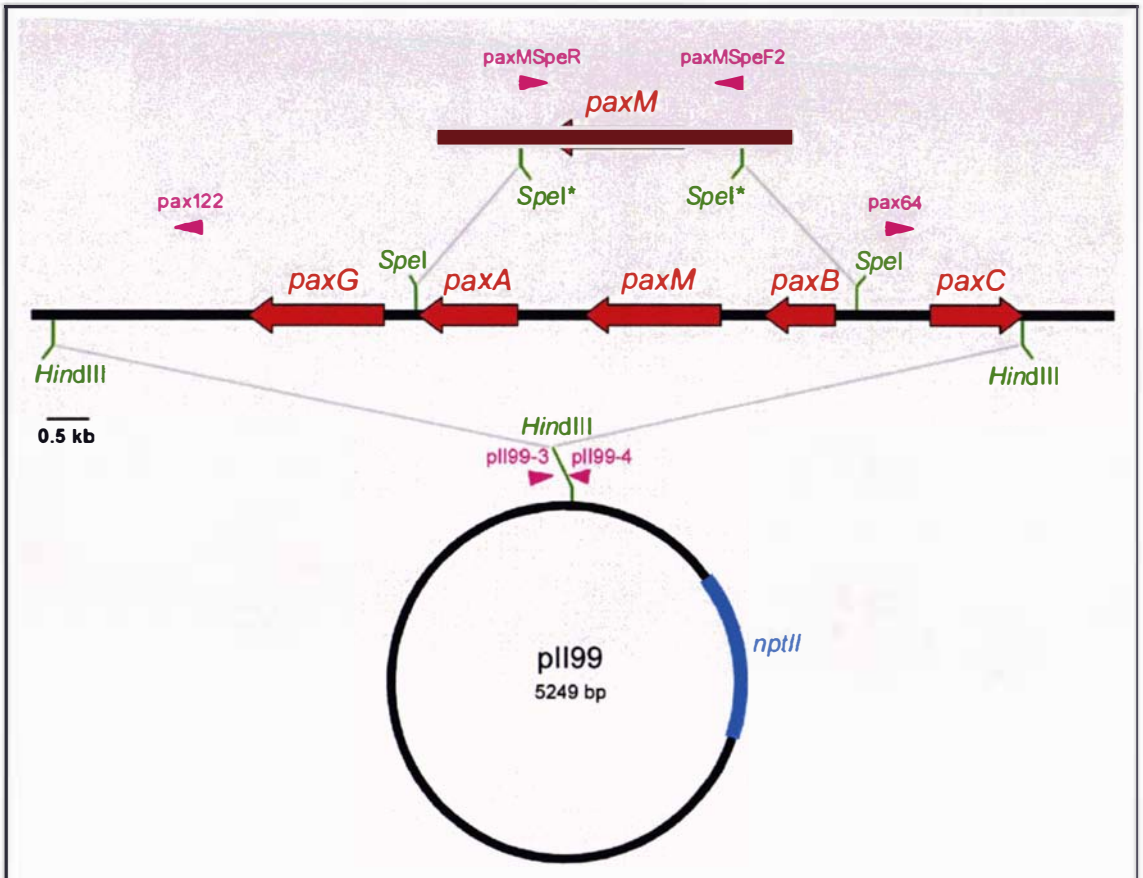

Figure 3.7 pSS16 (*paxGMC*) construct

The construct pSS16 was made by replacing the *Spe*I fragment containing *paxA*, *paxM* and *paxB* from pSS8 with a copy of *paxM* amplified with Expand High Fidelity PCR System using the primer pair paxMSpeF2 and paxMSpeR.
Restriction sites used for cloning and positions of primers used for PCR and screening transformants are shown in green and pink, respectively. * indicates restriction site introduced by PCR.

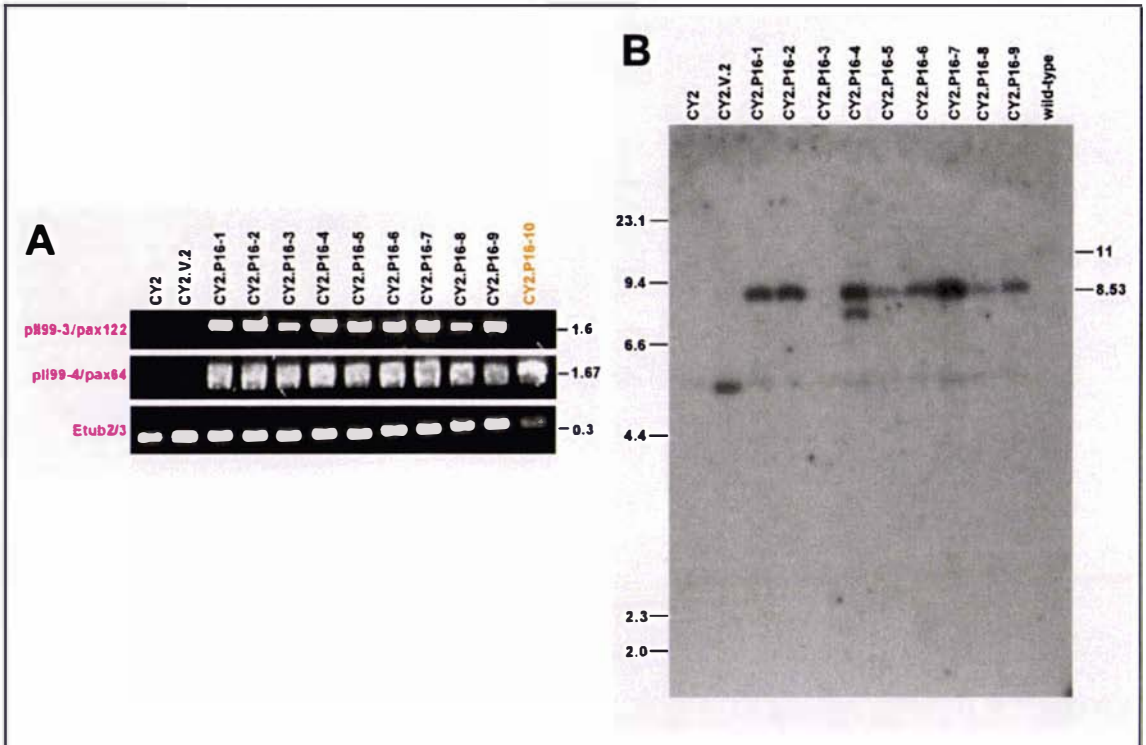

Figure 3.8 PCR screening and Southern analysis of CY2 transformants containing pSS16 (*paxGMC*)

(A) PCR screening for pSS16 (*paxGMC*) in CY2 background. Each transformant was screened with one primer set at either end of the construct (pII99-3/pax122 and pII99-4/pax64). The transformants (labelled black) that gave a PCR product for both sets of primers and also CY2 and CY2.V.2 (negative control and vector only control, respectively) were screened further by Southern analysis as shown in (B). See Figure 3.7 for primer positions. *tub2* was used as a control (amplified with primer set Etub2/3). **(B)** Southern analysis of CY2/*paxGMC* transformants. *Hin*dIII-digested genomic DNA from CY2/*paxGMC* transformants hybridised with the [^{32}P]-labelled *Hin*dIII fragment from the pSS8 construct. The numbers on the left correspond to the sizes of λDNA/*Hin*dIII fragments and those on the right correspond to the expected sizes of the restriction fragments that hybridised to the probe.
All fragment sizes are shown in kb. P16=pSS16; V=pII99 vector.

Standard PCR components (Section 2.14.2) were used with the following thermocycle conditions: 1 cycle of 94°C for 2 min; 30 cycles of 94°C for 30 sec, 55°C for 30 sec, 72°C for either 2 min (for pII99-3/pax122 and pII99-4/pax64) or 1 min (for Etub2/3); 1 cycle of 72°C for 5 min.

The TLC analysis (Section 2.21) of extracts of CY2/pSS16 transformants containing the pSS16 insert showed no detectable indole-diterpenes (Figure 3.9A). This was further confirmed by HPLC analysis (Section 2.21) (Figure 3.9B). These results confirmed that the introduction of pSS16 into CY2 was not sufficient to restore the ability to synthesise paspaline.

3.1.5 Preparation of pSS20

Since the introduction of pSS16 into CY2 failed to restore the ability to synthesise paspaline the construct pSS20 containing *paxGAMC* was prepared. To prepare this construct, a *paxA-paxM* fragment containing 479 bp of the sequence 5' of the *paxM* ATG, all 1559 bp of the *paxM* gene sequence, all 752 bp of the sequence between *paxM* and *paxA*, all 1131 bp of the *paxA* gene sequence and 22 bp of the sequence flanking the 3' end of *paxA* was PCR amplified from wild-type genomic DNA (Section 2.14.4) using the primers SS9 and paxMSpeF1, containing native and introduced *Spe*I sites, respectively (Figure 3.10). The *paxA-paxM* PCR product was subcloned into pGEM®-T Easy vector (Promega) to generate pSS19 and subsequently sequenced. A clone without any PCR-introduced error was then used to obtain the *Spe*I fragment, containing *paxA-paxM*, which was then ligated into the *Spe*I site of pSS8 to generate pSS20.

3.1.6 pSS20 transformation of *pax* deletion mutant CY2

Protoplasts of CY2 were transformed with 5 µg of circular pII99 or pSS20 and geneticin-resistant transformants selected on RG medium supplemented with 150 µg/ml of geneticin (Section 2.13.2). Ten arbitrarily selected geneticin resistant CY2/pSS20 transformants were screened for integration of the pSS20 insert by PCR (Section 2.14.2) using primer sets designed to amplify each end of the insert (Figure 3.11A). Eight out of ten transformants showed both products. The absence of PCR products in two transformants was not due to template quality as confirmed by the amplification of *tub2* product in these transformants. The positive transformants were further analysed by Southern blotting and hybridisation (Section 2.10) using a [^{32}P]-labelled *Hin*dIII restriction fragment from pSS8 as the probe (Figure 3.11B). In these transformants the size of the hybridising fragment (~9.94 kb) was different from that in wild-type

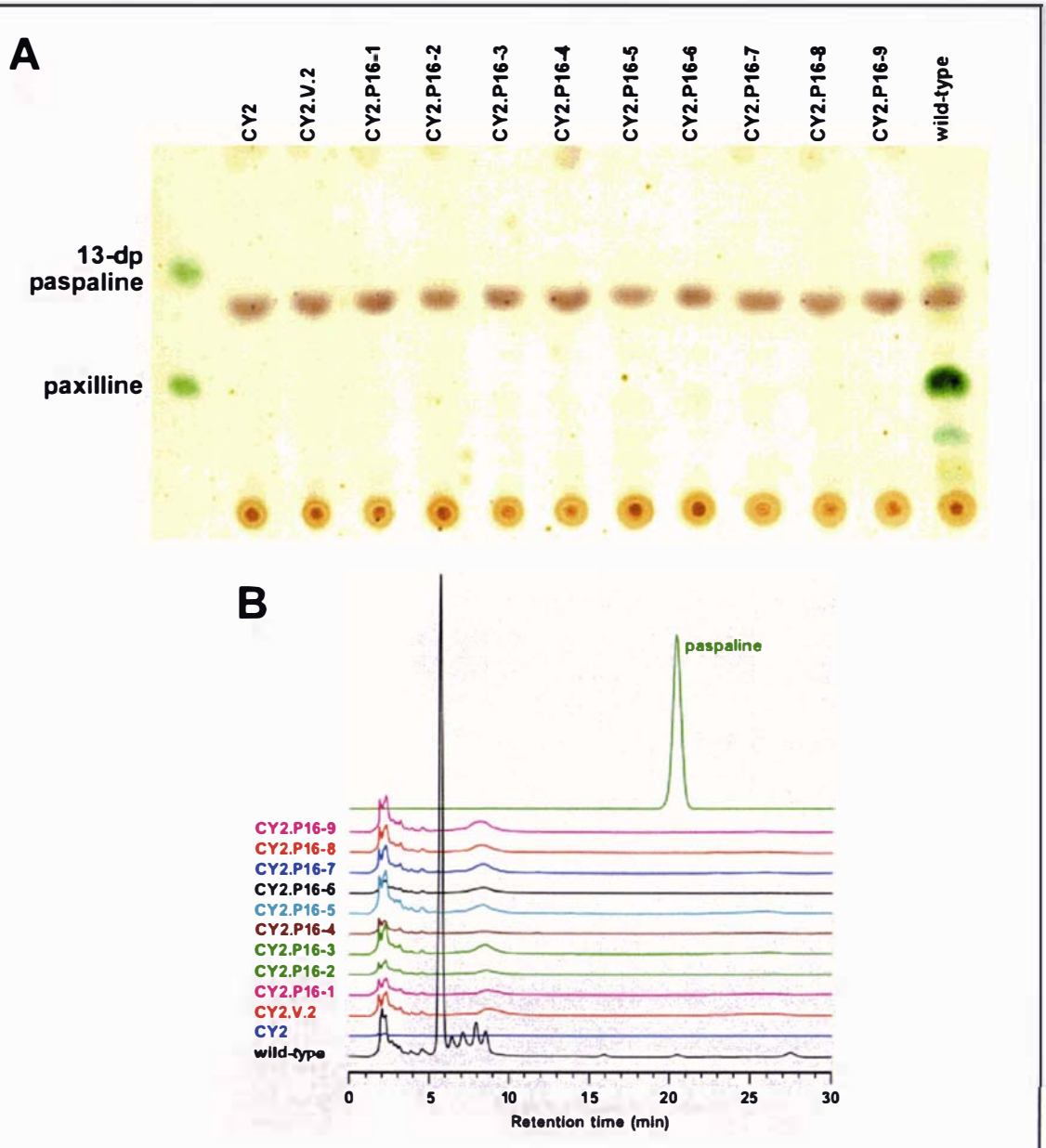

Figure 3.9 NP-TLC and RP-HPLC analysis of CY2/pSS16 transformants

CY2 transformants containing the construct pSS16 (*paxGMC*) were analysed by **(A)** NP-TLC and **(B)** RP-HPLC for the presence of indole-diterpenes (Section 2.21). Mycelium was grown for 7 days in CDYE, supplemented with trace element mix (Section 2.3.2), at 28ºC with shaking at 200 rpm, freeze-dried and extracted in 2:1 chloroform-methanol mixture. V=pII99 vector; P16=pSS16; 13-dp=13-desoxypaxilline.

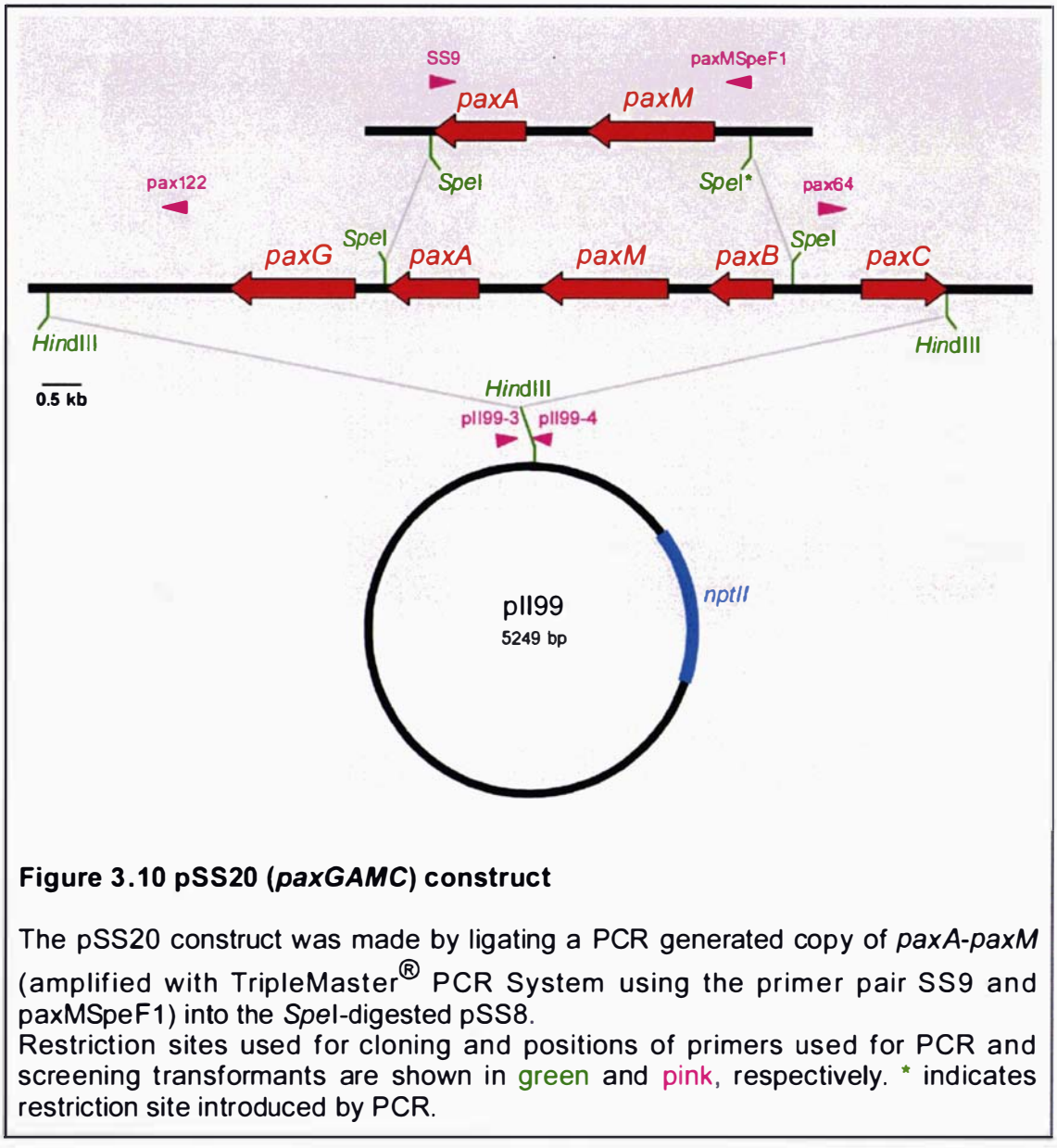

Figure 3.10 pSS20 (*paxGAMC*) construct

The pSS20 construct was made by ligating a PCR generated copy of *paxA-paxM* (amplified with TripleMaster® PCR System using the primer pair SS9 and paxMSpeF1) into the *Spe*I-digested pSS8.
Restriction sites used for cloning and positions of primers used for PCR and screening transformants are shown in green and pink, respectively. * indicates restriction site introduced by PCR.

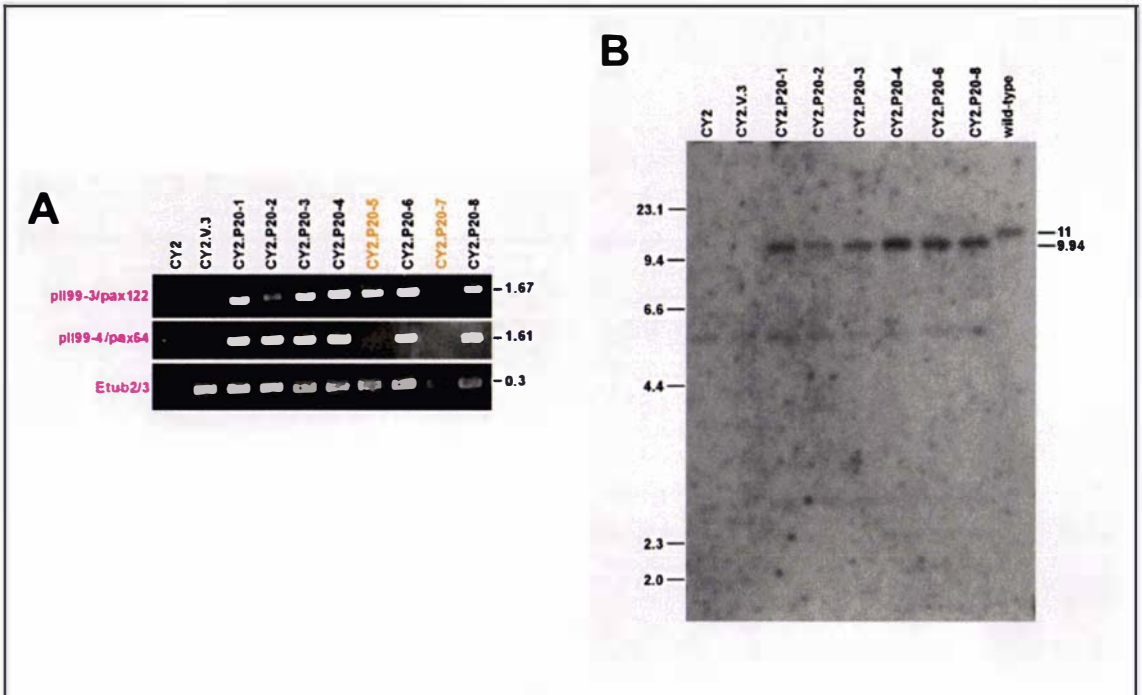

Figure 3.11 PCR screening and Southern analysis of CY2 transformants containing pSS20 (*paxGAMC*)

(A) PCR screening for pSS20 (*paxGAMC*) in CY2 background. Each transformant was screened with one primer set at either end of the construct (pII99-3/pax122 and pII99-4/pax64). The transformants (labelled black) that gave a PCR product for both sets of primers and also CY2 and CY2.V.3 (negative control and vector only control, respectively) were screened further by Southern analysis as shown in (B). See Figure 3.10 for primer positions. *tub2* was used as a control (amplified with primer set Etub2/3). **(B)** Southem analysis of CY2/*paxGAMC* transformants. *Hin*dIII-digested genomic DNA from CY2/*paxGAMC* transformants hybridised with the [^{32}P]-labelled *Hin*dIII fragment from the pSS8 construct. The numbers on the left correspond to the sizes of λDNA/*Hin*dIII fragments and those on the right correspond to the expected sizes of the restriction fragments that hybridised to the probe.
All fragment sizes are shown in kb. P20=pSS20; V=pII99 vector.

Standard PCR components (Section 2.14.2) were used with the following thermocycle conditions: 1 cycle of 94°C for 2 min; 30 cycles of 94°C for 30 sec, 55°C for 30 sec, 72°C for either 2 min (for pII99-3/pax122 and pII99-4/pax64) or 1 min (for Etub2/3); 1 cycle of 72°C for 5 min.

(~11 kb), since the *Spe*I fragment (5004 bp) from pSS8 was replaced by the *Spe*I-digested *paxA-paxM* PCR product of 3955 bp. The Southern hybridisation data showed that all CY2/SS20 transformants had at least one copy of the *Hin*dIII fragment containing *paxGAMC*.

Analysis of extracts (Section 2.21) of CY2/pSS20 transformants showed that all transformants were negative for any indole-diterpene (Figure 3.12A & B). Thus, the introduction of pSS20 into CY2 mutant was unable to restore to these strains the ability to synthesise paspaline.

3.1.7 Preparation of pSS17

The results described above showed that combinations of *paxGMC* and *paxGAMC* failed to restore the paspaline biosynthesis ability to CY2. To test if the *paxGMBC* combination was able to restore the paspaline biosynthesis ability, the construct pSS17 containing *paxGMBC* was prepared. In order to prepare this construct a *paxM-paxB* fragment containing 251 bp of the sequence 5' of the *paxB* ATG, all 819 bp of the *paxB* gene sequence, all 479 bp of the sequence between *paxB* and *paxM*, all 1559 bp of the *paxM* gene sequence and 282 bp of the sequence flanking the 3' end of *paxM* was PCR amplified from pSS8 (Section 2.14.3) using the primers paxMSpeR and SS8, containing introduced and native *Spe*I sites, respectively (Figure 3.13). The *paxM-paxB* PCR product was subcloned into pGEM®-T Easy vector (Promega) to create the plasmid pSS15 and subsequently sequenced. Error-free clones were selected to obtain the *Spe*I fragment containing *paxM-paxB*, which was then ligated into *Spe*I-digested pSS8 generating the construct pSS17.

3.1.8 pSS17 transformation of *pax* deletion mutant CY2

Protoplasts of CY2 were transformed with 5 µg of circular pII99 or pSS17 and the geneticin-resistant transformants selected on RG medium supplemented with 150 µg/ml of geneticin (Section 2.13.2). Ten arbitrarily selected geneticin-resistant CY2/pSS17 transformants were screened for integration of the pSS17 insert by PCR amplification (Section 2.14.2) using primer sets designed to amplify each end of the insert (Figure 3.14A). All the transformants showed both products and were further analysed by Southern blotting and hybridisation

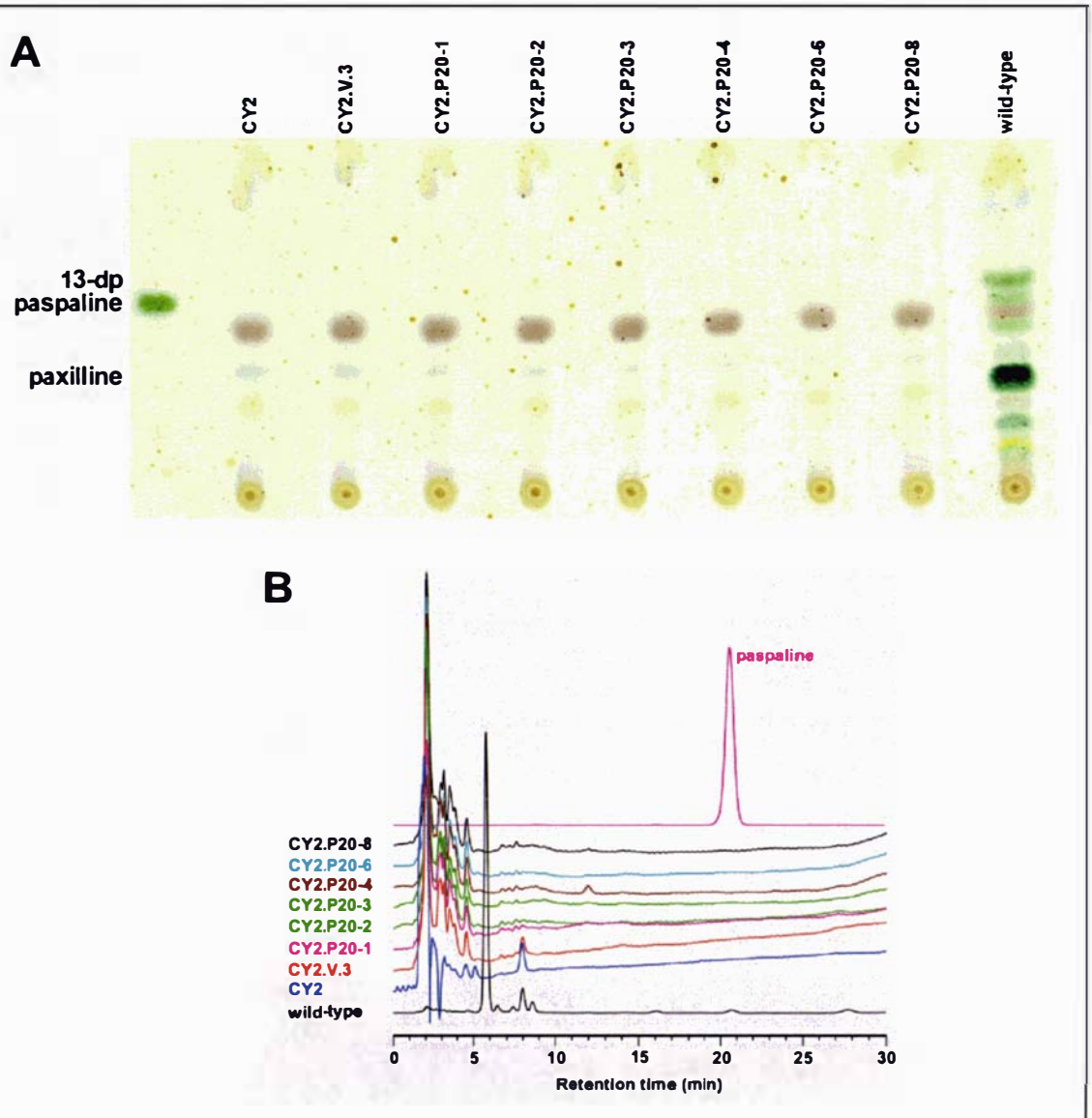

Figure 3.12 NP-TLC and RP-HPLC analysis of CY2/pSS20 transformants

CY2 transformants containing the construct pSS20 (*paxGAMC*) were analysed by **(A)** NP-TLC and **(B)** RP-HPLC for the presence of indole-diterpenes (Section 2.21). Mycelium was grown for 7 days in CDYE, supplemented with trace element mix (Section 2.3.2), at 28°C with shaking at 200 rpm, freeze-dried and extracted in 2:1 chloroform-methanol mixture. The mobility of paxilline and 13-dp is also shown on the TLC. V=pII99 vector; P20=pSS20; 13-dp=13-desoxypaxilline.

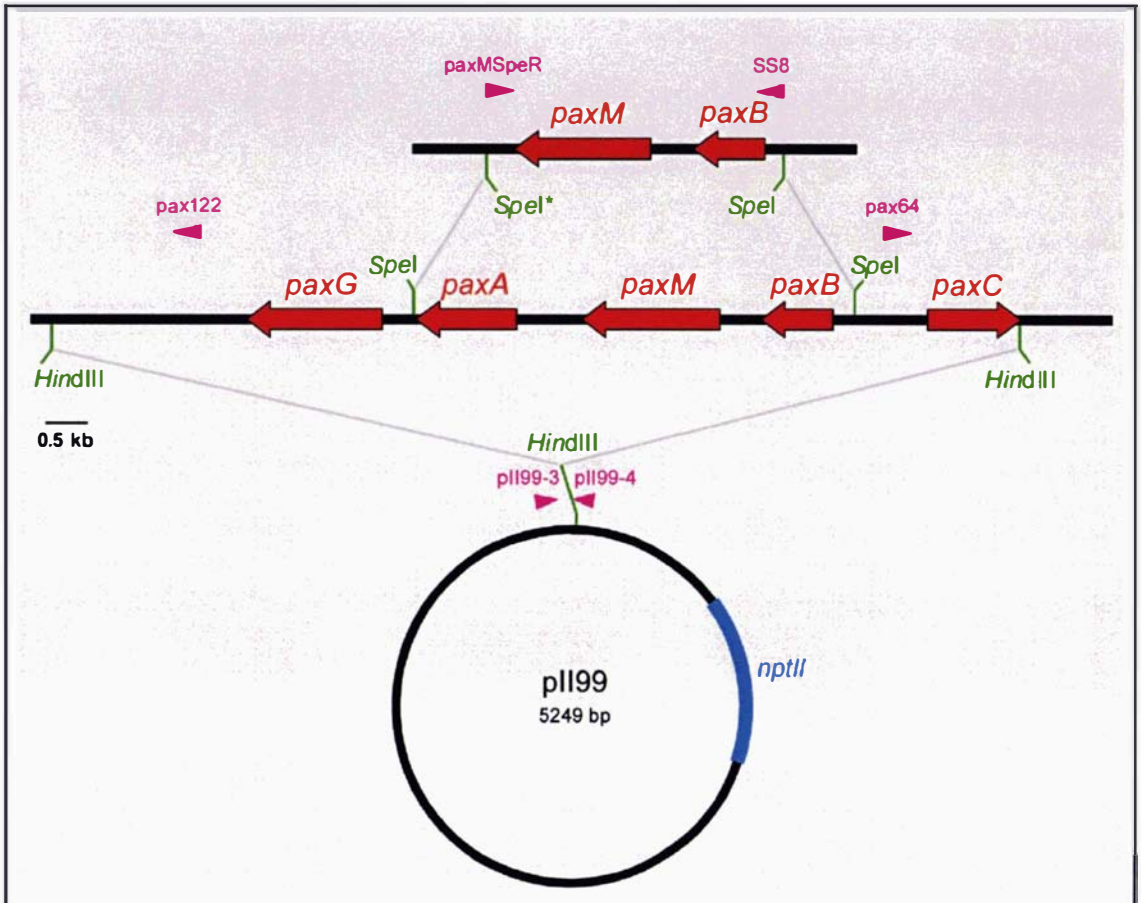

Figure 3.13 pSS17 (*paxGMBC*) construct

The construct pSS17 was made by ligating a PCR generated copy of *paxM-paxB* (amplified with Expand High Fidelity PCR System using the primer pair SS8 and paxMSpeR) into the *Spe*I-digested pSS8.
Restriction sites used for cloning and positions of primers used for PCR and screening transformants are shown in green and pink, respectively. * indicates restriction site introduced by PCR.

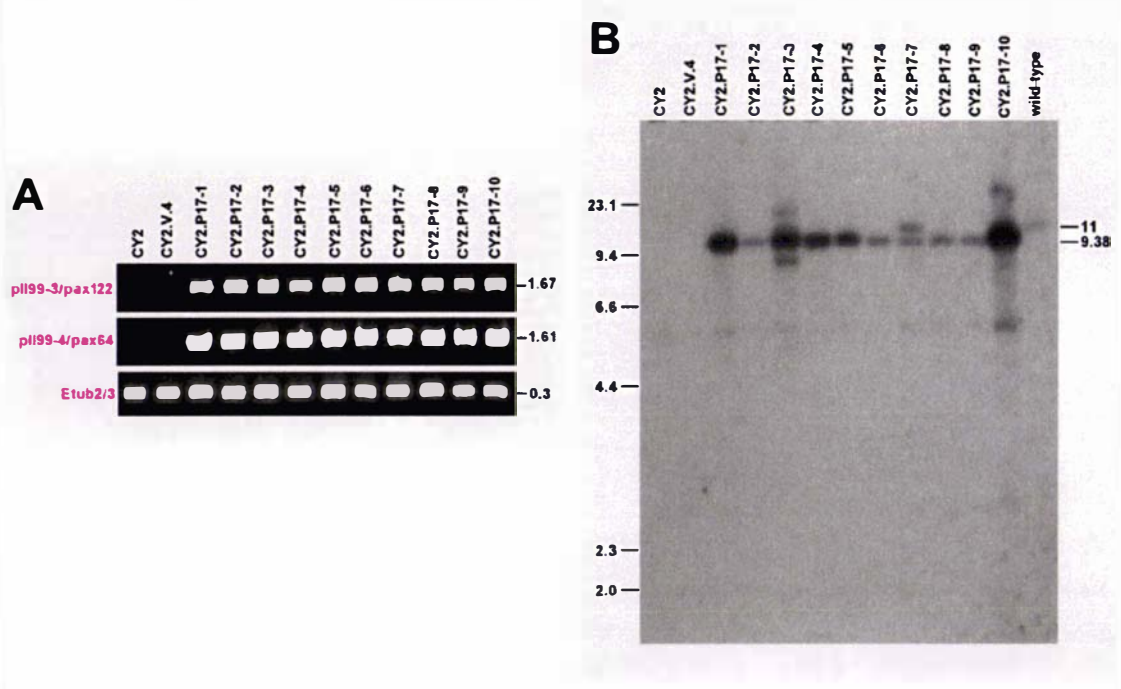

Figure 3.14 PCR screening and Southern analysis of CY2 transformants containing pSS17 (*paxGMBC*)

(A) PCR screening for pSS17 (*paxGMBC*) in CY2 background. Each transformant was screened with one primer set at either end of the construct (pII99-3/pax122 and pII99-4/pax64). The transformants (labelled black) that gave a PCR product for both sets of primers and also CY2 and CY2.V.4 (negative control and vector only control, respectively) were screened further by Southern analysis as shown in (B). See Figure 3.13 for primer positions. *tub2* was used as a control (amplified with primer set Etub2/3). **(B)** Southern analysis of CY2/*paxGMBC* transformants. *Hin*dIII-digested genomic DNA from CY2/*paxGMBC* transformants hybridised with the [^{32}P]-labelled *Hin*dIII fragment from the pSS8 construct. The numbers on the left correspond to the sizes of λDNA/*Hin*dIII fragments and those on the right correspond to the expected sizes of the restriction fragments that hybridised to the probe.
All fragment sizes are shown in kb. P17=pSS17; V=pII99 vector.

Standard PCR components (Section 2.14.2) were used with the following thermocycle conditions: 1 cycle of 94°C for 2 min; 30 cycles of 94°C for 30 sec, 55°C for 30 sec, 72°C for either 2 min (for pII99-3/pax122 and pII99-4/pax64) or 1 min (for Etub2/3); 1 cycle of 72°C for 5 min.

(Section 2.10) using a [^{32}P]-labelled *Hin*dIII restriction fragment from pSS8 as the probe (Figure 3.14B). In CY2/pSS17 transformants the size of the hybridising fragment (~9.38 kb) was different from that in wild-type (~11 kb) since the *Spe*I fragment (5004 bp) from pSS8 was replaced by the *Spe*I digested *paxM-paxB* PCR product of 3392 bp. The Southern hybridisation data showed that all transformants had at least two copies of the *Hin*dIII fragment containing *paxGMBC*.

TLC analysis (Section 2.21) of extracts of CY2/pSS17 transformants showed that three out of ten transformants viz. CY2.P17-3, CY2.P17-4, CY2.P17-10 had a green band with an R_f value similar to authentic paspaline (Figure 3.15A). On HPLC analysis (Section 2.21), one more transformant, CY2.P17-1, was found to contain the same metabolite with retention time (R_t = 20.5 min) similar to authentic paspaline (Figure 3.15B). These results showed that the introduction of pSS17 into CY2 mutant was able to restore to this strain the ability to synthesise paspaline.

In addition to paspaline, another green band, indicated by red rectangles in Figure 3.15A, was visible in extracts of the transformants CY2.P17-1, CY2.P17-3 and CY2.P17-4 that was not present in extracts of wild-type *P. paxilli*. The presence of this novel indole-diterpene metabolite was confirmed by HPLC analysis and had a retention time of 10.5 min (Figure 3.15B). However, this novel metabolite was not detected in CY2.P17-10 in which high levels of paspaline were detected.

In order to confirm the identity of the novel metabolite, an extract of CY2.P17-3 was analysed by LC-MSMS (Section 2.21) (Figure 3.16 & Figure 3.17). This analysis confirmed the presence of two major indole-diterpenes both with *m/z* values of 422 and with R_t 15.8 min and 24.2 min in the CY2.P17-3 extract (Figure 3.16). The fragmentation pattern of the metabolite eluting at 24.2 min was consistent with that of authentic paspaline (Figure 3.17). The fragmentation pattern of the metabolite eluting at 15.8 min was very similar to that of paspaline and showed just loss of two water molecules, while PC-M6 (the only other known indole-diterpene with an *m/z* of 422) shows loss of three

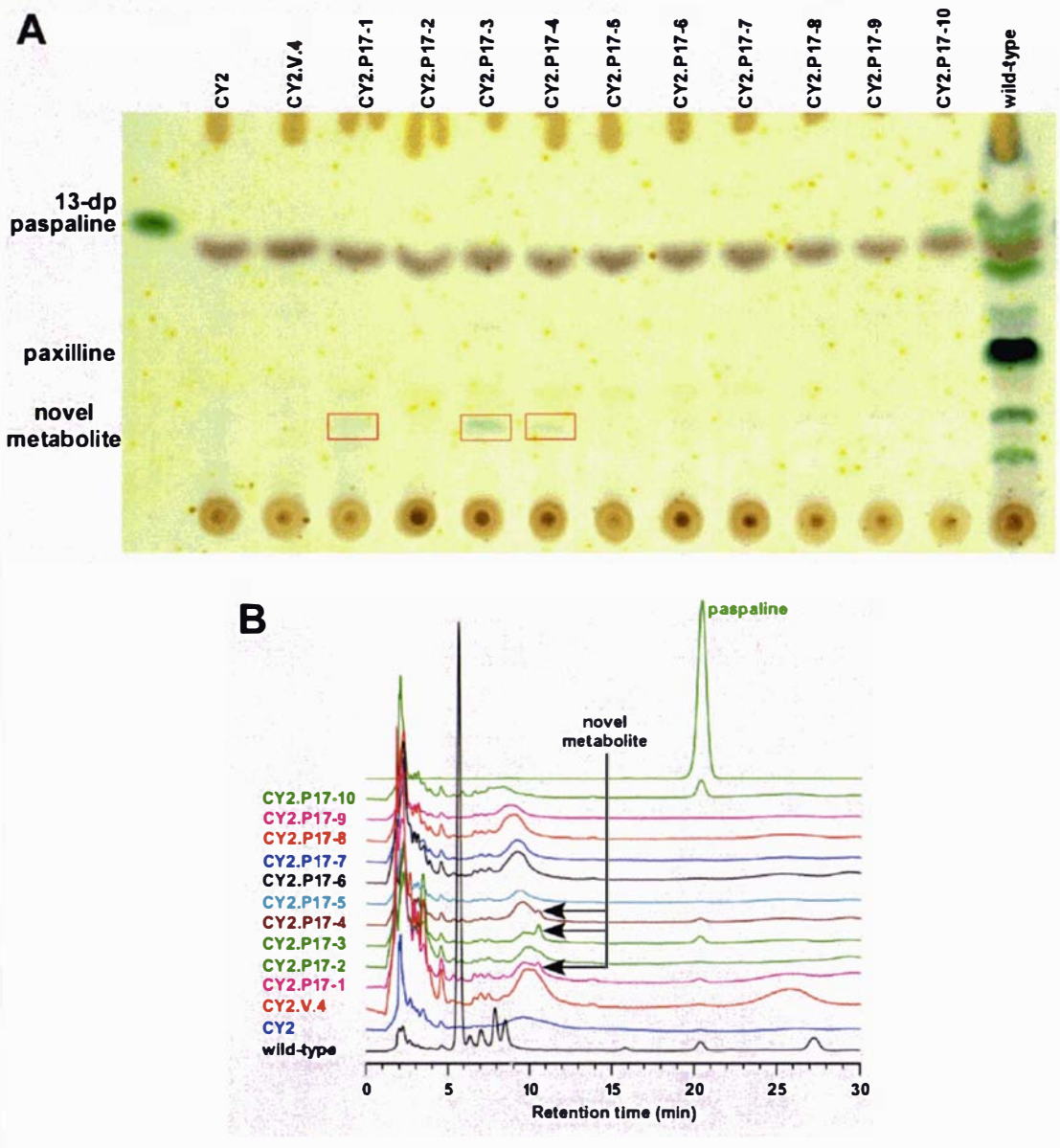

Figure 3.15 NP-TLC and RP-HPLC analysis of CY2/pSS17 transformants

CY2 transformants containing the construct pSS17 (*paxGMBC*) were analysed by **(A)** NP-TLC and **(B)** RP-HPLC for the presence of indole-diterpenes (Section 2.21). Mycelium was grown for 7 days in CDYE, supplemented with trace element mix (Section 2.3.2), at 28ºC with shaking at 200 rpm, freeze-dried and extracted in 2:1 chloroform-methanol mixture. The mobility of novel metabolite (marked by red rectangles), paxilline and 13-dp is also shown on the TLC. V=pII99 vector; P17=pSS17; 13-dp=13-desoxypaxilline.

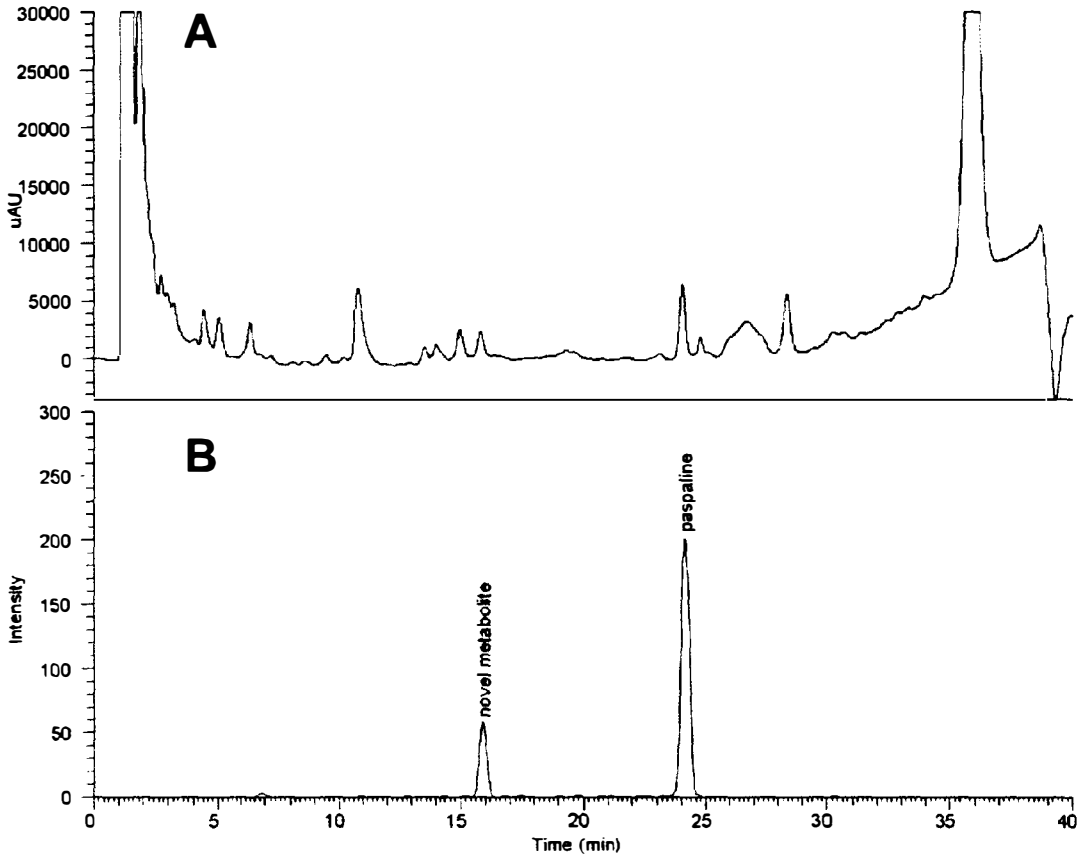

Figure 3.16 LC-MSMS analysis of CY2/pSS17 (*paxGMBC*) transformant, CY2.P17-3

Extract of CY2.P17-3, CY2 transformant containing the construct pSS17 (*paxGMBC*), was analysed by LC-MSMS (Section 2.21) for the presence of indole-diterpenes and to confirm the identity of a novel metabolite detected in the extracts by NP-TLC/ RP-HPLC analysis (See Figure 3.15). **(A)** UV trace at 275 nm. **(B)** LC-MSMS trace showing 422 ions (MS1 spectra) containing 130 *m/z* fragments characteristic of an indole moiety.

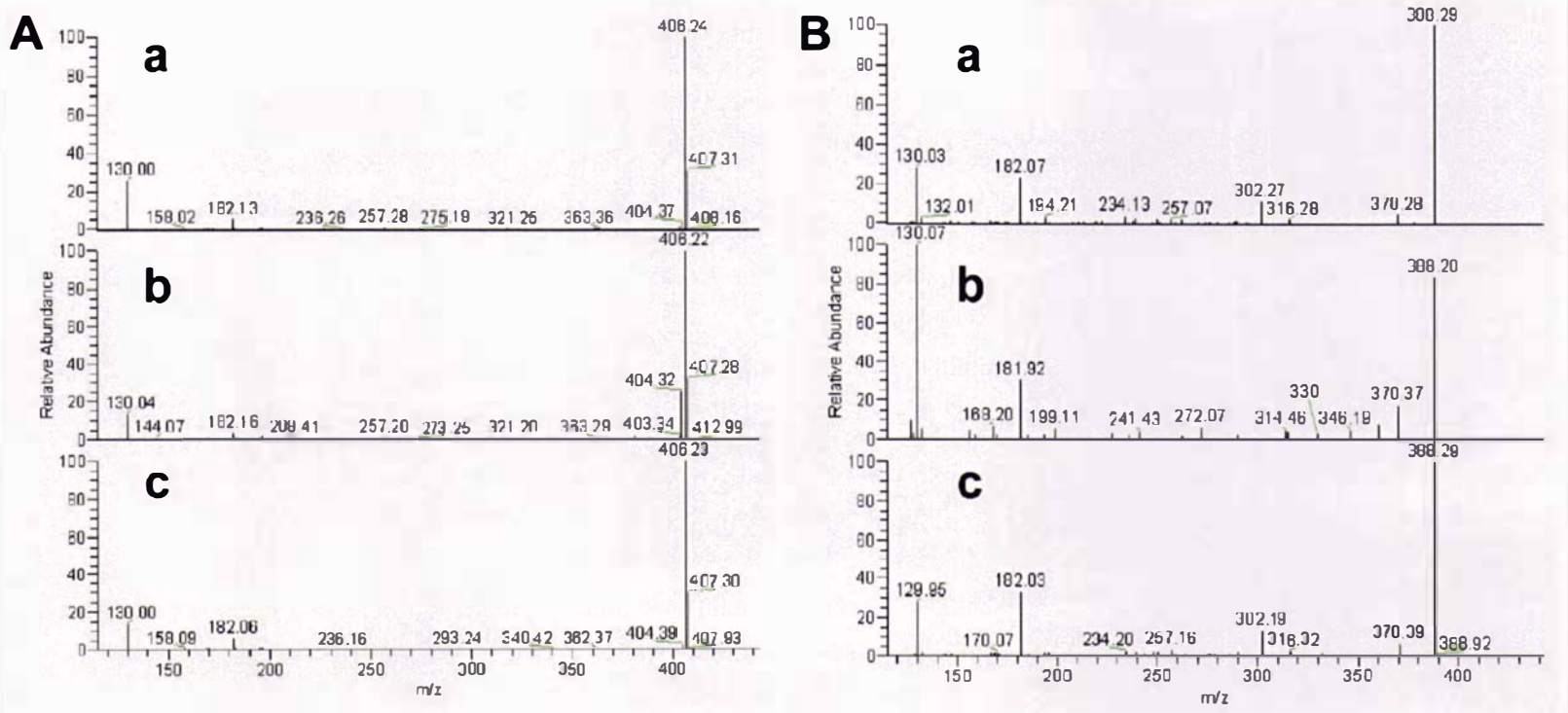

Figure 3.17 LC-MSMS analysis of CY2/pSS17 (*paxGMBC*) transformant, CY2.P17-3

Mass spectra of **(A)** 422 ions (MS2 spectra) and **(B)** 406 ions (most intense fragment in the mass spectrum of 422 *m/z*) (MS3 spectra) of (a) paspaline in CY2.P17-3, (b) novel metabolite in CY2.P17-3 and (c) authentic paspaline.

water molecules. The presence of a 406 ion, as the most intense fragment in the MS2 spectrum (Figure 3.17A), suggested the presence of a hydroxyl group at C-24 to give the ability to lose CH_4. The distinct difference between the mass spectra of the novel metabolite and paspaline was the higher intensity of the 404 ion which indicates that the oxygen in the F-ring was present as a free hydroxyl group. This was confirmed by the presence of an ion with *m/z* 330 in the MS3 spectrum (Figure 3.17B) which results from the loss of water consistent with a loss of the right end tail up to C-16. Such a loss in paspaline would be much more difficult and would result in an ion with *m/z* 332. Thus, the structure of the novel metabolite eluting at 15.8 min is predicted to be different from paspaline in having an open F-ring (Figure 3.18). The accumulation of this novel metabolite may be due to the absence of the complete paxilline biosynthetic machinery. Partial cyclisation products like emindoles and emeniveol have been isolated from *Emericella* species suggesting the possibility of alternative cyclisation pathways of indole and diterpene moieties without skeletal rearrangement or with only one epoxidation of the two terminal alkenes of the geranylgeranyl moiety (Kimura *et al.*, 1992; Nozawa *et al.*, 1988a, b; Nozawa *et al.*, 1988c).

3.1.9 Summary

The analyses of the *P. paxilli* strains containing different combinations of *pax* genes confirmed that four proteins PaxG, PaxM, PaxB and PaxC were required for the biosynthesis of the indole-diterpene paspaline. A scheme was proposed for paspaline biosynthesis (Figure 3.19) in which PaxG catalyses a series of iterative condensations of IPP with DMAPP, GPP, then FPP, to form GGPP. Although the precise details of the mechanism of condensation of the GGPP and indole moiety, and subsequent epoxidation and cyclisation events are not clear, roles for PaxM and PaxC are proposed in these steps. PaxM, a FAD-dependent monooxygenase, catalyses the epoxidation of the two terminal alkenes of the geranylgeranyl moiety of the 3-geranylgeranylindole intermediate and PaxC, a prenyl transferase, catalyses the cationic cyclisation giving rise to paspaline. The condensation of indole-3-glycerol phosphate with GGPP may be catalysed by either PaxG or PaxC. Although PaxB was required for paspaline biosynthesis, its role was not clear. The secondary structure

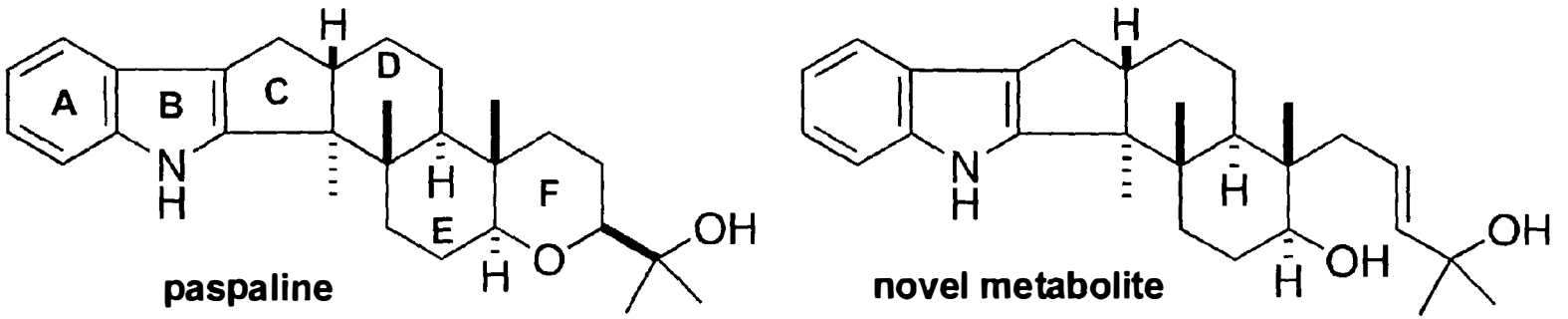

Figure 3.18 Structures of paspaline and the novel metabolite detected in the CY2/pSS17 transformant, CY2.P17-3

Based on the LC-MSMS analysis of the extract of CY2/pSS17 transformant CY2.P17-3, the novel metabolite is predicted to be a partially cyclised indole-diterpene in which the F-ring is open.

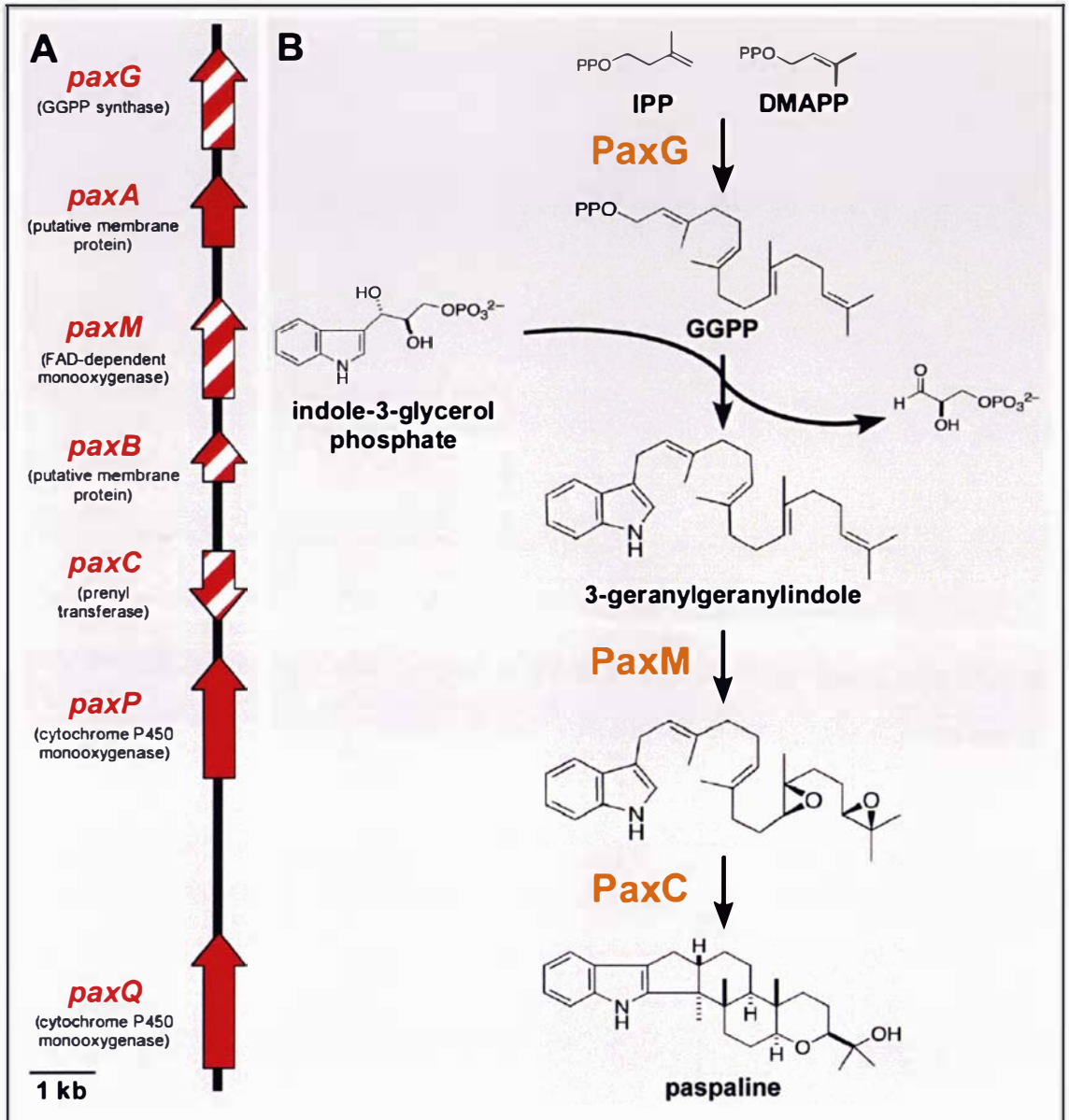

Figure 3.19 Proposed scheme for paspaline biosynthesis in *P. paxilli*

(A) Organisation of paxilline (*pax*) gene cluster. Paspaline-associated genes are shown as striped arrows. The proposed enzymatic function of each gene product, except PaxA and PaxB (no enzymatic function identified), is also indicated. **(B)** The proposed pathway for paspaline biosynthesis. IPP - isopentenyl diphosphate; DMAPP - dimethylallyl diphosphate; GGPP - geranylgeranyl diphosphate.

analysis of PaxB suggested that it may be a transporter. Unlike the major ATP-binding cassette (ABC) and major facilitator superfamily (MFS) fungal transporters, PaxB contained seven transmembrane domains. Most ABC and MFS transporters associated with secondary metabolite gene clusters appear to have a role in self-protection of the producing organism from the toxic effects of the metabolite (Del Sorbo *et al.*, 2000; Gardiner *et al.*, 2005). Given the novel structure of PaxB and the indole-diterpene negative phenotype of the *paxB* mutant (Monahan and Scott, unpublished results), PaxB was proposed to have a role in transporting substrate(s) to the vicinity of the biosynthetic enzyme complex, rather than a role in self-protection.

3.2 *paxP* and *paxQ* complementations

The deletion mutants of *paxP* and *paxQ* are blocked for paxilline biosynthesis and accumulate the indole-diterpenes paspaline and 13-desoxypaxilline, respectively (McMillan *et al.*, 2003). This suggested that *paxP* and *paxQ* are essential for paxilline biosynthesis and that paspaline and 13-desoxypaxilline are the most likely substrates for the corresponding enzymes. To test if the block for paxilline biosynthesis in LMP1 (Δ*paxP*) and LMQ226 (Δ*paxQ*) mutants could be released by complementation, *paxP* and *paxQ* complementation constructs were prepared. These complementation constructs were also used to investigate if paspaline and 13-desoxypaxilline are the true substrates for the corresponding enzymes and also to test the participation of other proposed intermediates in paxilline biosynthesis (Section 3.3).

3.2.1 Preparation of *paxP* and *paxQ* complementation constructs

To test if the *paxP* deletion in LMP1 mutant could be complemented, a *paxP* complementation construct pSS1 was prepared. A *paxP* fragment containing 583 bp of the sequence 5' of the *paxP* ATG, all 1849 bp of the gene sequence and 243 bp of the 3' sequence was PCR amplified from wild-type genomic DNA (Section 2.14.3) using the primers paxPEcoRIF2 and paxPEcoRIR, containing introduced *Eco*RI sites (Figure 3.20A). This product was subcloned into pGEM®-T Easy vector (Promega) and subsequently sequenced. This analysis identified one PCR-introduced error but was outside of *paxP* 60 bp downstream of the transcription stop site. The *Eco*RI fragment containing *paxP* was then cloned into the *Eco*RI site of pII99 to generate pSS1 (Figure 3.20A).

In order to test if the *paxQ* deletion in LMQ226 mutant could be complemented, a *paxQ* complementation construct pSS2 was prepared. A *paxQ* fragment consisting of 631 bp of the sequence 5' of the *paxQ* ATG, all 2087 bp of the gene sequence and 297 bp of the 3' sequence was PCR amplified from wild-type genomic DNA (Section 2.14.3) using the primers paxQHindIIIF2 and paxQHindIIIR, containing introduced *Hin*dIII sites (Figure 3.20B).

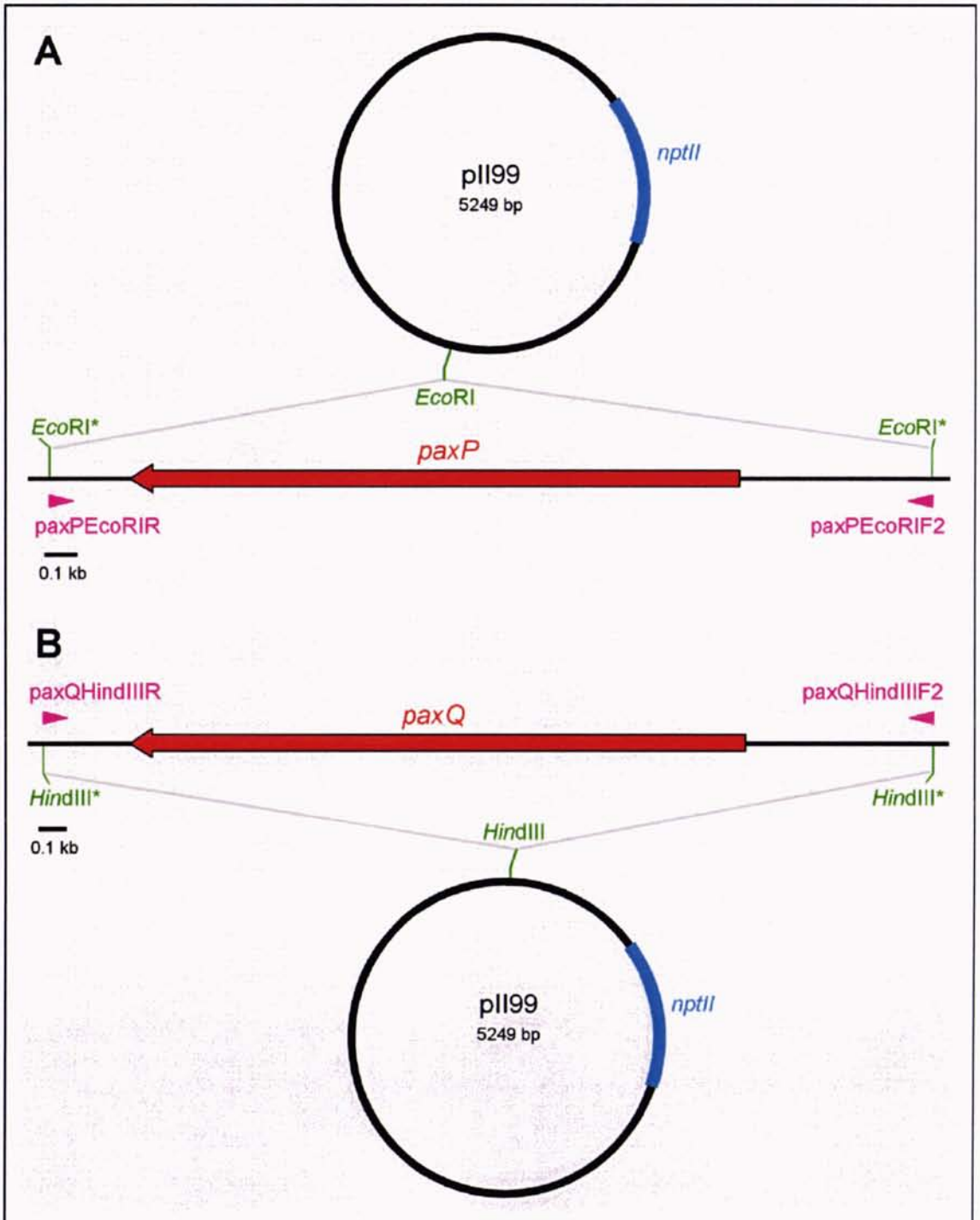

Figure 3.20 *paxP* and *paxQ* complementation constructs

(A) pSS1 contains the PCR-amplified copy of *paxP* from wild-type *P. paxilli* cloned into the *Eco*RI site of pII99. **(B)** pSS2 contains the PCR-amplified copy of *paxQ* from wild-type *P. paxilli* cloned into the *Hin*dIII site of pII99.
Restriction sites used for cloning and positions of primers used for PCR are shown in green and pink, respectively. * indicates restriction site introduced by PCR.

The *paxQ* PCR product was subcloned into pGEM®-T Easy vector (Promega) and subsequently sequenced. Sequence analysis confirmed that there were no PCR-introduced errors. The *Hin*dIII fragment containing *paxQ* was then ligated into the *Hin*dIII site of pII99 to generate pSS2 (Figure 3.20B).

3.2.2 Complementation of Δ*paxP* and Δ*paxQ* strains

Protoplasts of LMP1 (Δ*paxP*) and LMQ226 (Δ*paxQ*) mutants were transformed with 5 μg of circular pSS1 (*paxP*) and pSS2 (*paxQ*), respectively, and also with circular pII99 vector (Section 2.13.2). The transformants were selected on RG medium supplemented with 150 μg/ml of geneticin. Ten arbitrarily selected geneticin-resistant LMP1/pSS1 and LMQ226/pSS2 transformants were colony-purified and screened by TLC analysis (Section 2.21) for their ability to make paxilline (Figure 3.21).

Extracts of LMP1 and LMP1/pII99 contained a single indole-diterpene with an R_f value similar to authentic paspaline (Figure 3.21A). The presence of green bands with R_f values similar to authentic paxilline in seven out of ten LMP1/pSS1 transformants analysed confirmed that pSS1 was able to complement the *paxP* deletion in LMP1 (Figure 3.21A). These transformants had other green bands similar in mobility to those consistently observed in extracts of wild-type *P. paxilli* and, as shown later, correspond to other indole-diterpenes including β-paxitriol, PC-M6, paspaline and 13-desoxypaxilline. The variable levels of paxilline detected among the transformants could be due to the position of integration of the construct into the genome and/or differences in copy number (Malonek *et al.*, 2005a), or the presence of an incomplete promoter sequence in pSS1.

TLC analysis of extracts of *paxQ* mutant and *paxQ* mutant with pII99 detected intense green bands with R_f values similar to authentic 13-desoxypaxilline and other less intense green bands corresponding to other indole-diterpenes (Figure 3.21B). All the ten LMQ226/pSS2 transformants analysed had intense green bands with R_f values similar to authentic paxilline suggesting that pSS2 was able to complement the *paxQ* deletion in LMQ226 mutant (Figure 3.21B).

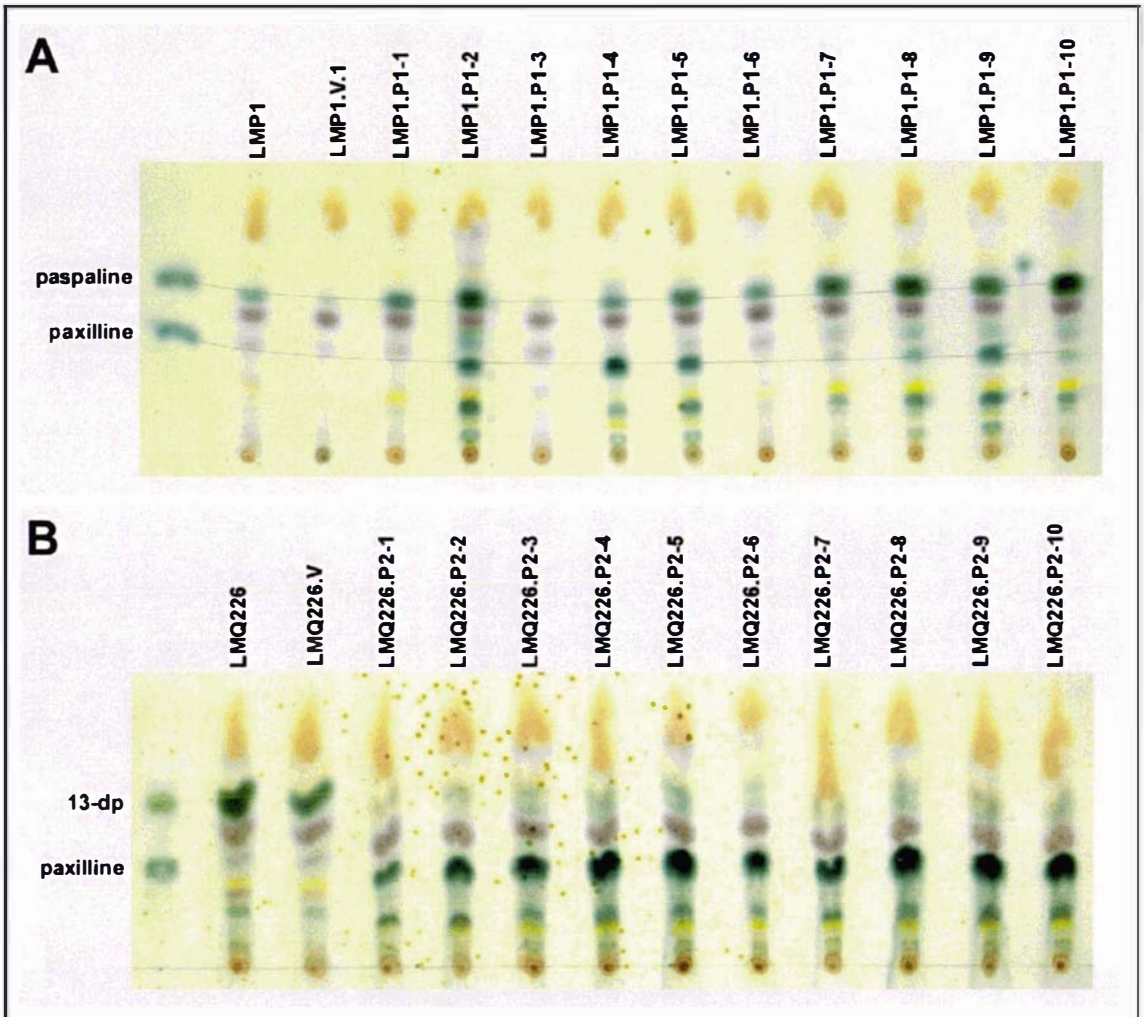

Figure 3.21 NP-TLC analysis of *paxP* and *paxQ* complementations

NP-TLC analysis of **(A)** *paxP* deletion mutant LMP1 containing the complementation construct pSS1 (lines are drawn to show the mobility of green bands corresponding to authentic paxilline and paspaline) and **(B)** *paxQ* deletion mutant LMQ226 containing the complementation construct pSS2, for the presence of indole-diterpenes (Section 2.21). Mycelium was grown for 7 days in CDYE, supplemented with trace element mix (Section 2.3.2), at 28ºC with shaking at 200 rpm, freeze-dried and extracted in 2:1 chloroform-methanol mixture. V=pII99 vector; P1=pSS1; P2=pSS2; 13-dp=13-desoxypaxilline.

Unlike the *paxP* complementation, the level of paxilline detected in each of the LMQ226/pSS2 transformants was similar. Additional green bands similar to those consistently observed in extracts of wild-type strain were also observed. As will be shown later, these correspond to other indole-diterpenes.

3.2.3 Preparation of pSS7 with longer *paxP* promoter sequence

To test if the variable levels of paxilline detected in LMP1/pSS1 transformants (Section 3.2.2) was due to an incomplete promoter sequence in pSS1, a second *paxP* complementation construct, pSS7, was prepared that contained a longer *paxP* promoter sequence (1584 bp) than in pSS1 (583 bp). A 915 bp *Eco*RI/*Sma*I fragment, containing part of the *paxP* gene sequence (483 bp) and 432 bp of the 3' untranslated region, from the lambda clone λCY56 (Young *et al.*, 2001) was cloned into the *Eco*RI/*Sma*I site of the pBlueScript II KS vector to generate pSS3 (Figure 3.22A). A 2950 bp *Sma*I fragment, containing 1584 bp of the sequence 5' of the *paxP* ATG plus the remaining part of the *paxP* gene sequence (1366 bp), was cloned from λCY56 into the *Sma*I site of pSS3 in the correct orientation to generate pSS7 (Figure 3.22B).

3.2.4 Complementation of Δ*paxP* strain with pSS7

Protoplasts of *paxP* deletion mutant LMP1 were co-transformed with 5 μg of circular pII99 vector and pSS7 (Section 2.13.2). Twenty six arbitrarily selected geneticin-resistant transformants were colony-purified and PCR-screened (Section 2.14.2) for integration of the pSS7 insert. Six positive transformants were further screened by TLC analysis (Section 2.21) for their ability to make paxilline. TLC analysis of extracts of LMP1 and LMP1/pII99 identified green bands with R_f values similar to authentic paspaline (Figure 3.23). Five out of six geneticin-resistant LMP1/pII99/pSS7 transformants had green bands with R_f values similar to authentic paxilline suggesting that the *paxP* deletion in LMP1 mutant was complemented by pSS7 (Figure 3.23). These transformants had other green bands that correspond to other indole-diterpenes. Although pSS7 was able to complement LMP1, variable levels of paxilline were once again observed.

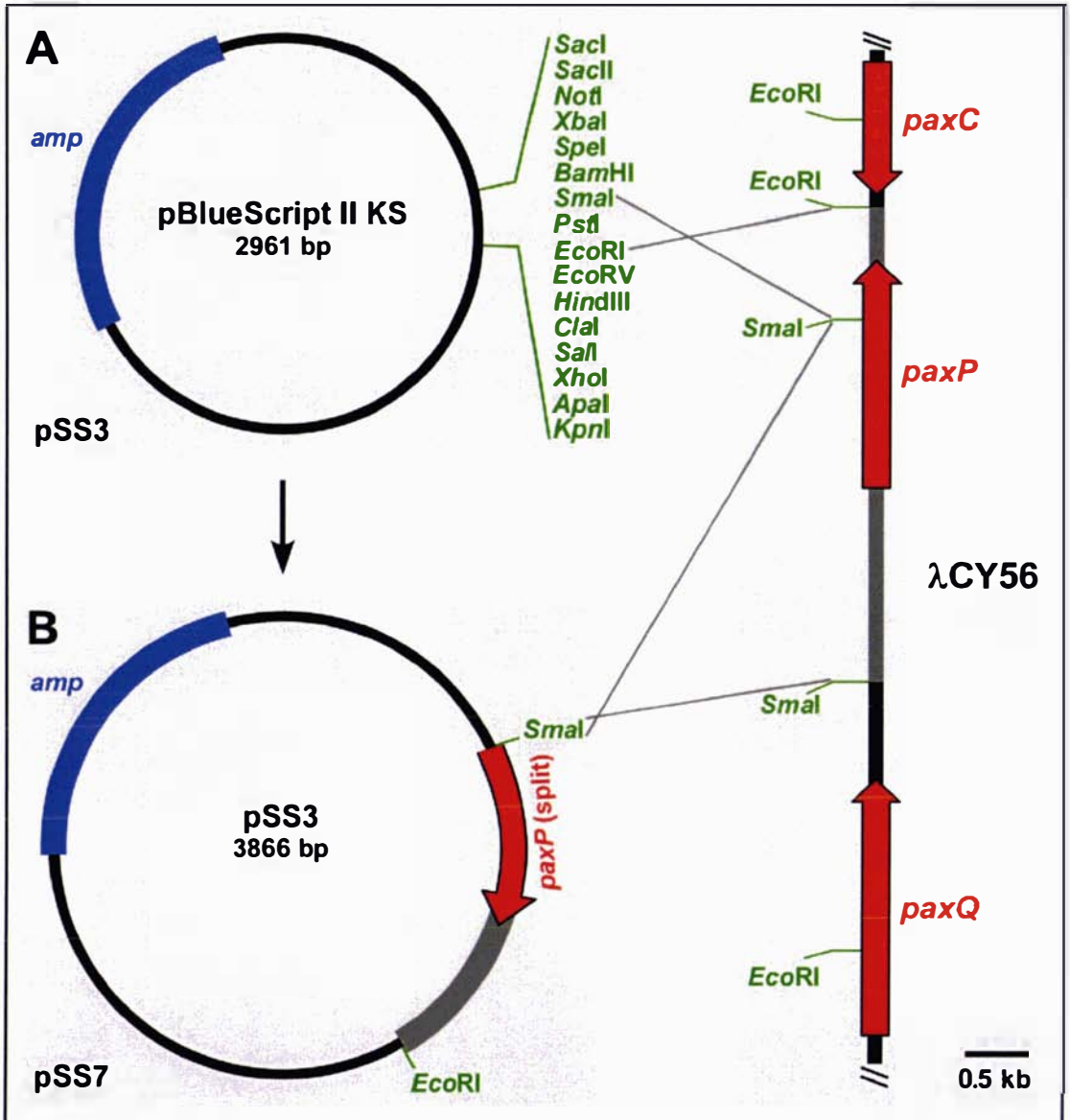

Figure 3.22 *paxP* complementation construct with different promoter length

(A) *Eco*RI/*Sma*I fragment, containing part of *paxP*, from λCY56 was cloned into pBlueScript II KS to give pSS3. **(B)** *Sma*I fragment, containing the promoter and remaining part of *paxP*, from λCY56 was cloned into pSS3 to give pSS7. pSS7 plasmid was used with pII99 in a co-transformation of LMP1 (Δ*paxP*) protoplasts.

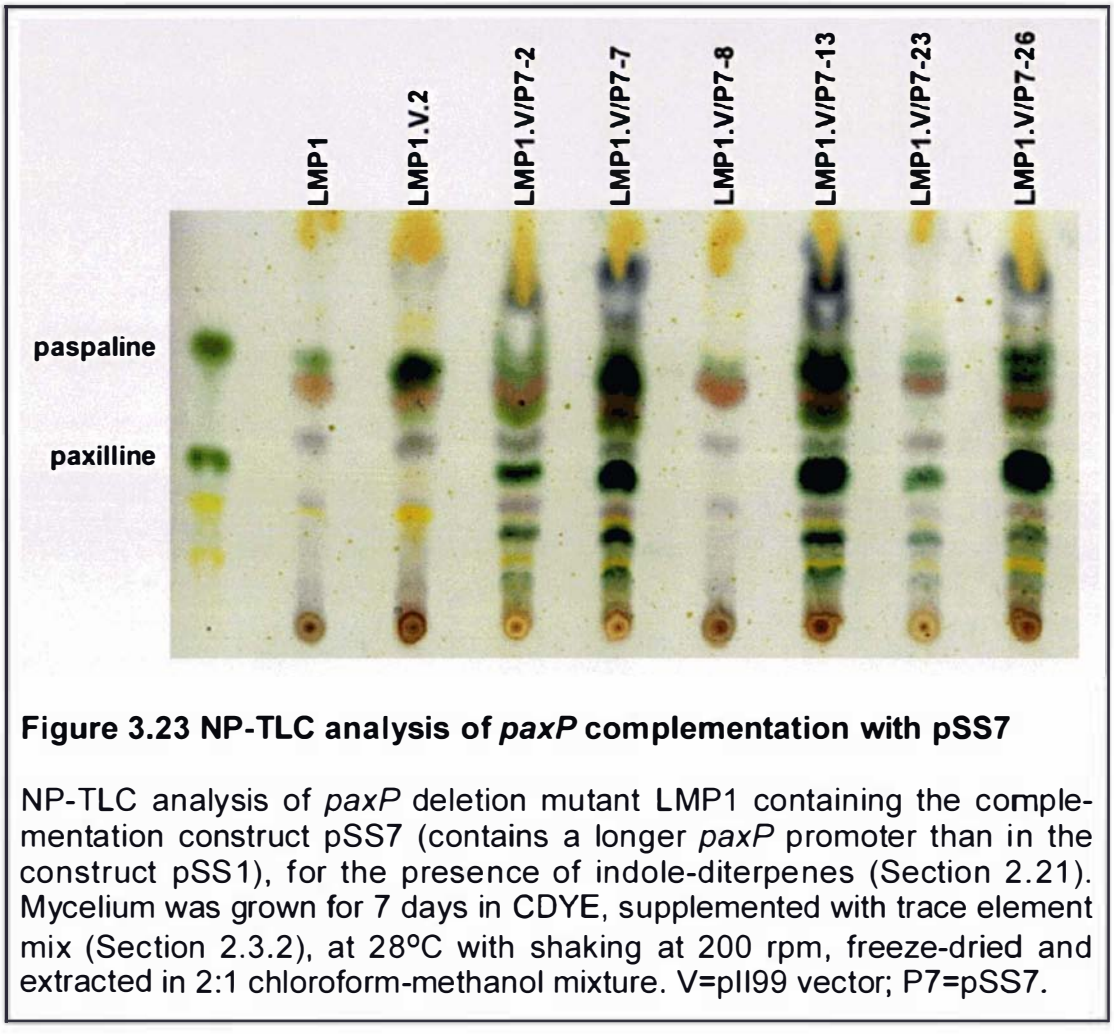

Figure 3.23 NP-TLC analysis of *paxP* complementation with pSS7

NP-TLC analysis of *paxP* deletion mutant LMP1 containing the complementation construct pSS7 (contains a longer *paxP* promoter than in the construct pSS1), for the presence of indole-diterpenes (Section 2.21). Mycelium was grown for 7 days in CDYE, supplemented with trace element mix (Section 2.3.2), at 28°C with shaking at 200 rpm, freeze-dried and extracted in 2:1 chloroform-methanol mixture. V=pII99 vector; P7=pSS7.

Given the primary aim of these experiments was to confirm that the *paxP* and *paxQ* constructs were functional, no detailed molecular analysis was carried out to confirm whether the variable levels of paxilline reflected copy number or position of integration.

3.3 Feeding studies with paxilline precursor metabolites

Previous work confirmed that just four proteins were required in the early steps in paxilline biosynthesis pathway to synthesise the first stable indole-diterpene metabolite, paspaline (Section 3.1). Later steps in the paxilline biosynthesis pathway involve two cytochrome P450 monooxygenases, PaxP and PaxQ, that are proposed to utilise paspaline and 13-desoxypaxilline as their respective substrates (McMillan *et al.*, 2003). These compounds together with paspaline B, PC-M6 and β-paxitriol have been proposed to form a metabolic grid for paxilline biosynthesis (Figure 3.24) (Munday-Finch *et al.*, 1996). Given the versatility of cytochrome P450 enzymes to catalyse multiple steps (Ro *et al.*, 2005; Tudzynski, 2005), it was considered possible that PaxP alone could catalyse the conversion of paspaline to PC-M6. The formation of paxilline from PC-M6 could occur either via 13-desoxypaxilline or via β-paxitriol. Conversion of PC-M6 to β-paxitriol requires a C-13 hydroxylation that could be catalysed by PaxQ, since this reaction is similar to the conversion of 13-desoxypaxilline to paxilline. Further, the conversion of PC-M6 to 13-desoxypaxilline and β-paxitriol to paxilline both require a C-10 oxidation suggesting the need for a dehydrogenase function. To test whether the metabolic scheme proposed by Munday-Finch *et al.* (Munday-Finch *et al.*, 1996) is correct and whether an additional unidentified dehydrogenase is required the proposed intermediates were purified and fed to *P. paxilli* deletion mutants and strains containing introduced *pax* genes, *paxP* or *paxQ*, in a *pax* cluster negative background for further analysis (Figure 3.25).

3.3.1 pSS1 transformation of *pax* deletion mutants LM662 and CY2

Protoplasts of LM662 and CY2 were transformed with 5 μg of circular pII99 vector or pSS1 (Section 2.13.2) and geneticin-resistant transformants selected on RG medium supplemented with 150 μg/ml of geneticin. An arbitrary selection of geneticin-resistant LM662/pSS1 and CY2/pSS1 transformants were PCR-screened (Section 2.14.2), using the primers paxPEcoRIF2 and paxPEcoRIR (data not shown), for integration of the insert from pSS1.

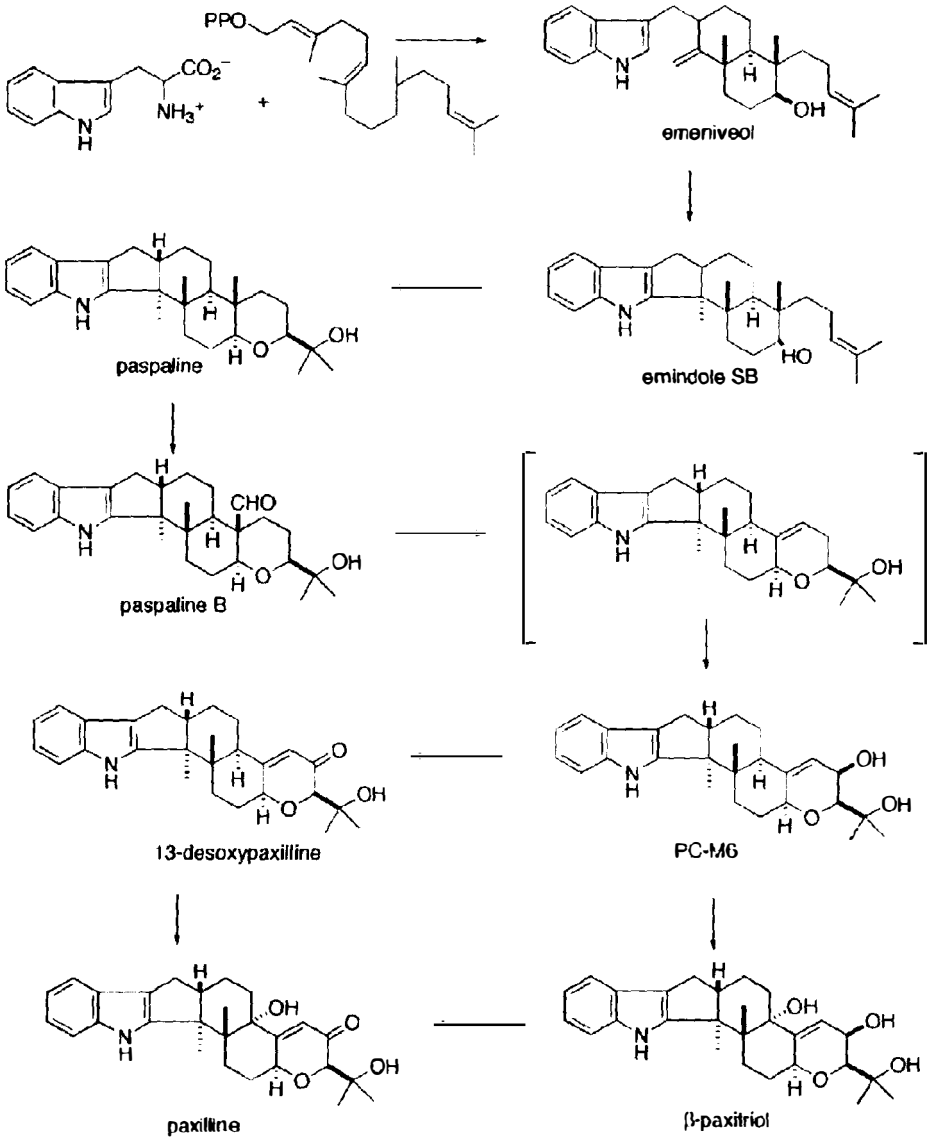

Figure 3.24 Metabolic pathway for paxilline biosynthesis as proposed by Munday-Finch *et al.* (1996)

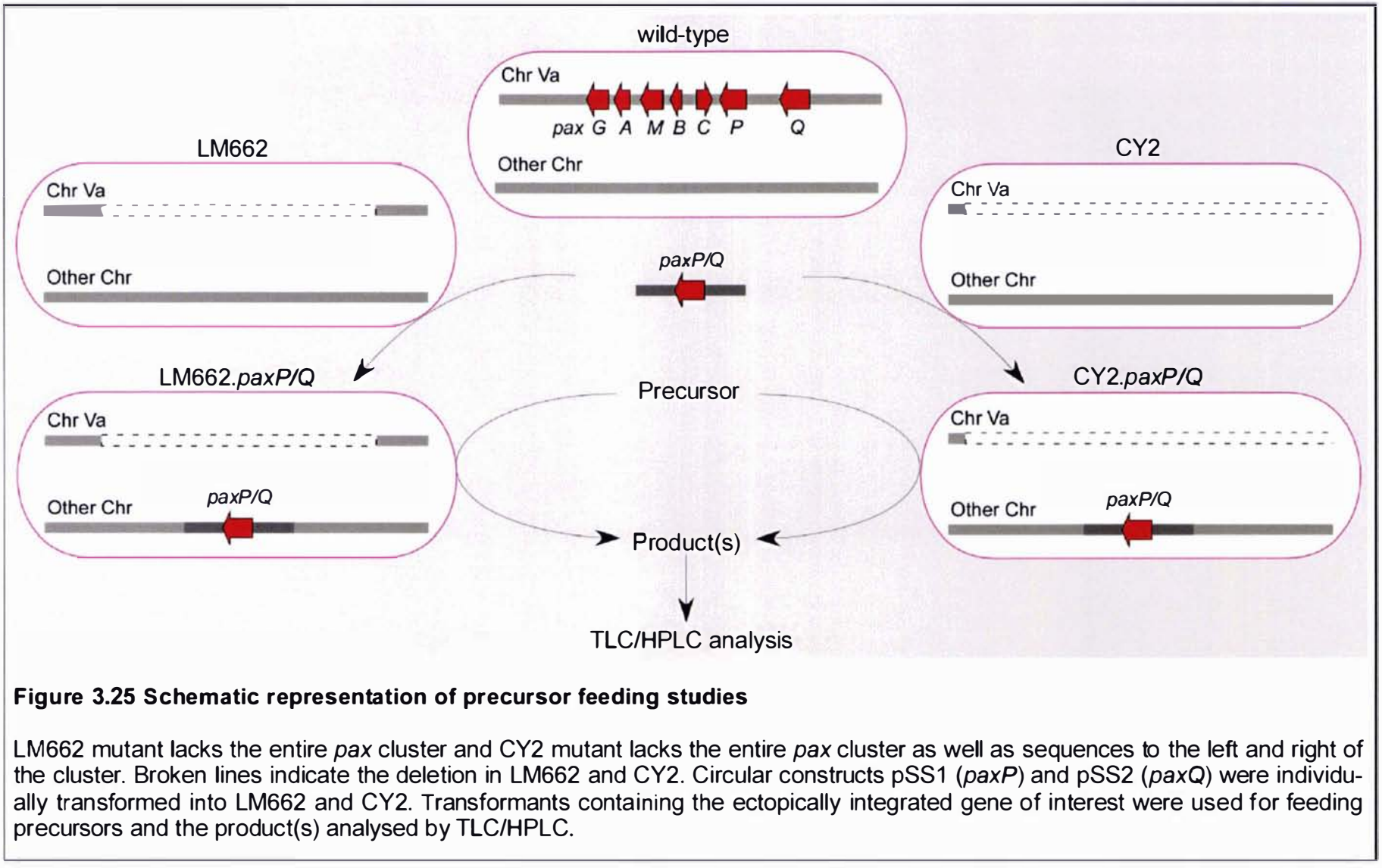

Figure 3.25 Schematic representation of precursor feeding studies

LM662 mutant lacks the entire *pax* cluster and CY2 mutant lacks the entire *pax* cluster as well as sequences to the left and right of the cluster. Broken lines indicate the deletion in LM662 and CY2. Circular constructs pSS1 (*paxP*) and pSS2 (*paxQ*) were individually transformed into LM662 and CY2. Transformants containing the ectopically integrated gene of interest were used for feeding precursors and the product(s) analysed by TLC/HPLC.

Transformants containing a PCR product of the correct size were further assessed for *paxP* expression by RT-PCR analysis (Section 2.14.5.2) using primers that spanned one of the introns so that targets only from RNA or cDNA would be primed (Figure 3.26A). The *tub2* was also amplified as a positive control for template quality.

A high level of *paxP* expression was detected in all LM662/pSS1 transformants (Figure 3.26B). However, the level of *paxP* expression was comparatively lower in CY2/pSS1 transformants (Figure 3.26C). Two LM662/pSS1 transformants viz. LM662.P1-2 & LM662.P1-10 and two CY2/pSS1 transformants viz. CY2.P1-9 & CY2.P1-10, with comparatively high levels of *paxP* expression, were selected for paspaline feeding studies.

3.3.2 Paspaline feeding of LM662/pSS1 and CY2/pSS1 transformants

One hundred μg of paspaline was added to the mycelia of LM662/pSS1 and CY2/pSS1 transformants, together with appropriate controls, on day four and day five (Section 2.20). Fungal mycelia that did not receive paspaline were also included as controls. All fungal mycelia were harvested on day six and freeze-dried for further analysis (Section 2.21).

TLC analysis of extracts of paspaline-fed LM662 and LM662/pII99 detected a single indole-diterpene corresponding to the added paspaline (Figure 3.27A). However, extracts of LM662/pSS1 transformants fed with paspaline contained a second major indole-diterpene besides the added paspaline (Figure 3.27A). HPLC analysis of these extracts confirmed that the second indole-diterpene had the same retention time as authentic 13-desoxypaxilline (R_t = 7.7 min) (Figure 3.27B). A minor additional peak (R_t = 8.25 min) corresponding to another indole-diterpene was also observed in the extracts of paspaline-fed LM662/pSS1 transformants. It is not surprising that this indole-diterpene was not visible on the TLC, given its trace amount (Figure 3.27A). The retention time of this metabolite, as shown later, corresponded to β-PC-M6. The two LM662 transformants containing pSS1 differed in their ability to convert

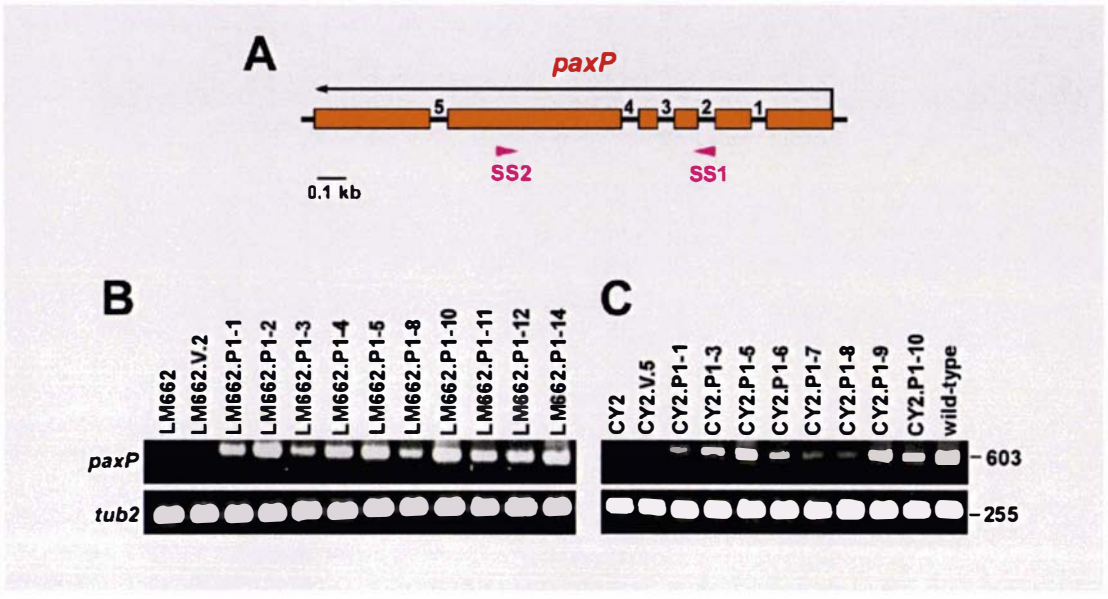

Figure 3.26 Expression analysis of *paxP* in LM662 and CY2 backgrounds

RT-PCR analysis of RNA isolated from 6 day old mycelia using the SuperScript™ One-Step RT-PCR system (Invitrogen). *tub2* was used as a positive control. Primer positions are shown in pink. Primer SS1 spans intron 2 and hence would only prime from RNA and cDNA targets.
All fragment sizes are shown in bp. V=pII99 vector; P1=pSS1.

The PCR components used per reaction were: 100 ng of total RNA, 1x SuperScript™ One-Step RT-PCR (Invitrogen) reaction mix, 200 nM of each primer and 0.5 µl of RT/ Platinum® *Taq* mix in a 25 µl reaction volume. The cycling conditions used were: 1 cycle of 50°C for 30 min, 94°C for 2 min; 35 cycles of 94°C for 30 sec, 55°C for 30 sec, 72°C for 1 min; 1 cycle of 72°C for 10 min.

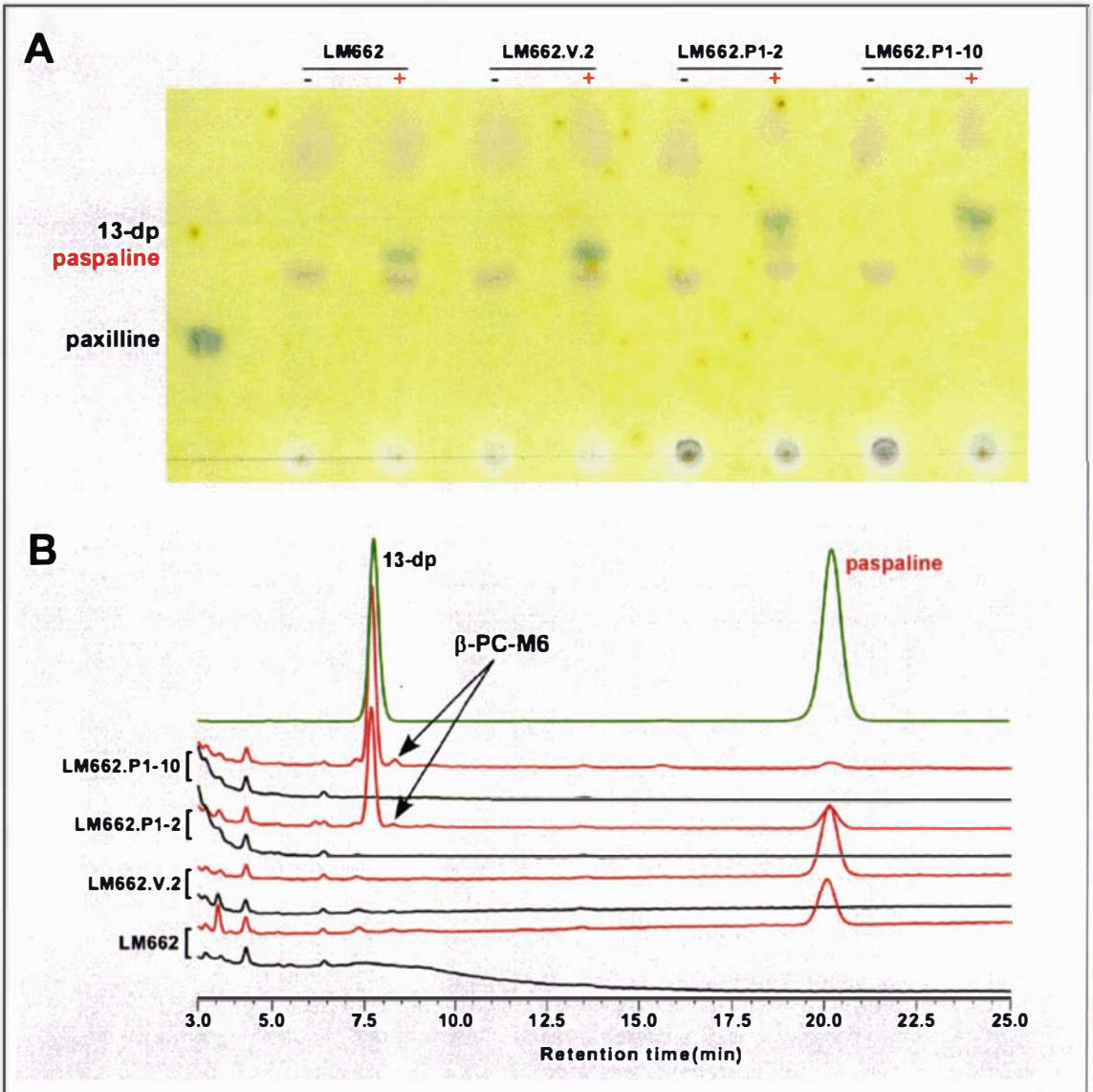

Figure 3.27 NP-TLC and RP-HPLC analysis of LM662/pSS1 transformants fed with paspaline

LM662 transformants containing pSS1 (*paxP*) were fed with paspaline (Section 2.20) and analysed by **(A)** NP-TLC ('-' without paspaline; '+' with paspaline; the mobility of paspaline and 13-dp are shown) and **(B)** RP-HPLC (black traces - without paspaline; red traces - with paspaline), for presence of indole-diterpenes (Section 2.21). Precursor fed is labelled red. V=pII99 vector; P1=pSS1; 13-dp=13-desoxypaxilline.

paspaline to 13-desoxypaxilline and β-PC-M6, with LM662.P1-10 having higher levels of 13-desoxypaxilline than the other transformant LM662.P1-2.

No other indole-diterpenes except the added paspaline were detected in extracts of paspaline-fed CY2 and CY2/pII99 (Figure 3.28A). In addition to the added paspaline, extracts of paspaline-fed CY2/pSS1 transformant, CY2.P1-9, contained two more indole-diterpenes, one with R_f value similar to 13-desoxypaxilline and the other (marked by red rectangle), as shown later, corresponded to β-PC-M6 (Figure 3.28A). Although accumulation of 13-desoxypaxilline and β-PC-M6 in paspaline-fed CY2.P1-10 extracts was not evident from TLC, HPLC analysis confirmed the accumulation of paspaline, 13-desoxypaxilline and β-PC-M6 in extracts of both CY2.P1-9 and CY2.P1-10 transformants (Figure 3.28B). The better conversion of paspaline to 13-desoxypaxilline and β-PC-M6 by the CY2.P1-9 transformant could be attributed to the comparatively higher level of *paxP* expression in CY2.P1-9 than in CY2.P1-10 transformant (Figure 3.26C). Although this is only a limited analysis, the CY2/pSS1 transformants appear to be less efficient in converting paspaline than the LM662/pSS1 transformants.

It was confirmed that paspaline is a substrate for PaxP and is converted to the major product 13-desoxypaxilline and also to β-PC-M6, and that PaxP is capable of catalysing more steps than originally proposed (McMillan *et al.*, 2003). In addition, the paspaline feeding results also support the proposed metabolic grid involving these metabolites as intermediates in paxilline biosynthesis (Figure 3.24).

3.3.3 pSS2 transformation of *pax* deletion mutants LM662 and CY2

Protoplasts of LM662 and CY2 were transformed with 5 μg of circular pII99 vector or pSS2 (Section 2.13.2) and the geneticin-resistant transformants were selected on RG medium supplemented with 150 μg/ml of geneticin. An arbitrary selection of geneticin-resistant LM662/pSS2 and CY2/pSS2 transformants were PCR-screened (Section 2.14.2), using the primers paxQHindIIIF2 and paxQHindIIIR (data not shown), for integration of the insert from pSS2 into the

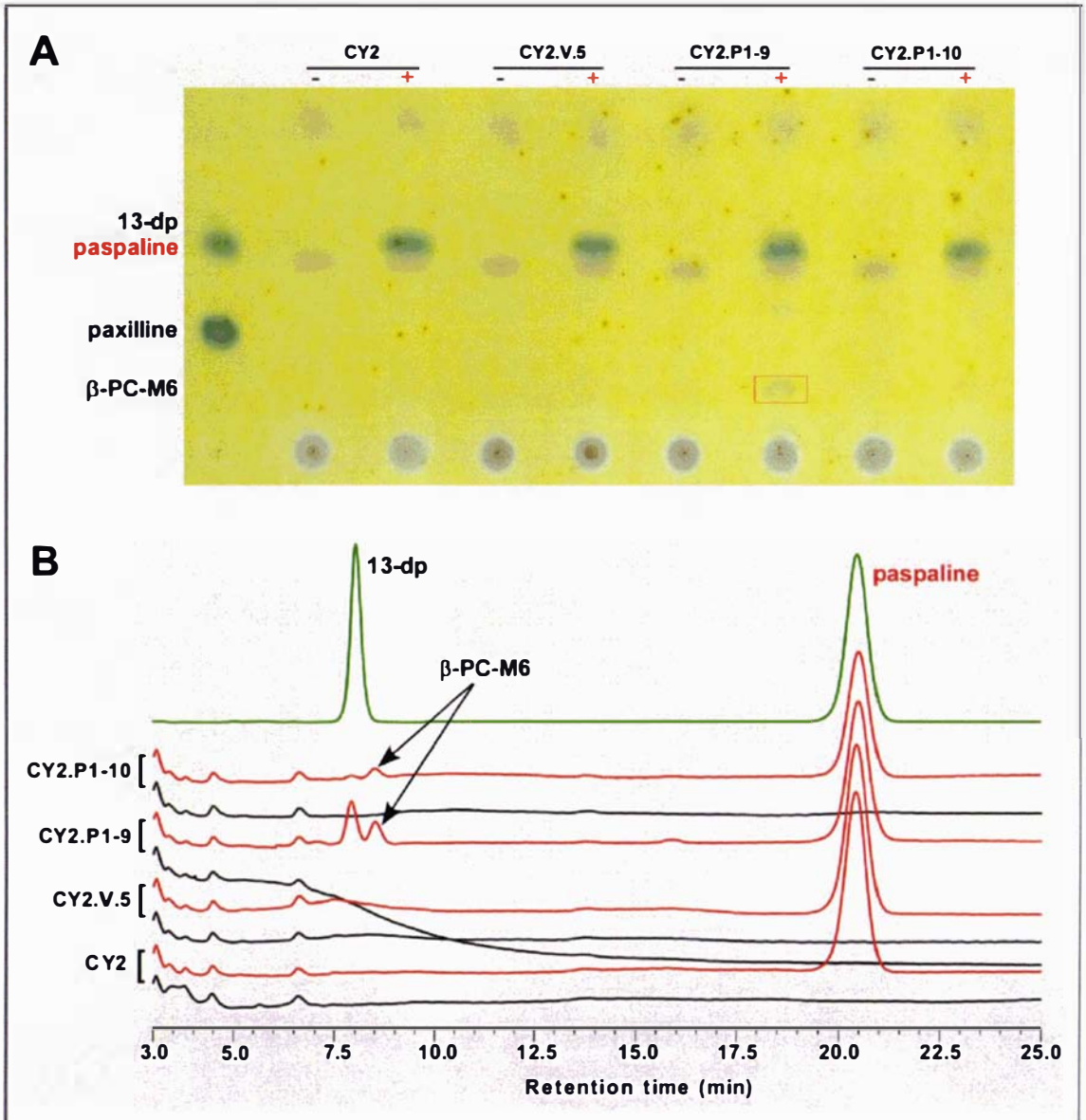

Figure 3.28 NP-TLC and RP-HPLC analysis of CY2/pSS1 transformants fed with paspaline

CY2 transformants containing pSS1 (*paxP*) were fed with paspaline (Section 2.20) and analysed by **(A)** NP-TLC ('-' without paspaline; '+' with paspaline) and **(B)** RP-HPLC (black traces - without paspaline; red traces - with paspaline), for presence of indole-diterpenes (Section 2.21). Precursor fed is labelled red. The mobility of β-PC-M6 (marked by a red rectangle) is also shown on TLC. V=pII99 vector; P1=pSS1; 13-dp=13-desoxypaxilline.

genome. The transformants that gave a PCR product of the correct size were further assessed for *paxQ* expression by RT-PCR analysis (Section 2.14.5.2) using primers that spanned one of the introns so that targets only from RNA or cDNA would be primed (Figure 3.29A). The *tub2* gene was also included as a positive control for template quality.

Expression of *paxQ* was observed in all LM662/pSS2 and CY2/pSS2 transformants (Figure 3.29B & C). However, in CY2/pSS2 transformants the level of *paxQ* expression was comparatively lower than that in LM662/pSS2 transformants. In all transformants multiple products were observed that could be the result of differences in splicing. For 13-desoxypaxilline feeding studies, two LM662/pSS2 transformants viz. LM662.P2-9 & LM662.P2-14 and two CY2/pSS2 transformants viz. CY2.P2-7 & CY2.P2-10 were selected.

3.3.4 13-desoxypaxilline feeding of LM662/pSS2 and CY2/pSS2 transformants

One hundred μg of 13-desoxypaxilline was added to the fungal mycelia of LM662/pSS2 and CY2/pSS2 transformants, together with appropriate controls, on day four and day five of their growth period (Section 2.20). Fungal mycelia that did not receive 13-desoxypaxilline were also included as controls. All fungal mycelia were harvested on day six and freeze-dried for further analysis (Section 2.21).

TLC analysis showed that no indole-diterpenes but the added 13-desoxypaxilline were detected in extracts of 13-desoxypaxilline-fed LM662 and LM662/pII99 strains (Figure 3.30A). However, extracts of 13-desoxypaxilline-fed LM662/pSS2 transformants each showed an intense green band with R_f value similar to authentic paxilline (Figure 3.30A). HPLC analysis of extracts of these transformants confirmed the accumulation of paxilline and traces of 13-desoxypaxilline (Figure 3.30B) indicating almost complete conversion of the added 13-desoxypaxilline to paxilline. In the extract of LM662 deletion mutant that did not receive 13-desoxypaxilline (Figure 3.30B), the signal observed at the same retention time as 13-desoxypaxilline was not due to an indole-

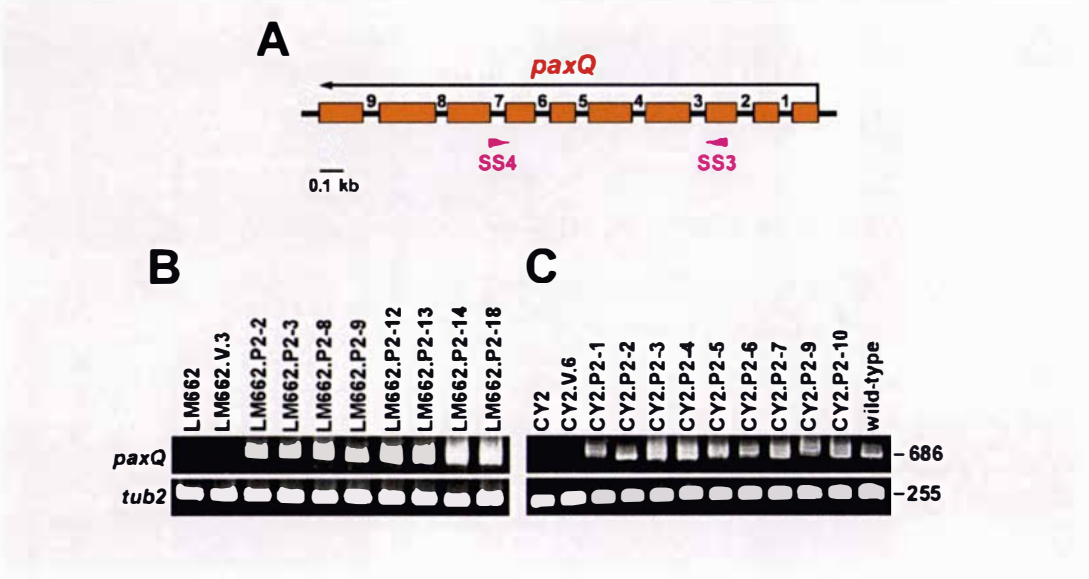

Figure 3.29 Expression analysis of *paxQ* in LM662 and CY2 backgrounds

RT-PCR analysis of RNA isolated from 6 day old mycelia using the SuperScript™ One-Step RT-PCR system (Invitrogen). *tub2* was used as a positive control. Primer positions are shown in pink. Primer SS4 spans intron 7 and hence would only prime from RNA and cDNA targets.
All fragment sizes are shown in bp. V=pII99 vector; P2=pSS2.

The PCR components used per reaction were: 100 ng of total RNA, 1x SuperScript™ One-Step RT-PCR (Invitrogen) reaction mix, 200 nM of each primer and 0.5 μl of RT/ Platinum® *Taq* mix in a 25 μl reaction volume. The cycling conditions used were: 1 cycle of 50°C for 30 min, 94°C for 2 min; 35 cycles of 94°C for 30 sec, 55°C for 30 sec, 72°C for 1 min; 1 cycle of 72°C for 10 min.

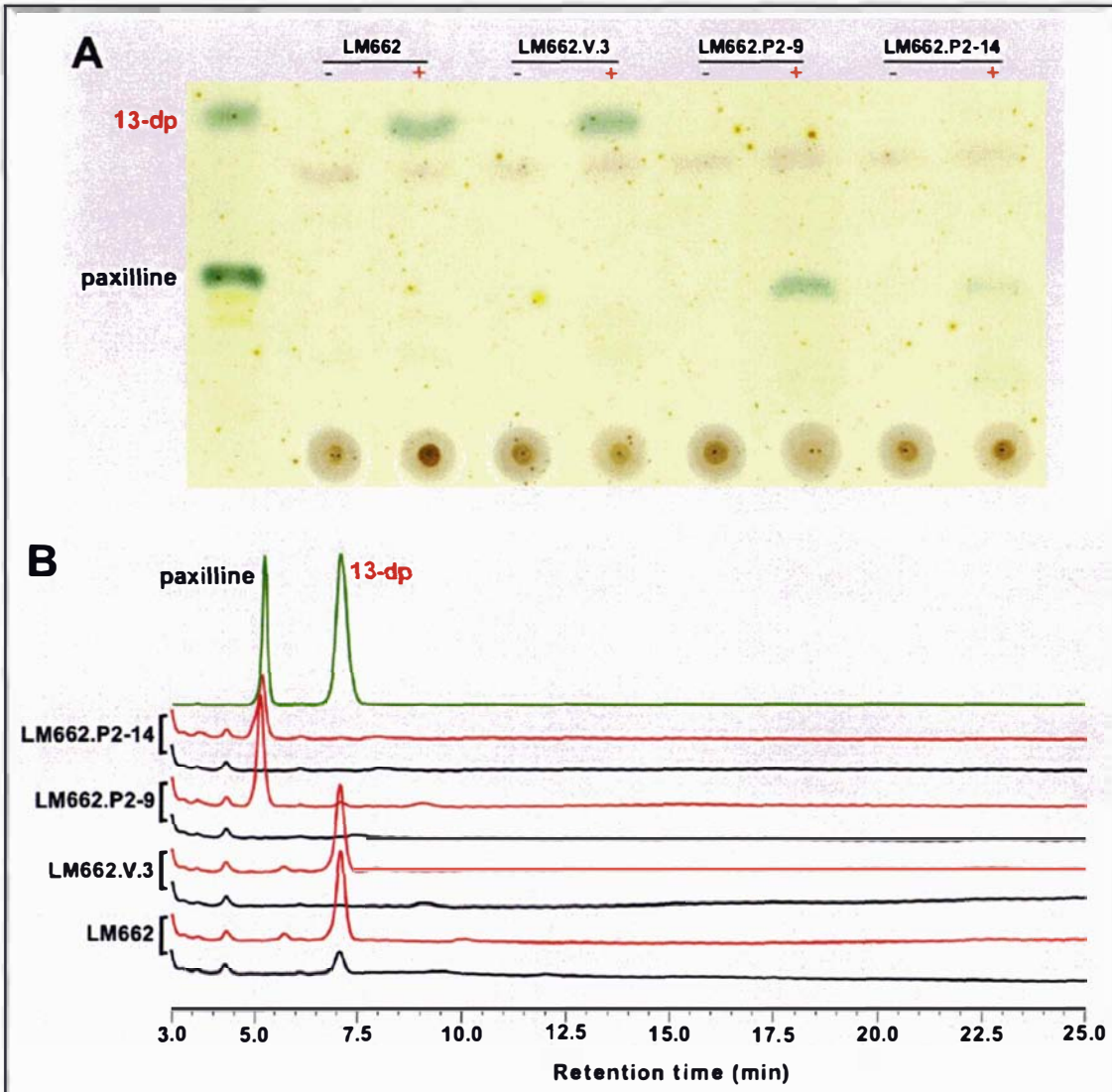

Figure 3.30 NP-TLC and RP-HPLC analysis of LM662/pSS2 transformants fed with 13-desoxypaxilline

LM662 transformants containing pSS2 (*paxQ*) were fed with 13-desoxypaxilline (Section 2.20) and analysed by **(A)** NP-TLC ('-' without 13-desoxypaxilline; '+' with 13-desoxypaxilline) and **(B)** RP-HPLC (black traces - without 13-desoxypaxilline; red traces - with 13-desoxypaxilline), for presence of indole-diterpenes (Section 2.21). Precursor fed is labelled red. V=pII99 vector; P2=pSS2; 13-dp=13-desoxypaxilline.

diterpene as it did not had the characteristic absorption feature of an indole moiety (Section 2.21). TLC analysis of extracts of 13-desoxypaxilline-fed CY2 and CY2/pII99 strains detected the accumulation of a single indole-diterpene corresponding to the added 13-desoxypaxilline (Figure 3.31A). Extracts of CY2/pSS2 transformants incubated with 13-desoxypaxilline accumulated a second indole-diterpene corresponding to paxilline besides the added 13-desoxypaxilline (Figure 3.31A). These results were further confirmed by HPLC analysis (Figure 3.31B). Unlike LM662/pSS2 transformants, extracts of CY2/pSS2 transformants accumulated substantial amounts of the fed precursor 13-desoxypaxilline suggesting that the added 13-desoxypaxilline was more efficiently converted by PaxQ in the LM662 background than in the CY2 background. These studies confirmed 13-desoxypaxilline as a substrate for PaxQ and thus supporting the proposed metabolic scheme for paxilline biosynthesis (Figure 3.24).

3.3.5 PC-M6 feeding of *pax* deletion mutants

The sodium borohydride reduction of 13-desoxypaxilline gave PC-M6, which was confirmed by LC-MSMS (Section 2.19.2). This reduction gave two products that were identified as the two diastereomers of PC-M6, α- and β-PC-M6 (ratio of α:β *ca* 2:3), based on their feeding studies (see below). The two diastereomers were purified by RP-HPLC and tested for their involvement as intermediates in paxilline biosynthesis. These diastereomers were individually fed to the *pax* deletion mutants LMP1 (Δ*paxP*), LMQ226 (Δ*paxQ*), LM662 and CY2; LM662 and CY2 mutants containing pII99 vector; and LM662 and CY2 mutants containing *paxQ* viz. LM662.P2-9 and CY2.P2-7. The *paxP* deletion mutant was included to test whether PC-M6 was metabolised in absence of PaxP, thereby supporting the concept of a separate dehydrogenase enzyme. The *paxQ* deletion mutant was selected as a negative control. LM662 and CY2 deletion mutants were included to test if the dehydrogenase function was encoded by an enzyme within the region defined by the LM662 deletion or that defined by the CY2 deletion. LM662 and CY2 strains containing *paxQ* were included to test if PC-M6 was a substrate for the corresponding enzyme PaxQ. LM662 and CY2 strains containing pII99 vector were selected as vector-only

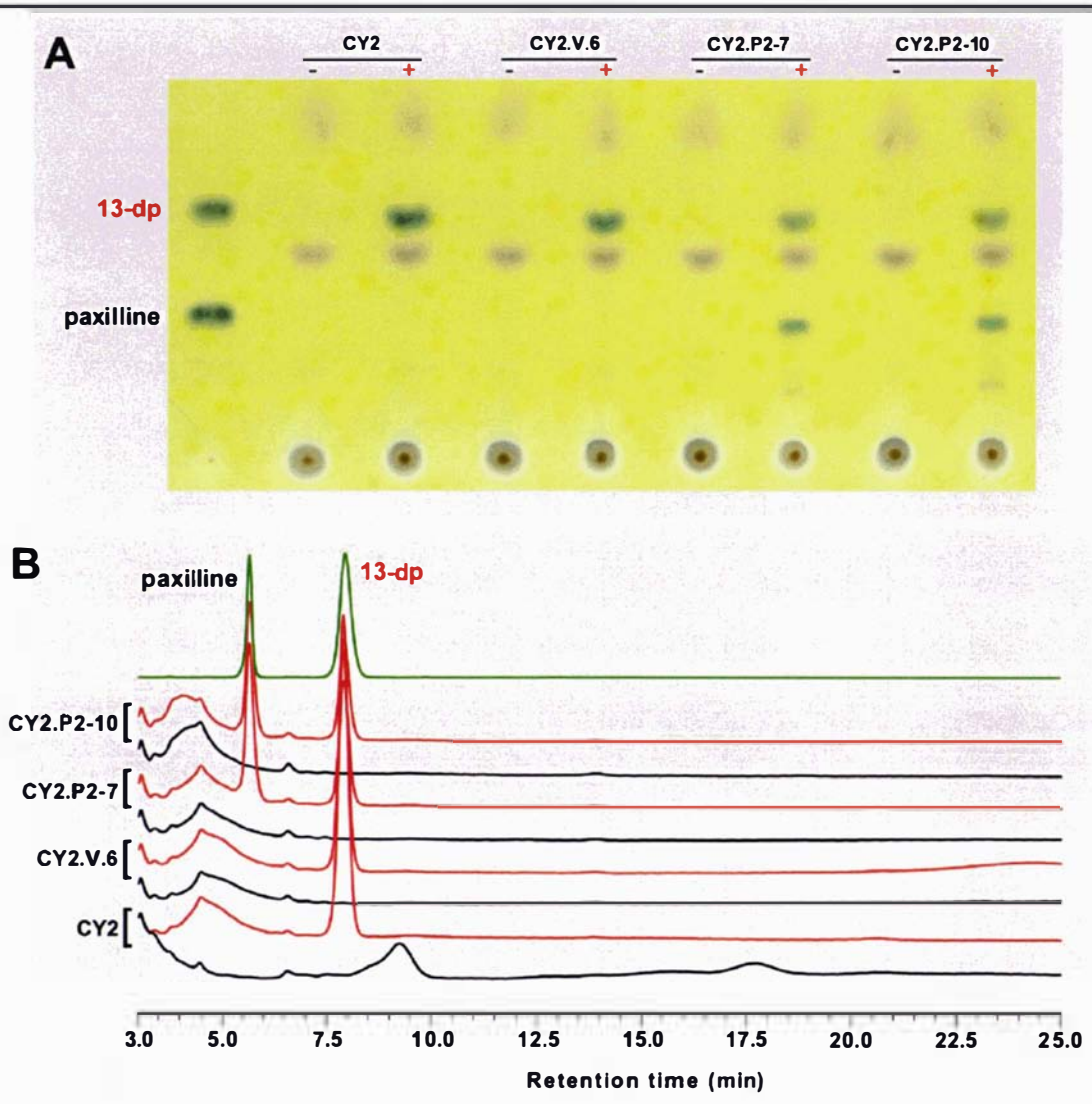

Figure 3.31 NP-TLC and RP-HPLC analysis of CY2/pSS2 transformants fed with 13-desoxypaxilline

CY2 transformants containing pSS2 (*paxQ*) were fed with 13-desoxypaxilline (Section 2.20) and analysed by **(A)** NP-TLC ('-' without 13-desoxypaxilline; '+' with 13-desoxypaxilline) and **(B)** RP-HPLC (black traces - without 13-desoxypaxilline; red traces - with 13-desoxypaxilline), for presence of indole-diterpenes (Section 2.21). Precursor fed is labelled red. V=pII99 vector; P2=pSS2; 13-dp=13-desoxypaxilline.

controls. One hundred μg of α- or β-PC-M6 was added to the mycelia of all these strains on day four and day five of their growth period (Section 2.20). Fungal mycelia that did not receive the precursors were also included as controls. All fungal mycelia were harvested on day six and freeze-dried for further analysis (Section 2.21).

TLC analysis of extracts of all strains when fed α-PC-M6 showed a single green band that had an R_f value similar to authentic α-PC-M6 and authentic paxilline which ran together on the TLC (Figure 3.32A). This metabolite was shown to be α-PC-M6 and not paxilline by HPLC analysis where it had a retention time (R_t = 5.85 min) similar to authentic α-PC-M6 and not to authentic paxilline (Figure 3.33A & Figure 3.34A). However, all three PaxQ containing strains, LM662.P2-9, CY2.P2-7 and LMP1, after incubations with α-PC-M6, accumulated another indole-diterpene with R_f value similar to authentic α-paxitriol besides the added α-PC-M6 (Figure 3.32A). The accumulation of α-paxitriol in these extracts was further confirmed by HPLC analysis where it was found to have the same retention time (R_t = 4.30 min) as authentic α-paxitriol (Figure 3.33A & Figure 3.34A).* Although the extracts of all the strains that did not receive α-PC-M6 appears to have α-paxitriol in them, none of these strains showed the presence of an indole containing metabolite at the same retention time as α-paxitriol as confirmed by the absence of the characteristic absorption feature of an indole moiety at 230 nm and 280 nm (Section 2.21). Interestingly, LMP1 mutant also showed an increased accumulation of paspaline in response to α-PC-M6 feeding. Extracts of α-PC-M6-fed LMQ226 mutant contained the added α-PC-M6, and other indole-diterpenes that were also present in extracts of LMQ226 mutant that did not receive α-PC-M6 (Figure 3.32A & Figure 3.33A). The presence of the added α-PC-M6 and the absence of α-paxitriol suggested that none of the added α-PC-M6 was metabolised by this mutant.

*These results form the basis of identification of the two sodium borohydride reduction products of 13-desoxypaxilline as α- and β-PC-M6. Conversion of the putative α-PC-M6 into α-paxitriol by PaxQ confirms it to be α-PC-M6. In addition, LC-MSMS analysis confirmed the presence of only PC-M6 in the 13-desoxypaxilline reduction product (Section 2.19.2). These results together confirm the other compound in the reduction product to be β-PC-M6.

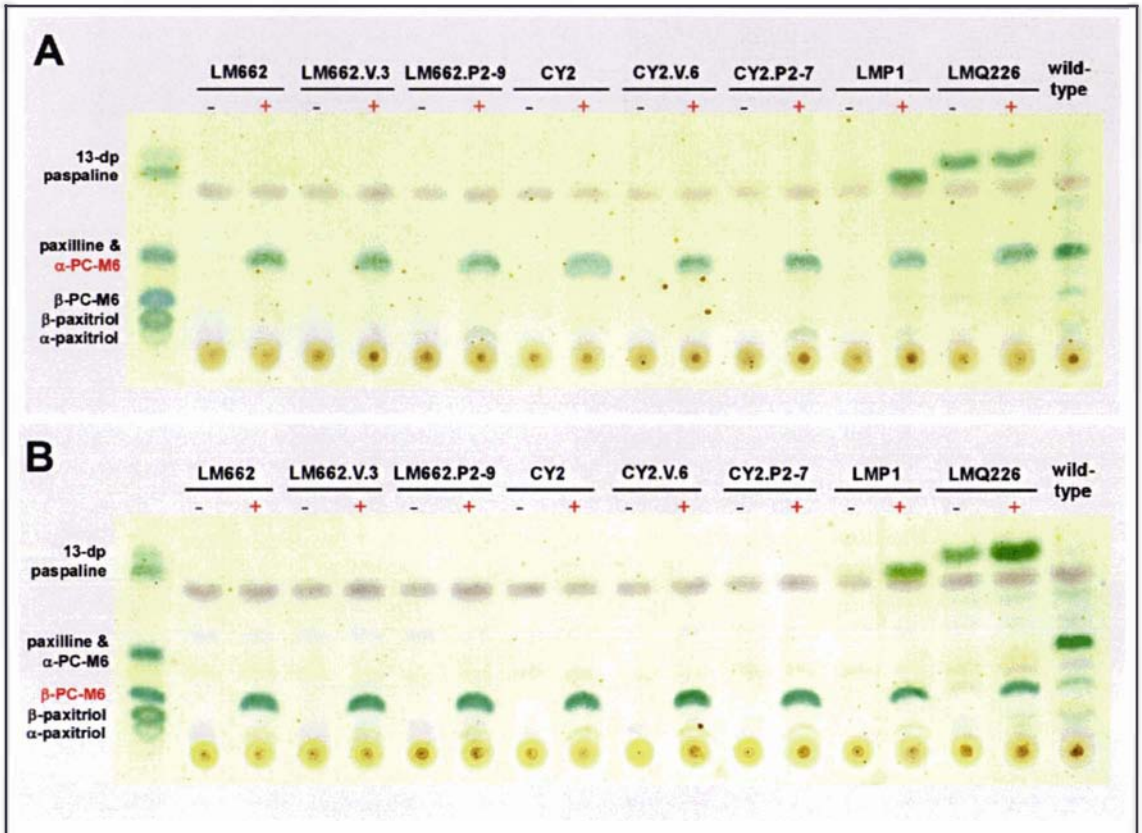

Figure 3.32 NP-TLC analysis of *P. paxilli* deletion mutants, LM662/pSS2 and CY2/pSS2 transformants fed with α- and β-PC-M6

LM662 and CY2 strains containing pSS2 (*paxQ*) and *P. paxilli* deletion mutants LMP1 (Δ*paxP*) and LMQ226 (Δ*paxQ*) were fed with α- and β-PC-M6 (Section 2.20) and analysed by NP-TLC for presence of indole-diterpenes (Section 2.21). **(A)** NP-TLC analysis of α-PC-M6-fed *P. paxilli* cultures. **(B)** NP-TLC analysis of β-PC-M6-fed *P. paxilli* cultures. '-' without α- or β-PC-M6; '+' with α- or β-PC-M6; precursor fed is labelled red. V=pII99 vector; P2=pSS2; 13-dp=13-desoxypaxilline.

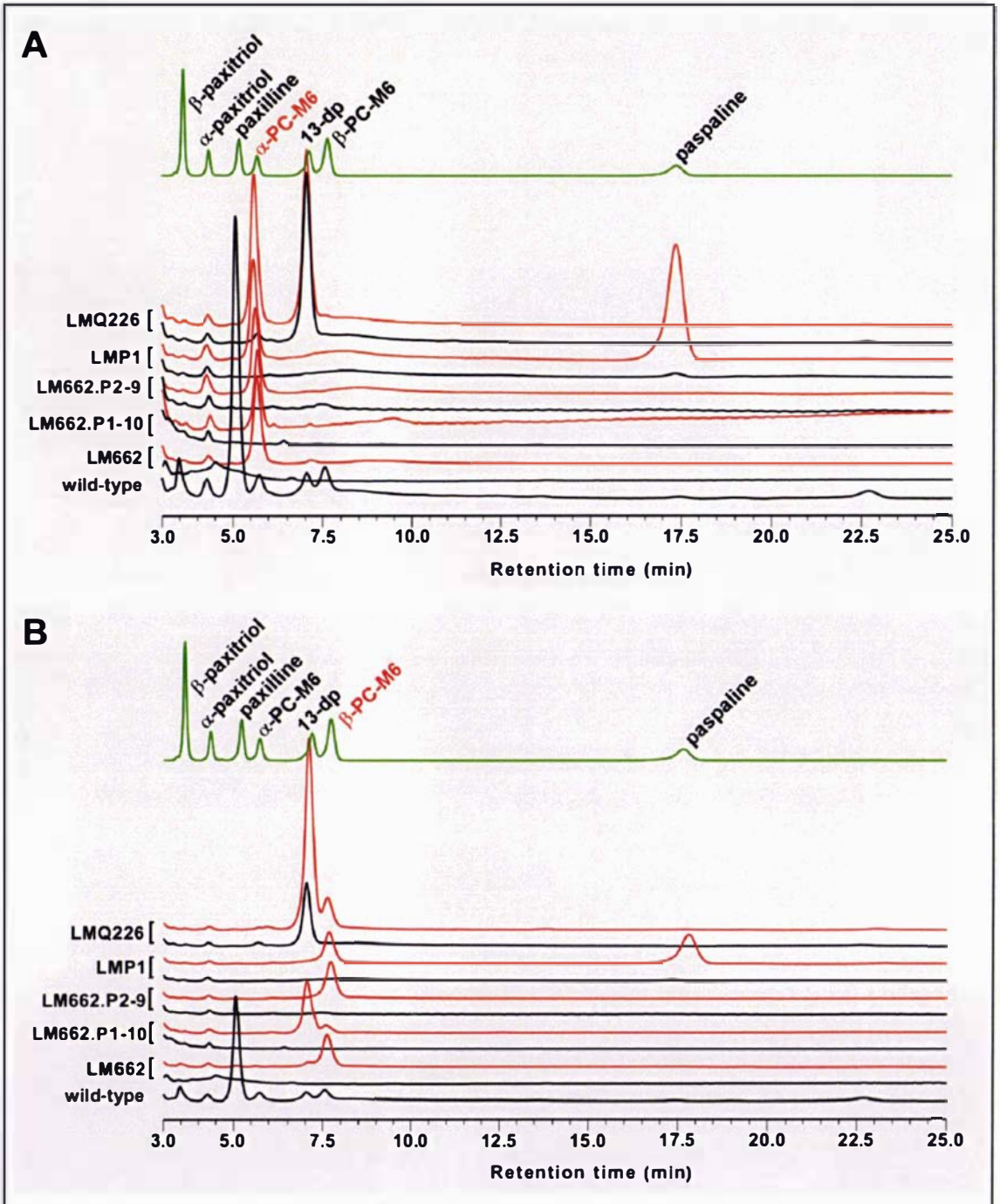

Figure 3.33 RP-HPLC analysis of *P. paxilli* deletion mutants, LM662/pSS1 and LM662/pSS2 transformants fed with α- and β-PC-M6

LM662 strains containing pSS1 (*paxP*) and pSS2 *(paxQ*) and *P. paxilli* deletion mutants LMP1 (Δ*paxP*) and LMQ226 (Δ*paxQ*) were fed with α- and β-PC-M6 (Section 2.20) and analysed by RP-HPLC for presence of indole-diterpenes (Section 2.21). **(A)** RP-HPLC analysis of α-PC-M6-fed *P. paxilli* cultures. **(B)** RP-HPLC analysis of β-PC-M6-fed *P. paxilli* cultures. black traces - without α- or β-PC-M6; red traces - with α- or β-PC-M6; precursor fed is labelled red. P1=pSS1; P2=pSS2; 13-dp=13-desoxypaxilline.

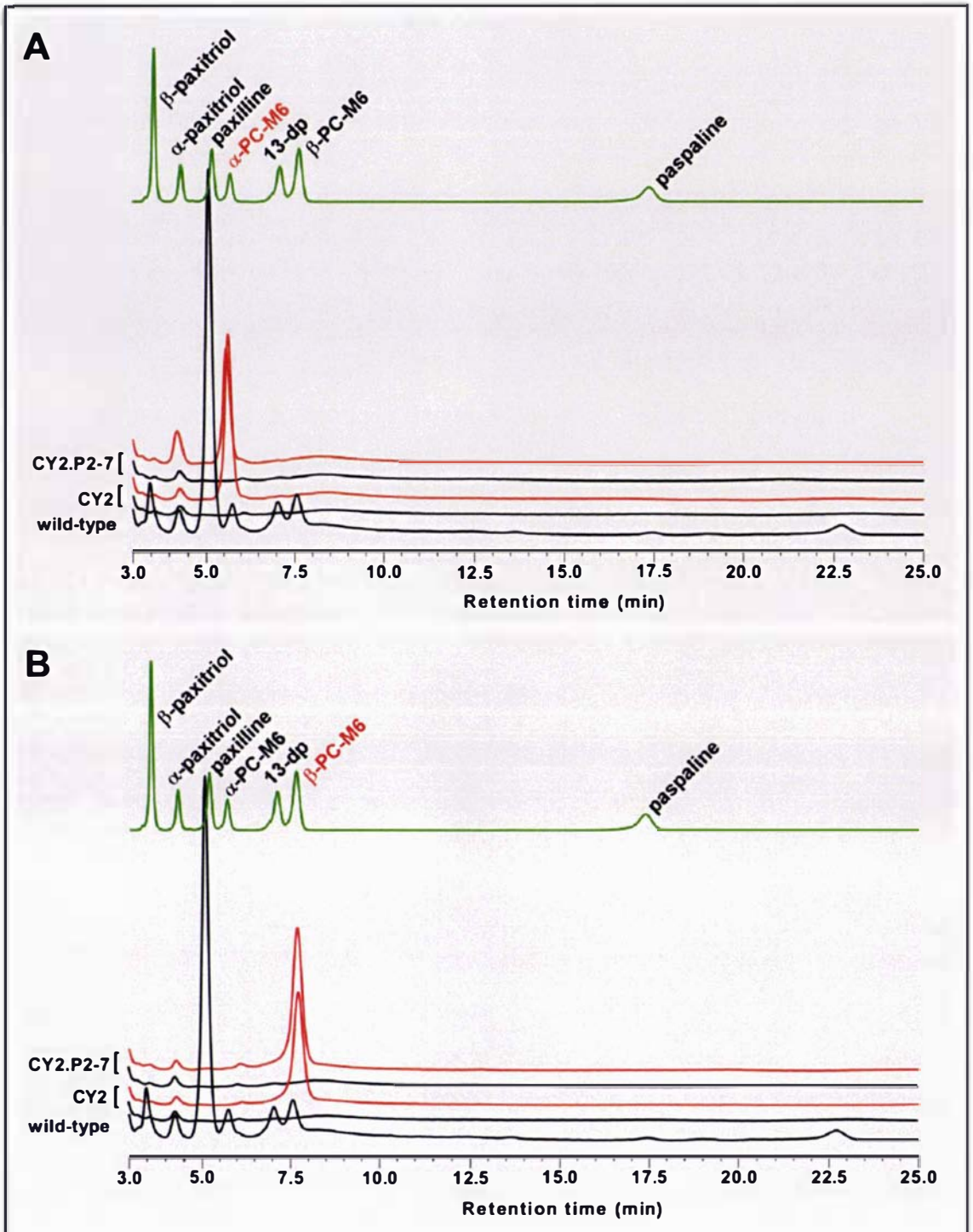

Figure 3.34 RP-HPLC analysis of CY2/pSS2 transformants fed with α- and β-PC-M6

CY2 strains containing pSS2 *(paxQ)* were fed with α- and β-PC-M6 (Section 2.20) and analysed by RP-HPLC for presence of indole-diterpenes (Section 2.21). **(A)** RP-HPLC analysis of α-PC-M6-fed transformants. **(B)** RP-HPLC analysis of β-PC-M6-fed transformants. black traces - without α- or β-PC-M6; red traces - with α- or β-PC-M6; precursor fed is labelled red. P2=pSS2; 13-dp=13-desoxypaxilline.

From the results described above it was observed that all the PaxQ containing strains were able to convert the added α-PC-M6 to α-paxitriol. Although these results suggested that α-PC-M6 was a substrate for PaxQ, it is most unlikely to be an intermediate in paxilline biosynthesis since paxilline precursors have a C-10 β-stereochemistry. Moreover, α-paxitriol is a proposed precursor in a pathway leading to the production of indole-diterpenes like lolitrems and terpendoles that have a C-10 α- stereochemistry (Parker and Scott, 2004).

Similar incubations with β-PC-M6 were carried out with the same strains. The precursor-fed LM662 and CY2 mutants, and LM662 and CY2 strains containing pII99 vector were unable to metabolise the added β-PC-M6 and showed the presence of the added β-PC-M6 only (Figure 3.32B, Figure 3.33B & Figure 3.34B). Similarly, cultures of LM662 and CY2 strains containing *paxQ*, LM662.P2-9 and CY2.P2-7, respectively, were also unable to metabolise the added β-PC-M6 and contained only the added β-PC-M6 (Figure 3.32B, Figure 3.33B & Figure 3.34B). However, extracts of β-PC-M6-fed LMP1 mutant showed an increased accumulation of paspaline similar to that observed in extracts of α-PC-M6-fed LMP1 mutant (Figure 3.32 & Figure 3.33). Extracts of β-PC-M6-fed LMQ226 mutant accumulated an increased amount of 13-desoxypaxilline (Figure 3.32B & Figure 3.33B) which could be the result of catalysis by PaxP. This result was also supported by the paspaline feeding study in which PaxP converted paspaline into 13-desoxypaxilline and β-PC-M6 (Section 3.3.2). This suggested that β-PC-M6 could be a substrate for PaxP.

In order to test if either α- or β-PC-M6 was a substrate for PaxP, incubations with α- or β-PC-M6 were carried out with an LM662 strain containing *paxP*, LM662.P1-10, since this strain efficiently converted paspaline to 13-desoxypaxilline (Section 3.3.2). Analysis of extracts of α-PC-M6-fed LM662/pSS1 transformant, LM662.P1.10, showed no conversion of α-PC-M6 and detected the added α-PC-M6 (Figure 3.33A & Figure 3.35). However, analysis of extracts of β-PC-M6-fed LM662.P1-10 transformant detected the added β-PC-M6 and a second indole-diterpene that had the R_f value similar to

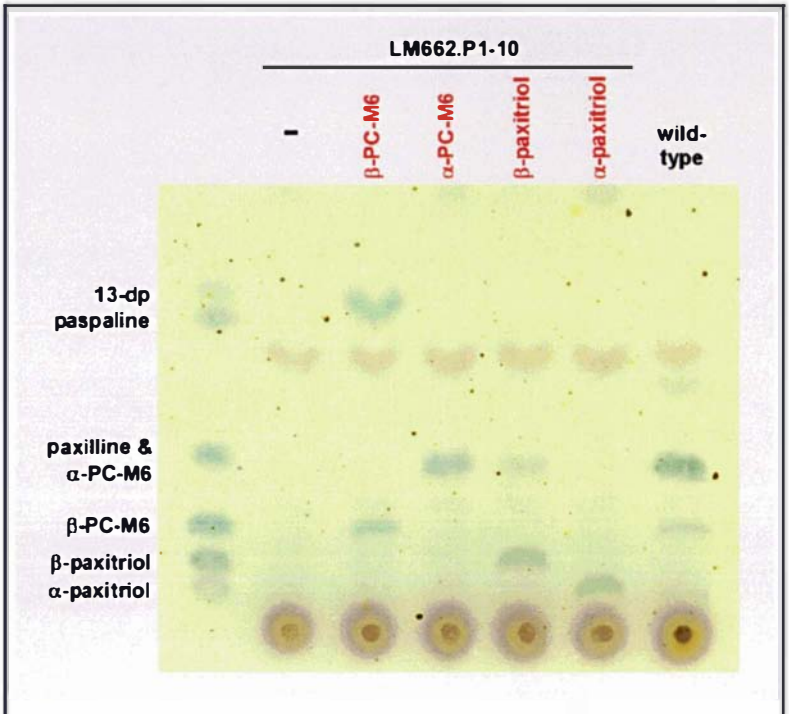

Figure 3.35 NP-TLC analysis of LM662/pSS1 transformant fed with α- and β-PC-M6 and α- and β-paxitriol

LM662 strain containing pSS1 (*paxP*) was fed with α- and β-PC-M6 and α- and β-paxitriol (Section 2.20) and analysed by NP-TLC for presence of indole-diterpenes (Section 2.21). '-' without any precursor; precursors fed are labelled red. P1=pSS1; 13-dp=13-desoxypaxilline.

authentic 13-desoxypaxilline (Figure 3.33B & Figure 3.35), which was confirmed by HPLC analysis (Figure 3.33B). These results confirmed that β-PC-M6 is a substrate for PaxP and is converted to 13-desoxypaxilline. The conversion of β-PC-M6 to 13-desoxypaxilline by PaxP also suggests that PaxP is able to catalyse the C-10 oxidation reaction which means that no distinct dehydrogenase enzyme needs to be involved for this conversion other than PaxP.

3.3.6 Paxitriol feeding of *pax* deletion mutants

Similar to the chemical synthesis of PC-M6 diastereomers, the sodium borohydride reduction of paxilline also gave two paxitriol diastereomers, α- and β-paxitriol (ratio α:β *ca* 1:2) (Section 2.19.3), which were tested for their involvement as intermediates in paxilline biosynthesis.

Both α- and β-paxitriol were individually fed to *pax* deletion mutants LM662, CY2 and LMQ226 (Δ*paxQ*), and LM662 strain containing *paxP* viz. LM662.P1-10. The LM662 and CY2 mutants were included to further test the involvement of a separate dehydrogenase enzyme. The *paxQ* mutant was selected to test if β-paxitriol was metabolised in the absence of PaxQ. The LM662 strain containing *paxP*, LM662.P1-10, which was earlier shown to convert β-PC-M6 to 13-desoxypaxilline (Section 3.3.5), was chosen to test if PaxP was also able to convert paxitriol to paxilline which also requires a C-10 oxidation. One hundred μg of α- or β-paxitriol was added to the mycelia of all these fungal strains on day four and day five of their growth period (Section 2.20). Fungal mycelia that did not receive the precursors were also included as controls. All fungal mycelia were harvested on day six and freeze-dried for further analysis (Section 2.21).

TLC analysis of extracts of α-paxitriol-fed LM662 and CY2 mutants, and LM662.P1-10 transformant identified a single indole-diterpene corresponding to the added α-paxitriol (Figure 3.35 & Figure 3.36A), which was confirmed by HPLC analysis (Figure 3.37A & Figure 3.38). Extracts of α-paxitriol-fed LMQ226 mutant contained the added α-paxitriol in addition to the indole-diterpenes that also accumulated in extracts of LMQ226 mutant that did not

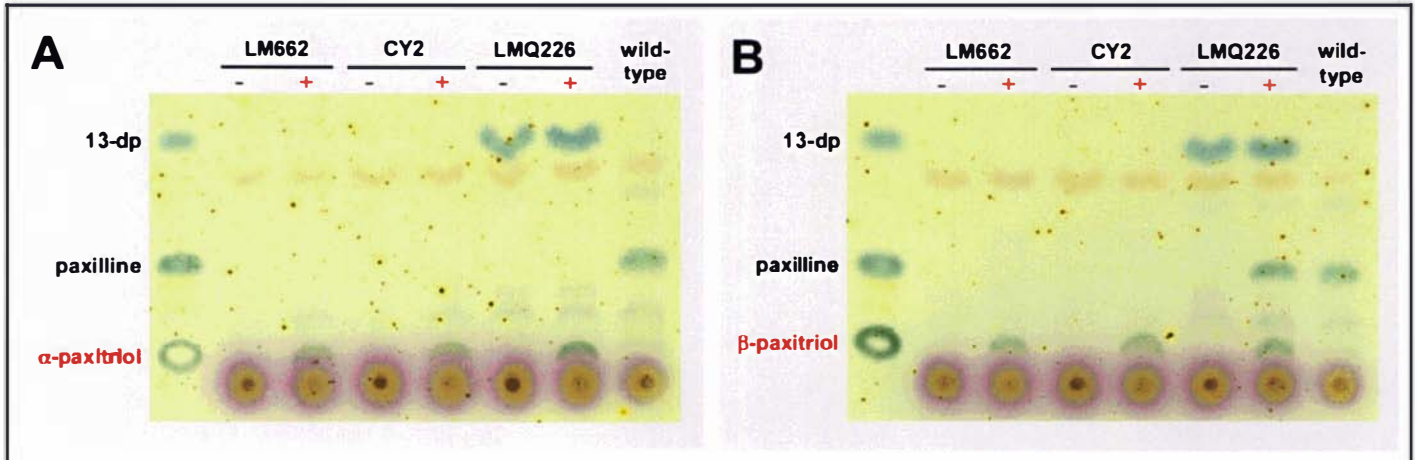

Figure 3.36 NP-TLC analysis of *P. paxilli* mutants fed with α- and β-paxitriol

P. paxilli mutants LM662, CY2 and LMQ226 (Δ*paxQ*) were fed with α- and β-paxitriol (Section 2.20) and analysed by NP-TLC for presence of indole-diterpenes (Section 2.21). **(A)** NP-TLC analysis of α-paxitriol-fed *P. paxilli* mutants and **(B)** NP-TLC analysis of β-paxitriol-fed *P. paxilli* mutants. '-' without α- or β-paxitriol; '+' with α- or β-paxitriol; precursor fed is labelled red. 13-dp=13-desoxypaxilline.

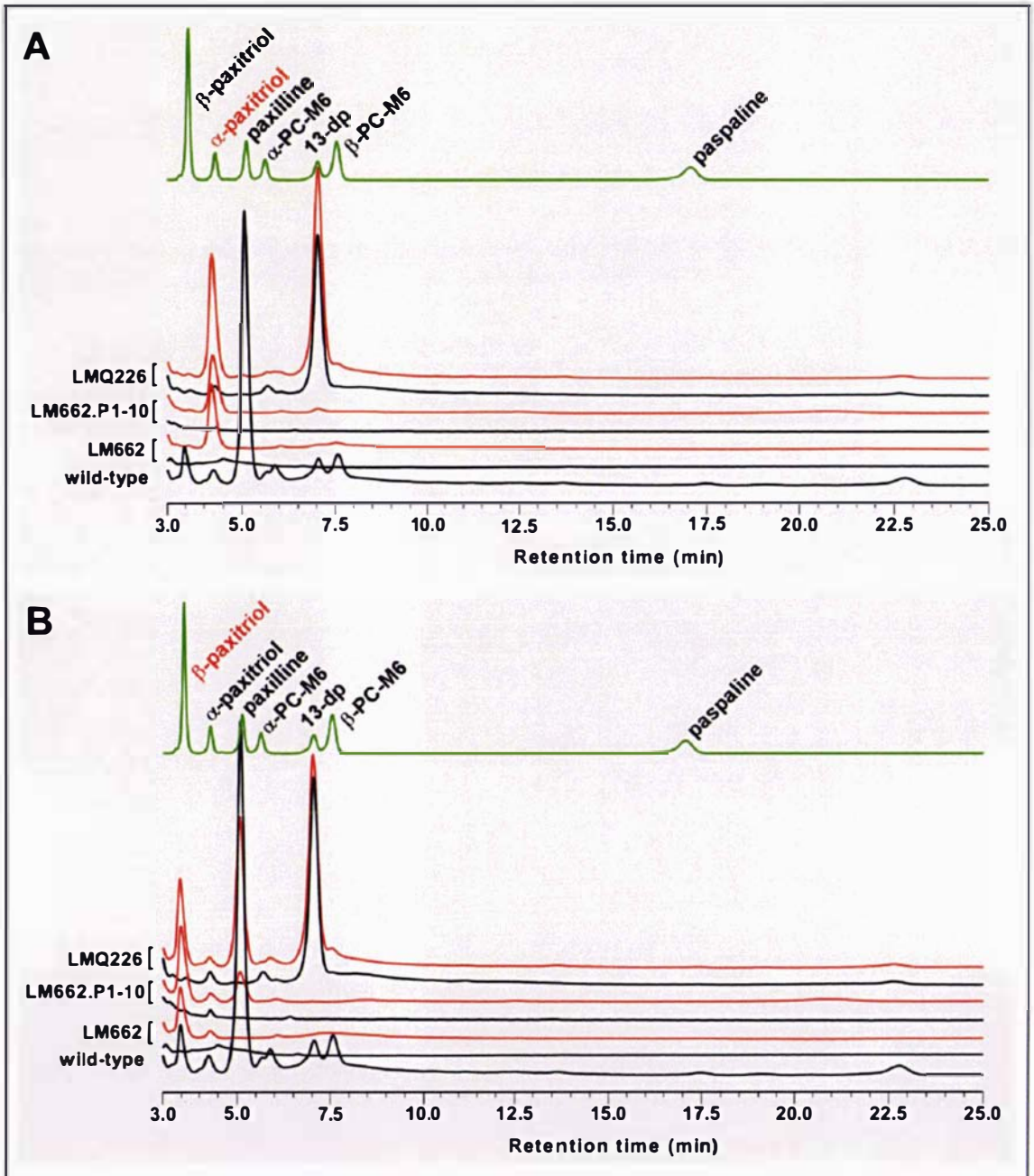

Figure 3.37 RP-HPLC analysis of *P. paxilli* mutants and LM662/pSS1 transformants fed with α- and β-paxitriol

LM662 strain containing pSS1 (*paxP*) and *P. paxilli* deletion mutant LMQ226 (Δ*paxQ*) were fed with α- and β-paxitriol (Section 2.20) and analysed by RP-HPLC for presence of indole-diterpenes (Section 2.21). **(A)** RP-HPLC analysis of α-paxitriol-fed *P. paxilli* cultures. **(B)** RP-HPLC analysis of β-paxitriol-fed *P. paxilli* cultures. black traces - without α- or β-paxitriol; red traces - with α- or β-paxitriol; precursor fed is labelled red. P1=pSS1; 13-dp=13-desoxypaxilline.

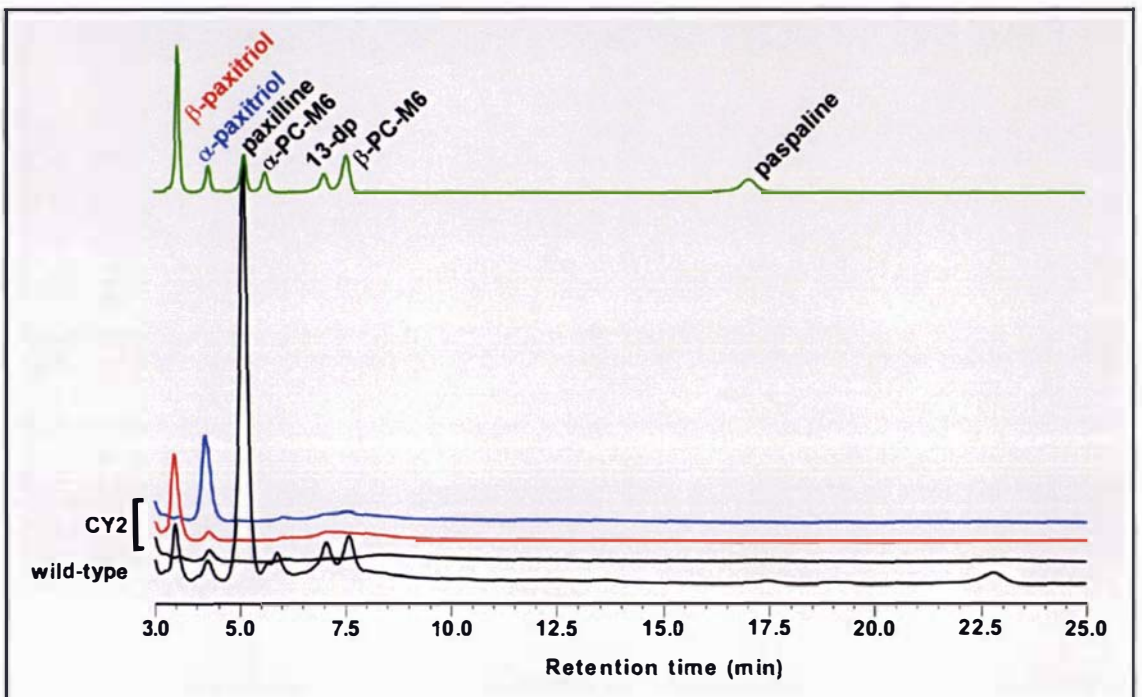

Figure 3.38 RP-HPLC analysis of *P. paxilli* mutant CY2 fed with α- and β-paxitriol

P. paxilli mutant CY2 was fed with α- and β-paxitriol (Section 2.20) and analysed by RP-HPLC for presence of indole-diterpenes (Section 2.21). black traces - without α- or β-paxitriol; red trace - with β-paxitriol; blue trace - with α-paxitriol; precursors fed are labelled red or blue. 13-dp=13-desoxypaxilline.

receive α-paxitriol (Figure 3.36A & Figure 3.37A). These results suggested that α-paxitriol is not a substrate for any Pax enzymes and hence not a true intermediate in paxilline biosynthesis.

Analysis of extracts of β-paxitriol-fed LM662 and CY2 mutants detected the added β-paxitriol (Figure 3.36B, Figure 3.37B & Figure 3.38). However, extracts of LMQ226 mutant incubated with β-paxitriol accumulated an indole-diterpene that had an R_f value similar to authentic paxilline, besides containing the added β-paxitriol and the indole-diterpenes that also accumulated in extracts of LMQ226 mutant that did not receive β-paxitriol (Figure 3.36B). This was confirmed by HPLC analysis (Figure 3.37B). The β-paxitriol-fed cultures of LM662.P1-10 also accumulated paxilline, in addition to the added β-paxitriol (Figure 3.35 & Figure 3.37B). Although none of the Pax enzymes were able to produce β-paxitriol, it was found to be a substrate for PaxP. The conversion of β-paxitriol to paxilline by the LMQ226 mutant suggests that the metabolism of β-paxitriol occurs after the steps catalysed by PaxQ. Taken together, these results suggest that β-paxitriol is not a true intermediate in paxilline biosynthesis. These results further confirm that the oxidation at C-10 is a catalytic function of PaxP, which catalyses the conversion of β-PC-M6 to 13-desoxypaxilline and β-paxitriol to paxilline, both requiring C-10 oxidation.

3.3.7 Summary

Based on the precursor feeding studies, paspaline was found to be a substrate for PaxP and was converted to 13-desoxypaxilline and β-PC-M6. These studies also showed that 13-desoxypaxilline was a substrate for PaxQ and was converted only to paxilline. However, the conversion of the substrates by both PaxP and PaxQ was more efficient in the LM662 background than in the CY2 background which could be due to the higher level of expression of the corresponding genes in the LM662 background. α-PC-M6 was a substrate only for PaxQ and was converted to α-paxitriol. However, β-PC-M6 was a substrate for PaxP and was converted to 13-desoxypaxilline. Thus, PaxP is able to catalyse the steps involved in the conversion of paspaline to 13-

desoxypaxilline, via β-PC-M6. Unlike α-paxitriol, which was not a substrate for any Pax enzymes, β-paxitriol was found to be a substrate for PaxP and was converted to paxilline. Based on these results, a scheme for paxilline biosynthesis is proposed (Figure 3.39). PaxP, a cytochrome P450 monooxygenase, catalyses the conversion of paspaline to β-PC-M6 via paspaline B as proposed by Munday-Finch *et al*. (Munday-Finch *et al*., 1996). Further, PaxP also catalyses the C-10 oxidation of β-PC-M6 to form 13-desoxypaxilline. As a side reaction, PaxP catalyses a similar C-10 oxidation of β-paxitriol to paxilline. No evidence for the proposed bifurcation (Figure 3.24) in the pathway between PC-M6 and paxilline was found. PaxQ, another cytochrome P450 monooxygenase, catalyses the C-13 hydroxylation of 13-desoxypaxilline to form paxilline. PaxQ also catalyses a side reaction involving the C-13 hydroxylation of α-PC-M6 to form α-paxitriol.

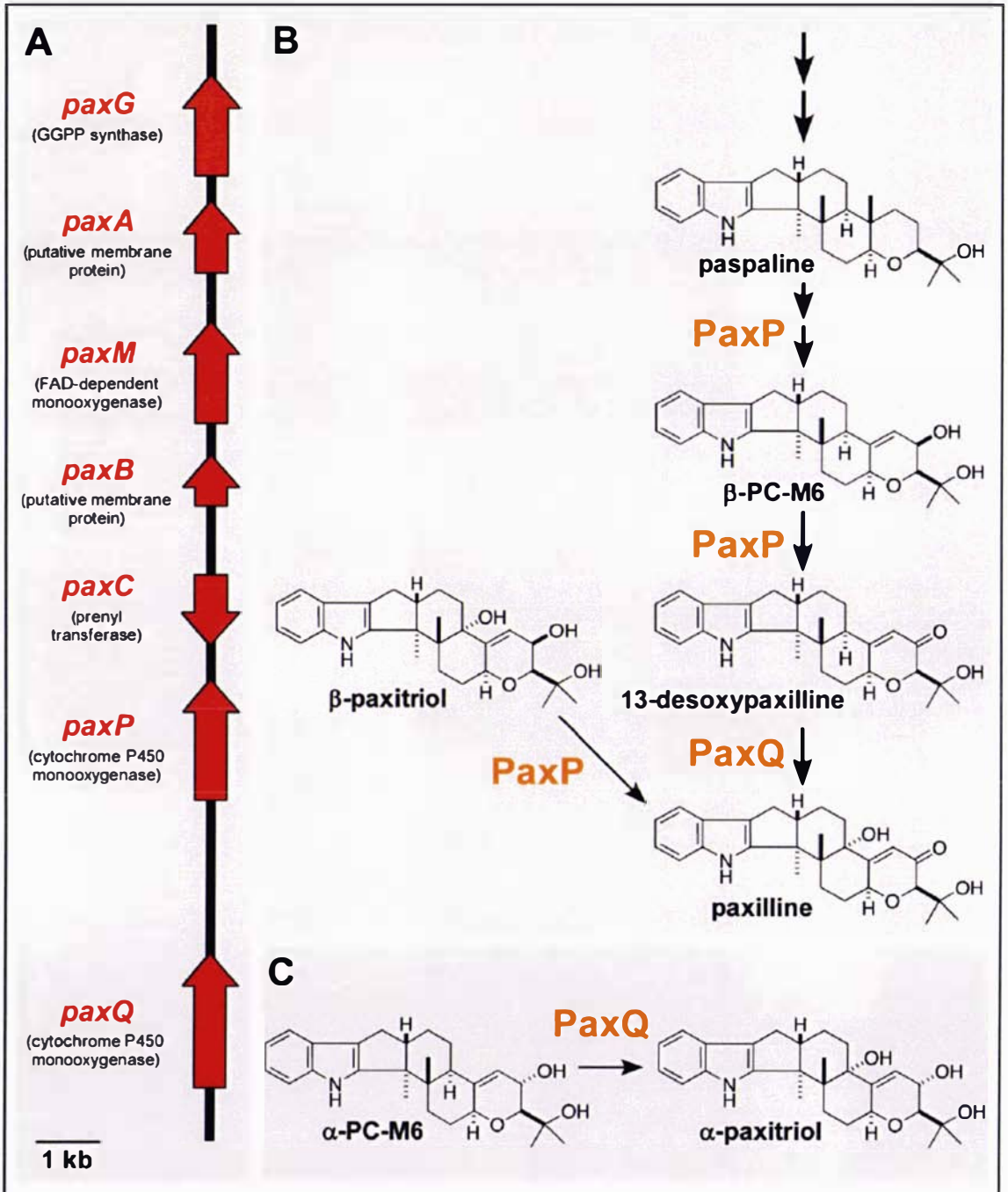

Figure 3.39 Formation of paxilline from paspaline

(A) Organisation of paxilline (*pax*) gene cluster. The proposed enzymatic function of each gene product, except PaxA and PaxB, is also indicated. No enzymatic function has been identified for PaxA and PaxB. **(B)** The proposed steps from paspaline to paxilline. **(C)** Side reaction catalysed by PaxQ. IPP - isopentenyl diphosphate; DMAPP - dimethyallyl diphosphate; GGPP - geranylgeranyl diphosphate.

3.4 Subcellular localisation of Ggs1 and PaxG

P. paxilli contains two copies of GGPP synthase genes viz. *ggs1* and *paxG* that are specific for primary and secondary metabolism, respectively (Young *et al.*, 2001). To test whether the two proteins are differentially localised enhanced GFP (EGFP) and DsRed fusion constructs of *ggs1* and *paxG* cDNA were transformed into wild-type *P. paxilli* and analysed by fluorescence microscopy.

3.4.1 Search for subcellular localisation signals

A BlastP (Altschul *et al.*, 1997) analysis of PaxG identified homologous sequences from other filamentous fungi including *A. nidulans* (AN0654, AN1592 and AN8143), *A. fumigatus* (AfA6E3.050c and Afu8g02400), *A. flavus* (AtmG), *F. graminearum* (FG10097 and FG04591), *F. fujikuroi* (Ff-Ggs1 and Ff-Ggs2), *Magnaportha grisea* (MG00758), *N. crassa* (Al-3) and *N. lolii* (Nl-Ggs1 and LtmG) which were aligned using ClustalX (Figure 3.40). This multiple sequence alignment showed variation among the sequences at their N-terminal region. Putative localisation signals at the N-terminus of GGPP synthases have been reported in other organisms (Okada *et al.*, 2000) suggesting that the variable N-terminal region observed among the PaxG homologues may harbour specific signals including that for localisation for the corresponding proteins. Phylogenetic analysis of these sequences revealed two distinct groups (Figure 3.41). One group contained Ggs1-related sequences and the other PaxG-related sequences. The sequences within the PaxG group were more divergent than those within the Ggs1 group.

A PSORT II (Nakai and Horton, 1999) analysis of these sequences for subcellular localisation signals identified peroxisomal targeting signals (indicated as red letters in Figure 3.40) in four of the PaxG-related sequences including PaxG, AtmG, AN8143 and FG04591. Although this search identified a peroxisomal targeting signal GRV in the C-terminus of PaxG, PaxG was predicted to be a cytoplasmic protein. Many variations of the C-terminus peroxisomal targeting signal type 1 (PTS 1) have been described with the consensus sequence (S/A/C/G)(K/R/H)(L/M) (Aitchison *et al.*, 1991; Gould *et al.*, 1989). The PaxG C-terminal tripeptide could be one of the variations of the

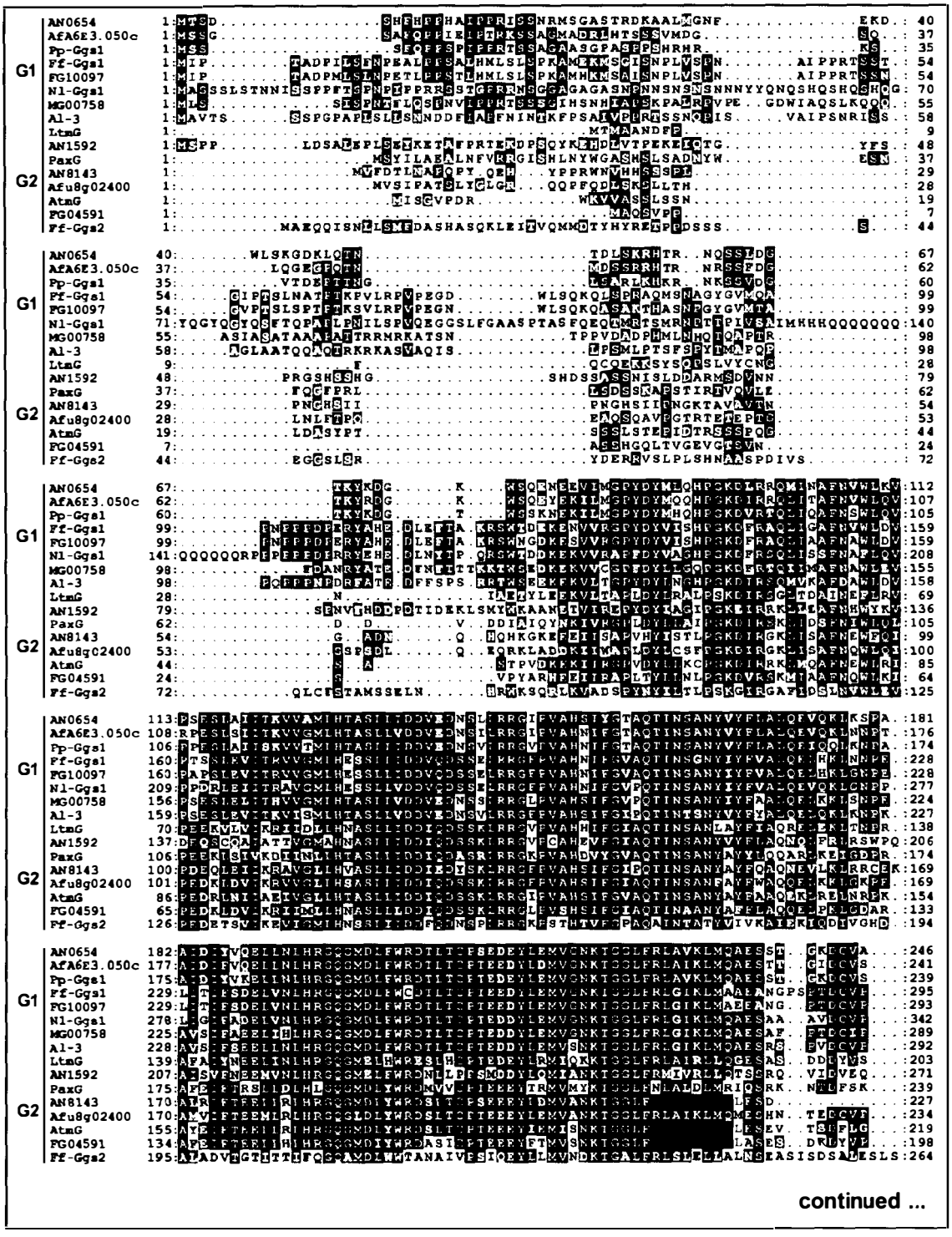
G1
G2
AN0654
AfA6E3.050c
Pp-Ggs1
Ff-Ggs1
FG10097
N1-Ggs1
MG00758
Al-3
LtmG
AN1592
PaxG
AN8143
Afu8g02400
AtmG
FG04591
Ff-Ggs2

continued ...

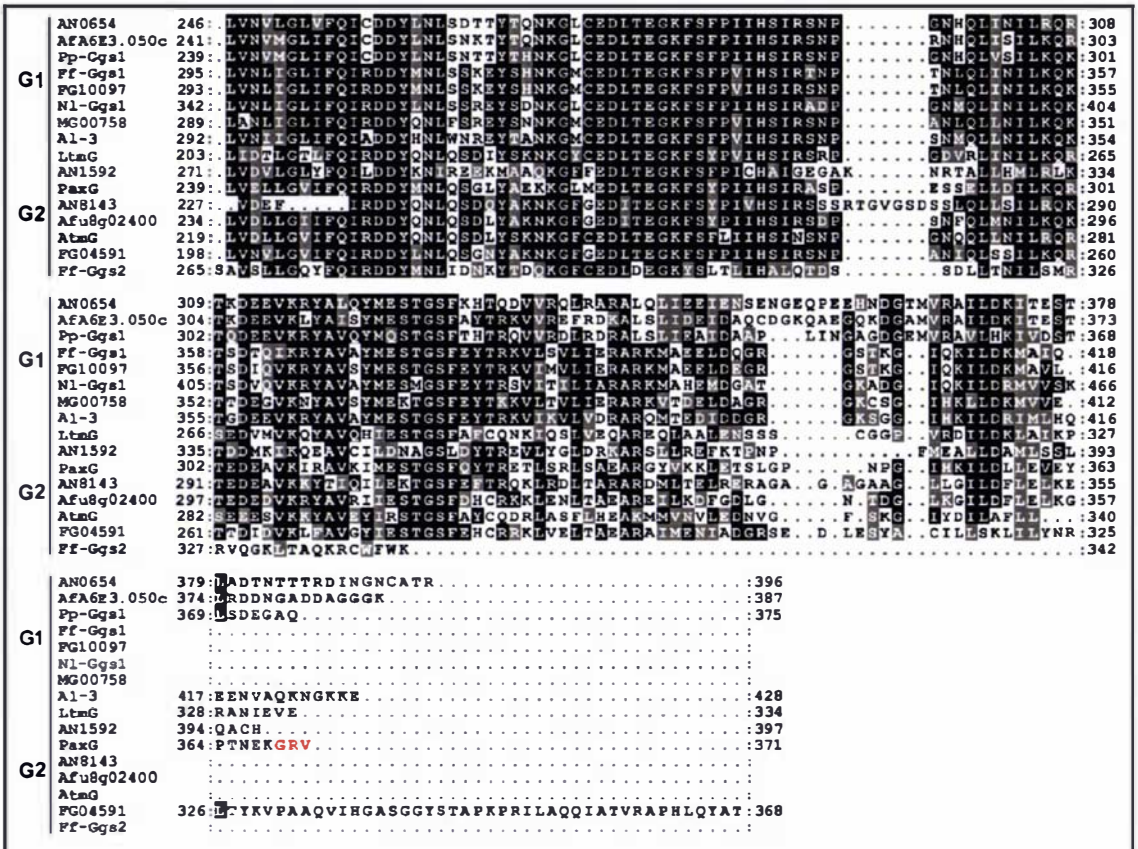

Figure 3.40 Multiple sequence alignment of GGPP synthases from filamentous fungi

The amino acid sequences of *P. paxilli* GGPP synthases were compared with those of other filamentous fungi. Amino acids identical in more than four sequences are indicated in white on black. Chemically conserved residues are indicated in white on gray. Amino acid residues that are similar to the conserved motif (R/K)(L/I)xxxxx(H/Q)(L/A) or (S/A/C/G)(K/R/H)(L/M) of peroxisomal proteins are shown as red letters. The sequences are grouped into G1 (Ggs1-related) and G2 (PaxG-related) based on a phylogenetic analysis (Figure 3.41). Accession numbers of the corresponding sequences are as follows: *A. nidulans* AN0654 - EAA65430, AN1592 - EAA64299, AN8143 - EAA59165; *A. fumigatus* AfA6E3.050c - CAF32032, Afu8g02400 - EAL84928; *A. flavus* AtmG - AAT65717; *P. paxilli* Pp-Ggs1 - AAK11525, PaxG - AAK11531; *F. fujikuroi* Ff-Ggs1 - CAA65644, Ff-Ggs2 - CAA75568; *F. graminearum* FG10097 - EAA68323, FG04591 - EAA72205; *N. lolii* Nl-Ggs1 - AAW88513, LtmG - AAW88510; *M. grisea* MG00758 - EAA49100; *N. crassa* Al-3 - P24322.

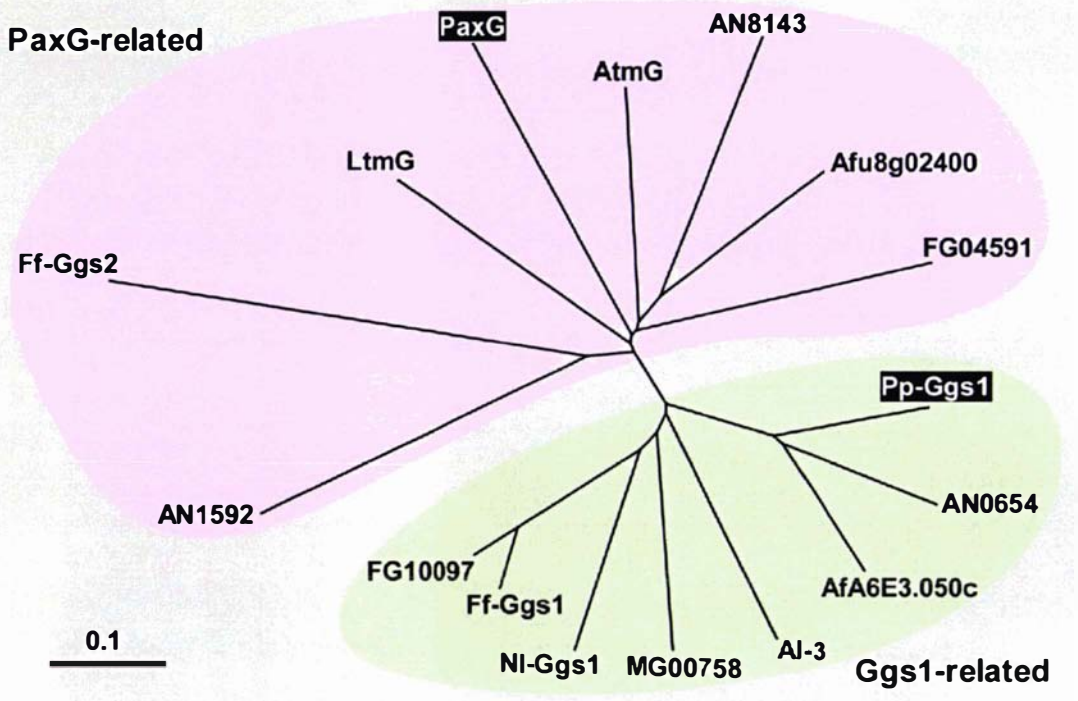

Figure 3.41 Phylogeny of GGPP synthases from filamentous fungi

A phylogenetic tree based on neighbour joining method was drawn using the TreeView program. The accession numbers of the corresponding sequences are as follows: *P. paxilli* Pp-Ggs1 - AAK11525, PaxG - AAK11531; *A. flavus* AtmG - AAT65717; *A. fumigatus* AfA6E3.050c - CAF32032, Afu8g02400 - EAL84928; *A. nidulans* AN0654 - EAA65430, AN1592 - EAA64299, AN8143 - EAA59165; *F. graminearum* FG10097 - EAA68323, FG04591 - EAA72205; *F. fujikuroi* Ff-Ggs1 - CAA65644, Ff-Ggs2 - CAA75568; *M. grisea* MG00758 - EAA49100; *N. crassa* Al-3 - P24322; *N. lolii* Nl-Ggs1 - AAW88513, LtmG - AAW88510.

PTS 1. The PSORT II analysis predicted *P. paxilli* Ggs1 and a related protein MG00758 as mitochondrial proteins. The N-terminal sequence of *P. paxilli* Ggs1 is over-represented by the amino acids Ser, Ala and Arg and lacks the negatively charged amino acids Asp and Glu, features characteristic of mitochondrial targeting peptides (Emanuelsson *et al.*, 2000).

3.4.2 Preparation of N- and C-terminal fusions of EGFP with *ggs1* cDNA

Plasmid pPN94 (Figure 3.42A) (Tanaka, unpublished results) carrying the *Aureobasidium pullulans TEF* promoter (Vanden Wymelenberg *et al.*, 1997), the *A. nidulans trpC* terminator (Mullaney *et al.*, 1985), and the *hph* gene for selection of transgenic strains was used for cloning and constitutive expression of the EGFP fusion constructs. A 1.12 kb *Xba*I/*Xho*I fragment and a 0.72 kb *Xho*I/*Not*I fragment containing the entire open reading frames (ORFs) of Ggs1 and EGFP, respectively, were cloned into the *Xba*I/*Not*I sites of pPN94 to generate pSS29 (Figure 3.43A).The *Xba*I/*Xho*I fragment was obtained by digesting a PCR product that was amplified with the primers ggs1-Xb-F and ggs1-Xh-R using wild-type cDNA as template (Section 2.14.4). The *Xho*I/*Not*I fragment was prepared by digesting a PCR product amplified with the primers EGFP-Xh-F and EGFP-No-R using pPN97 (Figure 3.42B) (Tanaka, unpublished results) as template (Section 2.14.3).

Plasmid pSS30 (Figure 3.43B) was prepared by cloning a 0.72 kb *Xba*I/*Xho*I fragment and a 1.12 kb *Xho*I/*Not*I fragment containing the entire ORFs of EGFP and Ggs1, respectively into the *Xba*I/*Not*I sites of pPN94. The 0.72 kb and 1.12 kb fragments were prepared by digesting PCR products that were amplified with the primers EGFP-Xb-F/EGFP-Xh-R (Section 2.14.3) and ggs1-Xh-F/ggs1-No-R (Section 2.14.4) using wild-type cDNA and pPN97 as templates, respectively.

All the primers contained mismatches relative to the wild-type sequence to introduce the appropriate enzyme recognition sites. All the PCR products were cloned into pBluescript II KS (+)-T vector (Section 2.8.3) and the sequences verified before their digestion with appropriate restriction endonucleases.

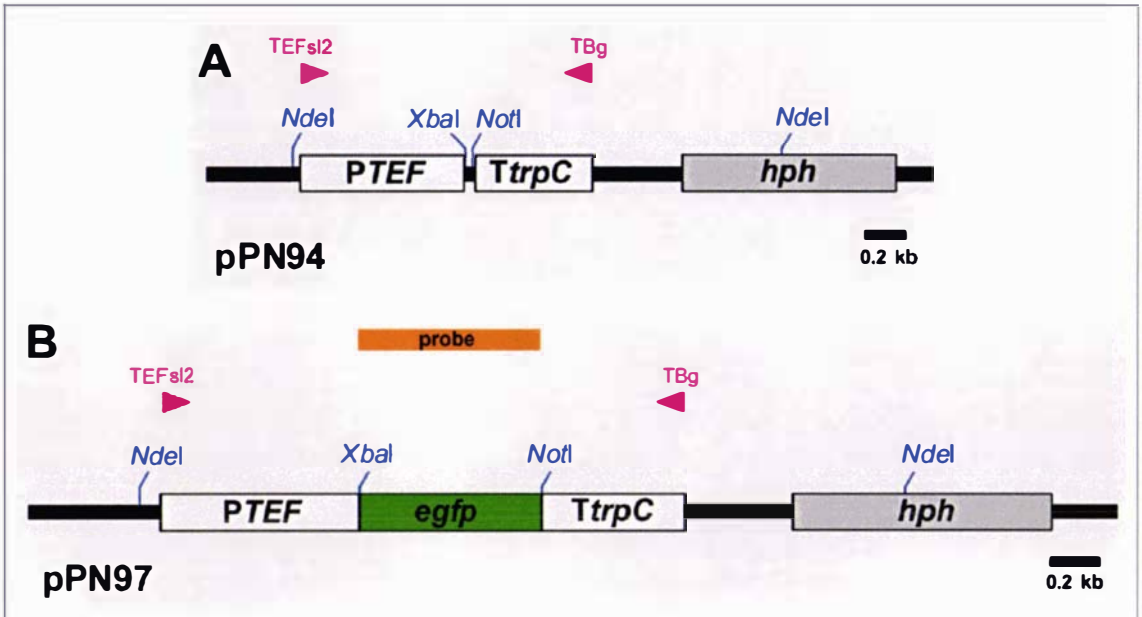

Figure 3.42 pPN94 and pPN97 constructs

(A) pPN94 construct (Tanaka, unpublished results). This was used as the base vector to prepare *egfp* fusion constructs. It contained the *TEF* promoter of *Aureobasidium pullulans* (Vanden Wymelenberg *et al.*, 1997), the *trpC* terminator of *A. nidulans* (Mullaney *et al.*, 1985) and the *hph* gene for selection of transgenic strains. **(B)** pPN97 construct (Tanaka, unpublished results). This was used as the '*egfp*-only' control. Primers TEFsl2/TBg were used for PCR screening of the transformants. The orange bar indicates the fragment used as the hybridisation probe. *Nde*I restriction sites were used for Southern analysis.

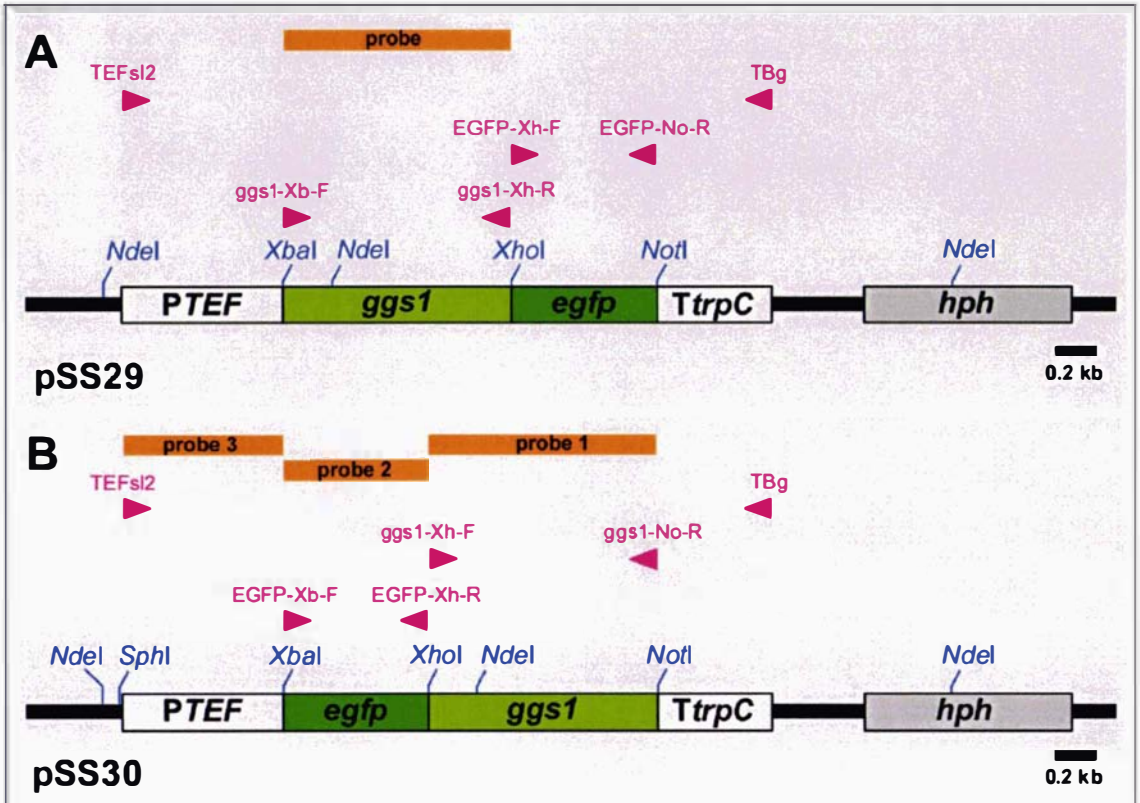

FIgure 3.43 Construction of reporter gene *egfp* fusions with *ggs1*

(A) pSS29 construct. *ggs1* and *egfp* cDNAs were amplified with primers ggs1-Xb-F/ggs1-Xh-R and EGFP-Xb-F/EGFP-No-R, respectively, sequence verified after TA-cloning, digested with *Xba*I/*Xho*I and *Xho*I/*Not*I, respectively, and cloned into *Xba*I/*Not*I-digested pPN94 (Figure 3.42A). **(B)** pSS30 construct. *egfp* and *ggs1* cDNAs were amplified with primers EGFP-Xb-F/EGFP-Xh-R and ggs1-Xh-F/ggs1-No-R, respectively, sequence verified after TA-cloning, digested with *Xba*I/*Xho*I and *Xho*I/*Not*I, respectively, and cloned into *Xba*I/*Not*I-digested pPN94 (Figure 3.42A).
Primers TEFsl2/TBg were used for PCR screening of the transformants. The orange bars indicate the fragments used as the hybridisation probe. *Nde*I and *Sph*I restriction sites were used for Southern analysis.

3.4.3 Subcellular localisation of Ggs1

Protoplasts of wild-type *P. paxilli* were transformed with 5 μg of either circular pSS29 (Ggs1-EGFP) or circular pSS30 (EGFP-Ggs1) (Section 2.13.2). Circular plasmid pPN97 containing EGFP alone was also included as a control. The resulting transgenic strains were selected on RG medium containing hygromycin (100 μg/ml). At least ten transgenic strains from each transformation were subjected to a primary screening by microscopy for EGFP fluorescence (Section 2.23). Four strains from each transformation, that showed comparatively high levels of EGFP fluorescence, were screened by PCR (data not shown) (Section 2.14.2) with the primers TEFsl2 and TBg that flank the insert including the *TEF* promoter and the *trpC* terminator. These strains were further analysed by Southern blotting and hybridisation (Section 2.10). Only one EGFP containing strain was used for Southern analysis. The Southern data showed that the transgenic strains contained at least one copy of the integrating construct (Figure 3.44). Fluorescence microscopy analysis (Section 2.23) of the strain carrying EGFP alone showed cytoplasmic distribution of EGFP fluorescence (Figure 3.45B). Similarly, the EGFP-Ggs1 fusion was found to express predominantly in the cytoplasm of all the four strains analysed (Figure 3.45D, H, J, P). However, in strains WT.P30-5 and WT.P30-7, the EGFP-Ggs1 fusion was observed to be localised in punctuate organelles in a few hyphae (Figure 3.45F, L, N). In contrast to the EGFP-Ggs1 fusion, the Ggs1-EGFP fusion was localised predominantly in punctuate organelles in all the four strains analysed (Figure 3.46D, E, F, G). Although Ggs1 is predicted to be a mitochondrial protein (Section 3.4.1), the pattern of Ggs1 localisation was not characteristic of mitochondrial localisation which typically forms a tubular network along the hyphae (Inoue *et al.*, 2002; Maggio-Hall and Keller, 2004).

To test if the punctuate organelles identified were mitochondria, the mitochondrial specific dye MitoTracker® Red CMXRos was used for staining (Section 2.22.1) mycelia of the strain WT.P29-12, since this strain showed comparatively more punctuate organelles expressing the chimeric protein. However, the pattern of Ggs1-EGFP fusion localisation was different from that

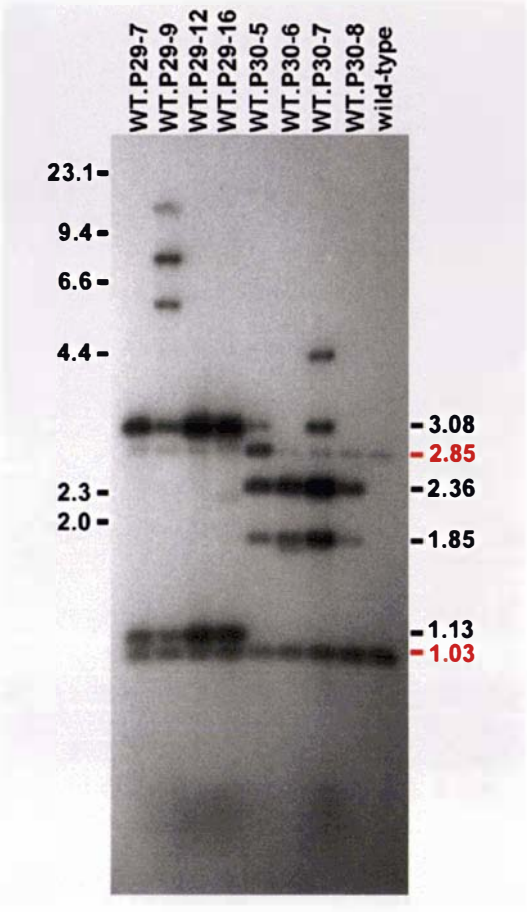

Figure 3.44 Southern analysis of wild-type strains containing pSS29 (Ggs1-EGFP) and pSS30 (EGFP-Ggs1)

*Nde*I-digested genomic DNA of wild-type strains containing Ggs1-EGFP and EGFP-Ggs1 was hybridised with the [^{32}P]-labelled *ggs1* probe (probe , Figure 3.43A; probe 1, Figure 3.43B). The numbers on the left correspond to the sizes of λDNA/*Hin*dIII fragments and those on the right correspond to the expected sizes of the restriction fragments that hybridised to the probe. The numbers labelled red correspond to the expected sizes of the restriction fragments in the parent wild-type strain. All fragment sizes are shown in kb. WT=wild-type; P29=pSS29; P30=pSS30.

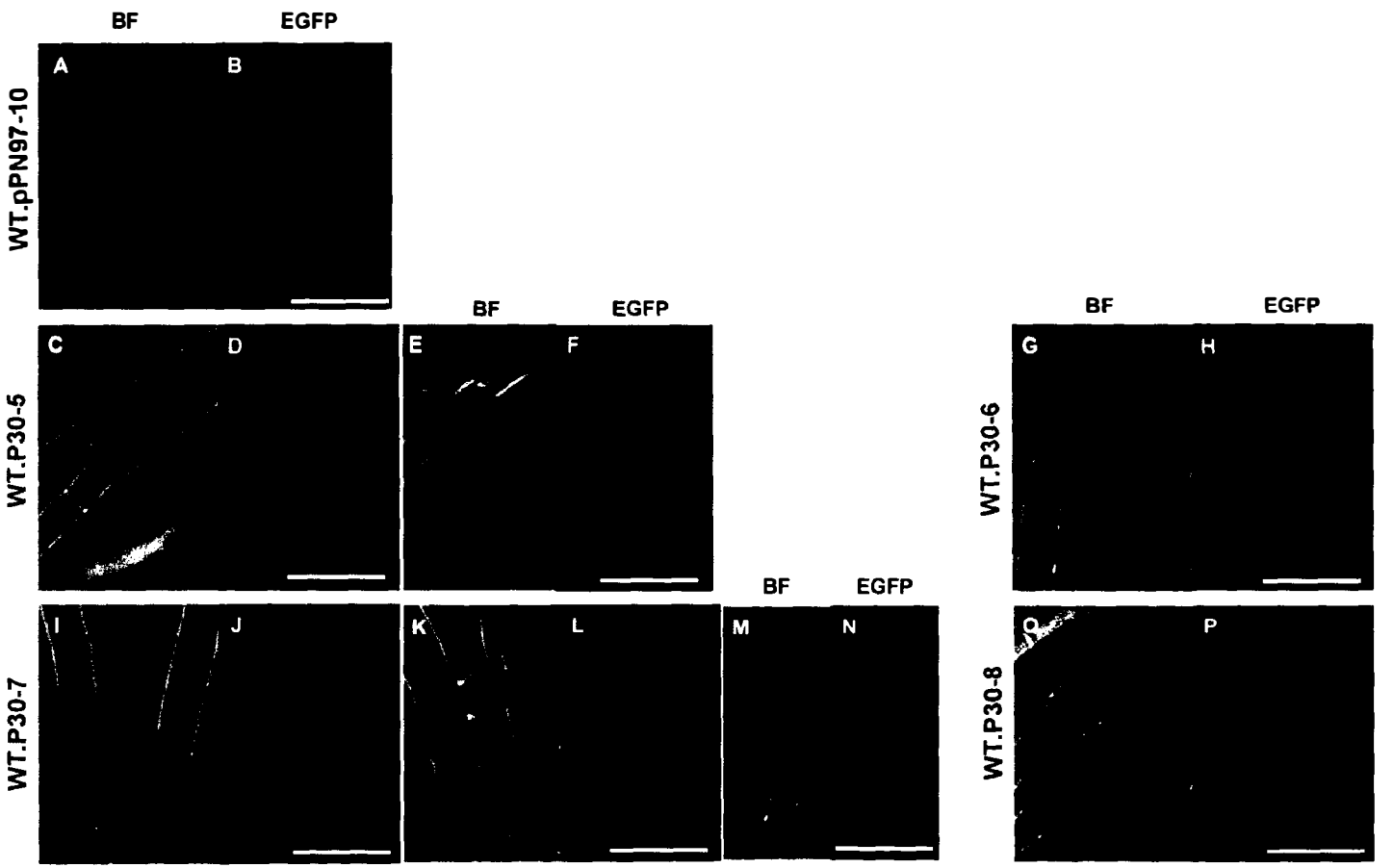

Figure 3.45 Subcellular localisation of EGFP-Ggs1 fusion

Wild-type strains containing pPN97 (EGFP-only) and pSS30 (EGFP-Ggs1) were grown on PDA at 22°C for 2 days (Section 2.23). Mycelia were observed by fluorescence microscopy. A, C, E, G, I, K, M, O - Bright Field (BF) images; B, D, F, H, J, L, N, P - EGFP fluorescence images. WT=wild-type; P30=pSS30. Bars=10 μm.

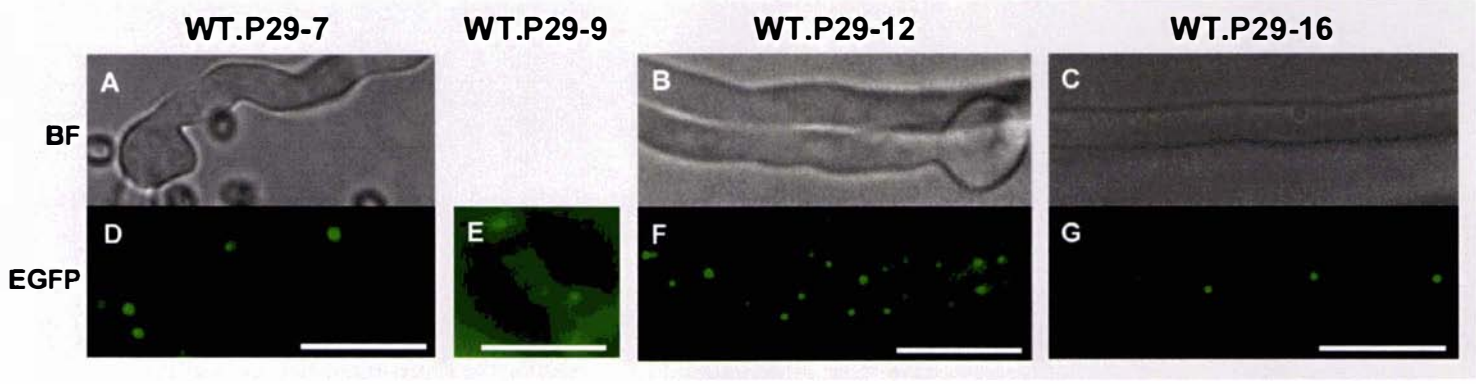

Figure 3.46 Subcellular localisation of Ggs1-EGFP fusion

Wild-type strains containing pSS29 (Ggs1-EGFP) were grown on PDA at 22ºC for 2 days (Section 2.23). Mycelia were observed by fluorescence microscopy. A-C Bright Field (BF) images; D-G EGFP fluorescence images. WT=wild-type; P29=pSS29. Bars=10 μm.

observed with MitoTracker (Figure 3.47), which stained mitochondria in a characteristic tubular pattern along the hyphae. These data suggested that the organelles expressing the Ggs1-EGFP fusion are not mitochondria. A membrane-selective fluorescent dye FM 4-64 was also used to check if the observed organelles are stained (Section 2.22.2). However, this dye also failed to stain the punctuate organelles (Figure 3.48).

3.4.4 Preparation of N- and C- terminal fusions of EGFP with *paxG* cDNA

A 1.11 kb *Spe*I/*Xho*I fragment and a 0.72 kb *Xho*I/*Not*I fragment containing the coding regions of PaxG and EGFP, respectively, were cloned into the *Xba*I/*Not*I sites of pPN94 to generate pSS27 (Figure 3.49A). The *Spe*I/*Xho*I fragment was prepared by digesting a PCR product amplified with the primers paxG-Sp-F and paxG-Xh-R using wild-type cDNA as template (Section 2.14.3). The *Xho*I/*Not*I fragment was prepared by digesting a PCR product amplified with the primers EGFP-Xh-F and EGFP-No-R using pPN97 (Figure 3.42B) as template (Section 2.14.3).

Plasmid pSS28 (Figure 3.49B) was prepared by cloning a 0.72 kb *Xba*I/*Xho*I fragment and a 1.11 kb *Xho*I/*Not*I fragment containing the coding regions of EGFP and PaxG, respectively, into the *Xba*I/*Not*I sites of pPN94. The *Xba*I/*Xho*I fragment was prepared by digesting a PCR product amplified with the primer set EGFP-Xb-F and EGFP-Xh-R using pPN97 as template (Section 2.14.3). The *Xho*I/*Not*I fragment was prepared by digesting a PCR product amplified with the primer set paxG-Xh-F2 and paxG-No-R2 using wild-type cDNA as template (Section 2.1.4.4).

All the primers were designed to generate the appropriate enzyme recognition sites and the PCR products were subcloned into pBluescript II KS (+)-T vector (Section 2.8.3) for sequence verification before their digestion with appropriate restriction endonucleases.

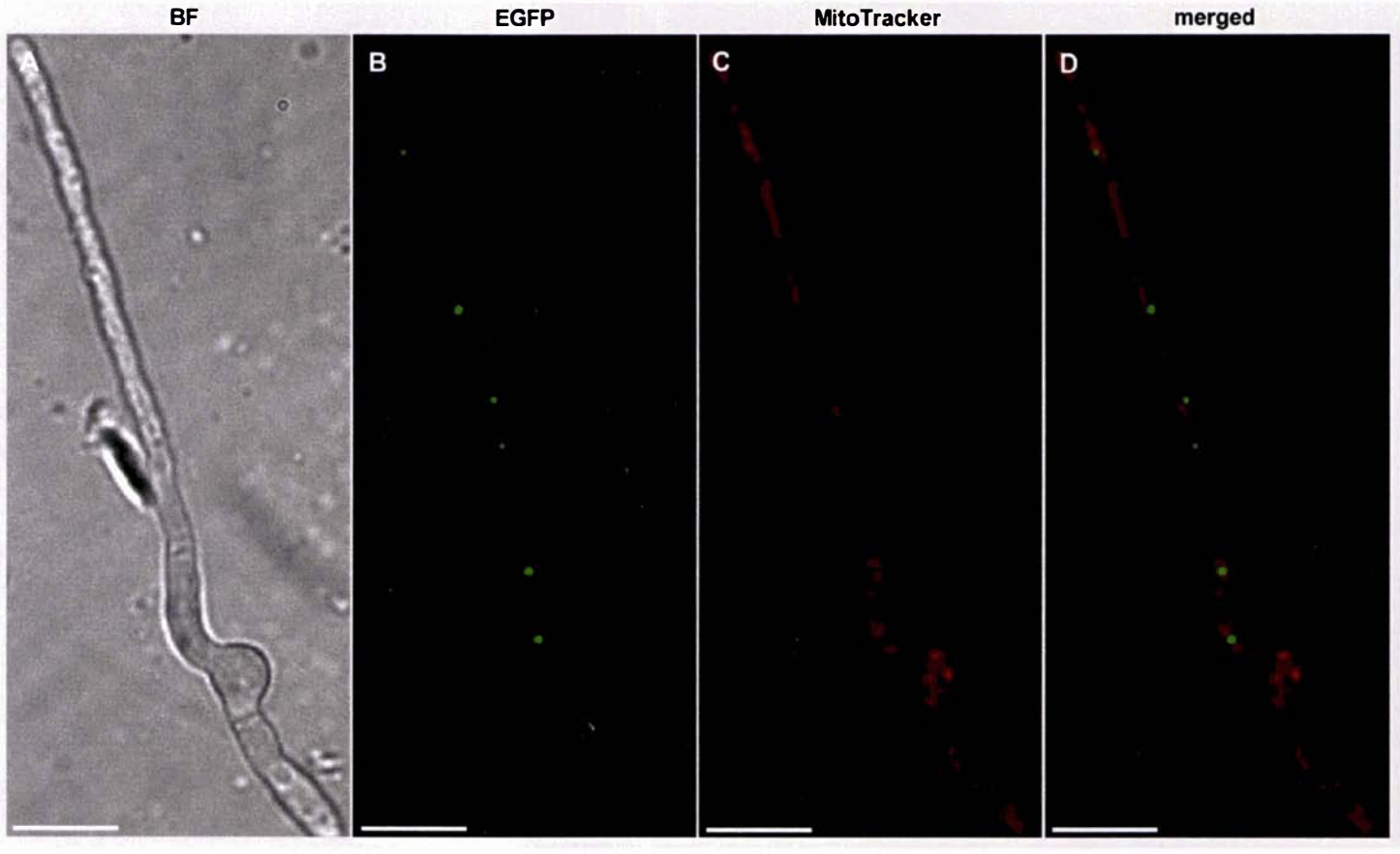

Figure 3.47 Visualisation of Ggs1-EGFP fusion

Strain WT.P29-12 (Ggs1-EGFP) was grown in PD broth at 22°C with shaking at 150 rpm for 2 days (Section 2.22). Mycelia were stained with MitoTracker® Red CMXRos for 30 min (Section 2.22.1) and observed by fluorescence microscopy. The same hyphal region is shown in all the images. A - Bright Field (BF) image; B - EGFP fluorescence image; C - MitoTracker staining image; D - merged image of B & C. Bars=10 μm.

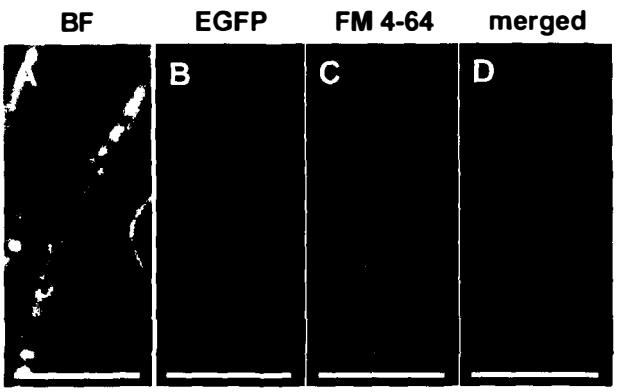

Figure 3.48 Visualisation of Ggs1-EGFP fusion

Strain WT.P29-12 (Ggs1-EGFP) was grown in PD broth at 22ºC with shaking at 150 rpm for 2 days (Section 2.22). Mycelia were stained with FM 4-64 for 30 min (Section 2.22.2) and observed by fluorescence microscopy. The same hyphal region is shown in all the images. A - Bright Field (BF) image; B - EGFP fluorescence image; C - FM 4-64 staining image; D - merged image of B & C. Bars=10 μm.

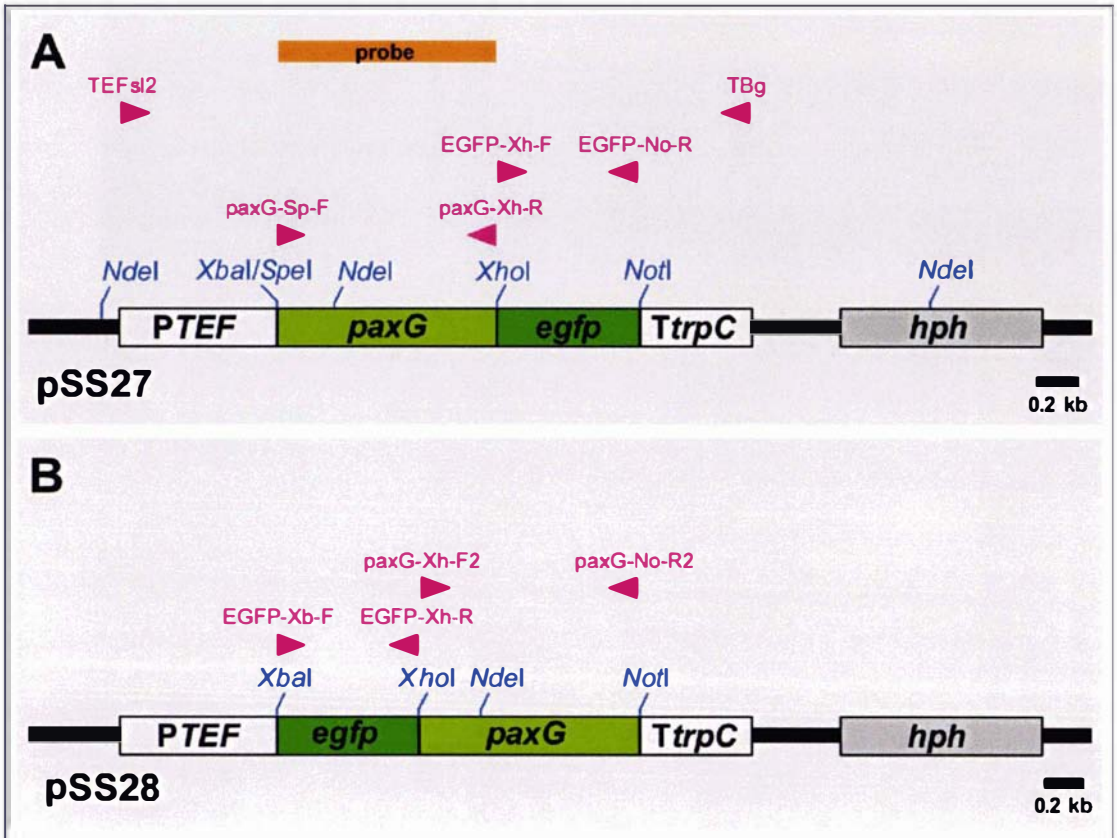

FIgure 3.49 Construction of reporter gene *egfp* fusions with *paxG*

(A) pSS27 construct. *paxG* and *egfp* cDNAs were amplified with primers paxG-Sp-F/paxG-Xh-R and EGFP-Xb-F/EGFP-No-R, respectively, sequence verified after TA-cloning, digested with *Spe*I/*Xho*I and *Xho*I/*Not*I, respectively, and cloned into *Xba*I/*Not*I-digested pPN94 (Figure 3.42A). Since *paxG* has a *Xba*I restriction site within the coding region, a *Spe*I restriction site was introduced by PCR at the 5' end of *paxG* cDNA to give a *Xba*I compatible 5' overhang for cloning into pPN94. **(B)** pSS28 construct. *egfp* and *paxG* cDNAs were amplified with primers EGFP-Xb-F/EGFP-Xh-R and paxG-Xh-F2/paxG-No-R2, respectively, sequence verified after TA-cloning, digested with *Xba*I/*Xho*I and *Xho*I/*Not*I, respectively, and cloned into *Xba*I/*Not*I-digested pPN94 (Figure 3.42A).
Primers TEFsl2/TBg were used for PCR screening of the transformants. The orange bar indicates the fragment used as the hybridisation probe. *Nde*I restriction sites were used for Southern analysis.

3.4.5 Subcellular localisation of PaxG

Five μg of either circular pSS27 (PaxG-EGFP) or circular pSS28 (EGFP-PaxG) was transformed into protoplasts of wild-type *P. paxilli* (Section 2.13.2). The resulting transgenic strains were selected on RG medium containing hygromycin (100 μg/ml). The introduction of pSS28 into protoplasts of wild-type *P. paxilli* did not give stable transformants. However, stable transformants were obtained with pSS27. At least ten transgenic strains were subjected to a primary screening by observing under the microscope for EGFP fluorescence (Section 2.23). No EGFP fluorescence was observed for the transgenic strains containing pSS27. Four pSS27 containing strains were arbitrarily selected for PCR screening (data not shown) (Section 2.14.2) with the primers TEFsI2 and TBg that flank the insert including the *TEF* promoter and the *trpC* terminator to ensure that their inability to fluoresce was not due to the absence of the PaxG-EGFP fusion construct. These strains were further analysed by Southern blotting and hybridisation (Section 2.10) which showed that all four strains contained the construct although with variable copy numbers (Figure 3.50).

3.4.6 Preparation of EGFP fusion with PaxG C-terminal tripeptide GRV

Since introduction of the EGFP construct with full length PaxG gave both unstable transformants and stable transformants that failed to express the PaxG-EGFP fusion (Section 3.4.5), a C-terminal EGFP fusion construct with the PaxG tripeptide GRV, a putative peroxisomal targeting motif (Section 3.4.1), was made. This plasmid pSS46 was prepared by cloning a 0.73 kb *Xba*I/*Not*I fragment containing the GRV tripeptide in frame at the C-terminus of the EGFP coding region into the corresponding restriction sites of pPN94 (Figure 3.51). The *Xba*I/*Not*I fragment was prepared by digesting a PCR product that was amplified with the primers EGFP-Xb-F and GRV-No-R, containing introduced *Xba*I and *Not*I sites, respectively, using pPN97 as template (Section 2.14.3). The primer GRV-No-R was designed to add the GRV tripeptide, in frame, to the C-terminus of the *egfp* gene. The sequence of the PCR product was verified by TA-cloning before restriction digestion.

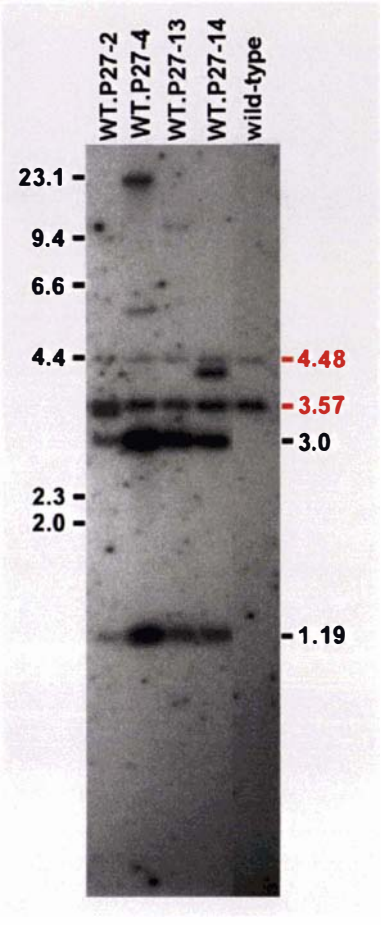

Figure 3.50 Southern analysis of wild-type strains containing pSS27 (PaxG-EGFP)

*Nde*I-digested genomic DNA of wild-type strains containing PaxG-EGFP was hybridised with the [^{32}P]-labelled *paxG* probe (Figure 3.49A). The numbers on the left correspond to the sizes of λDNA/*Hin*dIII fragments and those on the right correspond to the expected sizes of the restriction fragments that hybridised to the probe. The numbers labelled red correspond to the expected sizes of the restriction fragments in the parent wild-type strain. All fragment sizes are shown in kb. WT=wild-type; P27=pSS27.

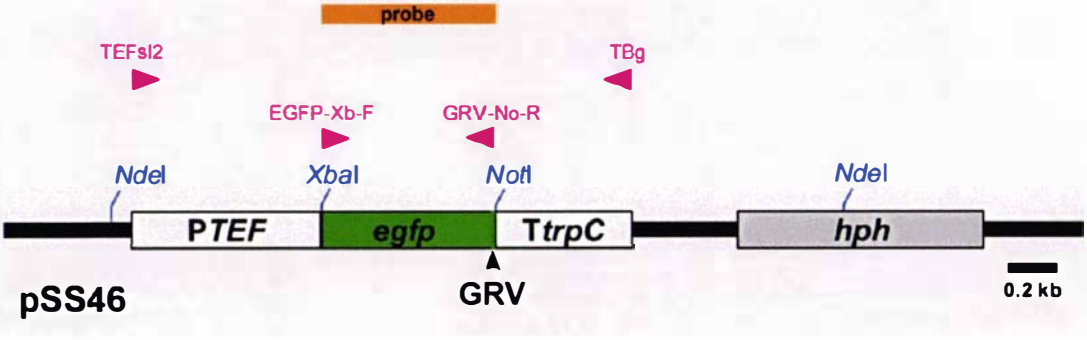

FIgure 3.51 Construction of reporter gene e*gfp* fusion with GRV tripeptide

pSS46 construct. *egfp* cDNA was amplified with primers EGFP-Xb-F/GRV-No-R. The 3' flanking primer, GRV-No-R, was designed to add in frame 9 additional base pairs, corresponding to GRV tripeptide, to the C-terminus of *egfp* cDNA. The PCR product was TA-cloned and sequence verified before digesting with *Xba*I/*Not*I and cloning into the corresponding restriction sites of pPN94 (Figure 3.42A).
Primers TEFsl2/TBg were used for PCR screening of the transformants. The orange bar indicates the fragment used as the hybridisation probe. *Nde*I restriction sites were used for Southern analysis.

3.4.7 Subcellular localisation of EGFP-GRV fusion

Protoplasts of wild-type *P. paxilli* were transformed with five μg of circular pSS46 (EGFP-GRV) (Section 2.13.2). At least ten stable transformants were subjected to a primary screening by microscopy (Section 2.23). Almost all the strains showed EGFP fluorescence under UV light and four of these strains, that exhibited comparatively high levels of EGFP fluorescence, were screened by PCR (data not shown) (Section 2.14.2) and then analysed by Southern blotting and hybridisation (Section 2.10) for the presence of the chimeric construct. The EGFP-GRV strains contained at least one copy of the insert (Figure 3.52). Strain WT.P30-8 that contained one copy of the chimeric *egfp-ggs1* gene (Figure 3.44) was used as a control for copy number. When examined by fluorescence microscopy (Section 2.23), this fusion protein was observed to be localised in punctuate organelles in all the four strains analysed (Figure 3.53B, D, F, H). Cytoplasmic expression of the EGFP-GRV fusion was also observed. The expression level of the EGFP-GRV fusion was variable among the strains and was not related to the copy number.

3.4.8 Preparation of DsRed-SKL fusion

In order to test if the punctuate organelles expressing the EGFP-GRV fusion (Section 3.4.7) were peroxisomes a reporter fusion construct with the consensus PTS 1 motif, SKL, was made. Vector pSS37 (Figure 3.54) was prepared to clone DsRed and DsRed-SKL fusion constructs. Plasmid pSS45 (Figure 3.55A) was prepared as a control by ligating a 0.67 kb *Xba*I/*Not*I fragment containing DsRed alone into the corresponding restriction sites of pSS37. The DsRed fragment was prepared by digesting a PCR product amplified with the primers DsRed-XbaI-F and DsRed-No-R, containing introduced *Xba*I and *Not*I sites, respectively, using pPgpd-DsRed as template (Section 2.14.3).

Plasmid pSS41 (Figure 3.55B) was prepared by cloning a 0.69 kb *Xba*I/*Not*I fragment containing DsRed-SKL into the corresponding restriction sites of pSS37. The *Xba*I/*Not*I fragment was prepared by digesting a PCR product that was amplified with the primers DsRed-XbaI-F and SKL-No-R, containing

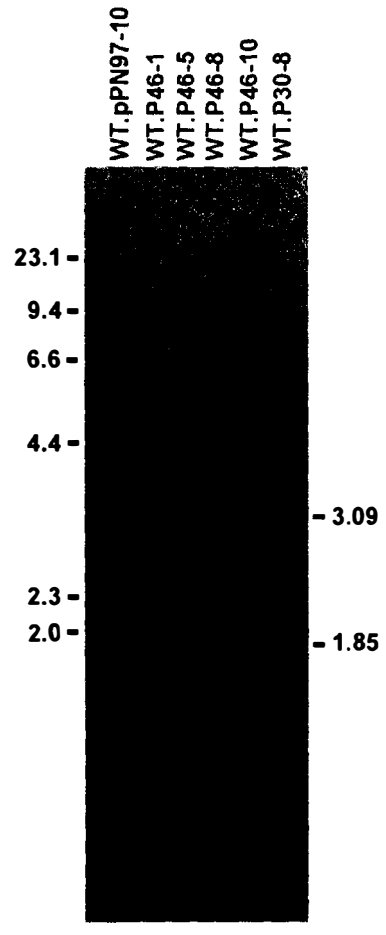

Figure 3.52 Southern analysis of wild-type strains containing pSS46 (EGFP-GRV) and pPN97 (EGFP)

*Nde*I-digested genomic DNA of wild-type strains containing EGFP-GRV and EGFP was hybridised with the [^{32}P]-labelled *egfp* probe (probe, Figure 3.42B & 3.51; probe 2, Figure 3.43B). Genomic DNA of WT.P30-8 was included as a control since it contained a single copy of the chimeric *egfp-ggs1* gene (Figure 3.44). The numbers on the left correspond to the sizes of λDNA/*Hin*dIII fragments and those on the right correspond to the expected sizes of the restriction fragments that hybridised to the probe. All fragment sizes are shown in kb. WT=wild-type; P46=pSS46; P30=pSS30 (EGFP-Ggs1).

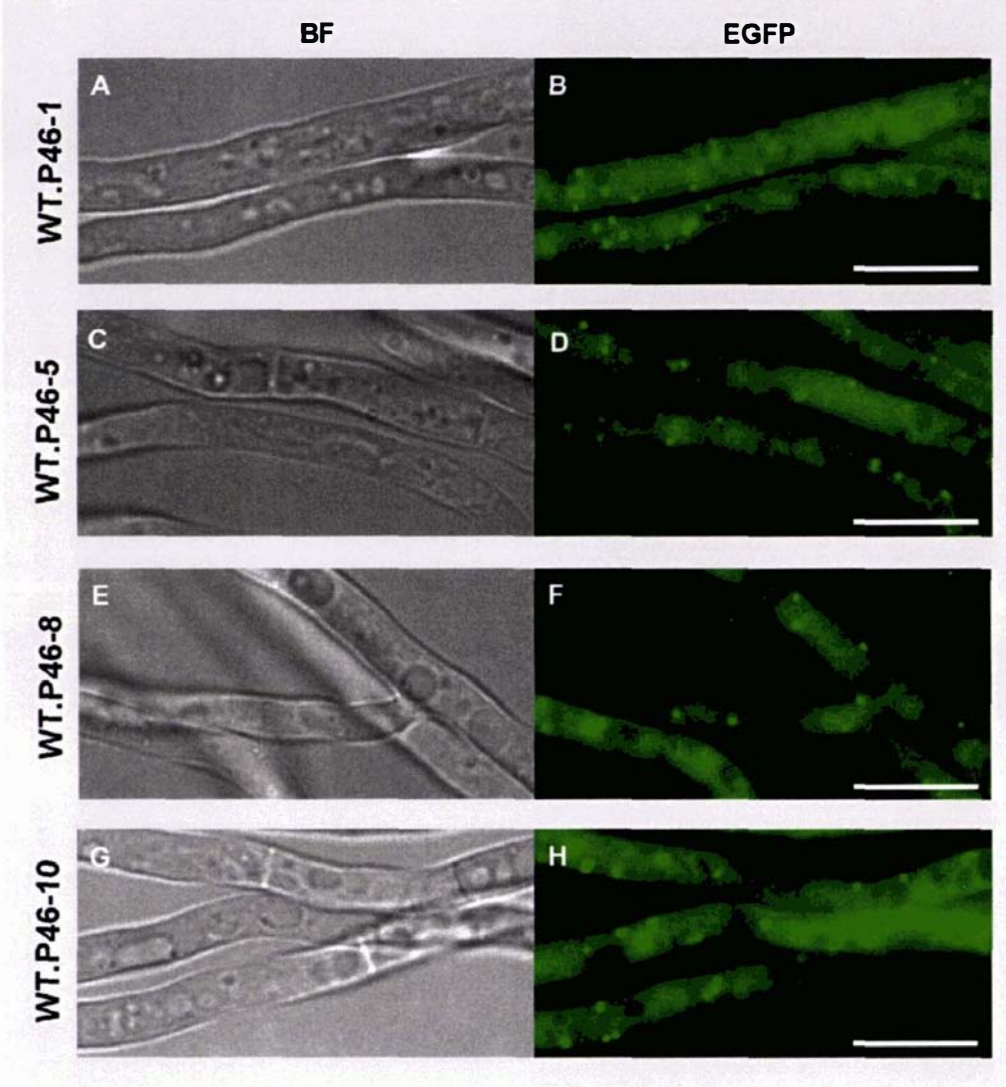

Figure 3.53 Subcellular localisation of EGFP-GRV fusion

Wild-type strains containing pSS46 (EGFP-GRV) were grown on PDA at 22°C for 2 days (Section 2.23). Mycelia were observed by fluorescence microscopy. A, C, E, G - Bright Field (BF) images; B, D, F, H - EGFP fluorescence images. WT=wild-type; P46=pSS46. Bars=10 μm.

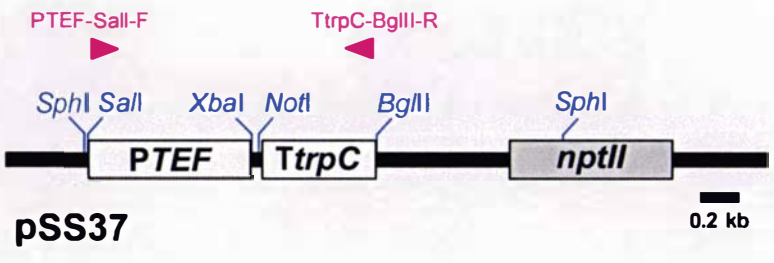

Figure 3.54 Construction of pSS37

A fragment containing the *TEF* promoter of *A. pullulans* (Vanden Wymelenberg *et al.*, 1997) and the *trpC* terminator of *A. nidulans* (Mullaney *et al.*, 1985) was prepared by PCR with primers PTEF-SalI-F/TtrpC-BglII-R using pPN94 (Figure 3.42A) as template. The PCR product was TA-cloned and the sequence verified before digesting with *SalI*/*Bgl*II. The *SalI*/*Bgl*II fragment was then cloned into the corresponding restriction sites of pPN16.17.cgi (Foster *et al.*, unpublished results) to generate pSS37. This was used as the base vector to prepare *dsred* fusion constructs. The presence of *nptII* gene in the base vector facilitated selection of transgenic strains.

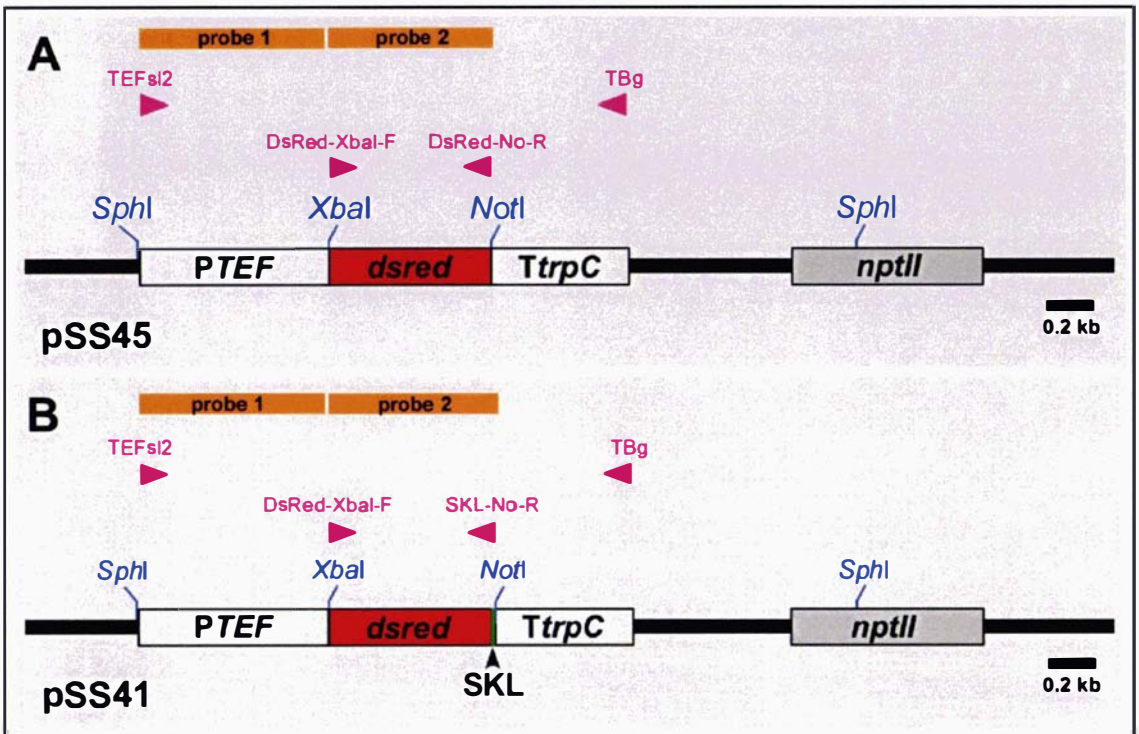

FIgure 3.55 Construction of reporter gene *dsred* fusion with SKL tripeptide

(A) pSS45 construct. *dsred* cDNA was amplified with primers DsRed-XbaI-F/DsRed-No-R, sequence verified after TA-cloning, digested with *Xba*I/*Not*I and cloned into *Xba*I/*Not*I-digested pSS37 (Figure 3.54). **(B)** pSS41 construct. *dsred* cDNA was amplified with primers DsRed-XbaI-F/SKL-No-R. The 3' flanking primer, SKL-No-R, was designed to add in frame 9 additional base pairs, corresponding to SKL tripeptide, to the C-terminus of *dsred* cDNA. The PCR product was TA-cloned and sequence verified before digesting with *Xba*I/*Not*I and cloning into the corresponding restriction sites of pSS37 (Figure 3.54).
The reporter gene constructs were under the control of the *TEF* promoter of *A. pullulans* (Vanden Wymelenberg *et al.*, 1997) and the *trpC* terminator of *A. nidulans* (Mullaney *et al.*, 1985). Primers TEFsl2/TBg were used for PCR screening of the transformants. The orange bars indicate the fragments used as the hybridisation probe. *Sph*I restriction sites were used for Southern analysis.

introduced *Xba*I and *Not*I sites, respectively, using pPgpd-DsRed as template (Section 2.14.3). The primer SKL-No-R contained nine additional bases 3' to the introduced *Not*I site to add in frame the SKL tripeptide to the DsRed gene. The sequences of all the PCR products were verified by TA-cloning before restriction digestion.

Like the EGFP fusion constructs (Section 3.4.2), the DsRed fusion constructs were also under the control of the strong constitutive *TEF* promoter of *A. pullulans* and the *trpC* terminator of *A. nidulans*. However, in contrast to the EGFP fusion constructs, the DsRed fusion constructs contained *nptII* gene as the dominant selectable marker for co-transformation of fungal protoplasts.

3.4.9 Subcellular localisation of DsRed-SKL fusion

Protoplasts of wild-type *P. paxilli* were transformed with five μg of either circular pSS45 (DsRed) or pSS41 (DsRed-SKL) (Section 2.13.2). The resulting transgenic strains were selected on RG medium containing geneticin (150 μg/ml). After primary microscopic screening (Section 2.23) one DsRed containing strain and four DsRed-SKL containing strains were screened by PCR (data not shown) (Section 2.14.2), followed by Southern blotting and hybridisation (Figure 3.56) (Section 2.10). Two of the strains containing the DsRed-SKL fusion viz. WT.P41-1 and WT.P41-10 had one copy of the insert. However, in all the four DsRed-SKL strains analysed, the DsRed-SKL chimeric protein was localised to punctuate organelles (Figure 3.57D, F, H, J) and was not observed in the cytoplasm. The strain containing DsRed alone showed cytoplasmic DsRed fluorescence (Figure 3.57B). Unlike the punctuate organelles observed in the Ggs1-EGFP strains (Section 3.4.3), these punctuate organelles were mobile and kept moving in and out of the focal plane. These data indicated that the SKL motif was able to function as the peroxisomal targeting signal in *P. paxilli*.

3.4.10 Co-localisation of EGFP-GRV and DsRed-SKL fusions

To check if the punctuate organelles to which the EGFP-GRV fusion was localised were peroxisomes, protoplasts of the DsRed-SKL strain WT.P41-1

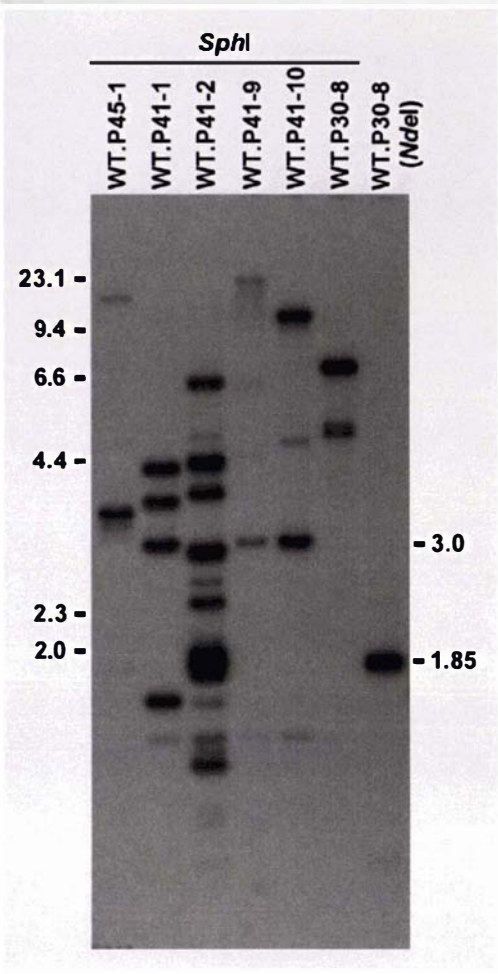

Figure 3.56 Southern analysis of wild-type strains containing pSS45 (DsRed) and pSS41 (DsRed-SKL)

*Sph*I-digested genomic DNA of wild-type strains containing DsRed and DsRed-SKL was hybridised with the [^{32}P]-labelled *PTEF* probe (probe 1, Figure 3.55; probe 3 Figure 3.43B). *Nde*I-digested genomic DNA of the strain WT.P30-8, which contained one copy of the chimeric *egfp-ggs1* gene (Figure 3.44), was also included as a control since there was only one *Sph*I site in pSS30. The numbers on the left correspond to the sizes of λDNA/*Hin*dIII fragments and those on the right correspond to the expected sizes of the restriction fragments that hybridised to the probe. All fragment sizes are shown in kb. WT=wild-type; P45=pSS45; P41=pSS41; P30=pSS30 (EGFP-Ggs1).

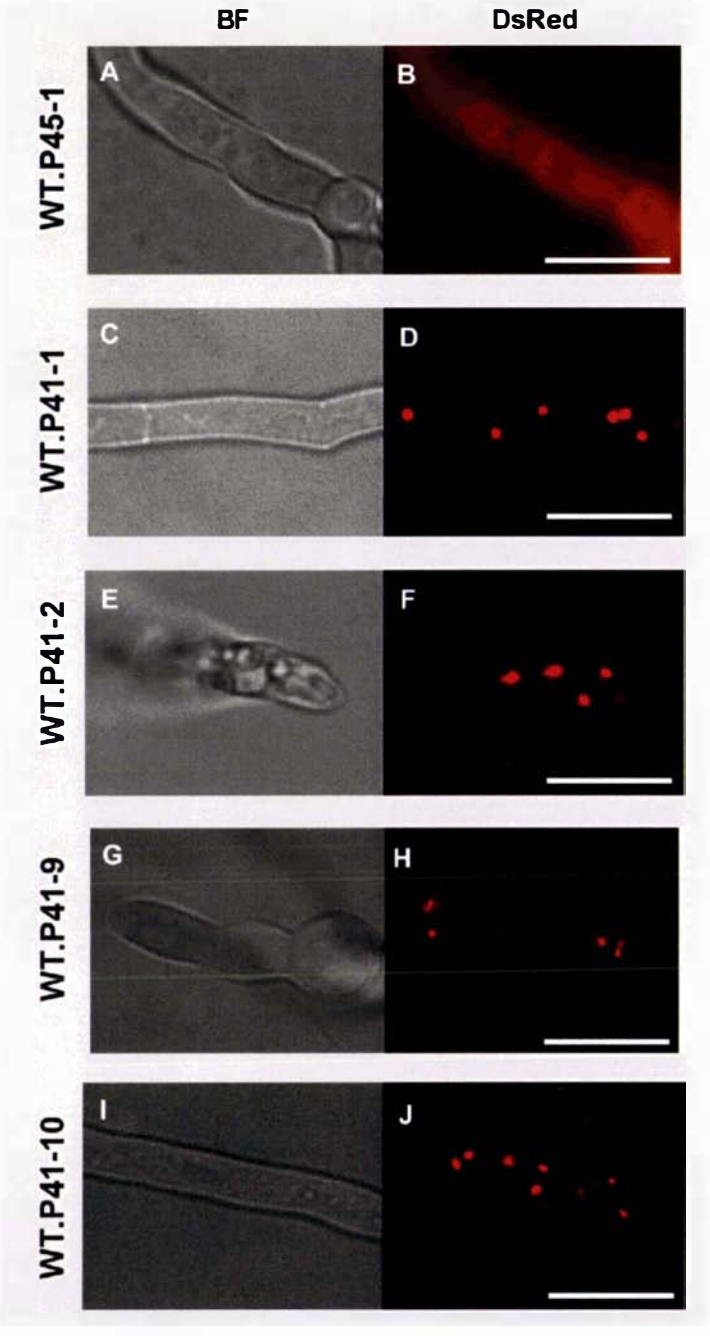

Figure 3.57 Subcellular localisation of DsRed-SKL fusion

Wild-type strains containing pSS45 (DsRed) and pSS41 (DsRed-SKL) were grown on PDA at 22ºC for 2 days (Section 2.23). Mycelia were observed by fluorescence microscopy. A, C, E, G, I - Bright Field (BF) images; B, D, F, H, J - DsRed fluorescence images. WT=wild-type; P45=pSS45; P41=pSS41. Bars=10 μm.

was transformed with 5 μg of circular plasmid pSS46 (EGFP-GRV) and the transgenic strains selected on RG medium containing hygromycin (100 μg/ml) (Section 2.13.2). Since all the strains carrying the *DsRed*-SKL gene showed a similar pattern of DsRed fluorescence, strain WT.P41-1 was arbitrarily chosen for differential labelling. Four transgenic strains that exhibited both EGFP and DsRed fluorescence after primary microscopic screening (Section 2.23) were arbitrarily selected for PCR analysis (data not shown) (Section 2.14.2) and Southern blotting and hybridisation (Section 2.10). These strains contained at least two copies of the EGFP-GRV insert (Figure 3.58). Strain WT.P30-8 that contained one copy of the chimeric *egfp-ggs1* gene (Figure 3.44) was included to determine the copy number of *egfp-GRV* (Figure 3.58B). All four strains showed co-localised expression of the EGFP-GRV and DsRed-SKL fusions (Figure 3.59). This confirmed that the EGFP-GRV expressing organelles are peroxisomes. Like the EGFP-GRV strains (Section 3.4.7), EGFP fluorescence was also observed in the cytoplasm of all four strains containing both the EGFP-GRV and DsRed-SKL fusions.

3.4.11 Oleic acid as a peroxisome proliferator

Since oleic acid is a known proliferator of peroxisomes (Maggio-Hall *et al.*, 2005), strains WT.P41-1 and WT.P46-10 containing the DsRed-SKL and EGFP-GRV fusions, respectively, were grown on PD medium supplemented with oleic acid (Section 2.23) to check if these strains show an increase in the number of organelles expressing the fusion proteins, as a result of oleic acid treatment. Strain WT.P46-10 was selected because the organelles expressing the EGFP-GRV fusion were more abundant in this strain than in the other EGFP-GRV strains. Both WT.P41-1 (DsRed-SKL) and WT.P46-10 (EGFP-GRV) strains showed a marked increase in the number of organelles that expressed the respective fusion proteins as a result of oleic acid induction (Figure 3.60). This data further supported that the punctuate organelles expressing the DsRed-SKL and EGFP-GRV fusions are indeed peroxisomes.

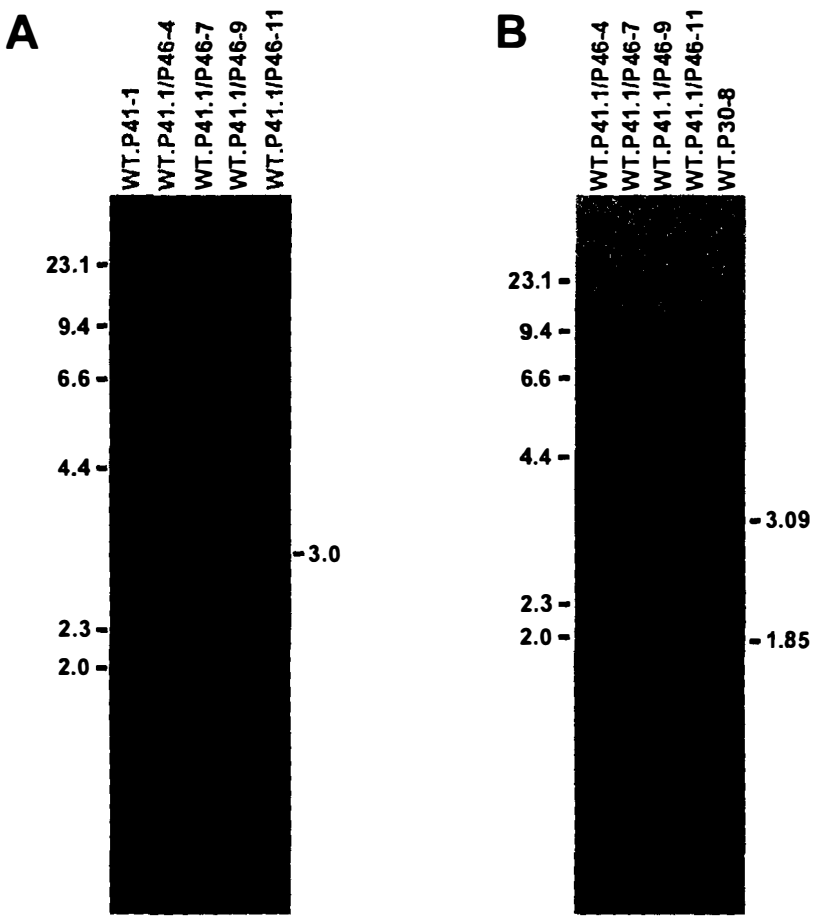

Figure 3.58 Southern analysis of wild-type strains containing both pSS41 (DsRed-SKL) and pSS46 (EGFP-GRV)

(A) *Sph*I-digested genomic DNA of wild-type strains containing both DsRed-SKL and EGFP-GRV was hybridised with the [^{32}P]-labelled *dsred* probe (probe 2, Figure 3.55B) to analyse the parent WT.P41-1 strain. **(B)** *Nde*I-digested genomic DNA of wild-type strains containing both DsRed-SKL and EGFP-GRV was hybridised with the [^{32}P]-labelled *egfp* probe (probe, Figure 3.51; probe 2, Figure 3.43B) to analyse the integration of EGFP-GRV. Genomic DNA of WT.P30-8 was included as a control since it contained one copy of the chimeric *egfp-ggs1* gene (Figure 3.44).
The numbers on the left correspond to the sizes of λDNA/*Hin*dIII fragments and those on the right correspond to the expected sizes of the restriction fragments that hybridised to the probe. All fragment sizes are shown in kb. WT=wild-type; P41=pSS41; P46=pSS46; P30=pSS30 (EGFP-Ggs1).

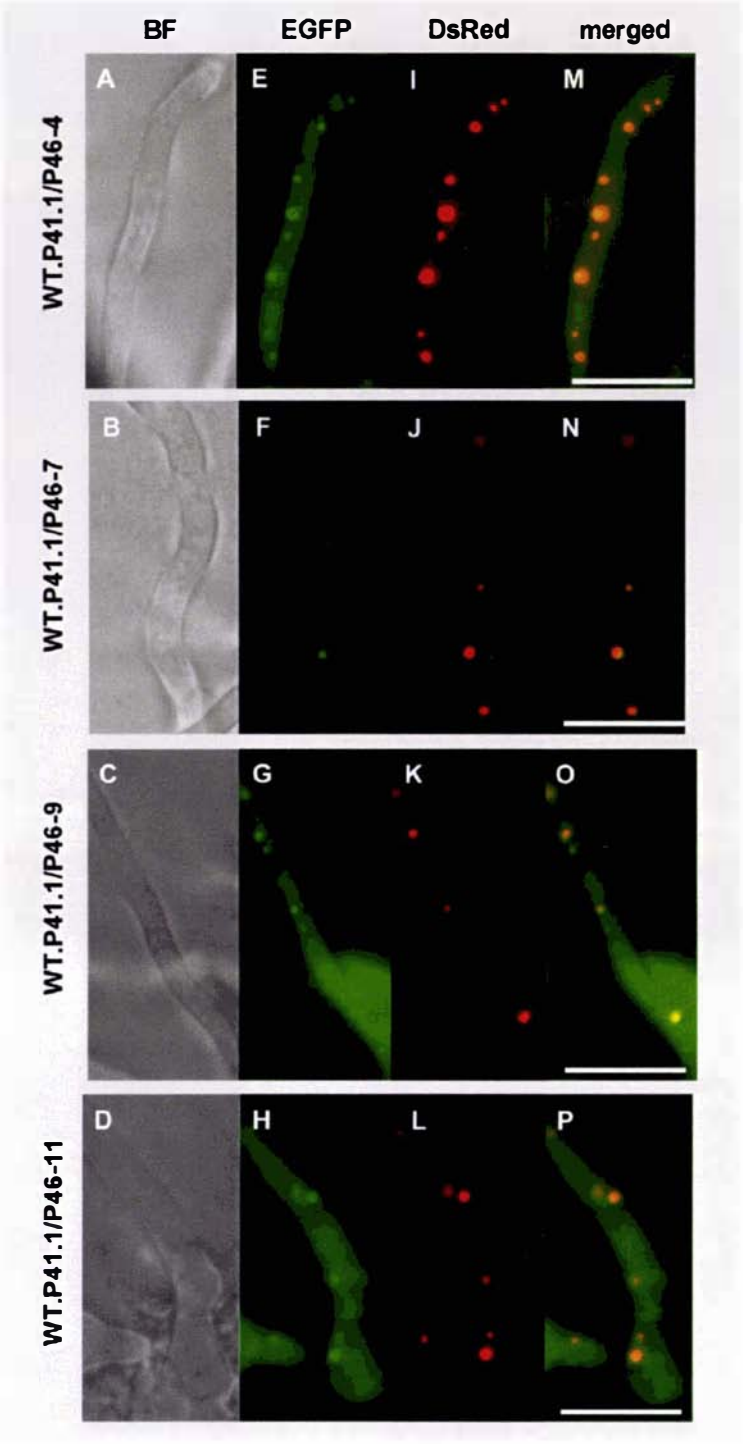

Figure 3.59 Co-localisation of EGFP-GRV and DsRed-SKL fusions

Wild-type strains containing both pSS41 (DsRed-SKL) and pSS46 (EGFP-GRV) were grown on PDA at 22ºC for 2 days (Section 2.23). Mycelia were observed by fluorescence microscopy. A-D Bright Field (BF) images; E-H EGFP fluorescence images; I-L DsRed fluorescence images; M-P merged images of EGFP and DsRed images, respectively. WT=wild-type; P41=pSS41; P46=pSS46. Bars=10 μm.

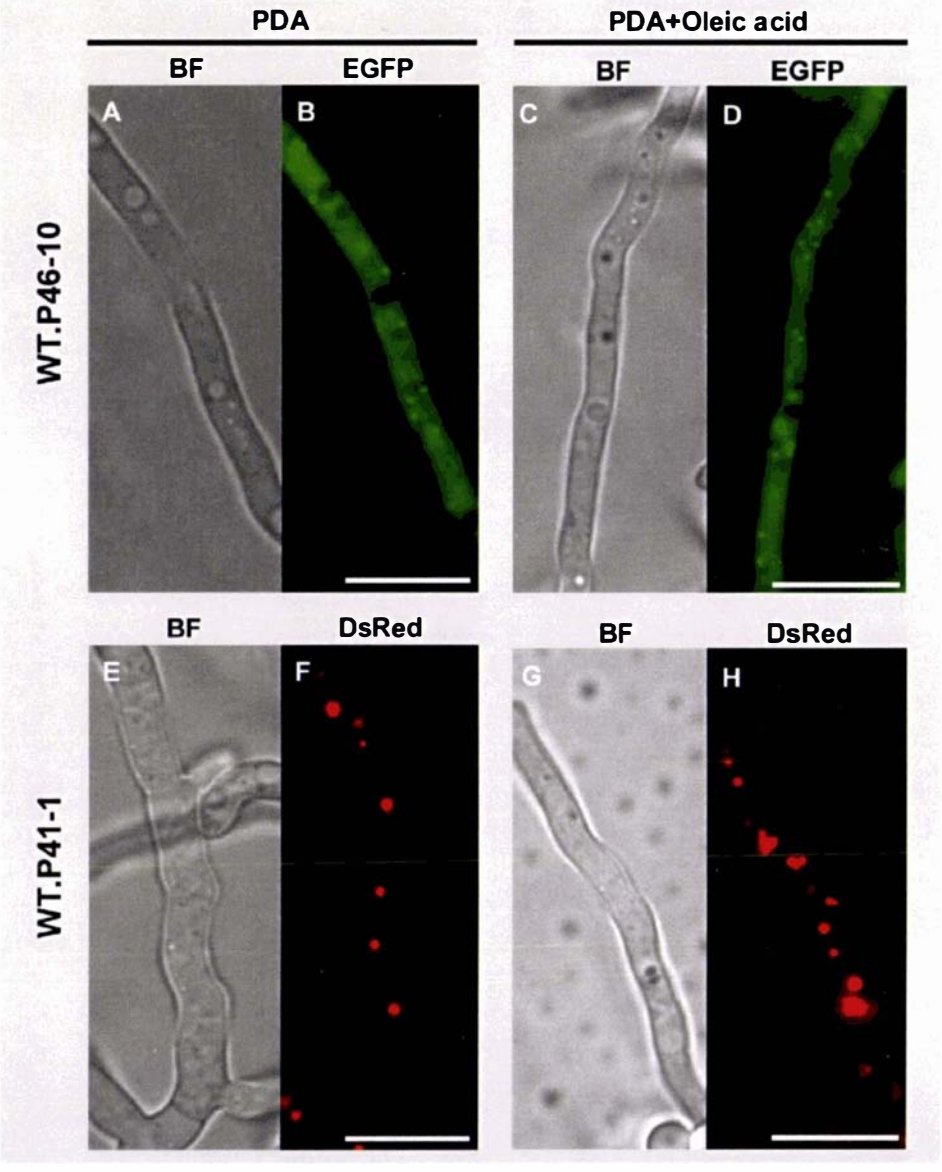

Figure 3.60 Visualisation of EGFP-GRV and DsRed-SKL fusions in oleic acid induced cultures

Wild-type strains containing pSS46 (EGFP-GRV) and pSS41 (DsRed-SKL) were grown on PDA and PDA + oleic acid at 22°C for 2 days (Section 2.23). Mycelia were observed by fluorescence microscopy. A, C, E, G - Bright Field (BF) images; B, D - EGFP fluorescence images; F, H - DsRed fluorescence images. WT=wild-type; P46=pSS46; P41=pSS41. Bars=10 μm.

3.4.12 Strains containing Ggs1-EGFP and DsRed-SKL fusions

Since the localisation pattern of the Ggs1-EGFP fusion resembled that of peroxisomal localisation (Sections 3.4.7, 3.4.9 & 3.4.10), strain WT.P29-12 containing the Ggs1-EGFP fusion was tested by differential labelling to check if the chimeric protein was localised to peroxisomes. Protoplasts of WT.P29-12 was transformed with 5 μg of circular pSS41 (DsRed-SKL) and the resulting transgenic strains selected on RG medium containing geneticin (150 μg/ml) (Section 2.13.2). Four strains were arbitrarily selected for PCR screening (data not shown) (Section 2.14.2) and Southern blotting and hybridisation (Section 2.10). The Southern data showed that two strains viz. WT.P29.12/P41-2 and WT.P29.12/P41-1(2) contained both the fusion constructs (Figure 3.61). When analysed by fluorescence microscopy (Section 2.23), it was observed that the two fusion proteins did not co-localise (Figure 3.62). This suggested that the organelles to which the Ggs1-EGFP fusion was targeted are not peroxisomes.

3.4.13 Summary

Strains containing the chimeric *ggs1-egfp* gene under the control of *TEF* promoter of *A. pullulans* showed that the fluorescent protein was localised to punctuate organelles. These organelles were not mitochondria as suggested by the inability of the MitoTracker dye to stain these organelles. Differential labelling with *DsRed* gene fused to the peroxisomal targeting signal SKL confirmed that these punctuate organelles were not peroxisomes. In contrast, transgenic strains containing the chimeric *egfp-ggs1* showed both cytoplasmic (major) and localised (minor) distribution of the fluorescent protein. The localised fluorescent pattern was similar to that observed for *ggs1-egfp* strains. This suggested that the localisation of Ggs1 to the punctuate organelles was affected by the N-terminal fusion of EGFP to this protein.

Introduction of the chimeric *egfp-paxG* gene into wild-type *P. paxilli* failed to give stable strains. Although stable transgenic strains containing *paxG-egfp* were obtained, no EGFP fluorescence was observed in these strains. However, the EGFP fusion with the C-terminal tripeptide GRV of PaxG was targeted to punctuate organelles. Differential labelling with *DsRed* gene fused to the

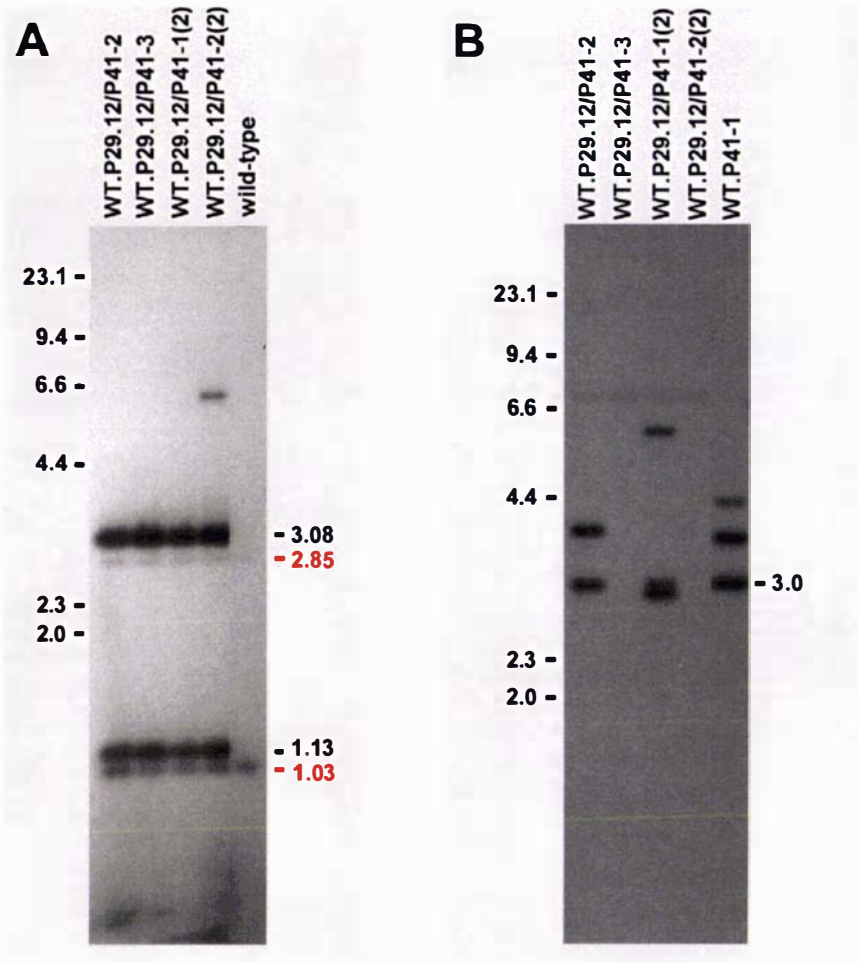

Figure 3.61 Southern analysis of wild-type strains containing both pSS29 (Ggs1-EGFP) and pSS41 (DsRed-SKL)

(A) *Nde*I-digested genomic DNA of wild-type strains containing both Ggs1-EGFP and DsRed SKL was hybridised with the [^{32}P]-labelled *ggs1* probe (Figure 3.43A) to analyse the parent WT.P29-12 strain. **(B)** *Sph*I-digested genomic DNA of wild-type strains containing both Ggs1-EGFP and DsRed-SKL was hybridised with the [^{32}P]-labelled *dsred* probe (probe 2, Figure 3.55B) to analyse the integration of DsRed-SKL.

The numbers on the left correspond to the sizes of λDNA/*Hin*dIII fragments and those on the right correspond to the expected sizes of the restriction fragments that hybridised to the probe. The numbers labelled red correspond to the expected sizes of the restriction fragments in the parent wild-type strain. All fragment sizes are shown in kb. WT=wild-type; P29=pSS29; P41=pSS41.

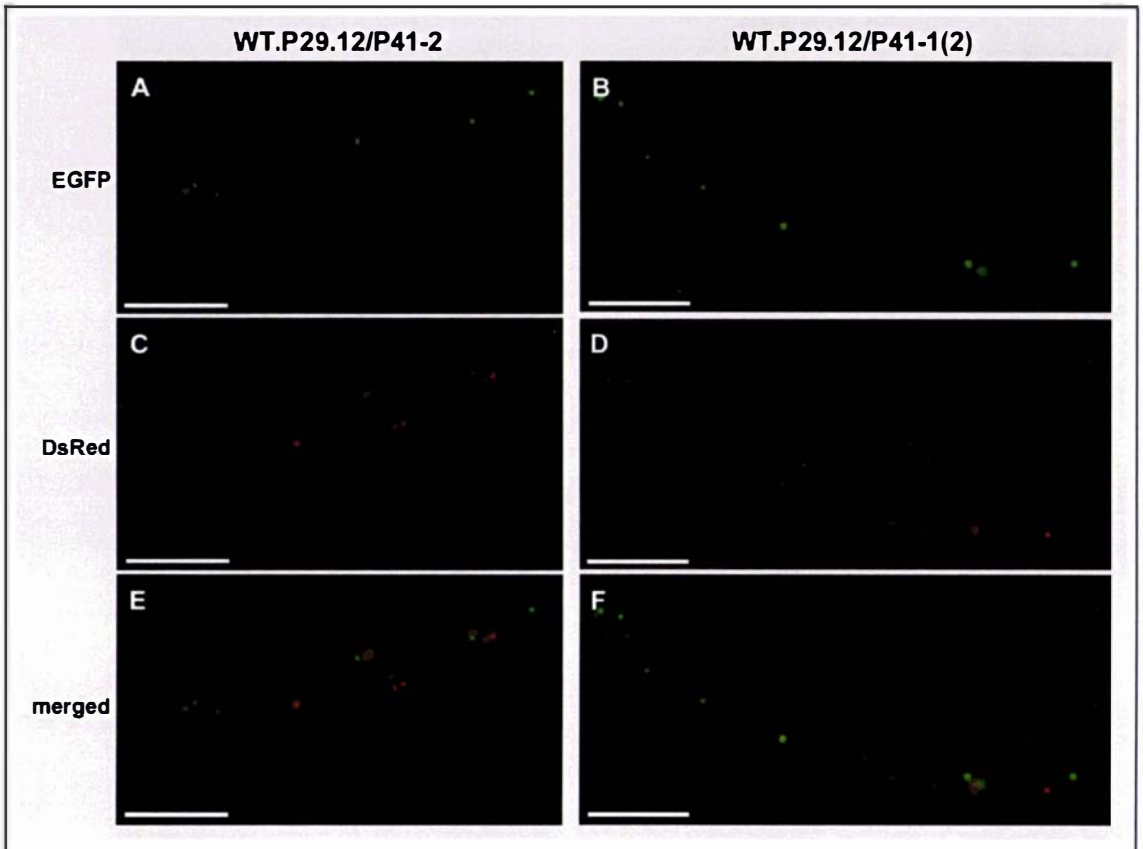

Figure 3.62 Visualisation of Ggs1-EGFP and DsRed-SKL fusions

Wild-type strains containing both pSS29 (Ggs1-EGFP) and pSS41 (DsRed-SKL) were grown on PDA at 22°C for 2 days (Section 2.23). Mycelia were observed by fluorescence microscopy. A, B - EGFP fluorescence images; C, D - DsRed fluorescence images; E, F - merged images of EGFP and DsRed fluorescence images, respectively. WT=wild-type; P29=pSS29; P41=pSS41. Bars=10 μm.

peroxisomal targeting signal SKL confirmed that the punctuate organelles expressing the EGFP-GRV fusion protein were peroxisomes. This was also confirmed by the proliferation of these organelles as a result of oleic acid induction.

Although the localisation of *ggs1* was a limited analysis, the two *P. paxilli ggpps* genes were differentially localised in the fungal cell.

CHAPTER FOUR
DISCUSSION

4.1 Biosynthesis of paxilline intermediates

Paxilline is produced by the filamentous fungus *P. paxilli* and belongs to a large group of indole-diterpene secondary metabolites that share a common core structure comprised of a cyclic diterpene skeleton and an indole moiety. The structural complexity of these metabolites is a result of additional prenylations, different ring substitutions and ring stereochemistry in the basic indole-diterpene ring structure. The cloning and characterisation of a paxilline biosynthesis gene cluster from *P. paxilli* has helped to understand the genetics and biochemistry of paxilline-like indole-diterpenes (Young *et al.*, 2001). The *pax* cluster contains seven genes that are necessary for paxilline biosynthesis. *paxG* encodes a GGPP synthase, *paxM* encodes a FAD-dependent monooxygenase, *paxC* encodes a prenyltransferase, *paxP* and *paxQ* encode two cytochrome P450 monooxygenases, and *paxA* and *paxB* encode two putative membrane proteins (McMillan *et al.*, 2003; Young *et al.*, 2001) (Monahan and Scott, unpublished results). Deletion mutants of *paxG* (Young *et al.*, 2001), *paxM* (McMillan and Scott, unpublished results), *paxC* (Young *et al.*, unpublished results), *paxA* and *paxB* (Monahan and Scott, unpublished results) lack the ability to synthesise any identifiable indole-diterpene suggesting that these genes are involved in early steps in the paxilline biosynthesis pathway. However, deletion mutants of *paxP* and *paxQ* accumulate paspaline and 13-desoxypaxilline, respectively (McMillan *et al.*, 2003). Taken together, these results suggest that paspaline is the first stable indole-diterpene intermediate and its biosynthesis requires up to five proteins PaxG, PaxA, PaxM, PaxB and PaxC. This was confirmed by the introduction of these five genes in a *pax* cluster negative background (Section 3.1.2) (Saikia *et al.*, 2006). The proposed function of PaxG, PaxM and PaxC suggest that these three enzymes alone might be sufficient for paspaline biosynthesis. However, *pax* cluster negative strains containing genes for the synthesis of these three enzymes alone failed to form paspaline or any other indole-diterpene (Section 3.1.4). This suggests a role for PaxA and/or PaxB in paspaline biosynthesis. Sequence analysis of PaxA and PaxB suggests that these are polytopic membrane proteins containing seven transmembrane domains. No identifiable enzymatic function was predicted for these two proteins. Introduction of *paxB* and not *paxA*, along with *paxG*, *paxM* and *paxC*, into a *pax* cluster negative background was able to

restore to the *pax* cluster negative strain the ability to form paspaline (Sections 3.1.6 & 3.1.8). This confirmed that paspaline biosynthesis requires the action of just four proteins PaxG, PaxM, PaxB and PaxC. Besides paspaline, these transformants also accumulated a novel, partially cyclised indole-diterpene intermediate (Section 3.1.8). The proposed structure of this novel metabolite differs from paspaline in having an open F-ring. Other partially cyclised indole-diterpenes that have been identified include emeniveol and emindoles (Figure 1.4), isolated from *Emericella* species (Kimura *et al.*, 1992; Nozawa *et al.*, 1988a, b; Nozawa *et al.*, 1988c). It has been suggested that formation of paspaline occurs via migration of the carbon skeleton to give emindole SB, which then undergoes epoxidation and cyclisation to form paspaline (Nozawa *et al.*, 1988b). However, to date, emeniveol and emindole SB have not been isolated from any *Penicillium* spp. or shown to be intermediates in the paxilline biosynthesis pathway by genetic or biochemical studies, giving rise to the hypothesis that the diterpene cyclises without skeletal rearrangement.

In the complementation studies, paspaline was detected mostly in *pax* cluster negative backgrounds that contained multiple copies of the introduced *pax* genes (Sections 3.1.2 & 3.1.8). However, some transformants failed to synthesise paspaline despite having multicopy integrations of *pax* genes in their genome. These data indicate that both copy number and site of integration are important for expression of the introduced *pax* genes (discussed below).

Based on the predicted functions of PaxG, PaxM, PaxB and PaxC, and the complementation studies (Section 3.1), a scheme for paspaline biosynthesis is proposed (Figure 4.1). PaxG is proposed to catalyse the first committed step in the pathway involving a series of iterative condensations of IPP with DMAPP, GPP, and FPP, to form GGPP. Contrary to a paxilline biosynthesis scheme proposed earlier in which GGPP was thought to condense with tryptophan to form the basic indole-diterpene core (Figure 3.24) (Munday-Finch *et al.*, 1996), here GGPP is proposed to condense with indole-3-glycerol phosphate to form the acyclic intermediate 3-geranylgeranylindole. The biosynthetic origins of the indole and the diterpene moiety of indole-diterpenes have been studied using labelled precursors. In *Claviceps paspali*, cultures fed with ^{13}C-labelled acetate

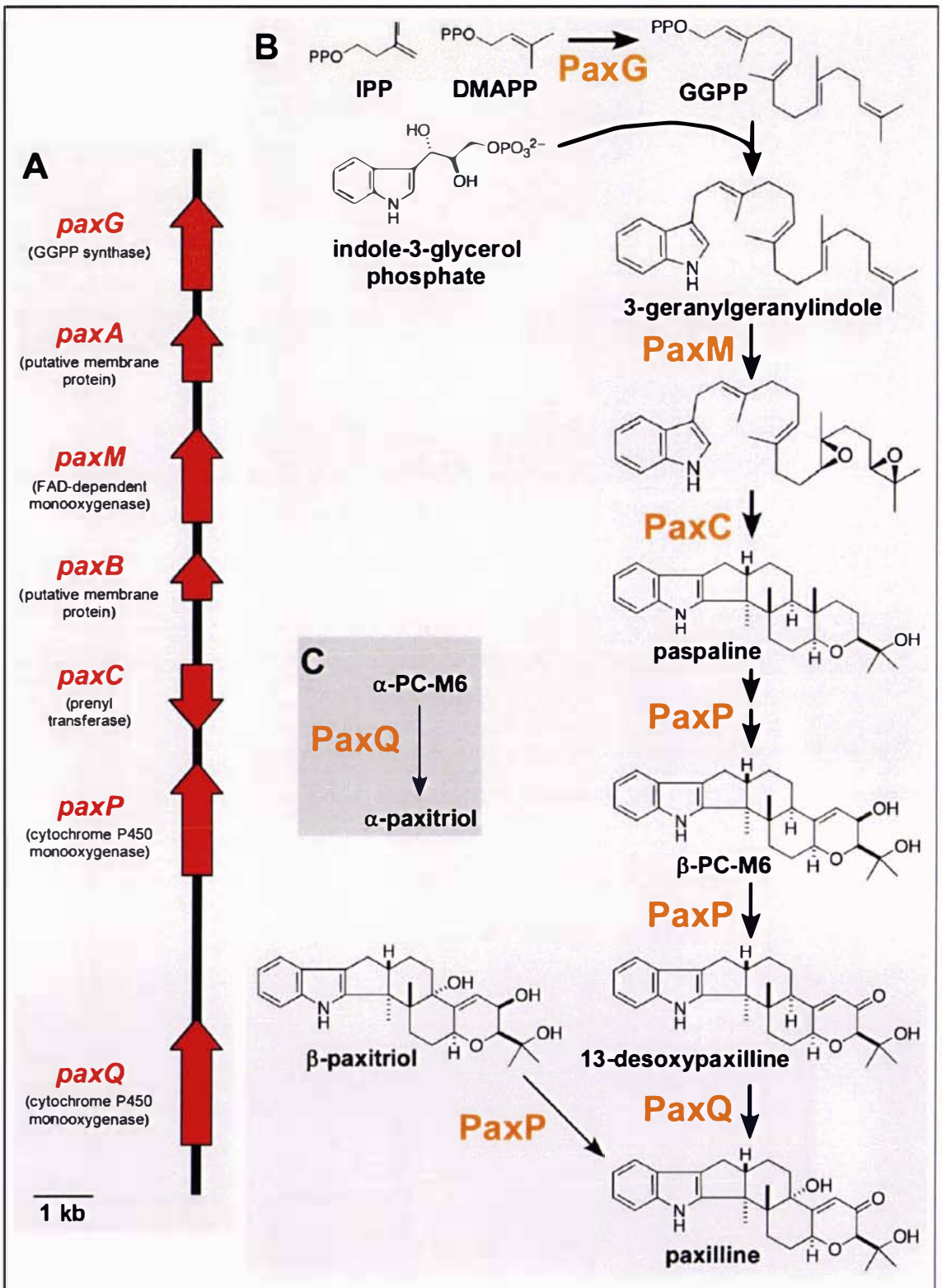

Figure 4.1 Proposed scheme for paxilline biosynthesis in *P. paxilli*

(A) Organisation of paxilline (*pax*) gene cluster. The proposed enzymatic function of each gene product, except PaxA and PaxB, is also indicated. No enzymatic function has been identified for PaxA and PaxB. **(B)** The proposed pathway for paxilline biosynthesis. **(C)** Side reaction catalysed by PaxQ. IPP - isopentenyl diphosphate; DMAPP - dimethyallyl diphosphate; GGPP - geranylgeranyl diphosphate

precursors showed the incorporation of label into the diterpene part of paspaline via mevalonate (Acklin *et al.*, 1977). de Jesus *et al.* (1983) observed similar pattern of incorporation of labelled acetate for penitrem A in *Penicillium crustosum* and also reported the incorporation of the indole moiety of tryptophan into penitrem A by feeding (2*RS*)-[*benzene-ring*-U-^{14}C]-tryptophan and (2*RS*)-[*indole*-2-^{13}C,2-^{15}N]-tryptophan to the fungal cultures. However, the rate of incorporation of the tryptophan indole moiety into penitrem A was low. Although a recent study on the biosynthesis of nodulisporic acid A (NAA), an indole-diterpene produced by the endophytic fungus *Nodulisporium*, also identified mevalonate as the biosynthetic origin of the diterpene part of NAA, the indole moiety was reported to be derived from anthranilic acid and not tryptophan (Byrne *et al.*, 2002). Incubation of a *Nodulisporium* sp. with tryptophan precursors ^{14}C-, ^{13}C-, and ^{15}N-anthranilic acid and ^{14}C- and ^{13}C-ribose showed high levels of incorporation of label into NAA. However, incubation with ^{14}C- and ^{13}C-tryptophan showed no incorporation of label into NAA which led the authors to propose indole-3-glycerol phosphate as the indole precursor for NAA. Frey and co-workers have shown that the indole incorporated into maize hydroxamic acids, 2,4-dihydroxy-1,4-benzoxazin-3-one and 2,4-dihydroxy-7-methoxy-1,4-benzoxazin-3-one, originates from indole-3-glycerol phosphate and not from tryptophan (Frey *et al.*, 1997) (Figure 4.2).

Evidence for the involvement of intermediates in the biosynthesis of indole-diterpenes has also come from the efforts of the synthetic chemistry community resulting in both total and biomimetic syntheses of indole-diterpenes (Clark *et al.*, 2003; Rainier and Smith, 2000; Smith *et al.*, 2006; Smith and Mewshaw, 1985; Smith *et al.*, 1990a; Smith *et al.*, 2000; Xiong *et al.*, 2003). Smith and co-workers have made several contributions towards the total syntheses of indole-diterpenes including (–)-paspaline (Smith and Mewshaw, 1985; Smith and Leenay, 1988, 1989), (+)-paspalicine (Smith *et al.*, 1990a; Smith *et al.*, 1992), (+)-paspalinine (Smith *et al.*, 1990a; Smith *et al.*, 1992), (–)-penitrem D (Smith *et al.*, 2000), and most recently (+)-nodulisporic acid F (Smith *et al.*, 2006). These studies support the involvement of 3-geranylgeranylindole as a common intermediate that undergoes epoxidation followed by cyclisation to give indole-diterpenes. Recently, Fueki and co-workers demonstrated the incorporation of

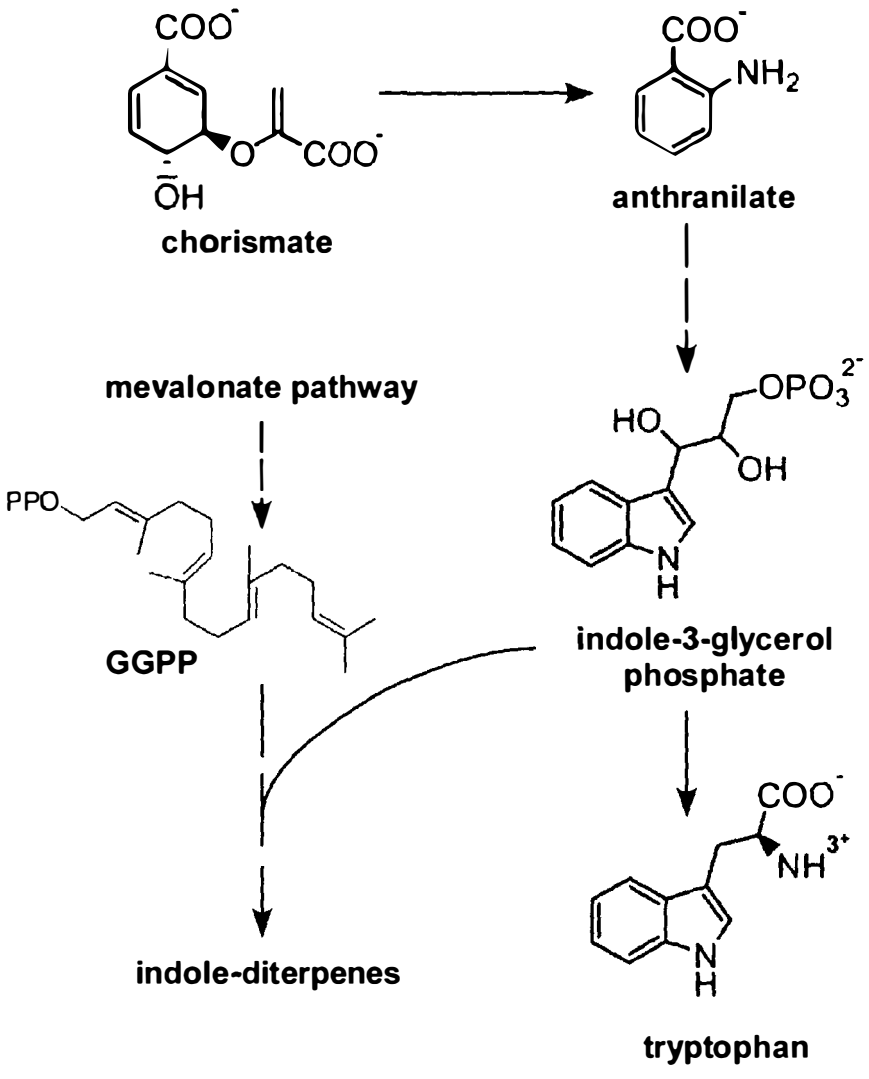

Figure 4.2 Sources of indole and diterpene moieties of indole-diterpenes

The indole moiety is proposed to originate from the tryptophan precursor, indole-3-glycerol phosphate. The diterpene moiety originates from the mevalonate pathway. GGPP=geranylgeranyl diphosphate.

deuterium labelled 3-geranylgeranylindole into the indole-diterpenes paxilline and emindole DA, evidence that supports the involvement of 3-geranylgeranylindole as a biosynthetic intermediate (Fueki *et al.*, 2004). Apart from these studies, schemes proposed for the biosynthesis of paxilline-like indole-diterpenes have been based on the chemical identification of likely intermediates and substrate feeding studies from the organism of interest and related filamentous fungi (Gatenby *et al.*, 1999; Mantle and Weedon, 1994; Munday-Finch *et al.*, 1996).

The condensation of GGPP with indole-3-glycerol phosphate may be catalysed by either PaxG or PaxC, as both are prenyltransferases. PaxM, a FAD-dependent monooxygenase, is proposed to catalyse the epoxidation of the two terminal alkenes of the geranylgeranyl moiety. The lack of precedence for a flavin monooxygenase catalysing a two-step epoxidation suggests that PaxM is a novel flavin monooxygenase. Subsequently, PaxC is proposed to catalyse the cationic cyclisation of the di-epoxy intermediate to form paspaline. Although PaxB is required for paspaline biosynthesis, its role in paspaline biosynthesis is not clear. Since the secondary structure analysis of PaxB suggests it is a membrane protein it may function as a transporter. Unlike the ATP-binding cassette (ABC) and major facilitator superfamily (MFS) fungal transporters, which contain 12 and 12-14 transmembrane domains, respectively, PaxB contains seven transmembrane domains. Most ABC and MFS transporters associated with secondary metabolite gene clusters have a role in self-protection of the producing organism from the toxic effects of the metabolite (Del Sorbo *et al.*, 2000; Gardiner *et al.*, 2005). However, the unique structure of PaxB and the indole-diterpene negative phenotype of the *paxB* mutant (Monahan and Scott, unpublished results) suggest that it may have a role in transporting substrate(s) to the vicinity of the biosynthetic enzyme complex, rather than a role in self-protection. Alternatively, PaxB may have a regulatory role. A large number of seven-transmembrane receptor proteins, G-protein coupled receptors (GPCRs), that are involved in G-protein signalling pathways have been identified (Lafon *et al.*, 2006; reviewed in Pierce *et al.*, 2002). These pathways have been shown to regulate sporulation and mycotoxin production in different filamentous fungi including *Aspergillus* spp. and *Fusarium* spp.

(reviewed in Brodhagen and Keller, 2006; Calvo *et al.*, 2002; Lengeler *et al.*, 2000). PaxA also has a unique secondary structure similar to PaxB containing seven transmembrane domains but, unlike PaxB, it is not required for paspaline biosynthesis (Section 3.1.6). However, the indole-diterpene negative phenotype of the *paxA* mutant (Monahan and Scott, unpublished results) suggests a role for PaxA in paxilline biosynthesis. Based on these data, it is difficult to assign a role for PaxA in paxilline biosynthesis and thus its function remains inconclusive.

Given the diverse array of indole-diterpenes that are structurally similar to the paspaline-like skeleton, it is tempting to propose that paspaline is the key intermediate for indole-diterpene biosynthesis providing the core structural skeleton for subsequent reactions. Recently, orthologues of *paxG*, *paxM*, *paxB* and *paxC* genes have been identified in a complex cluster for biosynthesis of the indole-diterpene, lolitrem B, in *N. lolii* (Young *et al.*, 2005; Young *et al.*, 2006). *ltmM* and *ltmC* have been shown to be functional orthologues of *P. paxilli* genes *paxM* and *paxC*, respectively. By analogy, LtmG, LtmM, LtmB and LtmC are likely to be involved in early steps forming paspaline as an intermediate in lolitrem B biosynthesis. In *A. flavus*, a gene cluster for the indole-diterpene, aflatrem, has been shown to contain orthologues of *paxG*, *paxM* and *paxC* (Zhang *et al.*, 2004). Complementation studies showed that the *atmM* gene was a functional orthologue of *P. paxilli paxM* (Zhang *et al.*, 2004). Recent analysis of the *A. flavus* genome sequence generated by Gary Payne and colleagues at North Carolina State University, USA (http://www.aspergillusflavus.org/genomics/), identified orthologues of *paxB* and *paxA*, together with orthologues of *paxP*, *paxQ* and *paxD* that formed a cluster at a different genomic location (Monahan *et al.*, unpublished results). This analysis again provides support for the involvement of orthologues of *paxG*, *paxM*, *paxB* and *paxC* in early steps of indole-diterpene biosynthesis.

Two other genes, *paxP* and *paxQ*, both encoding cytochrome P450 monooxygenases are proposed in later steps in the paxilline biosynthesis pathway (McMillan *et al.*, 2003). Deletion mutants of *paxP* and *paxQ* accumulate paspaline and 13-desoxypaxilline, respectively. These indole-

diterpenes together with others are proposed as intermediates in different metabolic grids for indole-diterpene biosynthesis (Gatenby *et al.*, 1999; Mantle and Weedon, 1994; Munday-Finch *et al.*, 1996). The position of the proposed intermediates and the sequence of reactions in the metabolic grids were based on a likely biochemical scheme involving sequential formation of more complex structures. These schemes showed paspaline as the basic indole-diterpene precursor for a large number of indole-diterpenes including paxilline, paspalicine, paspalinine, terpendoles, lolitrems, penitrems and janthitrems (Gatenby *et al.*, 1999; Mantle and Weedon, 1994; Munday-Finch *et al.*, 1996). The scheme for paxilline biosynthesis, as proposed by Munday-Finch and co-workers, involved a series of oxidation reactions starting with paspaline to give rise to paspaline B, PC-M6 and 13-desoxypaxilline (Munday-Finch *et al.*, 1996). In this scheme the penultimate substrate for paxilline biosynthesis was suggested to be either 13-desoxypaxilline or β-paxitriol. Based on a modification of this scheme using a similar approach, others have proposed schemes for biosynthesis of more complex indole-diterpenes such as lolitrems and terpendoles (Gatenby *et al.*, 1999; Parker and Scott, 2004).

Identification and characterisation of genes for the two cytochrome P450 monooxygenases, PaxP and PaxQ, within the paxilline biosynthesis gene cluster has helped to understand later steps in paxilline biosynthesis. Incubation of paspaline and 13-desoxypaxilline with two *pax* cluster deletion mutants, CY2 and LM662, containing either PaxP or PaxQ resulted in the conversion of fed compounds into indole-diterpene products confirming that these compounds are substrates for PaxP and PaxQ, respectively (Figure 4.1) (Sections 3.3.2 & 3.3.4). The conversion of these substrates by both PaxP and PaxQ was more efficient in the LM662 background than in the CY2 background (discussed below). Although paxilline was the only conversion product of 13-desoxypaxilline by PaxQ, paspaline was converted to 13-desoxypaxilline and β-PC-M6 by PaxP. These results confirmed that PaxP was able to catalyse the sequential oxidations involving removal of the C-30 methyl group followed by C-10 oxidation (Figure 4.3), via β-PC-M6. Similar sequential loss of a C-14 methyl group by a P450 enzyme has been reported in sterol biosynthesis

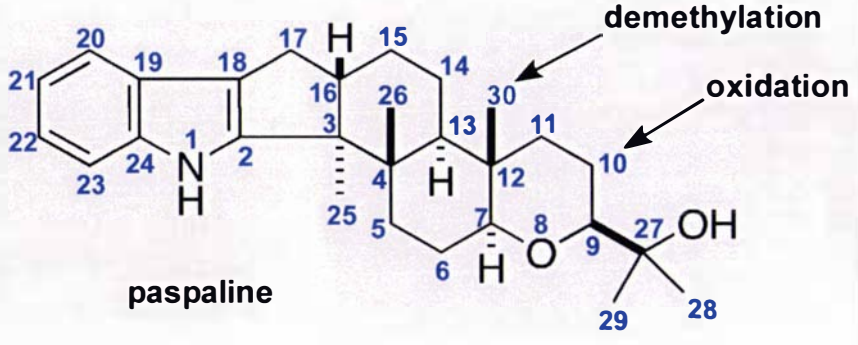

Figure 4.3 Modifications of paspaline by PaxP

Positions of paspaline carbon atoms acted upon by PaxP are shown by arrows.

(Fischer *et al.*, 1989; Lamb *et al.*, 1999). The proposed involvement of paspaline B as the first oxidised analogue of paspaline (Munday-Finch *et al.*, 1996) could not be tested due to the unavailability of an authentic sample of paspaline B. However, at least one unknown indole-diterpene compound was detected in extracts of wild-type *P. paxilli*. In addition, incubation of β-PC-M6 with a *pax* cluster negative strain containing only PaxP resulted in its conversion to 13-desoxypaxilline confirming that β-PC-M6 is a substrate for PaxP (Section 3.3.5). PaxP was also found to catalyse the C-10 oxidation of β-paxitriol to produce paxilline (Section 3.3.6). However, the source of β-paxitriol is not clear. It is possible that an enzyme outside the *pax* cluster is capable of converting paxilline to β-paxitriol. These results indicate that PaxP catalyses multiple oxidation steps both at a single carbon atom and at different carbon atoms. In *F. fujikuroi*, the multifunctional cytochrome P450 monooxygenase, GA_{14}-oxidase, was shown to catalyse four sequential oxidations at four different carbon atoms in a series of oxidations from *ent*-kaurenoic acid to GA_{14} (Rojas *et al.*, 2001). Oxidation at multiple sites by a single P450 enzyme has also been shown for the fungus *Curvularia lunata* in which the cytochrome P450 enzyme, P-450lun, catalyses bifunctionally 11β- and 14α-hydroxylations of 11-deoxycortisol to form cortisol (Suzuki *et al.*, 1993). In *F. fujikuroi*, another cytochrome P450 enzyme, *ent*-kaurene oxidase, catalyses three sequential oxidations at a single carbon atom in the conversion of *ent*-kaurene to *ent*-kaurenoic acid (Rojas *et al.*, 2001; Tudzynski *et al.*, 2001a). Similar multiple catalytic activities have been suggested for the cytochrome P450 enzymes encoded by genes within the GA cluster identified in *Phaeosphaeria* sp. (Kawaide, 2006).

No evidence for the proposed bifurcation in the paxilline pathway between PC-M6 and paxilline was found (Figure 3.24) (Munday-Finch *et al.*, 1996). Although incubation of β-paxitriol with a *paxQ* deletion mutant complemented paxilline biosynthesis, none of the *pax* gene products was able to convert either α- or β-PC-M6 to β-paxitriol (Section 3.3.6). β-paxitriol was only found to be a substrate for PaxP (discussed above). These precursor feeding studies have confirmed that β-paxitriol is not a part of the paxilline biosynthesis pathway but could be

involved in steps post-paxilline (Figure 4.1). Recently, two other *pax* genes, *paxD* encoding a prenyltransferase of the dimethylallyltryptophan (DMAT) synthase type and *paxO* encoding an oxidoreductase, that were earlier identified in the *pax* cluster (Young *et al.*, 2001) have been found to be co-regulated with other *pax* genes (Monahan *et al.*, unpublished results). A *paxD* deletion mutant (Young *et al.*, unpublished results) was found to accumulate indole-diterpenes that were not prenylated (Brian Tapper, personal communication) suggesting that PaxD may catalyse isoprenylation of the indole ring or the diterpene part of paxilline in steps post-paxilline. In *Claviceps purpurea*, the first step in ergot alkaloid biosynthesis has been shown to be catalysed by the DMAT synthase DmaW that involves the prenylation of the C-4 position of the tryptophan indole ring (Gebler and Poulter, 1992; Tsai *et al.*, 1995).

Incubation of α-paxitriol with strains containing *pax* cluster negative backgrounds and also with a PaxP containing strain confirmed that α-paxitriol was not a substrate for any Pax enzymes (Section 3.3.6). Interestingly, similar incubations of α-PC-M6 showed that it was a substrate for PaxQ and was converted by PaxQ to α-paxitriol (Section 3.3.5). Given that the paxilline intermediates have a β-configuration at C-10, acceptance of a substrate that has a α-configuration by a Pax enzyme is unusual. α-paxitriol is more likely a precursor for lolitrems and terpendoles that have the α-configuration at C-10 (Gatenby *et al.*, 1999; Miles *et al.*, 1992; Penn and Mantle, 1994). Based on the data presented here, it is highly unlikely that indole-diterpenes with a α-configuration are involved in the paxilline pathway. The formation of α-paxitriol by PaxQ could be a non-specific side reaction (Figure 4.1). The biosynthetic significance, if any, of this reaction is not known. In *Penicillium janczewskii* and *Penicillium janthinellum*, incorporation of labelled β-paxitriol and not α-paxitriol, into penitrem A and E and janthitrem B and C, respectively, suggested β-paxitriol as an immediate precursor for the complex indole-diterpenes with β-stereochemistry (Penn and Mantle, 1994). These observations emphasise the stereospecificity of enzymes involved in the biosynthesis of indole-diterpenes. Moreover, indole-diterpenes that have been reported from fungi belonging to

the taxonomic order Eurotiales (*Aspergillus* and *Penicillium*) have β-stereochemistry and those belonging to the order Clavicipitales (*Epichloë* and *Claviceps*) have α-stereochemistry (Parker and Scott, 2004, and references therein). In the present study, PaxP is shown to be a stereospecific enzyme that acts only on the substrates that have a β-configuration. Unlike PaxP, PaxQ appears to be a promiscuous enzyme that lacks substrate specificity. Although the reason for this promiscuous activity of PaxQ is not known, enzymes with promiscuous functions are thought to act as precursors for enzymes with higher specificity (Yoshikuni *et al.*, 2006, and references therein). Recent identification of PaxP and PaxQ homologues in the lolitrem gene cluster (Young *et al.*, 2006) could help in understanding the stereospecificities of these P450 enzymes in indole-diterpene biosynthesis. The data presented in this study suggest that the stereochemistry of the indole-diterpene intermediates is laid down by PaxP (and by analogy by LtmP). It is now possible to test this hypothesis by introducing either or both LtmP and LtmQ in *P. paxilli* and check if this introduction enables *P. paxilli* to form indole-diterpenes with α-stereochemistry.

In the chemical complementation studies, the ability of both PaxP and PaxQ to convert their respective substrates into products differed between the LM662 and CY2 backgrounds. Both P450 enzymes were more efficient in their ability to convert their respective substrates in the LM662 background than in the CY2 background (Sections 3.3.2 & 3.3.4). This could be attributed to a comparatively higher level expression of the corresponding genes in the LM662 background than in the CY2 background which in turn might be attributable to the site of integration (discussed below). Given that CY2 is a single crossover associated with a large deletion (> 100 kb) and that one end of this deletion is not yet defined (Young *et al.*, 1998), the presence of a regulatory element within the deleted region cannot be ruled out. Two putative regulatory genes *paxR* and *paxS* that encode putative transcription factors have been shown to be associated with the paxilline cluster (Young *et al.*, 2001). However, the *paxR* and *paxS* deletion mutants were positive for paxilline biosynthesis suggesting that these two genes do not have a regulatory function for the paxilline cluster (McMillan *et al.*, unpublished results). The *pax* gene cluster may be under the

control of the global nitrogen regulator, AreA, as has been shown for the regulation of gibberellin biosynthesis genes in *F. fujikuroi* (Mihlan *et al.*, 2003; Tudzynski *et al.*, 1999a). Recently, a global transcriptional regulator, LaeA, for secondary metabolism was reported in *Aspergillus* spp. (Bok and Keller, 2004; Bok *et al.*, 2005; Bok *et al.*, 2006). It was shown to positively regulate expression of genes in the penicillin and sterigmatocystin biosynthetic clusters of *A. nidulans*, the lovastatin cluster from *A. terreus*, and the gliotoxin cluster from *A. fumigatus.* This regulation of multiple gene clusters was attributed to possible involvement of LaeA in converting heterochromatin to euchromatin. Although genes containing the conserved *S*-adenosylmethionine domain found in LaeA are found in fungi such as *F. sporotrichioides*, *M. grisea* and *Coccidioides immitis*, whether these are functional homologues remains to be demonstrated.

The ability of PaxP to convert its substrate not only differed between the LM662 and CY2 backgrounds (discussed above) but also among the transformants having the same background. Transformants LM662.P1-10 and CY2.P1-9 exhibited a better conversion of the fed substrates into products than LM662.P1-2 and CY2.P1-10 transformants, respectively (Section 3.3.2). This difference in conversion was related to expression of the introduced genes. Since the introduced genes were ectopically integrated in the genome, the integration site appears to have an effect on expression of the introduced genes and thus on the function of the encoded enzymes. Similar results have been reported in other filamentous fungi. Expression of both *P450-4* and *P450-1* genes of either *F. fujikuroi* or *F. proliferatum* was not always detected after their introduction into the genome of *F. proliferatum* strain D02945 (Malonek *et al.*, 2005a). In some D02945 transformants, a high level of *F. fujikuroi P450-4* gene expression was associated with low levels of activity of the encoded *ent*-kaurene oxidase (Malonek *et al.*, 2005b). In *A. parasiticus*, β-glucuronidase (GUS) reporter assays with the aflatoxin biosynthetic gene *nor-1* showed that GUS activity was detected only when the fused P*nor-1*::*uidA* gene integrated at the *nor-1* locus and not when the fused gene integrated outside the aflatoxin gene cluster, at either the *niaD* or the *pyrG* locus (Chiou *et al.*, 2002). These

observations suggest the importance of the chromosomal location of a transgene in both gene expression and function of the encoded enzyme.

4.2 Subcellular localisation of GGPP synthases

In a eukaryotic cell many biochemical functions are compartmentalised, which warrants the need for targeting proteins to the correct cell organelle and structure. The information for protein targeting resides within the sequence and/ or structure of the targeted proteins and also at their destination. Well characterised signatures are known for proteins targeted to various organelles such as mitochondria, endoplasmic reticulum (ER), chloroplasts, nuclei, peroxisomes and vacuoles. The targeting signal is often at the N-terminus of the amino acid sequence of proteins targeted to mitochondria, chloroplast and ER. These signal sequences often do not form a part of the mature protein and are cleaved after protein targeting. In other proteins such as peroxisomal and ER proteins, the targeting signal may reside at the C-terminus of their amino acid sequences. Availability of genome sequences from different organisms has helped in identifying putative localisation signals in the protein of interest by performing a database search.

Fusion of reporter genes is one of the most powerful, commonly used methods to study the subcellular localisation of proteins. Green fluorescent protein (GFP) and its related variants have been used extensively in fusions to a target protein to enable visualisation by fluorescence microscopy (Lorang *et al.*, 2001; Tsien, 1998). Unlike the GUS reporter tags, GFP is not dependent upon exogenous substrates or cofactors but requires only oxygen. This has enabled the use of GFP and its variants in successfully monitoring the localisation of proteins, their movement, their interactions with other proteins and the dynamics of organelles to which these proteins are targeted (Cox *et al.*, 2002; Hoff and Kuck, 2005; Inoue *et al.*, 2002; Maggio-Hall and Keller, 2004; Maggio-Hall *et al.*, 2005; Okada *et al.*, 2000; Poggeler *et al.*, 2003; Shoji *et al.*, 2006; Tavoularis *et al.*, 2001). Another fluorescent protein, DsRed, has also been used as a marker protein (Eckert *et al.*, 2005; Mikkelsen *et al.*, 2003; Toews *et al.*, 2004). Besides fluorescent proteins, immunolabelling has also been used

as a tool to study protein localisation (Chiou *et al.*, 2004; Lee *et al.*, 2002a; Lee *et* al., 2004).

In the filamentous fungi, *P. paxilli*, *N. lolii* and *F. fujikuroi*, two GGPP synthase enzymes, one for primary metabolism and the other for secondary metabolism, have been reported (Tudzynski and Holter, 1998; Young *et al.*, 2001; Young *et al.*, 2005). The genomes of *A. nidulans* and *F. graminearum* also contain two copies of genes homologous to *paxG*, although the diterpene phenotypes of these two fungi are not known. The presence of two copies of GGPP synthases across these genera could mean that the two metabolic pathways are compartmentalised. In the present study, the subcellular localisation of the two *P. paxilli* GGPP synthases, Ggs1 and PaxG, was investigated using EGFP and DsRed reporter tags. Alignment of GGPP synthase sequences from different filamentous fungi showed variation among the sequences at their N-terminal region (Section 3.4.1). This variability suggests that the N-terminal region could harbour specific signals including that for protein targeting. Although detailed information on localisation of fungal GGPP synthases is not available, GGPP synthases with putative localisation signals at their N-terminal regions have been reported in plants. In *Arabidopsis*, five GGPP synthases have been shown to contain putative localisation signals at their N-terminal regions for their translocation into specific subcellular compartments (Okada *et al.*, 2000; Zhu *et al.*, 1997). Synthetic GFP (sGFP) was fused with an N-terminal sequence of 66 – 102 amino acids containing the putative localisation signal. It was shown that the fusion proteins of GGPS1-sGFP and GGPS3-sGFP localised to the chloroplast, GGPS2-sGFP and GGPS4-sGFP localised to the ER, and GGPS6-sGFP localised to the mitochondrion. In a similar study, a fusion protein containing the putative transit peptide of the *S. dulcis* GGPP synthase fused with sGFP was translocated to the chloroplast after its introduction into *Arabidopsis* leaves (Sitthithaworn *et al.*, 2001).

Analysis of the *P. paxilli* GGPP synthase Ggs1 using the PSORT II localisation algorithm suggested it to be a mitochondrial protein (Section 3.4.1). The N-terminal sequence of Ggs1 is over-represented by the amino acids Ser, Ala and Arg and lacks the negatively charged amino acids Asp and Glu, features

characteristic of mitochondrial targeting peptides (Emanuelsson *et al.*, 2000). Mitochondrial import of Ggs1 was investigated using strains expressing EGFP-tagged whole Ggs1 protein. It was observed that, unlike the EGFP-Ggs1 fusion, the Ggs1-EGFP fusion was predominantly targeted to punctuate organelles (Section 3.4.3). Only few hyphae showed similar targeting of the EGFP-Ggs1 fusion. These data suggest that a free N-terminal region is not absolutely necessary but is required for efficient targeting of the Ggs1 protein. In a similar study, the mitochondrial localisation of *Fusarium oxysporum* Fow1 was not affected by N- or C-terminal fusions of GFP to this protein (Inoue *et al.*, 2002). However, the punctuate organelles to which the Ggs1-EGFP fusion protein was targeted were not mitochondria as MitoTracker failed to stain these organelles (Section 3.4.3). Unlike the punctuate shape of these organelles, mitochondria usually appear as tubular structures within the hyphae, along the longitudinal axis of the cell (Inoue *et al.*, 2002; Koch *et al.*, 2003; Maggio-Hall and Keller, 2004; Suelmann and Fischer, 2000). Similar punctuate organelles to which the Ggs1-EGFP fusion protein was targeted have been reported in *Aspergillus* spp. using a membrane-selective fluorescent dye, FM 4-64, wherein FM 4-64 has been used to study membrane internalisation and vacuolar transport (Higuchi *et al.*, 2006; Penalva, 2005; Shoji *et al.*, 2006). Interestingly, FM 4-64 also failed to stain the punctuate organelles to which the Ggs1-EGFP fusion protein was targeted. Since peroxisomes form similar punctuate structures in the cell, strains expressing both Ggs1-EGFP and DsRed-SKL fusions were analysed (Sections 3.4.9 & 3.4.12). The tripeptide SKL is a standard PTS1 with a consensus sequence (S/A/C/G)(K/R/H)(L/M) that targets proteins to the peroxisomes (Gould *et al.*, 1989). However, the two fusion proteins failed to co-localise suggesting that Ggs1 is not in the peroxisomes (Section 3.4.12). Further detailed analysis is required to identify the punctuate organelles to which the Ggs1 protein is targeted. One approach could be to study the organelle movement by observing the localised protein over a time-course to test if the organelles are endosomes (Penalva, 2005). Although the Ggs1-targeted structures appeared static no detailed analysis was done to test the mobility of these structures. Another approach could be the use of drugs such as cytochalasin A and benomyl that destroy the actin and

microtubular cytoskeleton, respectively, and thus affect the morphology and movement of the attached organelles (Suelmann and Fischer, 2000).

For the *P. paxilli* PaxG, the localisation algorithm PSORT II identified a PTS1-like tripeptide GRV at the C-terminus of PaxG (Section 3.4.1). This tripeptide appears to be one of the many variations of the standard PTS1-like SKL motif (Aitchison *et al.*, 1991; Gould *et al.*, 1989). In addition, PaxG homologues in *A. flavus*, *A. nidulans* and *F. graminearum* (AtmG, AN8143 and FG04591, respectively) contain peroxisomal targeting signal type 2 (PTS2)-like sequences, RLAIKLMQL, RLAIKLIQL, RLAVKLMQL, respectively, that conform to the consensus sequence (R/K)(L/V/I)xxxxx(H/Q)(L/A) (Petriv *et al.*, 2004). The presence of either PTS1 or PTS2 in PaxG-related sequences suggests that these proteins may be peroxisomal proteins. In this study, the peroxisomal localisation of PaxG was investigated using strains expressing EGFP-tagged whole-PaxG protein. Attempts to obtain stable transformants containing the EGFP-PaxG fusion were unsuccessful (Section 3.4.5). The constitutive expression of the EGFP-PaxG fusion protein appeared to affect cell growth. In contrast, stable transformants, containing the PaxG-EGFP fusion protein, were obtained wherein the fusion protein was localised to the cytoplasm. From these results, it can be argued that a free PaxG C-terminus is required for its correct localisation. The role of the PaxG C-terminal tripeptide GRV in peroxisomal targeting was verified by analysing strains expressing both EGFP-GRV and DsRed-SKL fusion proteins (Sections 3.4.7, 3.4.9 & 3.4.10). Co-localisation of the two fusion proteins was observed (Section 3.4.10). Previous studies have reported that oleic acid promotes the proliferation of peroxisomes (Maggio-Hall *et al.*, 2005; Valenciano *et al.*, 1996; Veenhuis *et al.*, 1987; Yan *et al.*, 2005). In agreement to these studies, an increase in the number of organelles expressing the two fusion proteins was observed when corresponding *P. paxilli* strains were grown in the presence of oleic acid, suggesting that the organelles are peroxisomes (Section 3.4.11). Thus, the co-localisation and the oleic acid induction studies confirmed that the PaxG C-terminal tripeptide GRV functions as a peroxisomal targeting signal. It is interesting to note that other proteins involved in secondary metabolism are predicted/ verified to be peroxisomal. PTS1-like motifs have been reported for Akt1, Akt2, Akt3-1 and Akt3-2, proteins

required for biosynthesis of the secondary metabolite AK-toxin in *A. alternata* (Tanaka *et al.*, 1999; Tanaka and Tsuge, 2000). The acyltransferase enzyme catalysing the last step in penicillin biosynthesis contains a PTS1-like ARL sequence and was shown to localise to peroxisomes (Muller *et al.*, 1991; Muller *et al.*, 1992). In addition, expression of the acyltransferase enzyme lacking the ARL sequence was localised to the cytoplasm and vacuoles and failed to produce penicillin (Muller *et al.*, 1992). In *Aspergillus* spp., the sterigmatocystin and aflatoxin precursor, norsolorinic acid, was shown to accumulate in peroxisomes, although the catalysing enzymes, polyketide synthase and fatty acid synthase, were not predicted to have a peroxisomal location (Maggio-Hall *et al.*, 2005). However, studies have shown that proteins lacking the PTS1- and PTS2-like sequences are still translocated to the peroxisomes (Elgersma *et al.*, 1995; Klein *et al.*, 2002). These findings, on peroxisomal targeting of different proteins, involved in secondary metabolism, set precedence for this organelle's role in secondary metabolism. However, more such studies on subcellular localisation of proteins involved in fungal secondary metabolism are needed to establish the importance of this and other organelles in secondary metabolism.

4.3 Summary

In this study, biochemical analysis of *pax* gene products in *P. paxilli* viz. PaxG, PaxA, PaxM, PaxB, PaxC, PaxP and PaxQ was conducted. It was found that the combination of PaxG, PaxM, PaxB and PaxC was required for the synthesis of the first stable indole-diterpene, paspaline. Orthologues of these four genes have been identified in other filamentous fungi suggesting that paspaline is the key intermediate that provides the core structural backbone for the biosynthesis of indole-diterpenes. Although PaxA appears to have a role in paxilline biosynthesis, it was not required for paspaline biosynthesis. PaxP enzyme was stereospecific for substrates with β-configuration and catalysed multiple oxidation steps both at a single carbon atom and at different carbon atoms. The occurrence of indole-diterpenes with α- and β-stereochemistry in two different taxonomic orders suggest that PaxP and its orthologue may have a role in introducing the stereochemistry of indole-diterpenes. Unlike PaxP,

PaxQ was a promiscuous enzyme as shown by its ability to act on a substrate with α-configuration.

Although a pathway-specific regulator has not been found in the *pax* cluster, differences in the expression of *paxP* and *paxQ* genes in two different *pax* cluster deletion backgrounds suggests the presence of a regulatory factor.

The reporter fusion studies of the two *P. paxilli* GGPP synthases, Ggs1 and PaxG, showed their differential localisation. Ggs1-EGFP fusion protein was localised to punctuate structures whose identity could not be established. EGFP-GRV fusion protein, containing the C-terminal tripeptide GRV of PaxG, was localised to peroxisomes. Enzymes involved in other secondary metabolite pathways have been shown to either localised to peroxisomes or contain putative peroxisomal localisation signals suggesting that peroxisomes may have an important role in secondary metabolism.

Based on the results presented in this study, it is now possible to have a greater understanding of the various steps involved in indole-diterpene biosynthesis, which until now were speculative. The introduction of stereospecificities in the indole-diterpene intermediates can now be tested which would help in understanding the chemical diversity observed among the indole-diterpene producing fungi.

APPENDIX

Appendix 5.1

RP-HPLC analysis of authentic PC-M6 and paxitriol

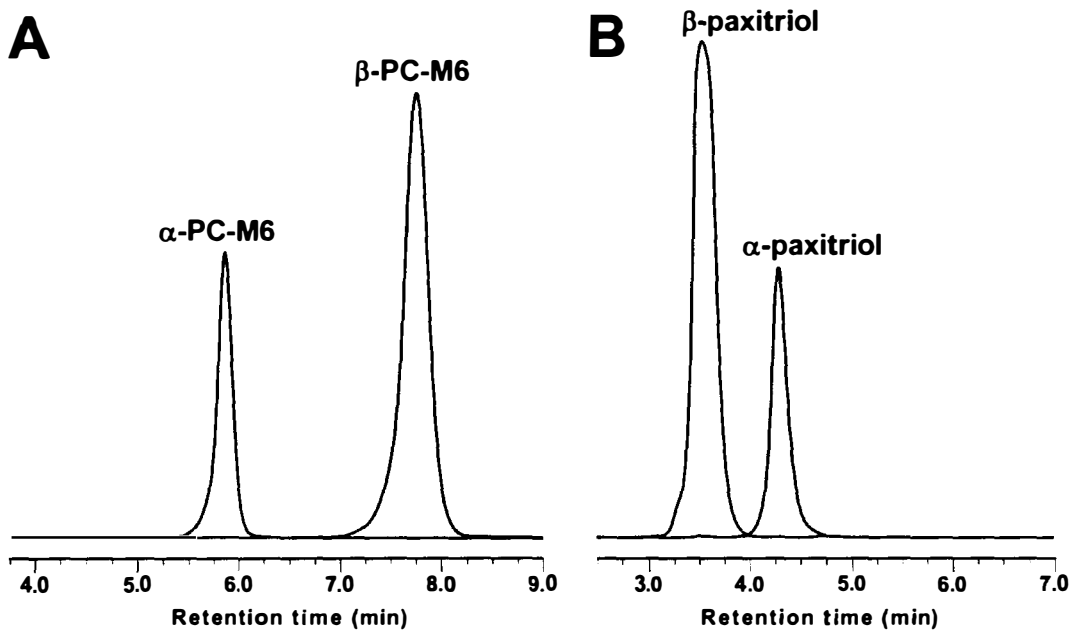

Appendix 5.1 RP-HPLC analysis of authentic PC-M6 and paxitriol

(A) PC-M6 stereoisomers: α-PC-M6 (R_t = 5.85 min) and β-PC-M6 (R_t = 7.75 min).
(B) Paxitriol stereoisomers: α-paxitriol (R_t = 4.30 min) and β-paxitriol (R_t = 3.55 min).

Appendix 5.2
Vector maps

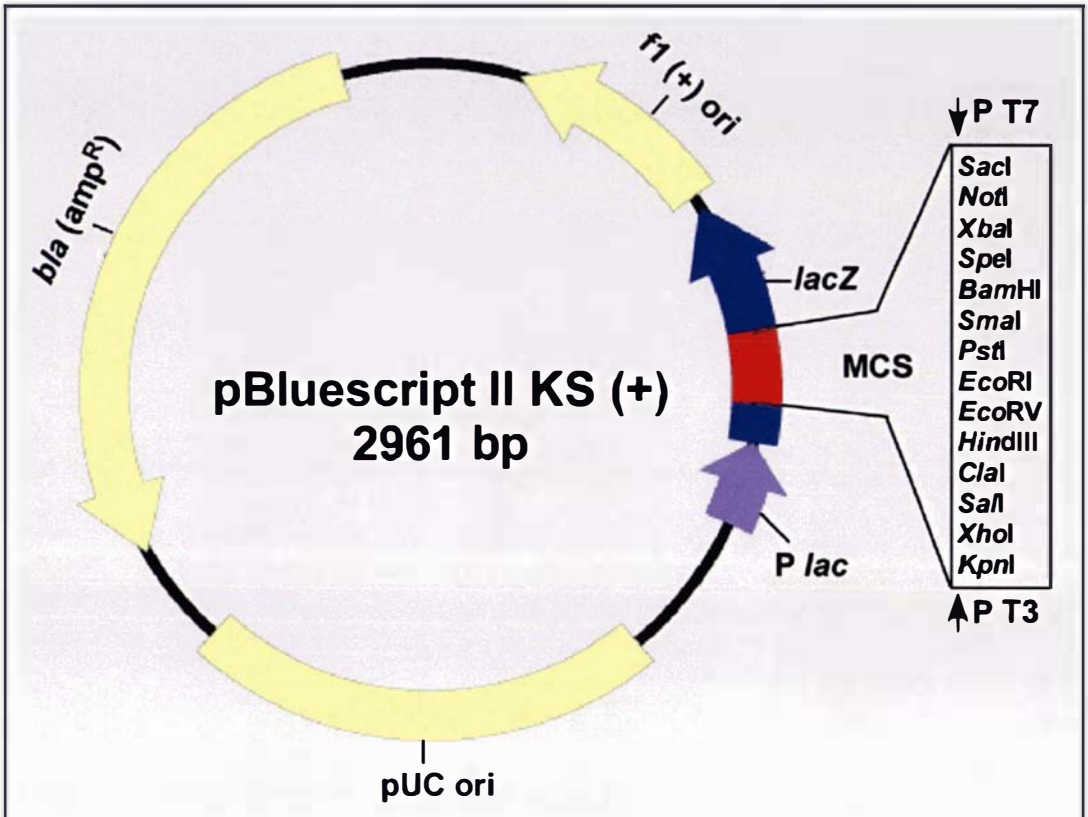

Appendix 5.2.1 pBluescript II KS (+) (Stratagene)

pBluescript II KS (+) vector sequence reference points:

f1 (+) origin of ss-DNA replication	135-441
β-galactoside α-fragment coding sequence (*lacZ*)	460-816
multiple cloning site	653-760
T7 promoter transcription initiation site	643
T3 promoter transcription initiation site	774
lac promoter	817-938
pUC origin of replication	1158-1825
ampicillin resistance (*bla*) ORF	1976-2833

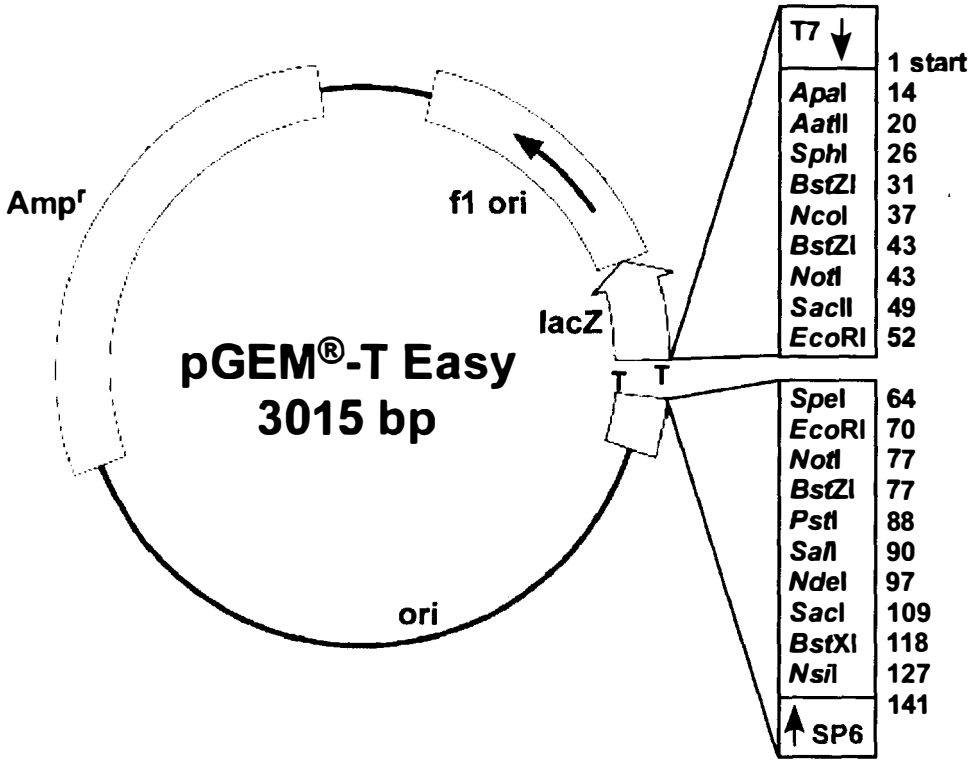

Appendix 5.2.2 pGEM®-T Easy (Promega)

pGEM®-T Easy vector sequence reference points:

T7 RNA polymerase transcription initiation site	1
SP6 RNA polymerase transcription initiation site	141
T7 RNA polymerase promoter	2999-3
SP6 RNA polymerase promoter	139-158
multiple cloning site	10-128
lacZ start codon	180
lac operon sequences	2836-2996, 166-395
lac operator	200-216
β-lactamase coding region	1337-2197
phage f1 region	2380-2835
pUC/M13 forward sequencing primer binding site	2949-2972
pUC/M13 reverse sequencing primer binding site	176-197

REFERENCES

Abe, Y., Suzuki, T., Ono, C., Iwamoto, K., Hosobuchi, M., and Yoshikawa, H. (2002) Molecular cloning and characterization of an ML-236B (compactin) biosynthetic gene cluster in *Penicillium citrinum*. *Mol Genet Genomics* **267**: 636-646.

Acklin, W., Weibel, F., and Arigoni, D. (1977) Zur biosynthese von paspalin und verwandten metaboliten aus *Claviceps paspali*. *Chimia* **31**: 63.

Ahn, J.H., and Walton, J.D. (1998) Regulation of cyclic peptide biosynthesis and pathogenicity in *Cochliobolus carbonum* by TOXEp, a novel protein with a bZIP basic DNA-binding motif and four ankyrin repeats. *Mol Gen Genet* **260**: 462-469.

Ahn, J.H., Cheng, Y.Q., and Walton, J.D. (2002) An extended physical map of the TOX2 locus of *Cochliobolus carbonum* required for biosynthesis of HC-toxin. *Fungal Genet Biol* **35**: 31-38.

Aitchison, J.D., Murray, W.W., and Rachubinski, R.A. (1991) The carboxyl-terminal tripeptide Ala-Lys-Ile is essential for targeting *Candida tropicalis* trifunctional enzyme to yeast peroxisomes. *J Biol Chem* **266**: 23197-23203.

Alexander, N.J., Hohn, T.M., and McCormick, S.P. (1998) The *TRI11* gene of *Fusarium sporotrichioides* encodes a cytochrome P-450 monooxygenase required for C-15 hydroxylation in trichothecene biosynthesis. *Appl Environ Microbiol* **64**: 221-225.

Alexander, N.J., McCormick, S.P., and Hohn, T.M. (1999) *TRI12*, a trichothecene efflux pump from *Fusarium sporotrichioides*: gene isolation and expression in yeast. *Mol Gen Genet* **261**: 977-984.

Alexander, N.J., McCormick, S.P., Larson, T.M., and Jurgenson, J.E. (2004) Expression of *Tri15* in *Fusarium sporotrichioides*. *Curr Genet* **45**: 157-162.

Altschul, S.F., Madden, T.L., Schaffer, A.A., Zhang, J., Zhang, Z., Miller, W., and Lipman, D.J. (1997) Gapped BLAST and PSI-BLAST: a new generation of protein database search programs. *Nucleic Acids Res* **25**: 3389-3402.

Barredo, J.L., Diez, B., Alvarez, E., and Martin, J.F. (1989) Large amplification of a 35-kb DNA fragment carrying two penicillin biosynthetic genes in

high penicillin producing strains of *Penicillium chrysogenum*. *Curr Genet* **16**: 453-459.

Bhatnagar, D., Ehrlich, K.C., and Cleveland, T.E. (2003) Molecular genetic analysis and regulation of aflatoxin biosynthesis. *Appl Microbiol Biotechnol* **61**: 83-93.

Bok, J.W., and Keller, N.P. (2004) *LaeA*, a regulator of secondary metabolism in *Aspergillus* spp. *Eukaryot Cell* **3**: 527-535.

Bok, J.W., Balajee, S.A., Marr, K.A., Andes, D., Nielsen, K.F., Frisvad, J.C., and Keller, N.P. (2005) LaeA, a regulator of morphogenetic fungal virulence factors. *Eukaryot Cell* **4**: 1574-1582.

Bok, J.W., Hoffmeister, D., Maggio-Hall, L.A., Murillo, R., Glasner, J.D., and Keller, N.P. (2006) Genomic mining for Aspergillus natural products. *Chem Biol* **13**: 31-37.

Bradshaw, R.E., Jin, H., Morgan, B.S., Schwelm, A., Teddy, O.R., Young, C.A., and Zhang, S. (2006) A polyketide synthase gene required for biosynthesis of the aflatoxin-like toxin, dothistromin. *Mycopathologia* **161**: 283-294.

Brakhage, A.A., Al-Abdallah, Q., Tuncher, A., and Sprote, P. (2005) Evolution of β-lactam biosynthesis genes and recruitment of *trans*-acting factors. *Phytochemistry* **66**: 1200-1210.

Brodhagen, M., and Keller, N.P. (2006) Signalling pathways connecting mycotoxin production and sporulatoin. *Mol Plant Pathol* **7**: 285-301.

Brown, D.W., McCormick, S.P., Alexander, N.J., Proctor, R.H., and Desjardins, A.E. (2001) A genetic and biochemical approach to study trichothecene diversity in *Fusarium sporotrichioides* and *Fusarium graminearum*. *Fungal Genet Biol* **32**: 121-133.

Brown, D.W., McCormick, S.P., Alexander, N.J., Proctor, R.H., and Desjardins, A.E. (2002) Inactivation of a cytochrome P-450 is a determinant of trichothecene diversity in *Fusarium* species. *Fungal Genet Biol* **36**: 224-233.

Brown, D.W., Yu, J.H., Kelkar, H.S., Fernandes, M., Nesbitt, T.C., Keller, N.P., Adams, T.H., and Leonard, T.J. (1996) Twenty-five coregulated

transcripts define a sterigmatocystin gene cluster in *Aspergillus nidulans*. *Proc Natl Acad Sci U S A* **93**: 1418-1422.

Buades, C., and Moya, A. (1996) Phylogenetic analysis of the isopenicillin-N-synthetase horizontal gene transfer. *J Mol Evol* **42**: 537-542.

Bullock, W.O., Fernandez, J.M., and Short, J.M. (1987) XL 1-blue: A high efficiency plasmid transforming recA *Escherichia coli* strain with β-galactosidase selection. *BioTechniques* **5**: 376-379.

Byrne, K.M., Smith, S.K., and Ondeyka, J.G. (2002) Biosynthesis of nodulisporic acid A: precursor studies. *J Am Chem Soc* **124**: 7055-7060.

Calvo, A.M., Wilson, R.A., Bok, J.W., and Keller, N.P. (2002) Relationship between secondary metabolism and fungal development. *Microbiol Mol Biol Rev* **66**: 447-459, table of contents.

Chang, P.K., Yu, J., Bhatnagar, D., and Cleveland, T.E. (2000) Characterization of the *Aspergillus parasiticus* major nitrogen regulatory gene, *areA*. *Biochim Biophys Acta* **1491**: 263-266.

Chiou, C.H., Lee, L.W., Owens, S.A., Whallon, J.H., Klomparens, K.L., Townsend, C.A., and Linz, J.E. (2004) Distribution and sub-cellular localization of the aflatoxin enzyme versicolorin B synthase in time-fractionated colonies of *Aspergillus parasiticus*. *Arch Microbiol* **182**: 67-79.

Chiou, C.H., Miller, M., Wilson, D.L., Trail, F., and Linz, J.E. (2002) Chromosomal location plays a role in regulation of aflatoxin gene expression in *Aspergillus parasiticus*. *Appl Environ Microbiol* **68**: 306-315.

Clark, J.S., Myatt, J., Wilson, C., Roberts, L., and Walshe, N. (2003) Exploration of the biomimetic synthesis of indole-diterpene mycotoxins: an unexpected cascade reaction during the attempted synthesis of emindole SB. *Chem Commun (Camb)*: 1546-1547.

Correia, T., Grammel, N., Ortel, I., Keller, U., and Tudzynski, P. (2003) Molecular cloning and analysis of the ergopeptine assembly system in the ergot fungus *Claviceps purpurea*. *Chem Biol* **10**: 1281-1292.

Cortes, J., Haydock, S.F., Roberts, G.A., Bevitt, D.J., and Leadlay, P.F. (1990) An unusually large multifunctional polypeptide in the erythromycin-

producing polyketide synthase of *Saccharopolyspora erythraea*. *Nature* **348**: 176-178.

Cox, K.H., Tate, J.J., and Cooper, T.G. (2002) Cytoplasmic compartmentation of Gln3 during nitrogen catabolite repression and the mechanism of its nuclear localization during carbon starvation in *Saccharomyces cerevisiae*. *J Biol Chem* **277**: 37559-37566.

Coyle, C.M., and Panaccione, D.G. (2005) An ergot alkaloid biosynthesis gene and clustered hypothetical genes from *Aspergillus fumigatus*. *Appl Environ Microbiol* **71**: 3112-3118.

Cramer, R.A., Jr., Gamcsik, M.P., Brooking, R.M., Najvar, L.K., Kirkpatrick, W.R., Patterson, T.F., Balibar, C.J., Graybill, J.R., Perfect, J.R., Abraham, S.N., and Steinbach, W.J. (2006) Disruption of a nonribosomal peptide synthetase in *Aspergillus fumigatus* eliminates gliotoxin production. *Eukaryot Cell* **5**: 972-980.

Cziferszky, A., Mach, R.L., and Kubicek, C.P. (2002) Phosphorylation positively regulates DNA binding of the carbon catabolite repressor Cre1 of *Hypocrea jecorina* (*Trichoderma reesei*). *J Biol Chem* **277**: 14688-14694.

de Jesus, A.E., Gorst-Allman, C.P., Steyn, P.S., van Heerden, F.R., Vleggaar, R., Wessels, P.L., and Hull, W.E. (1983) Tremorgenic mycotoxins from *Penicillium crustosum*. Biosynthesis of penitrem A. *J Chem Soc Perkin Trans 1*: 1863-1868.

Del Sorbo, G., Schoonbeek, H., and De Waard, M.A. (2000) Fungal transporters involved in efflux of natural toxic compounds and fungicides. *Fungal Genet Biol* **30**: 1-15.

Demain, A.L. (1992) Microbial secondary metabolism: a new theoretical frontier for academia, a new opportunity for industry. *Ciba Found Symp* **171**: 3-23.

Desjardins, A.E., Hohn, T.M., and McCormick, S.P. (1993) Trichothecene biosynthesis in *Fusarium* species: chemistry, genetics, and significance. *Microbiol Rev* **57**: 595-604.

Diez, B., Gutierrez, S., Barredo, J.L., van Solingen, P., van der Voort, L.H., and Martin, J.F. (1990) The cluster of penicillin biosynthetic genes. Identification and characterization of the *pcbAB* gene encoding the

alpha-aminoadipyl-cysteinyl-valine synthetase and linkage to the *pcbC* and *penDE* genes. *J Biol Chem* **265**: 16358-16365.

Doekel, S., and Marahiel, M.A. (2001) Biosynthesis of natural products on modular peptide synthetases. *Metab Eng* **3**: 64-77.

Dower, W.J., Miller, J.F., and Ragsdale, C.W. (1988) High efficiency transformation of *E. coli* by high voltage electroporation. *Nucleic Acids Res* **16**: 6127-6145.

Dowzer, C.E., and Kelly, J.M. (1991) Analysis of the *creA* gene, a regulator of carbon catabolite repression in *Aspergillus nidulans*. *Mol Cell Biol* **11**: 5701-5709.

Drysdale, M.R., Kolze, S.E., and Kelly, J.M. (1993) The *Aspergillus niger* carbon catabolite repressor encoding gene, *creA*. *Gene* **130**: 241-245.

Eckert, M., Maguire, K., Urban, M., Foster, S., Fitt, B., Lucas, J., and Hammond-Kosack, K. (2005) *Agrobacterium tumefaciens*-mediated transformation of *Leptosphaeria* spp. and *Oculimacula* spp. with the reef coral gene *DsRed* and the jellyfish gene *gfp*. *FEMS Microbiol Lett* **253**: 67-74.

Ehrlich, K.C., and Cotty, P.J. (2002) Variability in nitrogen regulation of aflatoxin production by *Aspergillus flavus* strains. *Appl Microbiol Biotechnol* **60**: 174-178.

Ehrlich, K.C., Montalbano, B.G., and Cary, J.W. (1999) Binding of the C6-zinc cluster protein, AFLR, to the promoters of aflatoxin pathway biosynthesis genes in *Aspergillus parasiticus*. *Gene* **230**: 249-257.

Eisendle, M., Oberegger, H., Buttinger, R., Illmer, P., and Haas, H. (2004) Biosynthesis and uptake of siderophores is controlled by the PacC-mediated ambient-pH regulatory system in *Aspergillus nidulans*. *Eukaryot Cell* **3**: 561-563.

Elgersma, Y., van Roermund, C.W., Wanders, R.J., and Tabak, H.F. (1995) Peroxisomal and mitochondrial carnitine acetyltransferases of *Saccharomyces cerevisiae* are encoded by a single gene. *EMBO J* **14**: 3472-3479.

Emanuelsson, O., Nielsen, H., Brunak, S., and von Heijne, G. (2000) Predicting subcellular localization of proteins based on their N-terminal amino acid sequence. *J Mol Biol* **300**: 1005-1016.

Fischer, R.T., Stam, S.H., Johnson, P.R., Ko, S.S., Magolda, R.L., Gaylor, J.L., and Trzaskos, J.M. (1989) Mechanistic studies of lanosterol 14 α-methyl demethylase: substrate requirements for the component reactions catalyzed by a single cytochrome P-450 isozyme. *J Lipid Res* **30**: 1621-1632.

Flaherty, J.E., and Woloshuk, C.P. (2004) Regulation of fumonisin biosynthesis in *Fusarium verticillioides* by a zinc binuclear cluster-type gene, *ZFR1. Appl Environ Microbiol* **70**: 2653-2659.

Flaherty, J.E., Pirttila, A.M., Bluhm, B.H., and Woloshuk, C.P. (2003) *PAC1*, a pH-regulatory gene from *Fusarium verticillioides. Appl Environ Microbiol* **69**: 5222-5227.

Fletcher, L.R., and Harvey, I.C. (1981) An association of a *Lolium* endophyte with ryegrass staggers. *NZ Vet J* **29**: 185-186.

Frey, M., Chomet, P., Glawischnig, E., Stettner, C., Grun, S., Winklmair, A., Eisenreich, W., Bacher, A., Meeley, R.B., Briggs, S.P., Simcox, K., and Gierl, A. (1997) Analysis of a chemical plant defense mechanism in grasses. *Science* **277**: 696-699.

Fueki, S., Tokiwano, T., Toshima, H., and Oikawa, H. (2004) Biosynthesis of indole diterpenes, emindole, and paxilline: involvement of a common intermediate. *Org Lett* **6**: 2697-2700.

Gaffoor, I., Brown, D.W., Plattner, R., Proctor, R.H., Qi, W., and Trail, F. (2005) Functional analysis of the polyketide synthase genes in the filamentous fungus *Gibberella zeae* (anamorph *Fusarium graminearum*). *Eukaryot Cell* **4**: 1926-1933.

Galagan, J.E., Calvo, S.E., Borkovich, K.A., Selker, E.U., Read, N.D., Jaffe, D., FitzHugh, W., Ma, L.J., Smirnov, S., Purcell, S., Rehman, B., Elkins, T., Engels, R., Wang, S., Nielsen, C.B., Butler, J., Endrizzi, M., Qui, D., Ianakiev, P., Bell-Pedersen, D., Nelson, M.A., Werner-Washburne, M., Selitrennikoff, C.P., Kinsey, J.A., Braun, E.L., Zelter, A., Schulte, U., Kothe, G.O., Jedd, G., Mewes, W., Staben, C., Marcotte, E., Greenberg, D., Roy, A., Foley, K., Naylor, J., Stange-Thomann, N., Barrett, R., Gnerre, S., Kamal, M., Kamvysselis, M., Mauceli, E., Bielke, C., Rudd, S., Frishman, D., Krystofova, S., Rasmussen, C., Metzenberg, R.L.,

Perkins, D.D., Kroken, S., Cogoni, C., Macino, G., Catcheside, D., Li, W., Pratt, R.J., Osmani, S.A., DeSouza, C.P., Glass, L., Orbach, M.J., Berglund, J.A., Voelker, R., Yarden, O., Plamann, M., Seiler, S., Dunlap, J., Radford, A., Aramayo, R., Natvig, D.O., Alex, L.A., Mannhaupt, G., Ebbole, D.J., Freitag, M., Paulsen, I., Sachs, M.S., Lander, E.S., Nusbaum, C., and Birren, B. (2003) The genome sequence of the filamentous fungus *Neurospora crassa*. *Nature* **422**: 859-868.

Gancedo, J.M. (1998) Yeast carbon catabolite repression. *Microbiol Mol Biol Rev* **62**: 334-361.

Gardiner, D.M., and Howlett, B.J. (2005) Bioinformatic and expression analysis of the putative gliotoxin biosynthetic gene cluster of *Aspergillus fumigatus*. *FEMS Microbiol Lett* **248**: 241-248.

Gardiner, D.M., Cozijnsen, A.J., Wilson, L.M., Pedras, M.S., and Howlett, B.J. (2004) The sirodesmin biosynthetic gene cluster of the plant pathogenic fungus *Leptosphaeria maculans*. *Mol Microbiol* **53**: 1307-1318.

Gardiner, D.M., Jarvis, R.S., and Howlett, B.J. (2005) The ABC transporter gene in the sirodesmin biosynthetic gene cluster of *Leptosphaeria maculans* is not essential for sirodesmin production but facilitates self-protection. *Fungal Genet Biol* **42**: 257-263.

Gatenby, W.A., Munday-Finch, S.C., Wilkins, A.L., and Miles, C.O. (1999) Terpendole M, a novel indole-diterpenoid isolated from *Lolium perenne* infected with the endophytic fungus *Neotyphodium lolii*. *J Agric Food Chem* **47**: 1092-1097.

Gebler, J.C., and Poulter, C.D. (1992) Purification and characterization of dimethylallyl tryptophan synthase from *Claviceps purpurea*. *Arch Biochem Biophys* **296**: 308-313.

Gloer, J.B. (1995) Antiinsectan natural products from fungal sclerotia. *Acc Chem Res* **28**: 343-350.

Gould, S.J., Keller, G.A., Hosken, N., Wilkinson, J., and Subramani, S. (1989) A conserved tripeptide sorts proteins to peroxisomes. *J Cell Biol* **108**: 1657-1664.

Haarmann, T., Machado, C., Lubbe, Y., Correia, T., Schardl, C.L., Panaccione, D.G., and Tudzynski, P. (2005) The ergot alkaloid gene cluster in

Claviceps purpurea: extension of the cluster sequence and intra species evolution. *Phytochemistry* **66**: 1312-1320.

Haarmann, T., Ortel, I., Tudzynski, P., and Keller, U. (2006) Identification of the cytochrome P450 monooxygenase that bridges the clavine and ergoline alkaloid pathways. *Chembiochem* **7**: 645-652.

Haas, H., and Marzluf, G.A. (1995) NRE, the major nitrogen regulatory protein of *Penicillium chrysogenum*, binds specifically to elements in the intergenic promoter regions of nitrate assimilation and penicillin biosynthetic gene clusters. *Curr Genet* **28**: 177-183.

Hanahan, D. (1983) Studies on transformation of *Escherichia coli* with plasmids. *J Mol Biol* **166**: 557-580.

Harris, L.J., Desjardins, A.E., Plattner, R.D., Nicholson, P., Butler, G., Young, J.C., Weston, G., Proctor, R.H., and Hohn, T.M. (1999) Possible role of trichothecene mycotoxins in virulence of *Fusarium graminearum* on maize. *Plant Dis* **83**: 954-960.

Hatta, R., Ito, K., Hosaki, Y., Tanaka, T., Tanaka, A., Yamamoto, M., Akimitsu, K., and Tsuge, T. (2002) A conditionally dispensable chromosome controls host-specific pathogenicity in the fungal plant pathogen *Alternaria alternata. Genetics* **161**: 59-70.

Higuchi, Y., Nakahama, T., Shoji, J.Y., Arioka, M., and Kitamoto, K. (2006) Visualization of the endocytic pathway in the filamentous fungus *Aspergillus oryzae* using an EGFP-fused plasma membrane protein. *Biochem Biophys Res Commun* **340**: 784-791.

Hoff, B., and Kuck, U. (2005) Use of bimolecular fluorescence complementation to demonstrate transcription factor interaction in nuclei of living cells from the filamentous fungus *Acremonium chrysogenum. Curr Genet* **47**: 132-138.

Hoff, B., Schmitt, E.K., and Kuck, U. (2005) CPCR1, but not its interacting transcription factor AcFKH1, controls fungal arthrospore formation in *Acremonium chrysogenum. Mol Microbiol* **56**: 1220-1233.

Hohn, T.M., and Beremand, P.D. (1989) Isolation and nucleotide sequence of a sesquiterpene cyclase gene from the trichothecene-producing fungus *Fusarium sporotrichioides. Gene* **79**: 131-138.

Hohn, T.M., Desjardins, A.E., and McCormick, S.P. (1995) The *Tri4* gene of *Fusarium sporotrichioides* encodes a cytochrome P450 monooxygenase involved in trichothecene biosynthesis. *Mol Gen Genet* **248**: 95-102.

Hohn, T.M., Krishna, R., and Proctor, R.H. (1999) Characterization of a transcriptional activator controlling trichothecene toxin biosynthesis. *Fungal Genet Biol* **26**: 224-235.

Ilmen, M., Thrane, C., and Penttila, M. (1996) The glucose repressor gene *cre1* of *Trichoderma*: isolation and expression of a full-length and a truncated mutant form. *Mol Gen Genet* **251**: 451-460.

Inoue, H., Nojima, H., and Okayama, H. (1990) High efficiency transformation of *Escherichia coli* with plasmids. *Gene* **96**: 23-28.

Inoue, I., Namiki, F., and Tsuge, T. (2002) Plant colonization by the vascular wilt fungus *Fusarium oxysporum* requires *FOW1*, a gene encoding a mitochondrial protein. *Plant Cell* **14**: 1869-1883.

Ito, K., Tanaka, T., Hatta, R., Yamamoto, M., Akimitsu, K., and Tsuge, T. (2004) Dissection of the host range of the fungal plant pathogen *Alternaria alternata* by modification of secondary metabolism. *Mol Microbiol* **52**: 399-411.

Itoh, Y., Johnson, R., and Scott, B. (1994) Integrative transformation of the mycotoxin-producing fungus, *Penicillium paxilli*. *Curr Genet* **25**: 508-513.

Johnson, R.D., Johnson, L., Itoh, Y., Kodama, M., Otani, H., and Kohmoto, K. (2000) Cloning and characterization of a cyclic peptide synthetase gene from *Alternaria alternata* apple pathotype whose product is involved in AM-toxin synthesis and pathogenicity. *Mol Plant Microbe Interact* **13**: 742-753.

Kawaide, H. (2006) Biochemical and molecular analyses of gibberellin biosynthesis in fungi. *Biosci Biotechnol Biochem* **70**: 583-590.

Keller, N.P., and Hohn, T.M. (1997) Metabolic pathway gene clusters in filamentous fungi. *Fungal Genet Biol* **21**: 17-29.

Keller, N.P., Nesbitt, C., Sarr, B., Phillips, T.D., and Burow, G.B. (1997) pH regulation of sterigmatocystin and aflatoxin biosynthesis in *Aspergillus* spp. *Phytopathology* **87**: 643-648.

Kennedy, J., Auclair, K., Kendrew, S.G., Park, C., Vederas, J.C., and Hutchinson, C.R. (1999) Modulation of polyketide synthase activity by

accessory proteins during lovastatin biosynthesis. *Science* **284**: 1368-1372.

Kim, J.E., Jin, J., Kim, H., Kim, J.C., Yun, S.H., and Lee, Y.W. (2006) GIP2, a putative transcription factor that regulates the aurofusarin biosynthetic gene cluster in *Gibberella zeae*. *Appl Environ Microbiol* **72**: 1645-1652.

Kim, Y.T., Lee, Y.R., Jin, J., Han, K.H., Kim, H., Kim, J.C., Lee, T., Yun, S.H., and Lee, Y.W. (2005) Two different polyketide synthase genes are required for synthesis of zearalenone in *Gibberella zeae*. *Mol Microbiol* **58**: 1102-1113.

Kimura, M., Kaneko, I., Komiyama, M., Takatsuki, A., Koshino, H., Yoneyama, K., and Yamaguchi, I. (1998) Trichothecene 3-*O*-acetyltransferase protects both the producing organism and transformed yeast from related mycotoxins. Cloning and characterization of *Tri101*. *J Biol Chem* **273**: 1654-1661.

Kimura, M., Tokai, T., O'Donnell, K., Ward, T.J., Fujimura, M., Hamamoto, H., Shibata, T., and Yamaguchi, I. (2003) The trichothecene biosynthesis gene cluster of *Fusarium graminearum* F15 contains a limited number of essential pathway genes and expressed non-essential genes. *FEBS Lett* **539**: 105-110.

Kimura, N., and Tsuge, T. (1993) Gene cluster involved in melanin biosynthesis of the filamentous fungus *Alternaria alternata*. *J Bacteriol* **175**: 4427-4435.

Kimura, Y., Nishibe, M., Nakajima, H., Hamasaki, T., Shigemitsu, N., Sugawara, F., Stout, T.J., and Clardy, J. (1992) Emeniveol; A new pollen growth inhibitor from the fungus, *Emericella nivea*. *Tetrahedron Lett* **33**: 6987-6990.

Klein, A.T., van den Berg, M., Bottger, G., Tabak, H.F., and Distel, B. (2002) *Saccharomyces cerevisiae* acyl-CoA oxidase follows a novel, non-PTS1, import pathway into peroxisomes that is dependent on Pex5p. *J Biol Chem* **277**: 25011-25019.

Koch, K.V., Suelmann, R., and Fischer, R. (2003) Deletion of *mdmB* impairs mitochondrial distribution and morphology in *Aspergillus nidulans*. *Cell Motil Cytoskeleton* **55**: 114-124.

Kroken, S., Glass, N.L., Taylor, J.W., Yoder, O.C., and Turgeon, B.G. (2003) Phylogenomic analysis of type I polyketide synthase genes in pathogenic and saprobic ascomycetes. *Proc Natl Acad Sci USA* **100**: 15670-15675.

Lafon, A., Han, K.H., Seo, J.A., Yu, J.H., and d'Enfert, C. (2006) G-protein and cAMP-mediated signaling in aspergilli: A genomic perspective. *Fungal Genet Biol* **43**: 490-502.

Lamas-Maceiras, M., Vaca, I., Rodriguez, E., Casqueiro, J., and Martin, J.F. (2006) Amplification and disruption of the phenylacetyl-CoA ligase gene of *Penicillium chrysogenum* encoding an aryl-capping enzyme that supplies phenylacetic acid to the isopenicillin N-acyltransferase. *Biochem J* **395**: 147-155.

Lamb, D.C., Kelly, D.E., Manning, N.J., Kaderbhai, M.A., and Kelly, S.L. (1999) Biodiversity of the P450 catalytic cycle: yeast cytochrome *b5*/NADH cytochrome *b5* reductase complex efficiently drives the entire sterol 14-demethylation (CYP51) reaction. *FEBS Lett* **462**: 283-288.

Lawrence, J.G. (2000) Clustering of antibiotic resistance genes: Beyond the selfish operon. *ASM News* **66**: 281-286.

Laws, I., and Mantle, P.G. (1989) Experimental constraints in the study of the biosynthesis of indole alkaloids in fungi. *J Gen Microbiol* **135**: 2679-2692.

Lee, L.W., Chiou, C.H., and Linz, J.E. (2002a) Function of native OmtA in vivo and expression and distribution of this protein in colonies of *Aspergillus parasiticus*. *Appl Environ Microbiol* **68**: 5718-5727.

Lee, L.W., Chiou, C.H., Klomparens, K.L., Cary, J.W., and Linz, J.E. (2004) Subcellular localization of aflatoxin biosynthetic enzymes Nor-1, Ver-1, and OmtA in time-dependent fractionated colonies of *Aspergillus parasiticus*. *Arch Microbiol* **181**: 204-214.

Lee, T., Han, Y.K., Kim, K.H., Yun, S.H., and Lee, Y.W. (2002b) *Tri13* and *Tri7* determine deoxynivalenol- and nivalenol-producing chemotypes of *Gibberella zeae*. *Appl Environ Microbiol* **68**: 2148-2154.

Lendenfeld, T., Ghali, D., Wolschek, M., Kubicek-Pranz, E.M., and Kubicek, C.P. (1993) Subcellular compartmentation of penicillin biosynthesis in

Penicillium chrysogenum. The amino acid precursors are derived from the vacuole. *J Biol Chem* **268**: 665-671.

Lengeler, K.B., Davidson, R.C., D'Souza, C., Harashima, T., Shen, W.C., Wang, P., Pan, X., Waugh, M., and Heitman, J. (2000) Signal transduction cascades regulating fungal development and virulence. *Microbiol Mol Biol Rev* **64**: 746-785.

Linnemannstons, P., Schulte, J., del Mar Prado, M., Proctor, R.H., Avalos, J., and Tudzynski, B. (2002) The polyketide synthase gene *pks4* from *Gibberella fujikuroi* encodes a key enzyme in the biosynthesis of the red pigment bikaverin. *Fungal Genet Biol* **37**: 134-148.

Litzka, O., Then Bergh, K., Van den Brulle, J., Steidl, S., and Brakhage, A.A. (1999) Transcriptional control of expression of fungal β-lactam biosynthesis genes. *Antonie Van Leeuwenhoek* **75**: 95-105.

Liu, B.H., and Chu, F.S. (1998) Regulation of *aflR* and its product, AflR, associated with aflatoxin biosynthesis. *Appl Environ Microbiol* **64**: 3718-3723.

Lorang, J.M., Tuori, R.P., Martinez, J.P., Sawyer, T.L., Redman, R.S., Rollins, J.A., Wolpert, T.J., Johnson, K.B., Rodriguez, R.J., Dickman, M.B., and Ciuffetti, L.M. (2001) Green fluorescent protein is lighting up fungal biology. *Appl Environ Microbiol* **67**: 1987-1994.

Lysoe, E., Klemsdal, S.S., Bone, K.R., Frandsen, R.J., Johansen, T., Thrane, U., and Giese, H. (2006) The *PKS4* gene of *Fusarium graminearum* is essential for zearalenone production. *Appl Environ Microbiol* **72**: 3924-3932.

Maggio-Hall, L.A., and Keller, N.P. (2004) Mitochondrial β-oxidation in *Aspergillus nidulans*. *Mol Microbiol* **54**: 1173-1185.

Maggio-Hall, L.A., Wilson, R.A., and Keller, N.P. (2005) Fundamental contribution of β-oxidation to polyketide mycotoxin production in planta. *Mol Plant Microbe Interact* **18**: 783-793.

Malonek, S., Rojas, M.C., Hedden, P., Gaskin, P., Hopkins, P., and Tudzynski, B. (2004) The NADPH-cytochrome P450 reductase gene from *Gibberella fujikuroi* is essential for gibberellin biosynthesis. *J Biol Chem* **279**: 25075-25084.

Malonek, S., Rojas, M.C., Hedden, P., Gaskin, P., Hopkins, P., and Tudzynski, B. (2005a) Functional characterization of two cytochrome P450 monooxygenase genes, *P450-1* and *P450-4*, of the gibberellic acid gene cluster in *Fusarium proliferatum* (*Gibberella fujikuroi* MP-D). *Appl Environ Microbiol* **71**: 1462-1472.

Malonek, S., Rojas, M.C., Hedden, P., Hopkins, P., and Tudzynski, B. (2005b) Restoration of gibberellin production in *Fusarium proliferatum* by functional complementation of enzymatic blocks. *Appl Environ Microbiol* **71**: 6014-6025.

Malz, S., Grell, M.N., Thrane, C., Maier, F.J., Rosager, P., Felk, A., Albertsen, K.S., Salomon, S., Bohn, L., Schafer, W., and Giese, H. (2005) Identification of a gene cluster responsible for the biosynthesis of aurofusarin in the *Fusarium graminearum* species complex. *Fungal Genet Biol* **42**: 420-433.

Mantle, P.G., and Weedon, C.M. (1994) Biosynthesis and transformation of tremorgenic indole-diterpenoids by *Penicillium paxilli* and *Acremonium lolii*. *Phytochemistry* **36**: 1209-1217.

Martin, J.F., Casqueiro, J., Kosalkova, K., Marcos, A.T., and Gutierrez, S. (1999) Penicillin and cephalosporin biosynthesis: mechanism of carbon catabolite regulation of penicillin production. *Antonie Van Leeuwenhoek* **75**: 21-31.

Marzluf, G.A. (1997) Genetic regulation of nitrogen metabolism in the fungi. *Microbiol Mol Biol Rev* **61**: 17-32.

McCormick, S.P., Alexander, N.J., Trapp, S.E., and Hohn, T.M. (1999) Disruption of *TRI101*, the gene encoding trichothecene 3-*O*-acetyltransferase, from *Fusarium sporotrichioides*. *Appl Environ Microbiol* **65**: 5252-5256.

McCormick, S.P., and Alexander, N.J. (2002) *Fusarium Tri8* encodes a trichothecene C-3 esterase. *Appl Environ Microbiol* **68**: 2959-2964.

McCormick, S.P., Hohn, T.M., and Desjardins, A.E. (1996) Isolation and characterization of *Tri3*, a gene encoding 15-*O*-acetyltransferase from *Fusarium sporotrichioides*. *Appl Environ Microbiol* **62**: 353-359.

McMillan, L.K., Carr, R.L., Young, C.A., Astin, J.W., Lowe, R.G., Parker, E.J., Jameson, G.B., Finch, S.C., Miles, C.O., McManus, O.B., Schmalhofer,

W.A., Garcia, M.L., Kaczorowski, G.J., Goetz, M., Tkacz, J.S., and Scott, B. (2003) Molecular analysis of two cytochrome P450 monooxygenase genes required for paxilline biosynthesis in *Penicillium paxilli*, and effects of paxilline intermediates on mammalian maxi-K ion channels. *Mol Genet Genomics* **270**: 9-23.

Meek, I.B., Peplow, A.W., Ake, C., Jr., Phillips, T.D., and Beremand, M.N. (2003) *Tri1* encodes the cytochrome P450 monooxygenase for C-8 hydroxylation during trichothecene biosynthesis in *Fusarium sporotrichioides* and resides upstream of another new *Tri* gene. *Appl Environ Microbiol* **69**: 1607-1613.

Mende, K., Homann, V., and Tudzynski, B. (1997) The geranylgeranyl diphosphate synthase gene of *Gibberella fujikuroi*: isolation and expression. *Mol Gen Genet* **255**: 96-105.

Meyers, D.M., Obrian, G., Du, W.L., Bhatnagar, D., and Payne, G.A. (1998) Characterization of *aflJ*, a gene required for conversion of pathway intermediates to aflatoxin. *Appl Environ Microbiol* **64**: 3713-3717.

Mihlan, M., Homann, V., Liu, T.W., and Tudzynski, B. (2003) *AREA* directly mediates nitrogen regulation of gibberellin biosynthesis in *Gibberella fujikuroi*, but its activity is not affected by NMR. *Mol Microbiol* **47**: 975-991.

Mikkelsen, L., Sarrocco, S., Lubeck, M., and Jensen, D.F. (2003) Expression of the red fluorescent protein DsRed-Express in filamentous ascomycete fungi. *FEMS Microbiol Lett* **223**: 135-139.

Miles, C.O., Wilkins, A.L., Gallagher, R.T., Hawkes, A.D., Munday, S.C., and Towers, N.R. (1992) Synthesis and tremorgenicity of paxitriols and lolitriol: Possible biosynthetic precursors of lolitrem B. *J Agric Food Chem* **40**: 234-238.

Miller, J.H. (1972) *Experiments in molecular genetics.* New York: Cold Spring Harbor.

Moffitt, M.C., and Neilan, B.A. (2000) The expansion of mechanistic and organismic diversity associated with non-ribosomal peptides. *FEMS Microbiol Lett* **191**: 159-167.

Motamedi, H., and Shafiee, A. (1998) The biosynthetic gene cluster for the macrolactone ring of the immunosuppressant FK506. *Eur J Biochem* **256**: 528-534.

Mullaney, E.J., Hamer, J.E., Roberti, K.A., Yelton, M.M., and Timberlake, W.E. (1985) Primary structure of the *trpC* gene from *Aspergillus nidulans*. *Mol Gen Genet* **199**: 37-45.

Muller, W.H., Bovenberg, R.A., Groothuis, M.H., Kattevilder, F., Smaal, E.B., Van der Voort, L.H., and Verkleij, A.J. (1992) Involvement of microbodies in penicillin biosynthesis. *Biochim Biophys Acta* **1116**: 210-213.

Muller, W.H., van der Krift, T.P., Krouwer, A.J., Wosten, H.A., van der Voort, L.H., Smaal, E.B., and Verkleij, A.J. (1991) Localization of the pathway of the penicillin biosynthesis in *Penicillium chrysogenum*. *EMBO J* **10**: 489-495.

Munday-Finch, S.C., Wilkins, A.L., and Miles, C.O. (1996) Isolation of paspaline B, an indole-diterpenoid from *Penicillium paxilli*. *Phytochemistry* **41**: 327-332.

Nakai, K., and Horton, P. (1999) PSORT: a program for detecting sorting signals in proteins and predicting their subcellular localization. *Trends Biochem Sci* **24**: 34-35.

Namiki, F., Matsunaga, M., Okuda, M., Inoue, I., Nishi, K., Fujita, Y., and Tsuge, T. (2001) Mutation of an arginine biosynthesis gene causes reduced pathogenicity in *Fusarium oxysporum* f. sp. *melonis*. *Mol Plant Microbe Interact* **14**: 580-584.

Nozawa, K., Nakajima, S., Kawai, K., and Udagawa, S. (1988a) Studies on fungal products. Part 17. Isolation and structures of novel indoloditerpenes, emindoles DA and DB, from *Emericella desertorum*: X-ray molecular structure of emindole DA acetate. *J Chem Soc Perkin Trans 1*: 1689-1694.

Nozawa, K., Nakajima, S., Kawai, K., and Udagawa, S. (1988b) Isolation and structures of indoloditerpenes, possible biosynthetic intermediates to the tremorgenic mycotoxin, paxilline, from *Emericella striata*. *J Chem Soc Perkin Trans 1*: 2607-2610.

Nozawa, K., Yuyama, M., Nakajima, S., Kawai, K., and Udagawa, S. (1988c) Studies on fungal products. Part 19. Isolation and structure of a novel indoloditerpene, emindole SA, from *Emericella striata*. *J Chem Soc Perkin Trans 1*: 2155-2160.

Oikawa, H., Toyomasu, T., Toshima, H., Ohashi, S., Kawaide, H., Kamiya, Y., Ohtsuka, M., Shinoda, S., Mitsuhashi, W., and Sassa, T. (2001) Cloning and functional expression of cDNA encoding aphidicolan-16 β-ol synthase: a key enzyme responsible for formation of an unusual diterpene skeleton in biosynthesis of DNA polymerase α inhibitor aphidicolin. *J Am Chem Soc* **123**: 5154-5155.

Okada, K., Saito, T., Nakagawa, T., Kawamukai, M., and Kamiya, Y. (2000) Five geranylgeranyl diphosphate synthases expressed in different organs are localized into three subcellular compartments in *Arabidopsis*. *Plant Physiol* **122**: 1045-1056.

Panaccione, D.G., Johnson, R.D., Wang, J., Young, C.A., Damrongkool, P., Scott, B., and Schardl, C.L. (2001) Elimination of ergovaline from a grass-*Neotyphodium* endophyte symbiosis by genetic modification of the endophyte. *Proc Natl Acad Sci U S A* **98**: 12820-12825.

Panaccione, D.G., Scott-Craig, J.S., Pocard, J.A., and Walton, J.D. (1992) A cyclic peptide synthetase gene required for pathogenicity of the fungus *Cochliobolus carbonum* on maize. *Proc Natl Acad Sci USA* **89**: 6590-6594.

Panozzo, C., Cornillot, E., and Felenbok, B. (1998) The CreA repressor is the sole DNA-binding protein responsible for carbon catabolite repression of the *alcA* gene in *Aspergillus nidulans* via its binding to a couple of specific sites. *J Biol Chem* **273**: 6367-6372.

Parker, E.J., and Scott, B. (2004) Indole-diterpene biosynthesis in ascomycetous fungi. In *Handbook of Industrial Mycology*. An, Z. (ed). New York: Marcel Dekker, pp. 405-426.

Pedley, K.F., and Walton, J.D. (2001) Regulation of cyclic peptide biosynthesis in a plant pathogenic fungus by a novel transcription factor. *Proc Natl Acad Sci USA* **98**: 14174-14179.

Penalva, M.A. (2005) Tracing the endocytic pathway of *Aspergillus nidulans* with FM4-64. *Fungal Genet Biol* **42**: 963-975.

Penalva, M.A., and Arst, H.N., Jr. (2002) Regulation of gene expression by ambient pH in filamentous fungi and yeasts. *Microbiol Mol Biol Rev* **66**: 426-446.

Penn, J., and Mantle, P.G. (1994) Biosynthetic intermediates of indole-diterpenoid mycotoxins from selected transformations at C-10 of paxilline. *Phytochemistry* **35**: 921-926.

Peplow, A.W., Meek, I.B., Wiles, M.C., Phillips, T.D., and Beremand, M.N. (2003a) *Tri16* is required for esterification of position C-8 during trichothecene mycotoxin production by *Fusarium sporotrichioides*. *Appl Environ Microbiol* **69**: 5935-5940.

Peplow, A.W., Tag, A.G., Garifullina, G.F., and Beremand, M.N. (2003b) Identification of new genes positively regulated by *Tri10* and a regulatory network for trichothecene mycotoxin production. *Appl Environ Microbiol* **69**: 2731-2736.

Petriv, O.I., Tang, L., Titorenko, V.I., and Rachubinski, R.A. (2004) A new definition for the consensus sequence of the peroxisome targeting signal type 2. *J Mol Biol* **341**: 119-134.

Pierce, K.L., Premont, R.T., and Lefkowitz, R.J. (2002) Seven-transmembrane receptors. *Nat Rev Mol Cell Biol* **3**: 639-650.

Poggeler, S., Masloff, S., Hoff, B., Mayrhofer, S., and Kuck, U. (2003) Versatile EGFP reporter plasmids for cellular localization of recombinant gene products in filamentous fungi. *Curr Genet* **43**: 54-61.

Proctor, R.H., Brown, D.W., Plattner, R.D., and Desjardins, A.E. (2003) Co-expression of 15 contiguous genes delineates a fumonisin biosynthetic gene cluster in *Gibberella moniliformis*. *Fungal Genet Biol* **38**: 237-249.

Proctor, R.H., Hohn, T.M., and McCormick, S.P. (1995a) Reduced virulence of *Gibberella zeae* caused by disruption of a trichothecene toxin biosynthetic gene. *Mol Plant Microbe Interact* **8**: 593-601.

Proctor, R.H., Hohn, T.M., McCormick, S.P., and Desjardins, A.E. (1995b) *Tri6* encodes an unusual zinc finger protein involved in regulation of trichothecene biosynthesis in *Fusarium sporotrichioides*. *Appl Environ Microbiol* **61**: 1923-1930.

Rainier, J.D., and Smith, A.B., III (2000) Polyene cyclizations to indole diterpenes. The first synthesis of (+)-emindole SA using a biomimetic approach. *Tetrahedron Lett* **41**: 9419-9423.

Riederer, B., Han, M., and Keller, U. (1996) D-Lysergyl peptide synthetase from the ergot fungus *Claviceps purpurea*. *J Biol Chem* **271**: 27524-27530.

Ro, D.K., Arimura, G., Lau, S.Y., Piers, E., and Bohlmann, J. (2005) Loblolly pine abietadienol/abietadienal oxidase *PtAO* (CYP720B1) is a multifunctional, multisubstrate cytochrome P450 monooxygenase. *Proc Natl Acad Sci U S A* **102**: 8060-8065.

Rojas, M.C., Hedden, P., Gaskin, P., and Tudzynski, B. (2001) The *P450-1* gene of *Gibberella fujikuroi* encodes a multifunctional enzyme in gibberellin biosynthesis. *Proc Natl Acad Sci U S A* **98**: 5838-5843.

Ruan, X., Stassi, D., Lax, S.A., and Katz, L. (1997) A second type-I PKS gene cluster isolated from *Streptomyces hygroscopicus* ATCC 29253, a rapamycin-producing strain. *Gene* **203**: 1-9.

Saikia, S., Parker, E.J., Koulman, A., and Scott, B. (2006) Four gene products are required for the fungal synthesis of the indole-diterpene, paspaline. *FEBS Lett* **580**: 1625-1630.

Sanger, F., Nicklen, S., and Coulson, A.R. (1977) DNA sequencing with chain-terminating inhibitors. *Proc Natl Acad Sci U S A* **74**: 5463-5467.

Scazzocchio, C. (2000) The fungal GATA factors. *Curr Opin Microbiol* **3**: 126-131.

Scott, B. (2001) *Epichloe* endophytes: fungal symbionts of grasses. *Curr Opin Microbiol* **4**: 393-398.

Scott, B., Jameson, G.B., and Parker, E.J. (2004) Isoprenoids: Gene clusters and chemical puzzles. In *Advances in Fungal Biotechnology for Industry, Agriculture, and Medicine*. Tkacz, J.S. and Lange, L. (eds). New York: Kluwer Academic/ Plenum Publishers, pp. 163-198.

Scott-Craig, J.S., Panaccione, D.G., Pocard, J.A., and Walton, J.D. (1992) The cyclic peptide synthetase catalyzing HC-toxin production in the filamentous fungus *Cochliobolus carbonum* is encoded by a 15.7-kilobase open reading frame. *J Biol Chem* **267**: 26044-26049.

Screen, S., Bailey, A., Charnley, K., Cooper, R., and Clarkson, J. (1997) Carbon regulation of the cuticle-degrading enzyme PR1 from

Metarhizium anisopliae may involve a trans-acting DNA-binding protein CRR1, a functional equivalent of the *Aspergillus nidulans* CREA protein. *Curr Genet* **31**: 511-518.

Sharma, Y.P., and Kim, Y.W. (1991) Trichothecenes. In *Mycotoxins and phytoalexins*. Tkacz, J.S. and Lange, L. (eds). Boca Raton, FL: CRC Press, pp. 339-359.

Shoji, J.Y., Arioka, M., and Kitamoto, K. (2006) Vacuolar membrane dynamics in the filamentous fungus *Aspergillus oryzae*. *Eukaryot Cell* **5**: 411-421.

Sitthithaworn, W., Kojima, N., Viroonchatapan, E., Suh, D.Y., Iwanami, N., Hayashi, T., Noji, M., Saito, K., Niwa, Y., and Sankawa, U. (2001) Geranylgeranyl diphosphate synthase from *Scoparia dulcis* and *Croton sublyratus*. Plastid localization and conversion to a farnesyl diphosphate synthase by mutagenesis. *Chem Pharm Bull (Tokyo)* **49**: 197-202.

Smith, A.B., 3rd, Davulcu, A.H., and Kurti, L. (2006) Indole diterpenoid synthetic studies. The total synthesis of (+)-nodulisporic acid F. *Org Lett* **8**: 1665-1668.

Smith, A.B., III, and Leenay, T.L. (1988) Indole-diterpene synthetic studies. 4. A stereocontrolled, second generation synthesis of (-)-paspaline. *Tetrahedron Lett* **29**: 2791-2792.

Smith, A.B., III, and Leenay, T.L. (1989) Indole diterpene synthetic studies. 5. Development of a unified synthetic strategy; a stereocontrolled, second-generation synthesis of (-)-Paspaline. *J Am Chem Soc* **111**: 5761-5768.

Smith, A.B., III, and Mewshaw, R. (1985) Total synthesis of (-)-paspaline. *J Am Chem Soc* **107**: 1769-1771.

Smith, A.B., III, Kanoh, N., Ishiyama, H., and Hartz, R.A. (2000) Total synthesis of (-)-penitrem D. *J Am Chem Soc* **122**: 11254-11255.

Smith, A.B., III, Kingery-Wood, J., Leenay, T.L., Nolen, E.G., and Sunazuka, T. (1992) Indole diterpene synthetic studies. 8. The total synthesis of (+)-paspalicine and (+)-paspalinine. *J Am Chem Soc* **114**: 1438-1449.

Smith, A.B., III, Sunazuka, T., Leenay, T.L., and Kingery-Wood, J. (1990a) Total syntheses of (+)-paspalicine and (+)-paspalinine. *J Am Chem Soc* **112**: 8197-8198.

Smith, D.J., Earl, A.J., and Turner, G. (1990b) The multifunctional peptide synthetase performing the first step of penicillin biosynthesis in

Penicillium chrysogenum is a 421,073 dalton protein similar to *Bacillus brevis* peptide antibiotic synthetases. *EMBO J* **9**: 2743-2750.

Southern, E.M. (1975) Detection of specific sequences among DNA fragments separated by gel electrophoresis. *J Mol Biol* **98**: 503-517.

Steyn, P.S., and Vleggaar, R. (1985) Tremorgenic mycotoxins. *Progress in the Chemistry of Organic Natural Products* **48**: 1-80.

Suarez, T., and Penalva, M.A. (1996) Characterization of a *Penicillium chrysogenum* gene encoding a PacC transcription factor and its binding sites in the divergent *pcbAB-pcbC* promoter of the penicillin biosynthetic cluster. *Mol Microbiol* **20**: 529-540.

Suelmann, R., and Fischer, R. (2000) Mitochondrial movement and morphology depend on an intact actin cytoskeleton in *Aspergillus nidulans*. *Cell Motil Cytoskeleton* **45**: 42-50.

Suzuki, K., Sanga, K., Chikaoka, Y., and Itagaki, E. (1993) Purification and properties of cytochrome P-450 (P-450lun) catalyzing steroid 11 β-hydroxylation in *Curvularia lunata*. *Biochim Biophys Acta* **1203**: 215-223.

Tag, A.G., Garifullina, G.F., Peplow, A.W., Ake, C., Jr., Phillips, T.D., Hohn, T.M., and Beremand, M.N. (2001) A novel regulatory gene, *Tri10*, controls trichothecene toxin production and gene expression. *Appl Environ Microbiol* **67**: 5294-5302.

Takashima, S., Nakamura, A., Iikura, H., Masaki, H., and Uozumi, T. (1996) Cloning of a gene encoding a putative carbon catabolite repressor from *Trichoderma reesei*. *Biosci Biotechnol Biochem* **60**: 173-176.

Tanaka, A., and Tsuge, T. (2000) Structural and functional complexity of the genomic region controlling AK-toxin biosynthesis and pathogenicity in the Japanese pear pathotype of *Alternaria alternata*. *Mol Plant Microbe Interact* **13**: 975-986.

Tanaka, A., Shiotani, H., Yamamoto, M., and Tsuge, T. (1999) Insertional mutagenesis and cloning of the genes required for biosynthesis of the host-specific AK-toxin in the Japanese pear pathotype of *Alternaria alternata*. *Mol Plant Microbe Interact* **12**: 691-702.

Tanaka, A., Tapper, B.A., Popay, A., Parker, E.J., and Scott, B. (2005) A symbiosis expressed non-ribosomal peptide synthetase from a

mutualistic fungal endophyte of perennial ryegrass confers protection to the symbiotum from insect herbivory. *Mol Microbiol* **57**: 1036-1050.

Tavoularis, S., Scazzocchio, C., and Sophianopoulou, V. (2001) Functional expression and cellular localization of a green fluorescent protein-tagged proline transporter in *Aspergillus nidulans*. *Fungal Genet Biol* **33**: 115-125.

Teichert, S., Schonig, B., Richter, S., and Tudzynski, B. (2004) Deletion of the *Gibberella fujikuroi* glutamine synthetase gene has significant impact on transcriptional control of primary and secondary metabolism. *Mol Microbiol* **53**: 1661-1675.

Then Bergh, K., and Brakhage, A.A. (1998) Regulation of the *Aspergillus nidulans* penicillin biosynthesis gene *acvA* (*pcbAB*) by amino acids: implication for involvement of transcription factor PACC. *Appl Environ Microbiol* **64**: 843-849.

Tilburn, J., Sarkar, S., Widdick, D.A., Espeso, E.A., Orejas, M., Mungroo, J., Penalva, M.A., and Arst, H.N., Jr. (1995) The *Aspergillus* PacC zinc finger transcription factor mediates regulation of both acid- and alkaline-expressed genes by ambient pH. *EMBO J* **14**: 779-790.

Toews, M.W., Warmbold, J., Konzack, S., Rischitor, P., Veith, D., Vienken, K., Vinuesa, C., Wei, H., and Fischer, R. (2004) Establishment of mRFP1 as a fluorescent marker in *Aspergillus nidulans* and construction of expression vectors for high-throughput protein tagging using recombination in vitro (GATEWAY). *Curr Genet* **45**: 383-389.

Tonukari, N.J., Scott-Craig, J.S., and Walton, J.D. (2003) Isolation of the carbon catabolite repressor (*CREA*) gene from the plant-pathogenic fungus *Cochliobolus carbonum*. *DNA Seq* **14**: 103-107.

Toyomasu, T., Nakaminami, K., Toshima, H., Mie, T., Watanabe, K., Ito, H., Matsui, H., Mitsuhashi, W., Sassa, T., and Oikawa, H. (2004) Cloning of a gene cluster responsible for the biosynthesis of diterpene aphidicolin, a specific inhibitor of DNA polymerase α. *Biosci Biotechnol Biochem* **68**: 146-152.

Trapp, S.C., Hohn, T.M., McCormick, S., and Jarvis, B.B. (1998) Characterization of the gene cluster for biosynthesis of macrocyclic trichothecenes in *Myrothecium roridum*. *Mol Gen Genet* **257**: 421-432.

Tsai, H.F., Wang, H., Gebler, J.C., Poulter, C.D., and Schardl, C.L. (1995) The *Claviceps purpurea* gene encoding dimethylallyltryptophan synthase, the committed step for ergot alkaloid biosynthesis. *Biochem Biophys Res Commun* **216**: 119-125.

Tsien, R.Y. (1998) The green fluorescent protein. *Ann Rev Biochem* **67**: 509-544.

Tudzynski, B. (2005) Gibberellin biosynthesis in fungi: genes, enzymes, evolution, and impact on biotechnology. *Appl Microbiol Biotechnol* **66**: 597-611.

Tudzynski, B., and Holter, K. (1998) Gibberellin biosynthetic pathway in *Gibberella fujikuroi*: evidence for a gene cluster. *Fungal Genet Biol* **25**: 157-170.

Tudzynski, B., Hedden, P., Carrera, E., and Gaskin, P. (2001a) The *P450-4* gene of *Gibberella fujikuroi* encodes ent-kaurene oxidase in the gibberellin biosynthesis pathway. *Appl Environ Microbiol* **67**: 3514-3522.

Tudzynski, B., Homann, V., Feng, B., and Marzluf, G.A. (1999a) Isolation, characterization and disruption of the *areA* nitrogen regulatory gene of *Gibberella fujikuroi*. *Mol Gen Genet* **261**: 106-114.

Tudzynski, B., Kawaide, H., and Kamiya, Y. (1998) Gibberellin biosynthesis in *Gibberella fujikuroi*: cloning and characterization of the copalyl diphosphate synthase gene. *Curr Genet* **34**: 234-240.

Tudzynski, B., Liu, S., and Kelly, J.M. (2000) Carbon catabolite repression in plant pathogenic fungi: isolation and characterization of the *Gibberella fujikuroi* and *Botrytis cinerea creA* genes. *FEMS Microbiol Lett* **184**: 9-15.

Tudzynski, B., Mihlan, M., Rojas, M.C., Linnemannstons, P., Gaskin, P., and Hedden, P. (2003) Characterization of the final two genes of the gibberellin biosynthesis gene cluster of *Gibberella fujikuroi*: *des* and *P450-3* encode GA4 desaturase and the 13-hydroxylase, respectively. *J Biol Chem* **278**: 28635-28643.

Tudzynski, B., Rojas, M.C., Gaskin, P., and Hedden, P. (2002) The gibberellin 20-oxidase of *Gibberella fujikuroi* is a multifunctional monooxygenase. *J Biol Chem* **277**: 21246-21253.

Tudzynski, P., Correia, T., and Keller, U. (2001b) Biotechnology and genetics of ergot alkaloids. *Appl Microbiol Biotechnol* **57**: 593-605.

Tudzynski, P., Holter, K., Correia, T., Arntz, C., Grammel, N., and Keller, U. (1999b) Evidence for an ergot alkaloid gene cluster in *Claviceps purpurea*. *Mol Gen Genet* **261**: 133-141.

Valenciano, S., Lucas, J.R., Pedregosa, A., Monistrol, I.F., and Laborda, F. (1996) Induction of β-oxidation enzymes and microbody proliferation in *Aspergillus nidulans*. *Arch Microbiol* **166**: 336-341.

Vanden Wymelenberg, A.J., Cullen, D., Spear, R.N., Schoenike, B., and Andrews, J.H. (1997) Expression of green fluorescent protein in *Aureobasidium pullulans* and quantification of the fungus on leaf surfaces. *Biotechniques* **23**: 686-690.

Vautard, G., Cotton, P., and Fevre, M. (1999) The glucose repressor CRE1 from *Sclerotinia sclerotiorum* is functionally related to CREA from *Aspergillus nidulans* but not to the Mig proteins from *Saccharomyces cerevisiae*. *FEBS Lett* **453**: 54-58.

Veenhuis, M., Mateblowski, M., Kunau, W.H., and Harder, W. (1987) Proliferation of microbodies in *Saccharomyces cerevisiae*. *Yeast* **3**: 77-84.

Walton, J.D. (2000) Horizontal gene transfer and the evolution of secondary metabolite gene clusters in fungi: an hypothesis. *Fungal Genet Biol* **30**: 167-171.

Wang, J., Machado, C., Panaccione, D.G., Tsai, H.F., and Schardl, C.L. (2004) The determinant step in ergot alkaloid biosynthesis by an endophyte of perennial ryegrass. *Fungal Genet Biol* **41**: 189-198.

Wong, S., and Wolfe, K.H. (2005) Birth of a metabolic gene cluster in yeast by adaptive gene relocation. *Nat Genet* **37**: 777-782.

Xiong, Q., Zhu, X., Wilson, W.K., Ganesan, A., and Matsuda, S.P. (2003) Enzymatic synthesis of an indole diterpene by an oxidosqualene

cyclase: mechanistic, biosynthetic, and phylogenetic implications. *J Am Chem Soc* **125**: 9002-9003.

Yan, M., Rayapuram, N., and Subramani, S. (2005) The control of peroxisome number and size during division and proliferation. *Curr Opin Cell Biol* **17**: 376-383.

Yang, G., Rose, M.S., Turgeon, B.G., and Yoder, O.C. (1996) A polyketide synthase is required for fungal virulence and production of the polyketide T-toxin. *Plant Cell* **8**: 2139-2150.

Yoder, O.C. (1988) *Cochliobolus heterostrophus*, cause of southern corn leaf blight. *Adv Plant Pathol* **6**: 93-112.

Yoon, Y.J., Kim, E.S., Hwang, Y.S., and Choi, C.Y. (2004) Avermectin: biochemical and molecular basis of its biosynthesis and regulation. *Appl Microbiol Biotechnol* **63**: 626-634.

Yoshikuni, Y., Ferrin, T.E., and Keasling, J.D. (2006) Designed divergent evolution of enzyme function. *Nature* **440**: 1078-1082.

Young, C., Itoh, Y., Johnson, R., Garthwaite, I., Miles, C.O., Munday-Finch, S.C., and Scott, B. (1998) Paxilline-negative mutants of *Penicillium paxilli* generated by heterologous and homologous plasmid integration. *Curr Genet* **33**: 368-377.

Young, C., McMillan, L., Telfer, E., and Scott, B. (2001) Molecular cloning and genetic analysis of an indole-diterpene gene cluster from *Penicillium paxilli*. *Mol Microbiol* **39**: 754-764.

Young, C.A., Bryant, M.K., Christensen, M.J., Tapper, B.A., Bryan, G.T., and Scott, B. (2005) Molecular cloning and genetic analysis of a symbiosis-expressed gene cluster for lolitrem biosynthesis from a mutualistic endophyte of perennial ryegrass. *Mol Genet Genomics* **274**: 13-29.

Young, C.A., Felitti, S., Shields, K., Spangenberg, G., Johnson, R.D., Bryan, G.T., Saikia, S., and Scott, B. (2006) A complex gene cluster for indole-diterpene biosynthesis in the grass endophyte *Neotyphodium lolii*. *Fungal Genet Biol* **43**: 679-693.

Yu, J., Chang, P.K., Ehrlich, K.C., Cary, J.W., Bhatnagar, D., Cleveland, T.E., Payne, G.A., Linz, J.E., Woloshuk, C.P., and Bennett, J.W. (2004) Clustered pathway genes in aflatoxin biosynthesis. *Appl Environ Microbiol* **70**: 1253-1262.

Zhang, S., Monahan, B.J., Tkacz, J.S., and Scott, B. (2004) Indole-diterpene gene cluster from *Aspergillus flavus*. *Appl Environ Microbiol* **70**: 6875-6883.

Zhu, X.F., Suzuki, K., Saito, T., Okada, K., Tanaka, K., Nakagawa, T., Matsuda, H., and Kawamukai, M. (1997) Geranylgeranyl pyrophosphate synthase encoded by the newly isolated gene *GGPS6* from *Arabidopsis thaliana* is localized in mitochondria. *Plant Mol Biol* **35**: 331-341.

FEBS Letters 580 (2006) 1625–1630

Four gene products are required for the fungal synthesis of the indole-diterpene, paspaline

Sanjay Saikia[a], Emily J. Parker[b], Albert Koulman[c], Barry Scott[a,*]

[a] *Institute of Molecular Biosciences, Massey University, Private Bag 11222, Palmerston North 5301, New Zealand*
[b] *Institute of Fundamental Sciences, Massey University, Private Bag 11222, Palmerston North 5301, New Zealand*
[c] *AgResearch Grasslands Research Centre, Tennent Drive, Private Bag 11008, Palmerston North 5301, New Zealand*

Received 9 December 2005; revised 7 February 2006; accepted 7 February 2006

Available online 17 February 2006

Edited by Ulf-Ingo Flügge

Abstract **Paspaline belongs to a large, structurally and functionally diverse group of indole-diterpenes synthesized by filamentous fungi. However, the identity of the gene products required for the biosynthesis of paspaline, a key intermediate for the synthesis of paxilline and other indole-diterpenes, is not known. Transfer of constructs containing different *pax* gene combinations into a paxilline negative deletion derivative of *Penicillium paxilli* demonstrated that just four proteins, PaxG, a geranylgeranyl diphosphate synthase, PaxM, a FAD-dependent monooxygenase, PaxB, a putative membrane protein, and PaxC, a prenyl transferase, are required for the biosynthesis of paspaline.**

Keywords: Indole-diterpenes; Paspaline; Paxilline; FAD-dependent monooxygenase; Prenyl transferase; *Penicillium paxilli*

1. Introduction

Indole-diterpenes are a large, structurally diverse group of natural products synthesized by filamentous fungi [1]. These natural products share a common core structure comprised of a cyclic diterpene skeleton derived from geranylgeranyl diphosphate (GGPP) and an indole moiety derived from tryptophan or a tryptophan precursor [2–6]. Further complexity of the basic indole-diterpene ring structure occurs by additional prenylations, different ring substitutions and ring stereochemistry. These metabolites have a number of biological activities including insect feeding deterrence, modulation of insect and mammalian ion channels and inhibition of specific enzymes [7,8]. The structural complexity and diverse biological activities of these compounds have attracted the attention of synthetic chemists resulting in both total and biomimetic syntheses of a number of paxilline-like indole-diterpenes [9–15]. The results of these studies suggest that 3-geranylgeranylindole is a common intermediate, which undergoes epoxidation followed by cyclization to give indole-diterpenes. More recently, feeding experiments with deuterium labeled 3-geranylgeranylindole demonstrated the incorporation of this compound into paxilline and emindole DA [16]. Although biosynthetic schemes have been proposed for paxilline-like compounds none of the enzymes responsible for catalyzing the proposed steps have been identified [6,17].

The cloning and characterization of a cluster of genes from *Penicillium paxilli* necessary for biosynthesis of the indole-diterpene, paxilline, has provided for the first time an insight into the gene products required for the synthesis of this important class of natural products and their biochemical function [18]. Systematic gene disruption and chemical complementation studies have shown that at least five enzymes are needed for paxilline biosynthesis [18,19]. *paxG* is proposed to encode a GGPP synthase that catalyzes the synthesis of GGPP, the determinant step in indole-diterpene biosynthesis. Deletion mutants of *paxM*, encoding a FAD-dependent monooxygenase (McMillan et al., unpublished results) and *paxC*, encoding a prenyl transferase (Young et al., unpublished results), lack the ability to synthesize any identifiable indole-diterpene indicating that these gene products catalyze early steps in paxilline biosynthesis. By contrast deletion of *paxP*, encoding a cytochrome P450 monooxygenase, resulted in a mutant strain that accumulates paspaline [19]. Taken together these results suggest that paspaline is the first stable indole-diterpene product, and that its synthesis requires the action of three enzymes viz. PaxG, PaxM and PaxC [20]. However, two additional genes, *paxA* and *paxB*, were recently identified within the core cluster of *paxG–paxM–paxC–paxP–paxQ* (Monahan et al., unpublished results). Sequence analysis of PaxA and PaxB suggests that these are polytopic membrane proteins containing seven transmembrane domains. Deletion derivatives of *paxA* and *paxB* were unable to synthesize any detectable indole-diterpenes. However, neither protein has any identifiable enzymatic function. The identification of these two new genes, the absence of detectable indole-diterpenes in *paxG*, *paxM* and *paxC* deletion mutants and accumulation of paspaline in the *paxP* deletion mutant suggests that up to five proteins PaxG, PaxA, PaxM, PaxB and PaxC are required for paspaline biosynthesis in *P. paxilli*. The objectives of this study were to define the minimum number of genes required for the synthesis of paspaline and to propose a biosynthetic scheme for the synthesis of this indole-diterpene. Our working hypothesis is that five gene products are required for paspaline biosynthesis.

*Corresponding author. Fax: +64 6 3505688.
E-mail address: d.b.scott@massey.ac.nz (B. Scott).

0014-5793/$32.00
doi:10.1016/j.febslet.2006.02.008

2. Materials and methods

2.1. Bacterial strains and plasmids

Escherichia coli strain DH5α (Invitrogen) served as the host for routine cloning. The transformants of this host were grown on LB agar plates supplemented with ampicillin (100 μg/ml) for selection. pGEM®-T Easy (Promega) and pII99 plasmids were used for cloning.

2.2. Fungal strains and growth conditions

Cultures of wild-type *P. paxilli* Bainier (PN2013 = ATCC 26601) and CY2 (PN2250) mutant derivatives were routinely grown in *Aspergillus* complete medium (ACM) [2% (w/v) malt extract (Oxoid, Basingstoke, England), 1% (w/v) mycological peptone (Oxoid), 2% (w/v) glucose, 1.5% (w/v) agar] and ACM supplemented with 0.8 M sucrose (RG medium), at 22 °C for 4–6 days. Liquid cultures were started using an inoculum of 5×10^6 spores per 25 ml of CDYE medium [3.34% (w/v) Czapex-Dox (Oxoid), 0.5% (w/v) yeast extract] supplemented with 0.5% (v/v) trace element mix [in 0.6 N HCl: 0.05% (w/v) $FeSO_4 \cdot 7H_2O$, 0.05% (w/v) $ZnSO_4 \cdot 7H_2O$, 0.01% (w/v) $MnSO_4 \cdot H_2O$, 0.005% (w/v) $CuSO_4 \cdot 5H_2O$, 0.004% (w/v) $CoCl_2 \cdot 6H_2O$], and shaken at 200 rpm at 28 °C for 7 days. Media were supplemented with geneticin (150 μg/ml), where necessary.

2.3. Molecular biology

Plasmid DNA was isolated and purified by alkaline lysis using either a Bio-Rad Quantum Prep® Plasmid Miniprep Kit (Bio-Rad Laboratories, CA, USA) or High Pure Plasmid Isolation Kit (Roche Diagnostics GmbH, Mannheim, Germany). Genomic DNA was isolated using a modification of the method of Yoder [21] as described previously [22]. Southern blotting and hybridization conditions were as described previously [22]. Genomic DNA for PCR screening was prepared from fungal spores. Spores from approximately 0.3 cm × 0.3 cm section of transformants on ACM were suspended in 1 ml TE (10 mM Tris–HCl, pH 7.5, 1 mM EDTA) with 0.01% (v/v) Triton X-100. 100 μl spore suspension was transferred into a 2 ml micro-tube PP (Sarstedt, Germany) containing sterile glass beads (425-600 μm). The spores were disrupted in a FastPrep® Cell Disrupter FP120 (Thermo Savant, NY, USA) for 20 s at 4 m/s and centrifuged at 13000 rpm for 10 min. The supernatant was collected and a 5 μl sample was used as the template for PCR. DNA fragments and PCR products were purified using QIAquick Gel Extraction and PCR Purification Kit (Qiagen). DNA fragments were sequenced by the dideoxynucleotide chain-termination method [23] using Big-Dye (Version 3) chemistry (Perkin–Elmer Applied Biosystems, Foster City, CA, USA) with oligonucleotide primers (Sigma Genosys). Products were separated on an ABI Prism 377 sequencer (Perkin–Elmer Applied Biosystems).

2.4. PCR conditions

PCR of *paxM* and *paxM–paxB* for cloning was carried out in 50 μl reaction volume containing 5 μl of 10× reaction buffer (Roche Diagnostics GmbH, Penzberg, Germany), 200 μM of each dNTP, 300 nM of each primer, 0.75 U of Expand High Fidelity Enzyme Mix (Roche) and 10 ng of plasmid. PCR of *paxA–paxM* for cloning was carried out in 50 μl reaction volume containing 5 μl of 10× reaction buffer (TripleMaster® PCR System, Eppendorf AG, Hamburg, Germany), 200 μM of each dNTP, 200 nM of each primer, 0.75 U of TripleMaster Polymerase Mix (Eppendorf) and 100 ng of genomic DNA. Genomic DNA, prepared from spores, was amplified in 50 μl reaction volume containing 5 μl of 10× reaction buffer (Roche Diagnostics GmbH), 100 μM of each dNTP, 200 nM of each primer and 2 U of *Taq* DNA polymerase (Roche).

The thermocycle conditions routinely used with *Taq* DNA polymerase and Expand High Fidelity Enzyme Mix were one cycle at 94 °C for 2 min, 30 cycles at 94 °C for 30 s, 55 °C for 30 s and 72 °C for 1 min (per kb) and one cycle at 72 °C for 5 min, and with TripleMaster Polymerase Mix were one cycle at 94 °C for 2 min, 30 cycles at 94 °C for 20 s, 55 °C for 20 s and 72 °C for 1 min (per kb) and one cycle at 72 °C for 3 min. Reactions were carried out in a PC-960, PC-960G (Corbett Research, Mortlake, Australia), or Mastercycler® gradient (Eppendorf, Hamburg, Germany) thermocycler.

2.5. Construction of expression constructs

Plasmid pSS8 (*paxG–paxA–paxM–paxB–paxC*) was constructed by ligating into pII99 an 11 kb *Hin*dIII fragment containing *paxG–paxA–paxM–paxB–paxC* from λCY55.

Plasmid pSS16 (*paxG–paxM–paxC*) was constructed by ligating into *Spe*I digested pSS8 a 2.54 kb *Spe*I fragment containing *paxM*. The fragment was prepared by digesting the PCR product amplified with primer set paxMSpeF2 and paxMSpeR from plasmid pSS8. Both primers contained mismatches relative to the genomic sequences in order to introduce *Spe*I sites at both ends.

Plasmid pSS17 (*paxG–paxM–paxB–paxC*) was constructed by ligating into *Spe*I digested pSS8 a 3.4 kb *Spe*I fragment containing *paxM–paxB*. The fragment was prepared by digesting the PCR product amplified with primer set paxMSpeR and SS8 from plasmid pSS8. Primer SS8 contained a native *Spe*I site.

Plasmid pSS20 (*paxG–paxA–paxM–paxC*) was constructed by ligating into *Spe*I digested pSS8 a 3.94 kb *Spe*I fragment containing *paxA–paxM*. The fragment was prepared by digesting the PCR product amplified with primer set paxMSpeF1 and SS9 from genomic DNA. Primer paxMSpeF1 contained mismatches relative to the genomic sequence in order to introduce a *Spe*I site at one end. Primer SS9 contained a native *Spe*I site.

2.6. Penicillium paxilli transformations and screening

Protoplasts of PN2250 (CY2) were prepared and transformed with circular plasmids pSS8, pSS16, pSS17 and pSS20 as described previously [19], except that the RG medium used for plating protoplasts was ACM supplemented with 0.8 M sucrose (see above). Transformants were selected on RG medium supplemented with geneticin (150 μg/ml) (Roche). The resulting stable transformants were maintained on ACM medium.

Screening of transformants for integration of the expression construct was carried out using genomic DNA from fungal spores (see above) as template and primer sets (see below) within, and external to, the gene fragment, to be integrated. The PCR conditions used were the standard conditions for *Taq* DNA polymerase (see above).

2.7. Indole-diterpene analysis

Mycelia from liquid cultures of *P. paxilli* grown for 7 days in CDYE, supplemented with trace element mix, were washed and freeze dried. Indole-diterpenes were extracted in 2:1 chloroform–methanol mixture. For thin-layer chromatography (TLC) analysis extracts were concentrated and redissolved in chloroform–methanol (2:1) and fractionated on SIL G (Macherey-Nagel, Germany) TLC plates using 9:1 chloroform–acetone mixture. Indole-diterpenes were identified with Ehrlich's reagent [2% (w/v) *p*-dimethylaminobenzaldehyde in 12% (v/v) HCl and 50% ethanol]. Analytical HPLC runs were performed on a Dionex Summit (Dionex Corporation, CA, USA) HPLC system equipped with a Luna (Phenomenex, CA, USA) C18 column (5 μm particle size, 4.6 × 250 mm). Indole-diterpenes were eluted with methanol–water (85:15) at a flow rate of 1.5 ml/min and UV detection at either 230 or 280 nm. LC–MSMS analysis was performed on a Thermo Finnigan Surveyor (Thermo Finnigan, CA, USA) HPLC system equipped with a Luna (Phenomenex) C18 column (5 μm particle size, 2 × 150 mm) at a flow rate of 200 μl/min with a solvent gradient starting with acetonitrile–water (60:40) in 0.1% formic acid and increasing to 95% acetonitrile over 30 min followed by a column wash at 99% acetonitrile. Mass spectra were determined with linear ion trap mass spectrometer (Thermo LTQ, Thermo Finnigan, CA, USA) using electro spray ionization (ESI) in positive mode. The spray voltage was 5.0 kV and the capillary temperature was 275 °C. The flow rates of sheath gas, auxiliary gas and sweep gas were set to 20, 5 and 10 (arbitrary units), respectively. Other parameters were optimized automatically by infusing authentic paspaline in water–acetonitrile–formic acid (75:25:0.1 v:v:v) at a flow rate of 200 μl/min. Paspaline and derivatives were detected in single reaction monitoring (SRM) mode, selecting 422 *m/z* ±2, 35% collision energy followed by data-dependent fragmentation of the three most intense ions in the mass spectrum above a 1000 (arbitrary unit) threshold.

2.8. Sequence of primers used in this study

Expression construct primers (restriction sites used for cloning are underlined and mismatches introduced are shown in bold).

For *paxM*:
paxMSpeF2: 5′ GGACTAGTCCGCTTCTTAGGATCAAC 3′
paxMSpeR: 5′ GTACTAGTGTCAGAGTACCCCTCTGC 3′
For *paxM–paxB*:
paxMSpeR: 5′ GTACTAGTGTCAGAGTACCCCTCTGC 3′
SS8: 5′ AGACTAGTTTAGATCTTGCAGGATCTCC 3′
For *paxA–paxM*:
paxMSpeF1: 5′ TTACTAGTGATCGGCAGTTGAGGGTG 3′
SS9: 5′ TGACTAGTCACAGGTCGTG 3′
Primers for screening transformants:
pII99-3: 5′ GGCTGGCTTAACTATGCG 3′
pII99-4: 5′ CCCAGAATGCACAGGTAC 3′
pax64: 5′ ACTGCATAGTTTGATATCTGC 3′
pax122: 5′ GCAGATAGTAGGTACTAC 3′
pax127: 5′ GGATTTGACCATGATGCG 3′

3. Results and discussion

Constructs containing all or different subsets of the five *pax* genes, *paxG*, *paxA*, *paxM*, *paxB*, and *paxC*, were cloned into the geneticin resistant vector pII99 [24] and transformed into protoplasts of CY2, a paxilline negative deletion mutant (>100 kb deletion) that lacks the entire *pax* gene cluster [22] (Fig. 1). Transformants were initially screened by PCR for the presence of the construct and then by Southern blot analysis to confirm integration of a complete copy of the construct in the recipient strain. The chemical phenotype of the positive transformants was determined by analyzing chloroform/methanol extracts by TLC and reverse-phase HPLC. A *Hin*dIII restriction fragment (11 kb) containing all 5 genes viz. *paxG*, *paxA*, *paxM*, *paxB* and *paxC* was sub-cloned from a lambda clone, λCY55, into pII99, to generate pSS8. Protoplasts of CY2 were transformed with pSS8 and an arbitrary selection of Gen^R transformants analyzed by TLC for the presence of indole-diterpenes. Four out of seven CY2/pSS8 transformants analyzed had a single green-staining compound with an R_f value similar to that of authentic paspaline (data not shown). Reverse-phase HPLC analysis of these extracts confirmed that the compound accumulated had the same retention time (R_t = 20.5 min) as authentic paspaline (Fig. 2A). Thus, the introduction of pSS8 into CY2 restored to this strain the ability to synthesize paspaline. The inability of some of the transformants to produce paspaline, despite containing the five genes, could be due to differences in copy number and/or position of integration of the construct in the genome [25]. These results suggest that five proteins are sufficient for paspaline biosynthesis. However, the proposed function of the enzymes PaxG, PaxM and PaxC suggested that these three enzymes alone might be sufficient for paspaline biosynthesis. To test this hypothesis a plasmid construct pSS16, containing *paxG–paxM–paxC*, was prepared by replacing a *Spe*I fragment containing *paxA–paxM–paxB* in pSS8 with a PCR amplified copy of *paxM*, and introduced into CY2. However, no detectable levels of any indole-diterpene were identified when extracts from nine of these CY2/pSS16 derivatives were analyzed by TLC (data not shown) or HPLC (Fig. 2B).

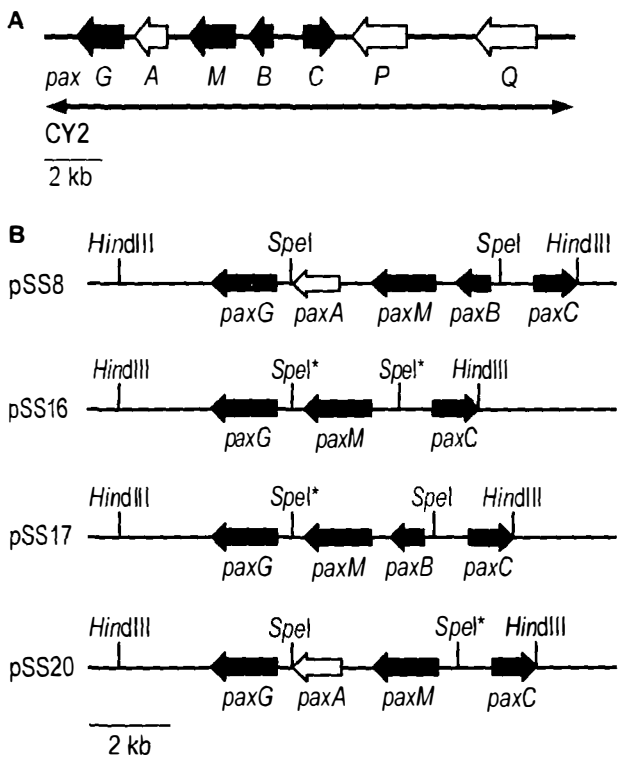

Fig. 1. (A) Organization of the paxilline (*pax*) gene cluster. Paspaline associated genes (black), and other *pax* genes within the core cluster (white). The double-headed arrow indicates that the deletion in CY2 includes the entire *pax* cluster as well as sequences to the left and right of the cluster. (B) Transformation constructs in linear form showing the subset of *pax* genes and the restriction sites used for cloning. * indicates restriction site introduced by PCR.

To test whether *paxA* and/or *paxB* are necessary for paspaline biosynthesis two additional constructs were prepared containing *paxG–paxM–paxC* and either *paxB* or *paxA*. Construct pSS20 (*paxG–paxA–paxM–paxC*) was prepared by ligating a PCR generated *paxA–paxM* fragment into *Spe*I digested pSS8. However, no detectable levels of any indole-diterpene were identified when extracts from eight of these CY2/pSS20 derivatives were analyzed by TLC (data not shown) or HPLC (Fig. 2C).

Construct pSS17 (*paxG–paxM–paxB–paxC*) was prepared by ligating a PCR generated *paxM–paxB* fragment into *Spe*I digested pSS8. Four out of ten CY2/pSS17 transformants analyzed produced a metabolite that eluted at the same retention time as authentic paspaline (Fig. 2D). In addition to paspaline (R_t = 20.5 min), a new more polar indole-diterpene (R_t = 10.5 min) was found to accumulate in the extracts of some of the CY2/pSS17 derivatives (Fig. 2D). This metabolite was not detected in extracts of wild-type *P. paxilli*. LC–MSMS analysis confirmed that two major indole-diterpenes were present in extracts from CY2/pSS17 transformant CY2.P17.3 (Fig. 3), both with *m/z* values of 422. The compound eluting at 24.2 min (Fig. 3) has a fragmentation pattern consistent with authentic paspaline whereas that eluting at 15.8 min has a fragmentation pattern indicative of a partially cyclized indole-diterpene (Supplementary material). The accumulation of this novel indole-diterpene metabolite may be due to the absence of the complete paxilline biosynthetic machinery. Products of partial cyclization like emindoles and emeniveol have been isolated from *Emericella* species suggesting that alternative cyclization pathways of indole and diterpene moieties are possible without skeletal rearrangement [26–29].

Identification of the proteins required for paspaline production now allows elucidation of the individual biosynthetic steps involved in its formation. We have shown here that just four proteins PaxG, PaxM, PaxB and PaxC are required for

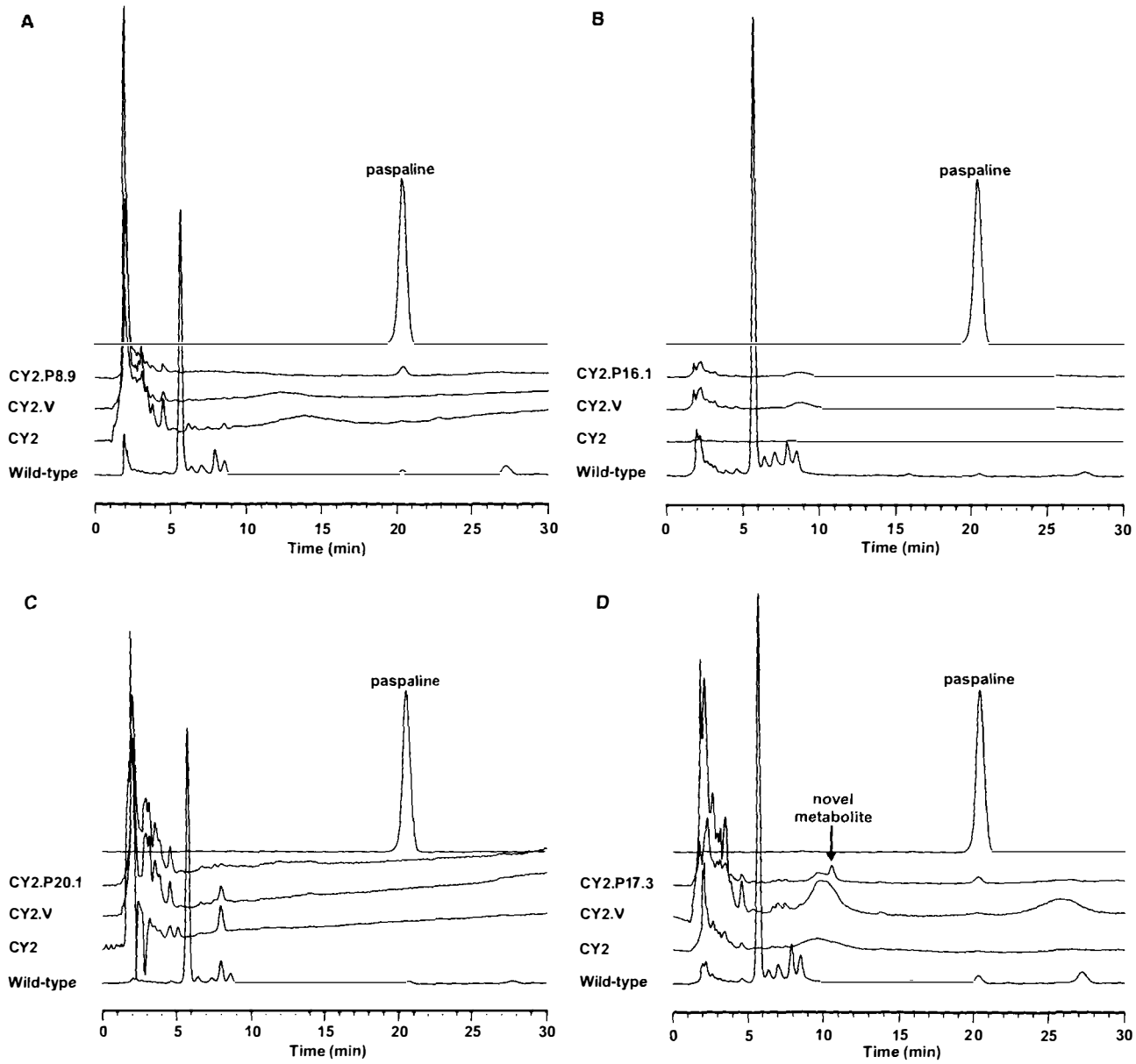

Fig. 2. Reverse-phase HPLC traces of CY2 derivatives containing: (A) pSS8 (*paxG–paxA–paxM–paxB–paxC*), (B) pSS16 (*paxG–paxM–paxC*), (C) pSS20 (*paxG–paxA–paxM–paxC*) and (D) pSS17 (*paxG–paxM–paxB–paxC*); CY2 – negative control; CY2.V – p1199 vector only control; P8 – pSS8; P16 – pSS16; P17 – pSS17; P20 – pSS20. The HPLC signal for wild-type is 6% of the original signal.

biosynthesis of paspaline. PaxG is proposed to catalyze a series of iterative condensations of IPP with DMAPP, GPP, then FPP, to form GGPP. Although the precise details of the mechanism of condensation of the GGPP and indole moiety, and subsequent epoxidation and cyclization events are not clear, our data implicate roles for PaxM and PaxC in these steps. We propose that PaxM, a FAD-dependent monooxygenase, catalyzes the epoxidation of the two terminal alkenes of the geranylgeranyl moiety (Fig. 4). Subsequently, PaxC, a prenyl transferase, catalyzes the cationic cyclization giving rise to paspaline. The condensation of indole-3-glycerol phosphate with GGPP may be catalyzed by either PaxG or PaxC.

Although our data clearly demonstrates that PaxB is required for paspaline biosynthesis, its role in paspaline biosynthesis is not clear. However, secondary structure analysis suggests that it may be a transporter. Unlike the major ABC (ATP-binding cassette) and MFS (major facilitator superfamily) fungal transporters, PaxB contains seven transmembrane domains. Most ABC and MFS transporters associated with secondary metabolite gene clusters appear to have a role in self-protection of the producing organism from the toxic effects of the metabolite [30,31]. Given the novel structure of PaxB and the indole-diterpene negative phenotype of the *paxB* mutant (Monahan et al., unpublished results), we propose that it is more likely to have a role in transporting substrate(s) to the vicinity of the biosynthetic enzyme complex, than a role in self-protection. Functional analysis of PaxM, PaxB and PaxC to confirm these predicted functions is currently underway as are reporter gene fusion experiments to localize these proteins in the cell.

In summary, we have successfully demonstrated that four proteins are required for paspaline biosynthesis. On the basis of this

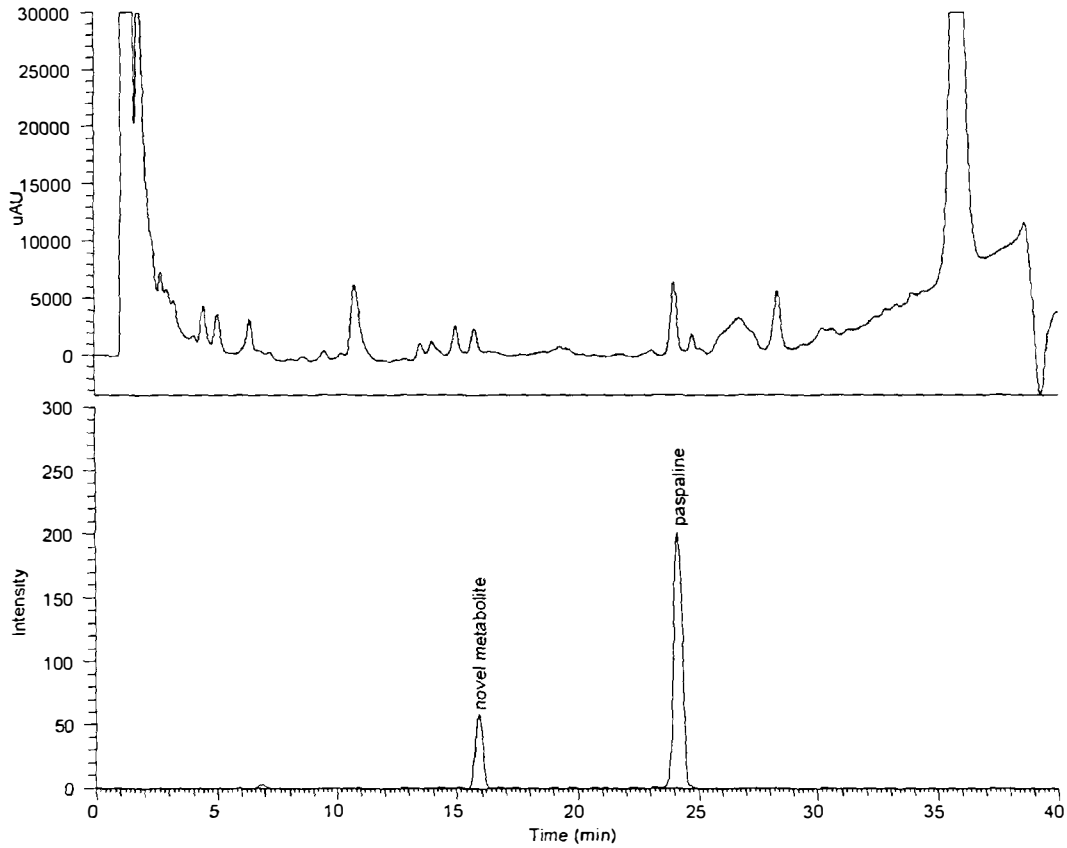

Fig. 3. Chromatogram of CY2/pSS17 (*paxG-paxM-paxB-paxC*) derivative, strain CY2.P17.3, showing the elution times for paspaline and a novel indole-diterpene metabolite. Top line: UV trace at 275 nm; Bottom line: LC–MSMS trace showing 422 ions containing 130 *m/z* fragments characteristic of indole moiety.

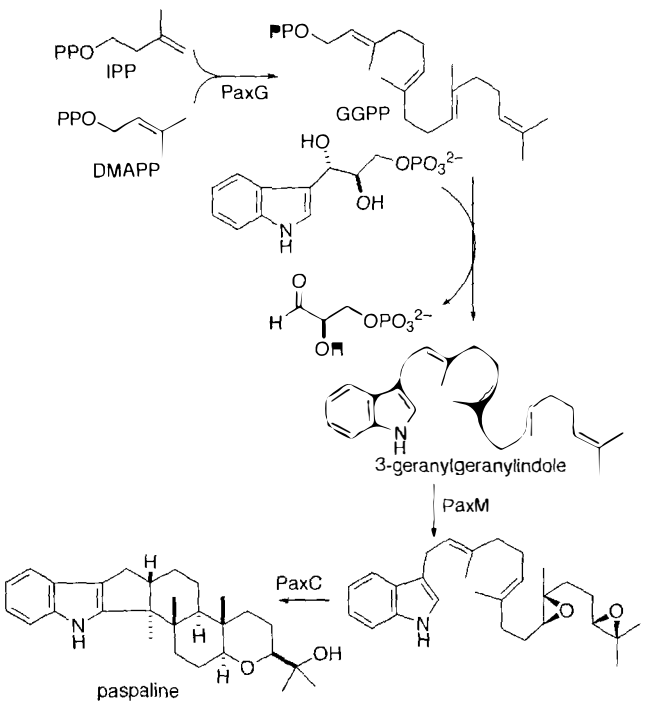

Fig. 4. Proposed scheme for paspaline biosynthesis in *P. paxilli*.

work, we predict that orthologues of these four genes will be common to other indole-diterpene biosynthetic gene clusters including those for aflatrem [32] and lolitrem [33] biosynthesis. We also propose that paspaline is the key intermediate for indole-diterpene biosynthesis, providing the core structural backbone for subsequent reactions that generate the chemical diversity within this important group of secondary metabolites.

Acknowledgements: The authors are grateful to Brendon Monahan for technical advice, and support from the Royal Society of New Zealand (Marsden Grant MAU010).

Appendix A. Supplementary data

Supplementary data associated with this article can be found, in the online version, at doi:10.1016/j.febslet.2006.02.008.

References

[1] Steyn, P.S. and Vleggaar, R. (1985) Tremorgenic mycotoxins. Prog. Chem. Org. Nat. Prod. 48, 1–80.
[2] Acklin, W., Weibel, F. and Arigoni, D. (1977) Zur biosynthese von paspalin und verwandten metaboliten aus *Claviceps paspali*. Chimia 31, 63.

[3] de Jesus, A.E., Gorst-Allman, C.P., Steyn, P.S., van Heerden, F.R., Vleggaar, R., Wessels, P.L. and Hull, W.E. (1983) Tremorgenic mycotoxins from *Penicillium crustosum*. Biosynthesis of penitrem A. J. Chem. Soc., Perkin Trans. 1, 1863–1868.
[4] Laws, I. and Mantle, P.G. (1989) Experimental constraints in the study of the biosynthesis of indole alkaloids in fungi. J. Gen. Microbiol. 135, 2679–2692.
[5] Byrne, K.M., Smith, S.K. and Ondeyka, J.G. (2002) Biosynthesis of nodulisporic acid A: precursor studies. J. Am. Chem. Soc. 124, 7055–7060.
[6] Munday-Finch, S.C., Wilkins, A.L. and Miles, C.O. (1996) Isolation of paspaline B, an indole-diterpenoid from *Penicillium paxilli*. Phytochemistry 41, 327–332.
[7] Cole, R.J. and Cox, R.H. (1981) Handbook of Toxic Fungal Metabolites, Academic Press, London.
[8] Li, C., Gloer, J.B., Wicklow, D.T. and Dowd, P.F. (2002) Thiersinines A and B: novel antiinsectan indole diterpenoids from a new fungicolous *Penicillium* species (NRRL 28147). Org. Lett. 4, 3095–3098.
[9] Smith III, A.B. and Mewshaw, R. (1985) Total synthesis of (−)-paspaline. J. Am. Chem. Soc. 107, 1769–1771.
[10] Smith III, A.B. and Leenay, T.L. (1989) Indole diterpene synthetic studies. 5. Development of a unified synthetic strategy: a stereocontrolled, second-generation synthesis of (−)-paspaline. J. Am. Chem. Soc. 111, 5761–5768.
[11] Smith III, A.B., Sunazuka, T., Leenay, T.L. and Kingery-Wood, J. (1990) Total syntheses of (+)-paspalicine and (+)-paspalinine. J. Am. Chem. Soc. 112, 8197–8198.
[12] Smith III, A.B., Kanoh, N., Minakawa, N., Rainier, J.D., Blase, F.R. and Hartz, R.A. (1999) Tremorgenic indole alkaloids. Studies directed toward the assembly of the A, F, and I rings of penitrem D: observation of an unexpected stereochemical outcome. Org. Lett. 1, 1263–1266.
[13] Rainier, J.D. and Smith III, A.B. (2000) Polyene cyclizations to indole diterpenes. The first synthesis of (+)-emindole SA using a biomimetic approach. Tetrahedron Lett. 41, 9419–9423.
[14] Clark, J.S., Myatt, J., Wilson, C., Roberts, L. and Walshe, N. (2003) Exploration of the biomimetic synthesis of indole-diterpene mycotoxins: an unexpected cascade reaction during the attempted synthesis of emindole SB. Chem. Commun. (Camb.), 1546–1547.
[15] Xiong, Q., Zhu, X., Wilson, W.K., Ganesan, A. and Matsuda, S.P. (2003) Enzymatic synthesis of an indole diterpene by an oxidosqualene cyclase: mechanistic, biosynthetic, and phylogenetic implications. J. Am. Chem. Soc. 125, 9002–9003.
[16] Fueki, S., Tokiwano, T., Toshima, H. and Oikawa, H. (2004) Biosynthesis of indole diterpenes, emindole, and paxilline: involvement of a common intermediate. Org. Lett. 6, 2697–2700.
[17] Mantle, P.G. and Weedon, C.M. (1994) Biosynthesis and transformation of tremorgenic indole-diterpenoids by *Penicillium paxilli* and *Acremonium lolii*. Phytochemistry 36, 1209–1217.
[18] Young, C., McMillan, L., Telfer, E. and Scott, B. (2001) Molecular cloning and genetic analysis of an indole-diterpene gene cluster from *Penicillium paxilli*. Mol. Microbiol. 39, 754–764.
[19] McMillan, L.K., Carr, R.L., Young, C.A., Astin, J.W., Lowe, R.G., Parker, E.J., Jameson, G.B., Finch, S.C., Miles, C.O., McManus, O.B., Schmalhofer, W.A., Garcia, M.L., Kaczorowski, G.J., Goetz, M., Tkacz, J.S. and Scott, B. (2003) Molecular analysis of two cytochrome P450 monooxygenase genes required for paxilline biosynthesis in *Penicillium paxilli*, and effects of paxilline intermediates on mammalian maxi-K ion channels. Mol. Genet. Genom. 270, 9–23.
[20] Parker, E.J. and Scott, B. (2004) in: Handbook of Industrial Mycology (An, Z., Ed.), pp. 405–426, Marcel Dekker, New York.
[21] Yoder, O.C. (1988) *Cochliobolus heterostrophus* cause of southern corn leaf blight. Adv. Plant Pathol. 6, 93–112.
[22] Young, C., Itoh, Y., Johnson, R., Garthwaite, I., Miles, C.O., Munday-Finch, S.C. and Scott, B. (1998) Paxilline-negative mutants of *Penicillium paxilli* generated by heterologous and homologous plasmid integration. Curr. Genet. 33, 368–377.
[23] Sanger, F., Nicklen, S. and Coulson, A.R. (1977) DNA sequencing with chain-terminating inhibitors. Proc. Natl. Acad. Sci. USA 74, 5463–5467.
[24] Namiki, F., Matsunaga, M., Okuda, M., Inoue, I., Nishi, K., Fujita, Y. and Tsuge, T. (2001) Mutation of an arginine biosynthesis gene causes reduced pathogenicity in *Fusarium oxysporum* f. sp. *melonis*. Mol. Plant Microb. Interact. 14, 580–584.
[25] Malonek, S., Rojas, M.C., Hedden, P., Gaskin, P., Hopkins, P. and Tudzynski, B. (2005) Functional characterization of two cytochrome P450 monooxygenase genes, *P450-1* and *P450-4*, of the gibberellic acid gene cluster in *Fusarium proliferatum* (*Gibberella fujikuroi* MP-D). Appl. Environ. Microbiol. 71, 1462–1472.
[26] Nozawa, K., Nakajima, S., Kawai, K. and Udagawa, S. (1988) Studies on fungal products. Part 17. Isolation and structures of novel indoloditerpenes, emindoles DA and DB, from *Emericella desertorum*: X-ray molecular structure of emindole DA acetate. J. Chem. Soc., Perkin Trans. 1, 1689–1694.
[27] Nozawa, K., Yuyama, M., Nakajima, S., Kawai, K. and Udagawa, S. (1988) Studies on fungal products. Part 19. Isolation and structure of a novel indoloditerpene, emindole SA, from *Emericella striata*. J. Chem. Soc., Perkin Trans. 1, 2155–2160.
[28] Nozawa, K., Nakajima, S., Kawai, K. and Udagawa, S. (1988) Isolation and structures of indoloditerpenes, possible biosynthetic intermediates to the tremorgenic mycotoxin, paxilline, from *Emericella striata*. J. Chem. Soc., Perkin Trans. 1, 2607–2610.
[29] Kimura, Y., Nishibe, M., Nakajima, H., Hamasaki, T., Shigemitsu, N., Sugawara, F., Stout, T.J. and Clardy, J. (1992) Emeniveol; A new pollen growth inhibitor from the fungus, *Emericella nivea*. Tetrahedron Lett. 33, 6987–6990.
[30] Del Sorbo, G., Schoonbeek, H. and De Waard, M.A. (2000) Fungal transporters involved in efflux of natural toxic compounds and fungicides. Fungal Genet. Biol. 30, 1–15.
[31] Gardiner, D.M., Jarvis, R.S. and Howlett, B.J. (2005) The ABC transporter gene in the sirodesmin biosynthetic gene cluster of *Leptosphaeria maculans* is not essential for sirodesmin production but facilitates self-protection. Fungal Genet. Biol. 42, 257–263.
[32] Zhang, S., Monahan, B.J., Tkacz, J.S. and Scott, B. (2004) Indole-diterpene gene cluster from *Aspergillus flavus*. Appl. Environ. Microbiol. 70, 6875–6883.
[33] Young, C.A., Bryant, M.K., Christensen, M.J., Tapper, B.A., Bryan, G.T. and Scott, B. (2005) Molecular cloning and genetic analysis of a symbiosis-expressed gene cluster for lolitrem biosynthesis from a mutualistic endophyte of perennial ryegrass. Mol. Genet. Genom. 274, 13–29.